Identifying Neurocircuitry Controlling Cardiovascular Function in Humans: Implications for Exercise Control

Shanika Deshani Basnayake

Merton College

University of Oxford

Trinity Term 2012

A thesis submitted in fulfilment of the requirements for the degree of Doctor of Philosophy at the University of Oxford

Shanika Basnayake
Merton College

ABSTRACT

Doctor of Philosophy
Trinity Term 2012

Identifying Neurocircuitry Controlling Cardiovascular Function in Humans: Implications for Exercise Control

This thesis is concerned with the neurocircuitry that underpins the cardiovascular response to exercise, which has thus far remained incompletely understood. Small animal studies have provided clues, but with the advent of functional neurosurgery, it has now been made possible to translate these findings to humans.

Chapter One reviews the background to the studies in this thesis. Our current understanding of the cardiovascular response to exercise is considered, followed by a discussion on the anatomy and function of various brain nuclei. In particular, the rationale for targeting the periaqueductal grey (PAG) and the subthalamic nucleus (STN) is reviewed.

Chapter Two reviews the use of deep brain stimulation (DBS), in which deep brain stimulating electrodes are implanted into various brain nuclei in humans, in order to treat chronic pain and movement disorders. This technique not only permits direct electrical stimulation of the human brain, but also gives the opportunity to record the neural activity from different brain regions during a variety of cardiovascular experiments. This chapter also gives a detailed methodological description of the experimental techniques performed in the studies in this thesis.

Chapter Three identifies the cardiovascular neurocircuitry involved in the exercise pressor reflex in humans using functional neurosurgery. It shows for the first time in humans that the exercise pressor reflex is associated with significantly increased neural activity in the dorsal PAG. The other sites investigated, which had previously been identified as cardiovascular active in both animals and humans, seem not to have a role in the integration of this reflex.

Chapter Four investigates whether changes in exercise intensity affect the neurocircuitry involved in the exercise pressor reflex. It demonstrates that the neural activity in the PAG is graded to increases in exercise intensity and corresponding increases in arterial blood pressure. This chapter also provides evidence to suggest that neural activity in the STN corresponds to the cardiovascular changes evoked by the remote ischaemic preconditioning stimulus in humans.

Chapter Five identifies the cardiovascular neurocircuitry involved during changes in central command during isometric exercise at constant muscle tension using muscle vibration. It shows that, in humans, central command is associated with significantly decreased neural activity in the STN. Furthermore, the STN activity is graded to the perception of the exercise task, i.e. the degree of central command. The other sites investigated appear not to have as significant a role in the integration of central command during the light exercise task that was undertaken.

Chapter Six studies the changes in muscle sympathetic nerve activity (MSNA) during stimulation of various brain nuclei in humans. Regrettably, the results presented in this chapter are not convincing enough to support the hypothesis that stimulation of particular subcortical structures corresponds to changes in MSNA. However, the cardiovascular changes that were recorded during stimulation of the different subcortical structures are congruous with previous studies in both animals and humans.

Chapter Seven presents a brief summary of the findings in this thesis.

For my parents

Table of Contents

CHAPTER 1

Introduction

Neurocircuitry Involved in Cardiovascular Function

It was in the 19th century that it was first speculated that the cardiovascular system was controlled by the brain. The eminent researchers Claude Bernard and Charles Edouard Brown-Séquard can be accredited with the 'discovery' of vasomotor nerves – Brown-Séquard observed the existence of sympathetic vasoconstrictor fibres, and Bernard demonstrated the presence of vasodilator nerves (as reviewed by Montastruc *et al*, 1996). However, their work was preceded by data obtained by others. For example, as early as 1630, Thomas Willis noted that artery diameter could be reduced by the 'contraction' of the surrounding nervous network. Although there was no experimental evidence at the time, several physiologists believed that arteries were supplied by sympathetic nerves. In 1840, Stilling coined the term 'nervus vasomotorius' for these nerves, and Henle described six layers that made up the arterial wall, one of which was composed of smooth muscle fibres with contractile filaments innervated by nerve fibres. Budge and Waller performed experiments in 1853 which demonstrated direct vasoconstrictor effects, as well as medullary pathways. They showed that galvanisation of the cervical sympathetic nerve induced an increase in pupil size, and that the effect had a medullary origin – the cilio-spinal centre in the medulla (see Montastruc *et al*, 1996). Ernst and Eduard Weber demonstrated the inhibitory action of the vagus nerve on the heart in 1854, when they stimulated the ends of isolated vagus nerves in frogs and showed dramatic slowing of the heartbeat - the pathway of this effect was also traced to the medulla (see Fye, 2000).

Since these early observations, there has been a tremendous amount of research in this field. Originally, much of this research was based around studies of the cardiovascular component of the 'defence reaction' in animals. It was demonstrated that regions in the hypothalamus, midbrain, pons and medulla acted together to produce a fully integrated defence response, including muscle vasodilatation, tachycardia, vasoconstriction in the skin, pupillary dilatation, and piloerection (Coote *et al*, 1973; Hilton, 1975). Guertzenstein and Silver (1974) were the first to suggest that a group of cells on the ventral surface of the medulla played a key role in the maintenance of arterial blood pressure. In 1985, Lovick and Hilton showed that excitatory amino acid microinjection into the ventrolateral medulla evokes a rise in arterial blood pressure and vasoconstriction in the hind limb muscles of cats. It is now widely accepted that the medulla contains the major nuclei that manipulate cardiorespiratory parameters, such as heart rate, blood pressure and respiration. Information passes from the peripheral arterial and cardiopulmonary baroreceptors and chemoreceptors to an area of the dorsomedial medulla; more specifically, the nucleus of the solitary tract (NTS) (Jordan and Spyer, 1977; Ciriello and Calaresu, 1981). Jordan and Spyer (1977) explored an area of the medulla in both cats and rabbits with tungsten stimulating electrodes in order to search for areas that evoked antidromic activity in the carotid sinus nerve, which contains primary afferent fibres that innervate the carotid sinus baroreceptors and the carotid body chemoreceptors. Action potentials in the carotid sinus nerve were evoked from sites in the ipsilateral medulla in the area of the NTS and also in the area postrema. The aortic depressor nerve has also been shown to project to the NTS using anterograde transport of horseradish peroxidise in cats (Ciriello and Calaresu, 1981). Degeneration studies after lesions in the NTS have shown diffuse projections to a number of locations in the brainstem (Calaresu *et al*, 1975). The majority of experimental evidence shows that afferent cardiovascular information is directly or indirectly relayed through the NTS to a variety of reticular nuclei, and also to the nucleus ambiguus and

the dorsal motor nucleus of the vagus (Calaresu *et al*, 1975). Furthermore, renal afferents influence the activity of brainstem regions that control blood pressure.

The control of arterial blood pressure is complex, as it is manipulated by both neural and hormonal pathways, influencing cardiovascular control areas in the brain down to individual cardiac and vascular myocytes. Short term (i.e. seconds to minutes) arterial blood pressure is regulated by feedback control systems which rely on the autonomic nervous system and also on circulating hormones as their effector mechanisms (Dampney *et al*, 2002). The arterial baroreflex originates from baroreceptors in the aortic arch and the carotid sinus, composed of unencapsulated free nerve endings in the arterial medial-adventitial borders (Sheehan *et al*, 1941; Sagawa, 1983). Changes in arterial blood pressure cause conformational changes in these mechanoreceptors, which leads to appropriate changes in the pattern of neuronal firing. Branches of the glossopharyngeal and vagus nerves carry impulses from the carotid and aortic baroreceptors, respectively. These afferent signals then converge in the NTS. When arterial blood pressure is raised, the baroreceptors stretch and trigger increased neuronal firing, whereas, when the arterial blood pressure is low, neuronal firing is decreased. In both scenarios, reflex-mediated autonomic neural adjustments occur so that resting arterial blood pressure operates around a set point (Heymans and Neil, 1958; Kirchheim, 1976; Fadel, 2008).

The neural control of arterial pressure operates via the two efferent arms of the autonomic nervous system – sympathetic and parasympathetic neurons which project from the brainstem (Guyenet, 2006). The parasympathetic system innervates the heart, and alters both heart rate and contractility via the vagus nerve. It is activated by the nucleus ambiguus and the dorsal motor nucleus of the vagus. The sympathetic system innervates the blood vessels, the heart, the kidneys and the adrenal medulla, and is primarily activated by the rostral ventrolateral medulla (RVLM). Blood pressure is determined by vascular resistance and cardiac output, which are both ultimately controlled by the autonomic nervous system. Cardiac

output is dependent on myocardial contractility, heart rate and end-diastolic volume, which, in turn, is determined by venous pressure. Venous pressure is related to blood volume and venous smooth muscle tone, both of which are sympathetically regulated. Myocardial contractility and heart rate are controlled by both the sympathetic and parasympathetic systems.

Changes in arterial blood pressure can be triggered either via reflex arcs from peripheral receptors (e.g. baro- / chemo-receptor reflexes, exercise pressor reflex), or as part of a centrally mediated response (e.g. at the onset of exercise). Signals originating from a variety of peripheral receptors can have influence on the activity of cardiovascular autonomic nerves. The arterial baroreflex originates from arterial baroreceptors which project to the NTS, where they excite second-order neurons, which in turn project to caudal and intermediate parts of the ventrolateral medulla; these latter neurons then project to and inhibit sympathoexcitatory neurons in the RVLM (Dampney, 1994). Blockade of this synapse abolishes the reflex, which illustrates the fundamental role that the RVLM plays in cardiovascular reflexes (Dampney *et al*, 2002). This reflex arc provides beat-to-beat information about the pressure of the arterial system, the cardiac chambers, and the greater veins.

Another short-term feedback regulator of blood pressure is the chemoreceptor reflex. Chemoreceptors are situated in the carotid and aortic bodies, and are stimulated by a decrease in the partial pressure of oxygen in arterial blood. It was in the early twentieth century that the physiologist Heinrich Hering first described the respiratory reflex and studied the carotid sinus in a reflexogenic context; at the same time, Heymans and Heymans studied the aortic reflexogenic region. However, it was De Castro who first described cells in the carotid bodies that specifically detected changes in the chemical composition of the blood (see De Castro, 2009). It is now understood that the carotid and aortic chemoreceptors project to the NTS via the glossopharyngeal and vagus nerves, similar to the baroreceptors. However,

unlike the baroreflex, there are direct excitatory projections from the NTS to the presympathetic neurons in the RVLM. Blocking this synapse abolishes the sympathetic component of the reflex, providing further evidence for the crucial role of the RVLM in cardiovascular reflexes (Dampney *et al*, 2002).

It is not only the afferent fibres of the glossopharyngeal and vagus nerves that contribute to the feedback mechanisms controlling cardiovascular function, but also afferent inputs entering the spinal cord via dorsal roots. These originate from various somatic and visceral receptors, including mechanoreceptors and chemoreceptors in skeletal muscle, skin nociceptors, and receptors in organs such as the heart, the kidneys, and the pulmonary vasculature (Dampney, 1994). All of the aforementioned mechanisms and pathways act reflexly in order to maintain cardiovascular homeostasis, but neural control of the cardiovascular system is far more complicated than this. The purpose of the human cardiovascular system is to provide adequate blood flow to different vascular beds under varying physiological conditions, thus facilitating the exchange of gas and nutrients in metabolically active tissues. The maintenance of a narrow blood pressure range via the baro- and chemoreceptor reflexes does not account for the rises in blood pressure that occur at times of increased activity, for example during exercise.

The Cardiovascular Response to Exercise

It is known that during an isometric contraction, large increases in arterial blood pressure and heart rate are observed (Lind *et al*, 1966). This occurs due to the requirement of increased perfusion of skeletal muscles, in order to meet their metabolic demands. An increase in metabolic activity will result in local vasodilatation and a consequent increase in blood flow – this is caused by the direct effect of endothelial factors and metabolites on vascular smooth muscle (Delp and Laughlin, 1998). This is an effective way of matching blood flow to metabolic

demands, as long as systemic arterial blood pressure is maintained at an appropriate level, via central cardiovascular control mechanisms. This is regulated by means of increased cardiac output through raised cardiac activity and venous return, and increased vascular resistance in inactive tissues, such as the skin and viscera (Armstrong *et al*, 1987).

Complex behavioural responses can evoke neurally mediated cardiovascular adjustments. At the onset of exercise, for example, there is an increase in ventilation, heart rate, skeletal muscle blood flow and the activity of sympathetic nerves supplying other vascular beds (e.g. the kidneys). The idea that signals descending from the brain could influence cardiovascular responses to exercise was first suggested at the close of the 19th century (Zuntz and Geppert, 1886). Johannson (1893) proposed that two distinct neural control mechanisms regulated these responses to exercise in animals – one originating peripherally in the skeletal muscle and the other originating centrally in the brain. These control mechanisms mediating the cardiovascular and respiratory changes associated with the onset of exercise have now been identified as the result of a cortically-initiated feed-forward regulatory response known as 'central command' (Goodwin *et al*, 1972). This concept was first introduced by Krogh and Lindhard (1913) as 'cortical irradiation' – they proposed that neural impulses from higher brain centres control cardiorespiratory parameters in a 'top-down' manner in order to match the anticipated metabolic demand of exercising muscles. With human subjects, perception of exercise resulted in a cardiorespiratory response that was related to the perceived work rate.

In 1960, Smith *et al* attempted to identify the higher brain centres involved in cardiovascular control by stereotaxically stimulating specific areas of the diencephalon in dogs. They noted that stimulating the periventricular grey area surrounding the third ventricle and the H_1 and H_2 fields of Forel caused the same cardiovascular responses to those which resulted from treadmill exercise. Asmussen *et al* (1965) investigated the influence of central command on the responses to exercise using curare-induced partial neuromuscular blockade. They found

that when strength was reduced by partial paralysis, there were exaggerated cardiovascular and ventilatory responses to a set level of dynamic exercise.

Goodwin *et al* (1972) conducted a range of experiments to investigate whether the 'central command' signals descending from higher neural control centres to working muscle provided an element of cardiorespiratory control. They applied vibration stimuli to the biceps tendons in humans holding sustained isometric contractions with either their biceps muscle or their triceps muscle. The vibration stimulus was used to either assist or inhibit a voluntary isometric contraction. During contraction of the biceps muscle, the activation of the primary afferents of the biceps muscle spindles via vibration provided a degree of reflex excitation. Therefore, less central command than usual was necessary to hold a given tension. On the other hand, during contraction of the triceps muscle, vibration of the primary afferents of its antagonist muscle spindles (the biceps spindles) provided a degree of reflex inhibition. Therefore, more central command was necessary to hold a given tension. Consequently, Goodwin *et al* (1972) were able to investigate the cardiovascular responses to an isometric effort during varying degrees of central command. They reported that blood pressure and heart rate both increase during an isometric effort, and that this increase was greater when the central command was increased, and lessened when the central command was decreased. This led them to the conclusion that there was 'irradiation' of the cardiovascular control centres by descending central command signals during voluntary isometric muscle contraction in humans.

Eldridge *et al* (1981; 1985) used unanaesthetised decorticate cats (which had been shown to move normally when placed on treadmills) to investigate the relationship between locomotion and respiration. This allowed the influence of feedback mechanisms to be eliminated, as these animals moved both spontaneously and also during stimulation of the 'subthalamic locomotor region'. It was observed that there was an increase in respiration and arterial pressure before the onset of movement, and once movement had ceased there was a rapid decrease in

respiration. Both arterial pressure and respiration increased proportionately depending on the level of exercise. In paralysed cats, stimulation of the subthalamic locomotor region resulted in 'fictive' locomotion, again preceded by increases in arterial pressure and phrenic activity. These findings supported the idea that a neural mechanism requiring no feedback from working muscle and originating above the cardiorespiratory centres of the medulla caused both locomotion and the increase in respiration associated with it.

A further demonstration of the 'central command' response was shown by Gandevia *et al* (1993), who studied artificially ventilated human subjects who had undergone total neuromuscular blockade. During paralysis, they noted marked increases in arterial pressure and heart rate during attempted isometric contractions of the arm, leg and trunk muscles. When the subjects attempted handgrip contractions, the increases in mean arterial pressure and heart rate were comparable to those observed during actual handgrip contractions. It was found that these increases in cardiovascular parameters were graded according to the intensity of the contraction. These responses are evidently not part of a feedback regulatory mechanism since the subjects were paralysed. Therefore, they can be considered feed-forward responses. It is clear that signals originating from the cortex can result in activation of sympathetic outflow to the heart and blood vessels.

Originally, it was believed that central command of the cardiovascular system was closely linked with the parallel feedforward motor system. However, Williamson *et al* (2006) proposed that central command in fact involves the simultaneous activation of two distinct networks: one intended for central motor control and one intended for central cardiorespiratory control. Experiments in which a subject's perception of exercise has been shown to determine their cardiovascular response (as opposed to the exercise itself) provides evidence for this. Thornton *et al* (2001) were able to demonstrate this response by performing positron emission tomography (PET) scanning on hypnotically induced subjects. They showed

that the right dorsolateral prefrontal cortex, the supplementary motor areas, the right premotor area, the superolateral sensorimotor area, the thalamus and the cerebellum were active during the imagination of exercise. During volitional hyperventilation to match that caused by the imagination of exercise, the supplementary motor areas and the lateral sensorimotor cortical areas were active. This suggested that a component of the respiratory response to exercise could be activated by a behavioural response, without afferent motor feedback.

During exercise, the muscle pressor reflex provides afferent feedback signals from working muscle, thereby providing additional influence on cardiovascular control. This idea was first proposed in 1937 by Alam and Smirk, who demonstrated that arresting the circulation from working muscle in humans, causes maintained elevated arterial blood pressure. This would only take place when nerves formed the only communication between the working muscle and the rest of the body, due to circulatory arrest. Therefore, it was thought that the metabolic 'by-products' of muscle contraction were accumulating within the muscle on occlusion of blood flow, thereby allowing the stimulation of afferent fibres. Thus, the sustained increase in blood pressure was believed to be due to a reflex.

Coote *et al* (1971) provided direct evidence for the muscle pressor reflex using anaesthetised cats. They stimulated the ventral roots of the hind limb muscles to cause tetanic contractions, and observed an increase in arterial blood pressure with slight increases in heart rate and respiration. They were able to increase the pressor response by increasing the intensity of the stimulation. However, on sectioning of the dorsal roots of the hind limb muscle, ventral root stimulation failed to produce a pressor response. This suggested that the rise in blood pressure was the result of a reflex mechanism originating in the contracting muscles. Direct current anodal block can be used to preferentially block the large myelinated fibres of the dorsal roots receiving afferents from the working muscle – this does not abolish the pressor

response caused by ventral root stimulation (McCloskey and Mitchell, 1972). However, local anaesthetic block of the dorsal roots, which preferentially blocks small myelinated and unmyelinated fibres, does abolish the pressor response to ventral root stimulation (McCloskey and Mitchell, 1972). Therefore, the muscle pressor reflex is thought to be mediated by group III (small myelinated) and group IV (unmyelinated) afferent fibres, respectively stimulated by mechanical stretch and metabolic products (McCloskey and Mitchell, 1972; Kaufman *et al*, 1983).

The afferent pathways of the exercise pressor reflex have been studied extensively in animals. Both the rostral and caudal regions of the ventrolateral medulla have been implicated in modulating the reflex during exercise (Bauer *et al*, 1989; Ally, 1998). However, thus far, the involvement of higher central circuits has not been clearly defined.

It is clear that there is much left to be established regarding the organisation of the central pathways involved in mediating cardiovascular reflexes. Thus far, the majority of research has been focused on identifying the key medullary areas that mediate these reflexes; little is known about the involvement of supramedullary nuclei in the midbrain and of higher cortical areas, and their roles in driving cardiovascular function. The hypothalamus has been identified as a neural site that is important for the integration of the somatic and visceral components of the 'defence' response in rats (Abrahams *et al*, 1960). Other higher cortical areas have also been shown to have projections to cardiovascular control areas, and some even have functionally opposite pressor and depressor regions: for example, the prefrontal cortex (Bandler *et al*, 2000; Thornton *et al*, 2001), the primary motor cortex (along with the premotor and supplementary areas) (Fink *et al*, 1995; Thornton *et al*, 2001), the insular cortex (Hilton and Spyer, 1980; Oppenheimer *et al*, 1992; Williamson *et al*, 2001), the cingulate cortex (Burns and Wyss, 1985) and the thalamus (Risold *et al*, 1997). However, the focus of this thesis is the midbrain areas, particularly the periaqueductal grey (PAG) and the subthalamic nucleus (STN).

The Periaqueductal Grey

Anatomy

The midbrain periaqueductal grey (PAG) denotes a region of grey matter which surrounds the cerebral aqueduct along its entire length, from the levels of the posterior commissure and the rostral portion of the third nucleus all the way to the level of the dorsal tegmental nucleus (Behbehani, 1995). It is known to be organised into distinct longitudinal columns – there is debate as to how many columns there are, and whether these distinctions can be applied across all species (Beitz, 1985), although its overall boundaries vary little across mammals (Carrive, 1993). Nevertheless, it is accepted that the typical mammalian PAG can be subdivided into five columns in a radial manner – dorsomedial, dorsolateral, lateral, ventrolateral and ventromedial (Bandler *et al*, 1991) (Fig. 1.1). PAG neurons stain intensely for NADPH-diaphorase. Therefore, the boundaries of these columns can be revealed very clearly (Gonzalez-Hernandez *et al*, 1992; Herbert and Saper, 1992).

The columns of the PAG have both morphological and functional differences. For example, their sizes and shapes vary along the rostrocaudal axis: in both cats and rats, the dorsolateral PAG is well developed in the middle third, but is much smaller in the caudal third (Carrive, 1993). In addition, five different cell types have been identified within the PAG, and although all five types are present in each column, their distribution varies (Gioia *et al*, 1985). In humans, the periventricular grey (PVG) is situated rostrally compared to the PAG and is continuous with it. The PVG area is not functionally divided into the same columns as the PAG, but into a dorsal section and a ventral section (Green *et al*, 2005).

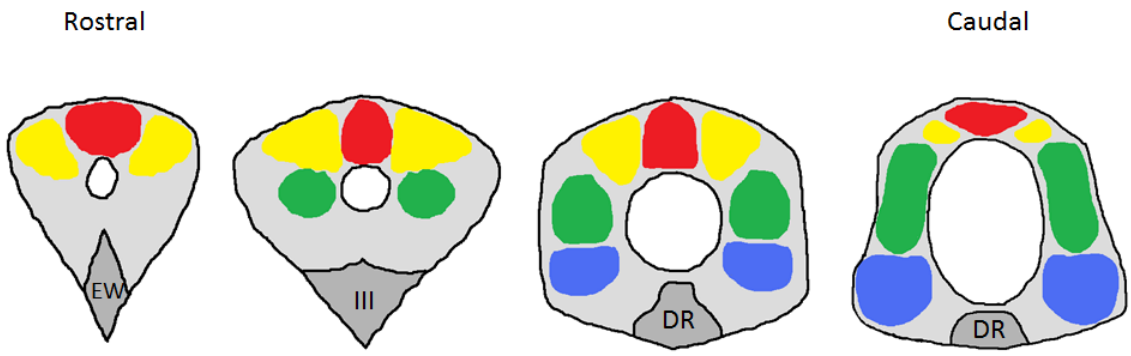

Figure 1.1 – *Schematic diagram showing four coronal slices of a typical mammalian PAG to demonstrate the columnar organisation: dorsomedial (red); dorsolateral (yellow); lateral (green); ventrolateral (blue). The ventromedial column is not shown as it is occupied by the Edinger-Westphal nucleus (EW), the occulomotor nucleus (III), and the dorsal raphe nucleus (DR).*

Local intrinsic projections between the columns of the PAG themselves have been demonstrated using anterograde axonal markers (Jansen *et al*, 1998). Each column was shown to project bilaterally to every other column. Each PAG column also receives afferent projections from a variety of other sites, including the prefrontal cortex (Bandler *et al*, 2000), the thalamus (Krout and Loewy, 2000), the anterior hypothalamus (Cameron *et al*, 1995), the rostral raphe (Marcinkiewicz *et al*, 1989), the amygdala (Rizvi *et al*, 1991), and even the spinal cord (Yezierski, 1988). The PAG projects efferents to sympathetic premotor neurons in a number of sites, including the hypothalamus, the pons and the medulla, which influence sympathetic outflow (Farkas *et al*, 1998). The PAG also sends efferents to vagal preganglionic neurons (Farkas *et al*, 1997). Beitz *et al* (1983) demonstrated projections from separate neuronal populations within the PAG to various brainstem nuclei, including the spinal trigeminal nucleus, the raphe magnus nucleus, the gigantocellular reticular nucleus pars alpha, and the paragigantocellular reticular nucleus.

Furthermore, the PAG has efferent connections (via the medulla) to the intermediate lateral cell column within the thoracolumbar spinal cord (Granata *et al*, 1985; Calaresu and Yardley,

1988). Carrive *et al* (1988) showed that in cats there is a direct projection from the PAG to the subretrofacial nucleus (SRF) of the rostral ventrolateral medulla (RVLM). Studies in the rat, based on electrolytic lesions in the RVLM (Lovick, 1985) have shown that this area serves as an important relay site, and a pathway has been described projecting directly from the PAG to the RVLM (Li and Lovick, 1985; Luiten *et al*, 1987; Van Bockstaele *et al*, 1989); more specifically from the lateral and ventrolateral columns (Beitz *et al*, 1983; Lovick, 1986; Luiten *et al*, 1987; Sun *et al*, 1988).

Role in Cardiovascular Function

Traditionally, the midbrain periaqueductal grey (PAG) is known to mediate a variety of different functions. It is thought to have a role in the control of motor function (Skultety, 1962), cardiorespiratory function (Abrahams *et al*, 1960; Ward and Darlington, 1987a; Ward and Darlington, 1987b; Ni *et al*, 1990), analgesia (Liebeskind *et al*, 1973; Yaksh *et al*, 1976), and vocalisation (Skultety, 1965; Jurgens and Pratt, 1979; Larson and Kistler, 1986). These functions can be triggered by stimulation of the PAG, as part of complex coordinated responses with parallel autonomic and somatomotor effects, for example the 'defence' reaction in animals (Abrahams *et al*, 1960). This reaction consists of two components: (1) the 'fight or flight' response in preparation for high intensity exercise, which involves increased blood pressure and heart rate, non-opioid-mediated analgesia, and emotional reactions including fear, (Hilton, 1982; Bandler and Carrive, 1988), and (2) a 'withdrawal' response, which involves decreased blood pressure and heart rate, opioid-mediated analgesia, immobility and sympathoinhibition (Liebman *et al*, 1973; Dennis *et al*, 1980; Zhang *et al*, 1990). Animals will often undergo this passive 'withdrawal' phase for recuperative purposes following an encounter involving active defensive behaviour, such as 'fight or flight';

alternatively, if escape from danger is impossible, the 'withdrawal' phase can be used to remain undetected, or to 'play dead' (Finnegan *et al*, 2005).

It has been demonstrated that activation of the dorsomedial, dorsolateral and lateral PAG columns produces the 'fight or flight' defence response, whereas activation of the ventrolateral PAG column evokes the 'withdrawal' defence response (Duggan and Morton, 1983; Lovick, 1985; Carrive and Bandler, 1991a). This strongly suggests that the PAG has a role in autonomic control of the cardiovascular system, particularly during periods of environmental stress. Other aspects of the 'defence' reaction include changes in rate and depth of respiration, changes in pupil size, exophthalmos, piloerection, micturition, and changes in skeletal blood flow (Hilton and Redfern, 1986; Yardley and Hilton, 1986; Carrive *et al*, 1987; Schenberg *et al*, 2005).

Carrive and Bandler (1991a) stimulated cell bodies in different PAG regions using microinjections of excitatory amino acids (EAAs). Different patterns of cardiovascular change were elicited depending on the exact location of the stimulation. A viscerotopic organisation was observed, in terms of the PAG's influence on vascular resistance in different vascular beds (Fig. 1.2). Stimulation of the lateral PAG column resulted in increased blood pressure. However, they found that stimulation of the rostral (or 'pretentorial') end of the lateral column caused an increase in blood pressure with accompanying skeletal muscle vasoconstriction and slight extracranial vasodilatation (with no significant change to renal vascular resistance). On the other hand, stimulation of the caudal (or 'subtentorial') end of the lateral PAG caused an increase in blood pressure, this time accompanied by extracranial and renal vasoconstriction with minor skeletal muscle vasodilatation. Stimulation with EEAs of the ventrolateral column of the PAG, on the other hand, can evoke depressor and vasodilator effects (Carrive and Bandler, 1991b). Stimulation of the rostral portion of this column is characterised by skeletal muscle vasodilatation accompanied by decreased blood pressure and

heart rate, whereas stimulation of the caudal part is characterised by renal vasodilatation accompanied by decreased blood pressure and heart rate (Carrive and Bandler, 1991b). These effects were demonstrated in both anaesthetised and unanaesthetised decerebrate cats, and also in unparalysed freely-moving cats (Goodchild *et al*, 1982). Therefore, although the rostral and caudal ends have opposite vasomotor effects, the viscerotopic representation of the vascular beds within each column is the same. The skeletal muscle vasculature is represented in the rostral region of both columns, whereas the renal vasculature is represented in the caudal regions.

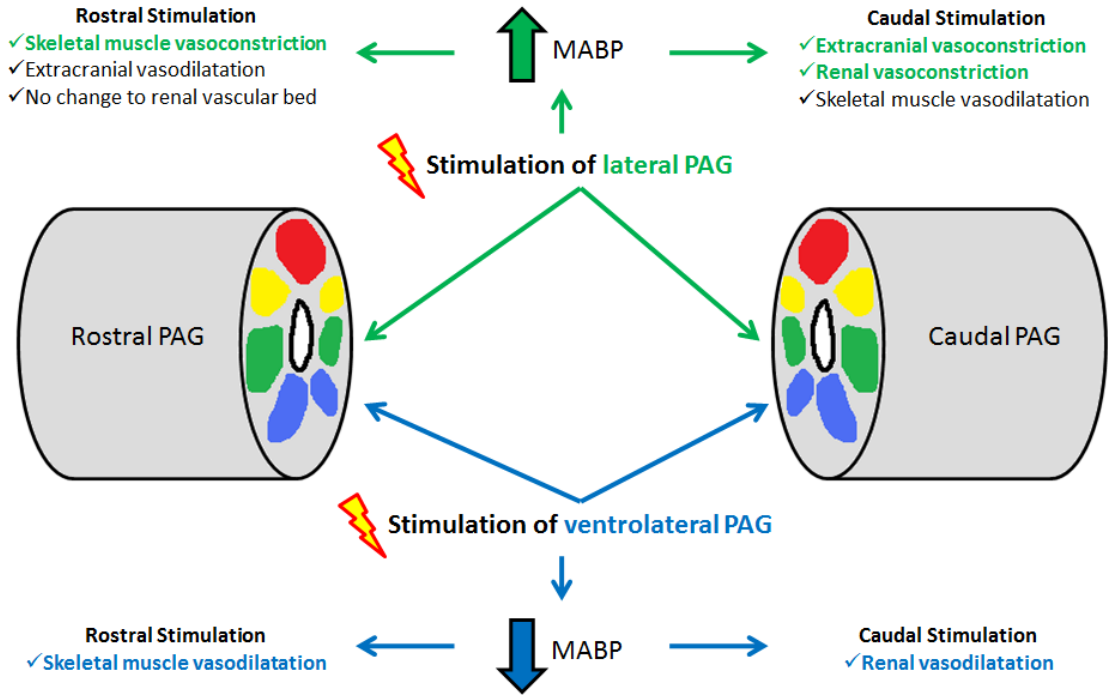

Figure 1.2 – *Schematic diagram showing viscerotopic organisation of PAG.*

It has been suggested that the PAG cardiovascular responses are most likely to be mediated by a relay pathway through the rostral ventolateral medulla (RVLM) pressor region, as opposed to a direct pathway from the PAG to the spinal cord, as lesions of the RVLM (both electrolytic and with kainic acid) reduce PAG-induced pressor responses (Verberne and Struyker Boudier, 1991). The presence of a direct pathway cannot be completely ruled out, as neither method

entirely abolishes the pressor responses elicited by consequent PAG stimulation. However, there is strong evidence to support the existence of a projection from the lateral and ventrolateral PAG to the RVLM (Beitz *et al*, 1983; Lovick, 1986; Luiten *et al*, 1987; Sun *et al*, 1988; Verberne and Struyker Boudier, 1991).

Neurons from both the rostral and caudal areas of the PAG are thought to project to an area of the RVLM called the subretrofacial (SRF) nucleus (Carrive *et al*, 1988; Carrive *et al*, 1989). There is evidence that this nucleus has an important role in the control of sympathetic vasomotor activity, as it consists of a large number of cardiovascular sympathetic premotor neurons (Dampney *et al*, 1985; Ciriello *et al*, 1986; McAllen and Dampney, 1990). The rostral PAG has been shown to project to the caudal SRF nucleus, while the caudal PAG projects to the rostral SRF nucleus (Carrive *et al*, 1989). This viscerotopic organisation of the two pathways is consistent with the separate patterns of vasomotor changes, as the caudal SRF preferentially modulates sympathetic vasoconstriction of the hind limb skeletal muscles, and the rostral SRF preferentially modulates sympathetic renal vasoconstriction (Lovick, 1987; Carrive *et al*, 1989; McAllen and Dampney, 1990). It is possible that the excitation of neurons in the lateral PAG (both in the rostral and caudal areas) evokes an increase in sympathetic vasomotor tone, and excitation of neurons in the ventrolateral PAG evokes a decrease in sympathetic vasomotor tone. Therefore, there could be both excitatory and inhibitory input from the PAG to the same subgroup of SRF neurons. For example, the rostral lateral PAG might have an excitatory input to the caudal SRF, whereas the rostral ventrolateral PAG might have an inhibitory input to the same neurons in the caudal SRF.

It has been suggested by Carrive and Bandler (1991b) that the PAG neurons from the ventrolateral PAG (both rostral and caudal areas) directly inhibit the pressor neurons within their respective SRF targets. However, other indirect pathways may also contribute. For example, it is well established that the PAG projects to the parabrachial pons and the nucleus

raphe magnus (Abols and Basbaum, 1981). In turn, the Kolliker-Fuse nucleus of the parabrachial pons projects to the SRF (Dampney *et al*, 1987), and is believed to have a role in cardiovascular function (McCall, 1984; Haselton *et al*, 1988a; Haselton *et al*, 1988b). However, it is unknown whether indirect pathways such as this are viscerotopically organised.

Studies in rats have shown that the neurons in the functionally different areas of the PAG elicit their respective cardiovascular responses via either excitation or inhibition of sympathetic premotor neurons in the RVLM (Lovick, 1992a; Lovick, 1992b). Electrical stimulation of the dorsal PAG in anaesthetised rats evokes increased blood pressure, tachycardia, hind limb vasodilatation and hyperpnoea. Lovick (1992a) demonstrated that microinjection of EAAs into the caudal portion of the ventrolateral PAG (at the level of the decussation of the superior cerebellar peduncle) significantly attenuated the magnitude of the cardiovascular response of the defence reaction evoked by electrical stimulation of the dorsal PAG. However, there was no effect on pressor responses evoked distally, for example, by electrical stimulation in the RVLM. Therefore, the activation of neurons in the caudal ventrolateral PAG seems to manipulate activity in the descending pathway of the dorsal PAG-evoked defence response. This suggests that neurons in the ventrolateral PAG have an inhibitory influence on the cardiovascular component of the defence response evoked by the dorsal/lateral PAG (the 'fight or flight' response). This inhibitory effect of the ventrolateral PAG could be a means of limiting active defensive responses and allowing the cardiovascular components of recuperative behaviour to prevail (Lovick, 1992a).

Further evidence for a role of the PAG in cardiovascular function is provided by the numerous connections which have been shown between the PAG and other brain areas associated with cardiovascular function (Fig. 1.3). For example, PAG neurons are known to project to cardiac vagal preganglionic neurons in the nucleus ambiguus, the dorsal motor nucleus of the vagus, and the nucleus of the solitary tract (Farkas *et al*, 1997). The PAG also has reciprocal

connections with 'higher' centres, including the hypothalamic nuclei, many of which manipulate blood pressure and heart rate (Pajolla *et al*, 2005; Martin *et al*, 2006; Horiuchi *et al*, 2009).

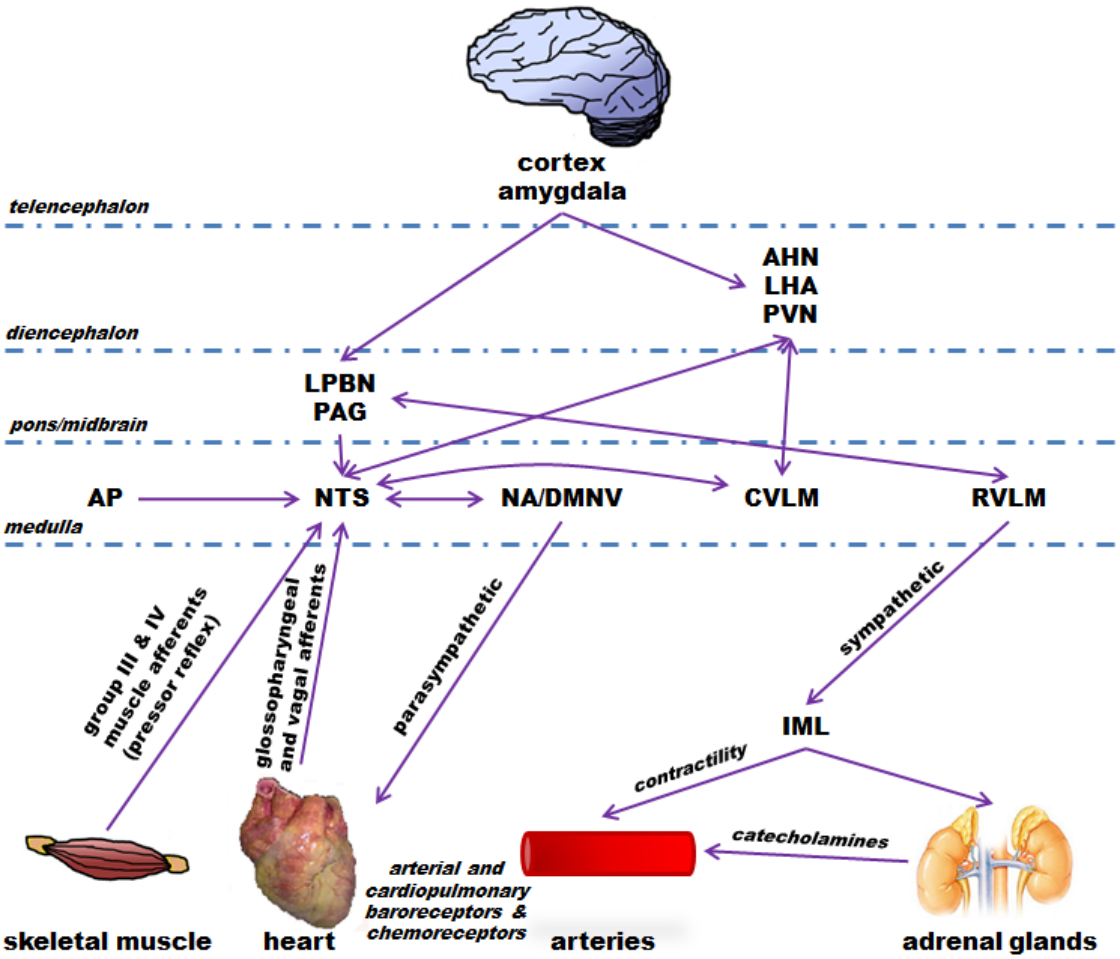

Figure 1.3 *– Diagram demonstrating numerous connections between PAG and other cardiovascularly active brain areas, and their visceral and somatic inputs and outputs. AHN, anterior hypothalamic nucleus; LHA, lateral hypothalamic nucleus; PVN, paraventricular nucleus of the hypothalamus; LPBN, lateral parabrachial nucleus; PAG, periaqueductal grey; NTS, nucleus of the solitary tract; CVLM, caudal ventrolateral medulla; RVLM, rostral ventrolateral medulla; NA, nucleus ambiguus, DMNV, dorsal motor nucleus of the vagus; AP, area postrema; IML, intermediolateral cell column. Modified from Green and Paterson (2008) – Experimental Physiology*

On top of the extensive animal data underpinning the role of the PAG in cardiovascular function, there is also evidence from awake humans. Green *et al* (2005) provided evidence

that the PAG is involved in the control of blood pressure by measuring the cardiovascular responses to electrical stimulation of the periventricular grey (PVG)/PAG in humans. A significant decrease in mean arterial blood pressure was observed upon stimulation of the ventral PVG/PAG and a significant increase in mean arterial blood pressure upon stimulation of the dorsal PVG/PAG. In addition, there were analogous changes in diastolic blood pressure, pulse pressure, and maximum d*P*/d*t*. However, there was no change in heart rate. This suggests that the cardiovascular responses are a result of altered myocardial contractility (shown by the changes in d*P*/d*t*) and altered total peripheral resistance (shown by the changes in pulse pressure). Therefore, the responses evoked by PAG stimulation are believed to be due to changes in sympathetic activity, with hardly any change in parasympathetic activity.

The Subthalamic Nucleus

Anatomy

The subthalamic nucleus (STN) is a small structure lying ventral to the zona incerta and dorsal to the cerebral peduncle. A densely neuronally-populated and highly vascularised structure, it consists of major myelinated fibre bundles. Therefore, it is regarded as a 'closed' nucleus, except for the medial border which is continuous with the lateral region of the hypothalamus (Parent and Hazrati, 1995). The STN is a central integrating component of the basal ganglia circuitry. The basal ganglia influence multiple aspects of cortical function via parallel cortico-basal ganglia-thalamocortical circuits (Benarroch, 2008). Each of these circuits originates from specific regions of the cerebral cortex, are then processed by the striatum, the globus pallidus and the substantia nigra pars reticulata (SNr), and finally project back to the input areas in the cortex via thalamic nuclei. The STN acts as a control site for these circuits (DeLong and Wichmann, 2007).

Traditionally, the STN is subdivided into three functional regions: the majority of the STN is comprised of the dorsolateral region which corresponds to motor function; the ventromedial region corresponds to associative behaviour; and the medial tip is associated with limbic function (Parent and Hazrati, 1995) (Fig. 1.4). Studies using anterograde tracers in the rat have shown that the majority of STN neurons are glutamatergic and provide excitatory input to the external globus pallidus (GPe), the internal globus pallidus (GPi), and the SNr (Kita and Kitai, 1987). The latter two nuclei act as output structures of the basal ganglia, and have a tonic inhibitory influence on the thalamic relay neurons and on other brainstem targets (Parent and Hazrati, 1995). The STN receives excitatory afferent projections from the cerebral cortex and inhibitory afferent projections from the GPe (Benarroch, 2008) (Fig. 1.4): the dorsolateral motor region receives somatotopic inputs from the primary motor cortex and projects to both the GPi and the GPe; the ventromedial associative region receives inputs from both the dorsolateral portion of the prefrontal cortex and the frontal eye fields, and projects to the SNr; and the medial limbic region receives inputs from medial portion of the prefrontal cortex and from the anterior cingulate cortex, and projects to the ventral pallidum. Despite the distinct inputs and outputs of the different STN regions, there is evidence of integration of information between the STN neurons themselves (Mallet *et al*, 2007).

The STN receives direct excitatory inputs from the centromedian nucleus and the parafascicular nucleus of the thalamus, both of which also project to the striatum and receive projections from the GPi and SNr (Benarroch, 2008). The STN has reciprocal connections with the pedunculopontine tegmental nucleus, which is another integral component of the basal ganglia circuits (Pahapill and Lozano, 2000; Mena-Segovia *et al*, 2004; Muthusamy *et al*, 2007), and with the dopaminergic neurons of the substantia nigra pars compacta (Francois *et al*, 2000; Grace *et al*, 2007).

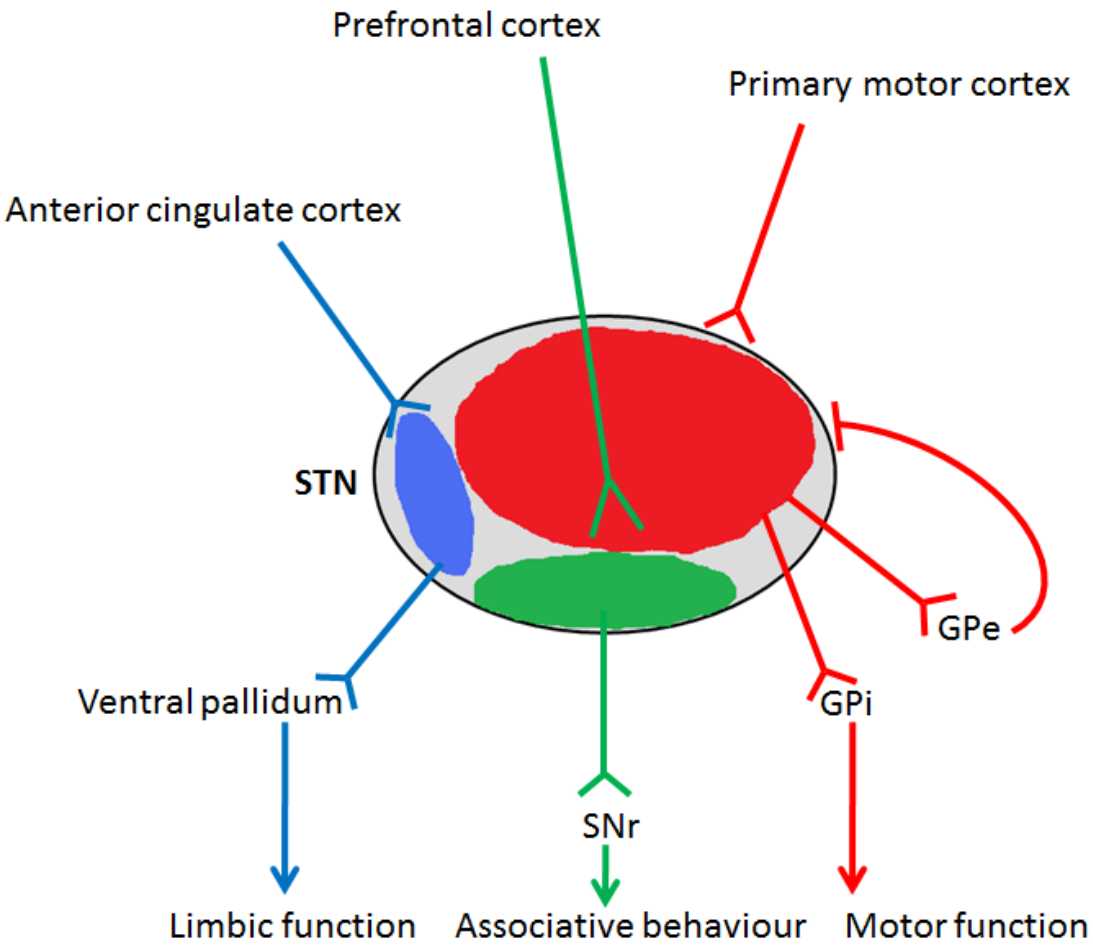

Figure 1.4 – *Schematic diagram showing the subdivisions of the STN: dorsolateral (red); ventromedial (green); medial (blue). STN, subthalamic nucleus; SNr, substantia nigra pars reticulata; GPi, internal globus pallidus; GPe, external globus pallidus.*

Role in Cardiovascular Function

It is well established that the basal ganglia (including the subthalamic nucleus [STN]) play a vital role in initiating somatomotor activity. However, the idea that the basal ganglia influence cardiovascular function has had relatively little experimental support. Classically, the STN has been thought of as a relay site of the 'indirect' pathway through which the striatum controls the basal ganglia output, thereby controlling motor function (DeLong and Wichmann, 2007) (Fig. 1.5). The striatum is thought to disinhibit the STN via inhibitory inputs to the external globus pallidus (GPe), thereby increasing internal globus pallidus (GPi) and substantia nigra

pars reticulata (SNr) activity. Therefore, this pathway inhibits motor function that could impede the execution of selected motor programs activated by the 'direct' striatal pathway to the GPi and SNr (Benarroch, 2008). In addition, there is much experimental evidence that demonstrates the STN having a role within complex neural networks, not only controlling motor function, but also emotion, cognition and thalamocortical excitability.

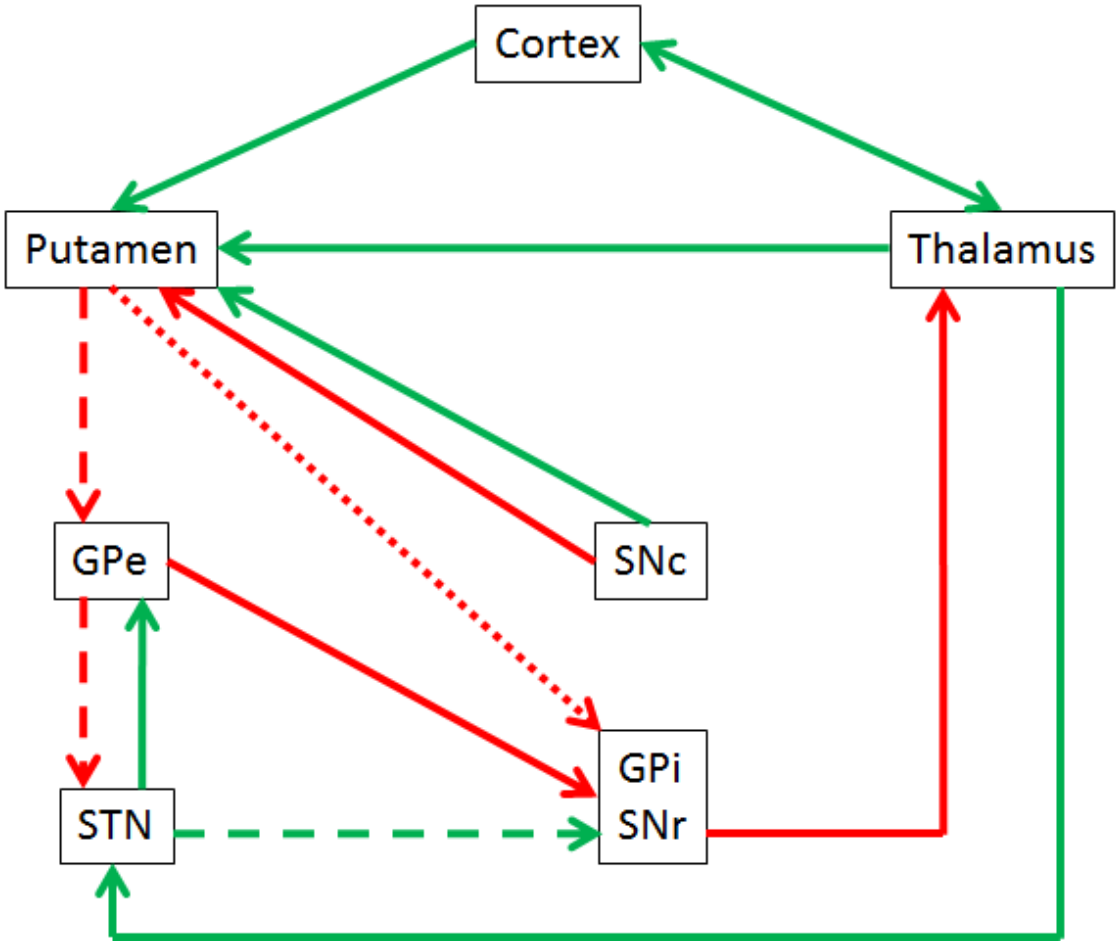

Figure 1.5 – *Circuit diagram showing intrinsic connections of the motor control circuit, including the 'direct' (dotted line) and 'indirect' (dashed lines) pathways. Excitatory (glutamatergic) connections are shown in green and inhibitory (GABA-ergic) connections are shown in red. GPe, external globus pallidus; SNc, substantia nigra pars compacta; STN, subthalamic nucleus; GPi, internal globus pallidus; SNr, substantia nigra pars reticulata.*

The STN can also be considered a cardiovascularly active area, as there is evidence for its involvement in the parallel activation of the cardiorespiratory system and the locomotor

system. Electrical stimulation of the STN in both freely moving and anaesthetised cats elicits a significant increase in arterial blood pressure, heart rate, and respiratory rate (e.g. Angyan and Angyan, 1999b). STN stimulation causes significant cardiorespiratory changes in anaesthetised cats, despite the absence of visible somatomotor activity, suggesting that the STN is directly involved in adjusting cardiorespiratory function, and that the cardiovascular responses to STN stimulation are not secondary to electrically elicited movement.

The above study implicates the STN itself in the control of cardiovascular function, but there have been numerous studies examining the entire subthalamic area, including the subthalamic locomotor region which lies in the area of the lateral hypothalamus that merges with the medial border of the STN. Smith *et al* (1960) demonstrated in dogs that electrical stimulation of the H_2 fields of Forel (which includes the dorsal region of the STN) evokes cardiovascular responses similar to those which result from volitional exercise. Eldridge *et al* (1981) stimulated the subthalamic locomotor region in unanaesthetised decorticate cats and suggested that this area drives both cardiovascular and locomotor activity. Moreover, c-Fos expression has been used to identify brainstem sites active during dynamic treadmill exercise in conscious rats (Iwamoto *et al*, 1996), further implicating the subthalamic locomotor region as having a role in the integration of the cardiovascular response to exercise.

Studies have been performed involving high frequency stimulation of the STN in humans (Kaufmann *et al,* 2002; Thornton *et al*, 2002; Benedetti *et al*, 2004), in which stimulation evoked increased heart rate and facilitation of movement. Only in the Thornton *et al* (2002) experiments did mean arterial blood pressure increase during stimulation of the STN in all patients; in the other studies, blood pressure changes were either not significant, or not consistent in the direction of change. Thornton *et al* (2002) also observed that heart rate, mean arterial blood pressure and facilitation of movement all increased upon stimulation of the thalamus and the substantia nigra. Stimulation of the GPi had no effect on cardiovascular

parameters, but did facilitate movement. Benedetti *et al* (2004) stimulated the different subdivisions of the STN, and observed that stimulation of the dorsal area (including the zona incerta) induced constant increases in heart rate, regardless of experimental conditions, whereas stimulation of the ventral area (including the adjacent SNr) elicited increases in heart rate which varied according to experimental conditions. These results suggested that the dorsal STN is involved in cardiovascular and autonomic control, whereas the ventral STN is likely to be involved in associative or limbic-related autonomic activity.

Other Nuclei

Apart from the periaqueductal grey (PAG) and the subthalamic nucleus (STN), several other brain nuclei have been investigated in order to understand their roles in mediating cardiovascular function during exercise, including the globus pallidus interna (GPi), the sensory thalamus, the posterior hypothalamus, and the anterior cingulate cortex.

There is some animal evidence for the GPi having a role in integrating cardiorespiratory function with somatomotor function. Electrical stimulation of the GPi in freely moving cats results in a complex sequence of cardiovascular changes (Angyan and Angyan, 1999a). Arterial blood pressure increases with pulse pressure, initially decreasing, and then increasing within 2-3 seconds. Heart rate, on the other hand, decreases. However, in humans, experimental evidence has shown no change in cardiovascular parameters on electrical stimulation of the GPi (Thornton *et al*, 2002), although stimulation did result in facilitation of movement and improved motor activity. Green *et al* (2007) reported increased activity in the GPi during exercise, which is consistent with studies by Chang *et al* (2006) in the rat, showing increased firing rates during locomotion. These changes in activity are believed to be behavioural context-dependent changes, related to locomotion. Critchley *et al* (2001) performed PET studies to show increased cerebral blood flow within the GPi which was associated with the

intent to relax. This is consistent with the idea that the GPi supplies the major inhibitory output of the basal ganglia.

The thalamus was implicated as having a role in cardiovascular control as far back as the late 19th century, when Ott (1891) performed lesioning studies in anaesthetised rabbits. In humans, the sensory thalamus has also been associated with the generation and processing of angina (Lenz *et al*, 1994; Rosen *et al*, 1996). Oppenheimer *et al* (1998) used extracellular recording techniques to evaluate human thalamic cells for phasic cardiovascular activity, and found clusters of cardiovascularly active cells within the ventrocaudal nucleus (the main sensory nucleus of the thalamus). They suggested that this nucleus could be involved in the integration of the baroreceptor reflex. It has also been observed that stimulation of the sensory thalamus evokes an increase in both heart rate and arterial blood pressure (Thornton *et al*, 2002).

Electrical stimulation of multiple sites within the hypothalamus of the conscious cat elicits skeletal muscle vasodilatation, along with increased arterial blood pressure, increased cardiac output and increased heart rate (Abrahams *et al*, 1960). These cardiovascular changes occur as part of the 'defence reaction', as they are accompanied by vasoconstriction in the skin and viscera, pupil dilation, piloerection, and retraction of the nictitating membrane. Tan and Dampney (1983) stimulated these sites in anaesthetised rabbits using glutamate ions (which excite nerve cell bodies selectively, as opposed to their axons of passage) and found the vasodilator response was confined to far more restricted regions, for example the ventromedial nucleus of the hypothalamus. Their results suggested that cell bodies within the ventromedial nucleus are capable of inducing skeletal muscle vasodilatation. Other hypothalamic nuclei have also been implicated in rat studies including the medial preoptic area, the periventricular nucleus, the suprachiasmatic nucleus, the supraoptic nucleus, the paraventricular nucleus, the anterior hypothalamic area, the arcuate nucleus and the posterior

hypothalamic nucleus (Coote, 1995; Ichiyama *et al*, 2002; Soya *et al*, 2007). Moreover, there is abundant evidence for a role of the hypothalamus in cardiovascular control in humans, not only during defensive behaviour but also specifically during dynamic exercise (Hilton, 1966; Dampney *et al*, 2008).

Burns and Wyss (1985) investigated the cardiovascular effects of electrical stimulation of the anterior cingulate cortex in both anaesthetised and non-anaesthetised rats. They observed that in anaesthetised rats, there was a consistent depressor response upon stimulation, with no change in heart rate. In awake rats, stimulation resulted in opposite blood pressure responses dependent on the rostrocaudal location of the stimulation. Stimulation in the rostral area resulted in a pressor response, and stimulation in the caudal area resulted in a depressor response. More recently in humans, positron emission tomography and functional magnetic resonance imaging data have shown that the anterior cingulate is part of a vital network that is essential for regulating the central autonomic nervous system (Nagai *et al*, 2010).

Aims

The introduction of functional neurosurgery, in which deep brain stimulating electrodes are implanted into various brain nuclei for the treatment of chronic pain and movement disorders, has given us the unique opportunity to investigate these nuclei in terms of their potential roles in integrating cardiovascular function in humans. This technique not only allows us to stimulate these regions of the brain and observe the cardiovascular effects, but also gives us the opportunity to record the activity of different nuclei during a range of experiments designed to separate the different control systems of exercise, including central command and the exercise pressor reflex.

The aims of this thesis (Fig. 1.6) were three-fold:

(1) To investigate the cardiovascular neurocircuitry involved in the exercise pressor reflex;

(2) To investigate the cardiovascular neurocircuitry involved in central command;

(3) To determine the efferent cardiovascular effects of each of these control systems.

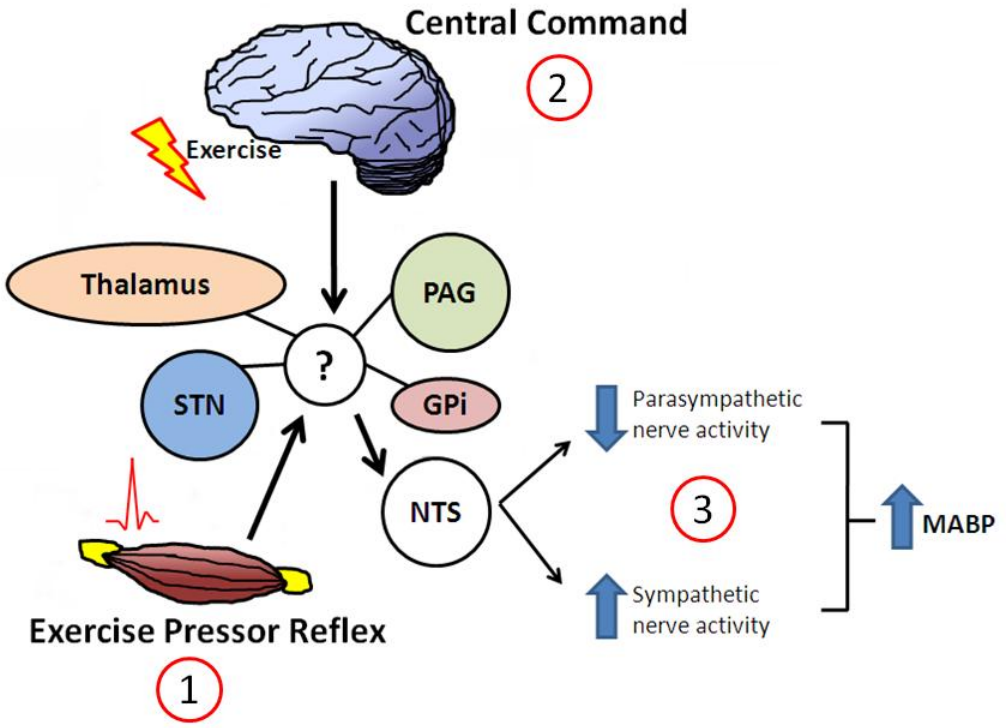

Figure 1.6 – *Diagram to illustrate the aims of this thesis: (1) To investigate the cardiovascular neurocircuitry involved in the exercise pressor reflex; (2) To investigate the cardiovascular neurocircuitry involved in central command; (3) To determine the efferent cardiovascular effects of each of these control systems. PAG, periaqueductal grey; STN, subthalamic nucleus; GPi, internal globus pallidus; NTS, nucleus of the solitary tract; MABP, mean arterial blood pressure.*

CHAPTER 2

General Methods

History of Deep Brain Stimulation

Certain features of the deep brain stimulation (DBS) procedure, such as its adaptability, reversibility, the fact that it is non-ablative, and its potential for conducting in vivo research, have attracted the interest of neurosurgeons and researchers alike. It is considered to be one of the most important and most rapidly expanding functional neurosurgical therapies to date (Schwalb and Hamani, 2008).

The advent of modern day DBS began with the development of the stereotactic frame in 1947 (Spiegel *et al*, 1947), followed by a surge of stereotactic functional neurosurgery in the 1950s, which included thalamotomy and pallidotomy for the treatment of Parkinson's disease and dystonia (Tasker, 2004). Originally, stimulation was used to identify optimal lesioning sites, although temporary electrodes were successfully being implanted into various sites in the brain for pain control. However, in the early 1970s, Bechtereva suggested using subcortical stimulation as a 'permanent' therapy (Hariz *et al*, 2010), and chronic DBS systems were introduced for implantation into both the thalamus and the periventricular/periaqueductal grey in order to treat chronic pain (Hosobuchi *et al*, 1973; Richardson and Akil, 1977a; Richardson and Akil, 1977b). The success rate of DBS as a treatment for chronic pain is somewhat variable, with some studies showing an effective response in as few as 25% of patients (Awan *et al*, 2009). In the 1990s, groups were reporting on thalamic DBS for the treatment of tremor, and the procedure was shown to be much safer than thalamotomy (Benabid *et al*, 1991). At the same time, it was discovered that either lesions or high frequency stimulation (which was believed to mimic the effects of surgical lesioning) of the subthalamic nucleus in 1-methyl-4-phenyl-1,2,3,6-tetrahyrdopyridine monkeys (primate models of

Parkinson's disease) could improve the symptoms of tremor, rigidity and bradykinesia (Bergman *et al*, 1990; Aziz *et al*, 1991; Benazzouz *et al*, 1993). In addition, DBS of the internal globus pallidus was introduced as a treatment for generalised dystonia (Gross *et al*, 1997; Pahwa *et al*, 1997).

In more recent years, a variety of new targets have been explored for the treatment of conditions that were previously thought to be out of the realm of neurosurgical therapy. For example, the hypothalamus has been identified as an effective target for treating cluster headaches (Franzini *et al*, 2003). Stimulation of the pedunculopontine nucleus has been introduced as a successful target for treating postural instability and gait in Parkinson's disease (Mazzone *et al*, 2005; Plaha and Gill, 2005). Psychiatric disorders, such as Tourette syndrome, obsessive-compulsive disorder and depression, can now also be treated with DBS (Kopell and Greenberg, 2008; Gubellini *et al*, 2009).

The underlying principles and neural mechanisms of DBS are still not fully understood. Original attempts to explain its mechanisms concentrated on the hypothesis that DBS mimics ablative lesioning. However, it was later believed that high frequency stimulation was likely to inhibit neural activity and low frequency stimulation was likely to drive it (Green and Paterson, 2008). There are many hypotheses as to the mechanism of inhibition of high frequency stimulation, including depolarisation blockade, synaptic inhibition, and synaptic depression (McIntyre *et al*, 2004). More recent efforts have investigated the broader changes in neural activity that are generated throughout the brain network being stimulated (McIntyre and Hahn, 2010). It is now believed that DBS is most likely to work by restoring normal oscillatory activity within a network of major neural sites (Kringelbach *et al*, 2010). The stimulation settings of therapeutic benefit have mostly been determined through trial and error, by observing the effects in patients on the operating table (Volkmann *et al*, 2002). The exact stimulation parameters vary depending on the targeted brain region; normally, amplitude is between 1 V and 9 V, pulse

width is between 60 µs and 240 µs, and frequency is either high (130-180 Hz) or low (5-50 Hz) (Kuncel and Grill, 2004).

The DBS system comprises either one or two quadripolar electrodes which are implanted in the brain, extension leads which run behind the ear, and an implantable pulse generator (IPG) which is implanted subcutaneously in the chest wall (Fig. 2.1). The IPG acts as both a power source and a device for modulating the stimulation parameters. It can be programmed transcutaneously by telemetry, and the patients are given a controller which allows them to turn the stimulation on and off, and also to vary the voltage of the stimulation.

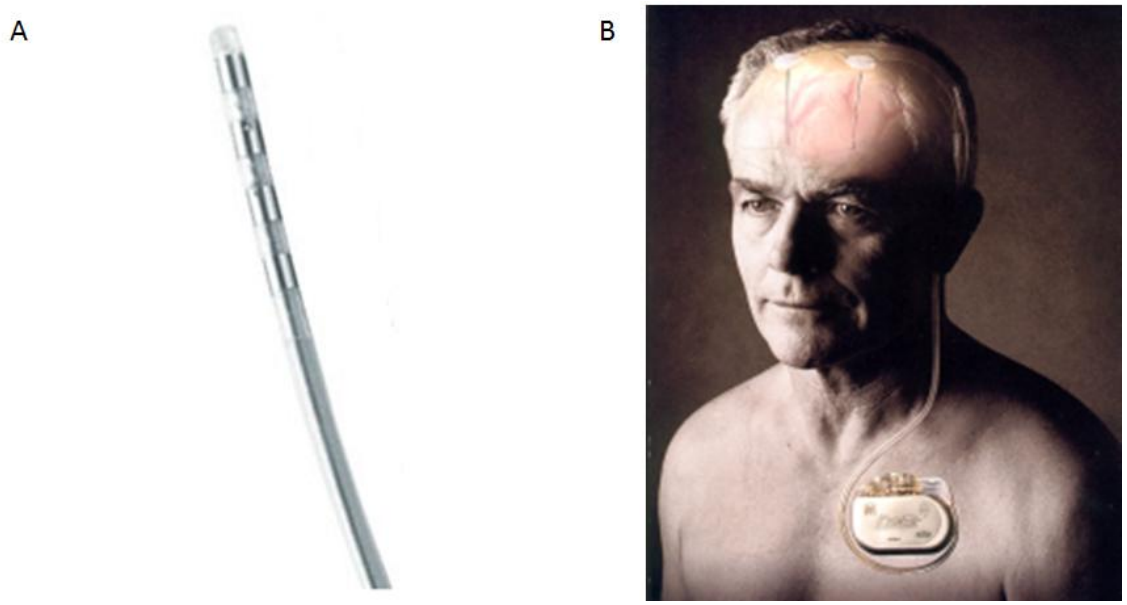

Figure 2.1 – *(A) Model 3387 DBS lead (Medtronic, Minneapolis, MN) consisting of four 1.5 mm wide circumferential contacts spaced at 1.5 mm apart. (B) Picture showing tunnelling of extension leads from the electrodes in the brain to the implantable pulse generator located subcutaneously in the chest wall. Used with permission from AL Green.*

DBS patients can provide us with a unique insight into the neurocircuitry underpinning cardiovascular control in humans, via two aspects: (1) there is a week-long postoperative period before the electrodes are connected to the IPG, during which they are externalised and can thus be used to record neural activity (in terms of local field potentials) from their target

nuclei, and (2) the electrodes can be used to stimulate the nuclei in which they are implanted to investigate what effects they have on cardiovascular parameters.

Subjects

Informed consent to take part in the following studies was obtained from every patient. Each of the experiments was approved by the local hospital ethics committee (Oxfordshire REC C: 05/Q1605/47), and the study conformed to the Declaration of Helsinki.

Owing to the clinical and therapeutic benefits of deep brain stimulation, I was presented with a wide range of target nuclei to study. Patients had electrodes implanted in the periaqueductal grey for the treatment of chronic pain. Electrodes were implanted in the sensory thalamus, also for the treatment of chronic pain, either in the ventroposterolateral or ventroposteromedial nucleus for the treatment of limb pain or facial pain, respectively. Electrodes in the subthalamic nucleus were for the treatment of Parkinson's disease. Electrodes in the inferior posterior hypothalamus were for the treatment of cluster headaches. Patients had electrodes in the internal globus pallidus for the treatment of generalised dystonia, and in the anterior cingulate cortex for the treatment of chronic pain.

Surgical Procedure

The deep brain stimulation (DBS) surgical procedure consists of two stages. Stage 1 involves identifying the target site, placing the stimulating electrode(s), and determining effective stimulation parameters (Bittar *et al*, 2005). An axial magnetic resonance image (MRI) brain scan of the subject's brain is taken preoperatively, with a slice thickness of 2.0 mm. Using Radionics Image Fusion™ and Stereoplan™ software (Radionics, Burlington, MA, USA) (Papanastassiou *et al*, 1998), the MRI is fused to a computed tomography (CT) scan of 1.9 mm

slice thickness and zero gantry tilt, which is obtained on the day of surgery whilst the subject has the Cosman-Roberts-Wells™ stereotactic frame applied to their scalp, under local anaesthetic. This allows the benefit of both the excellent geometric accuracy of CT and the superior tissue definition of MRI. Using the fused image, the target site and electrode trajectory can be mapped (Fig. 2.2). The avoidance of the surface vessels on the cortex and the ventricles can lead to some inter-patient variability in electrode placement (Fig. 2.3). Ultimately, the position of the electrode is decided intra-operatively, based on the therapeutic response to stimulation.

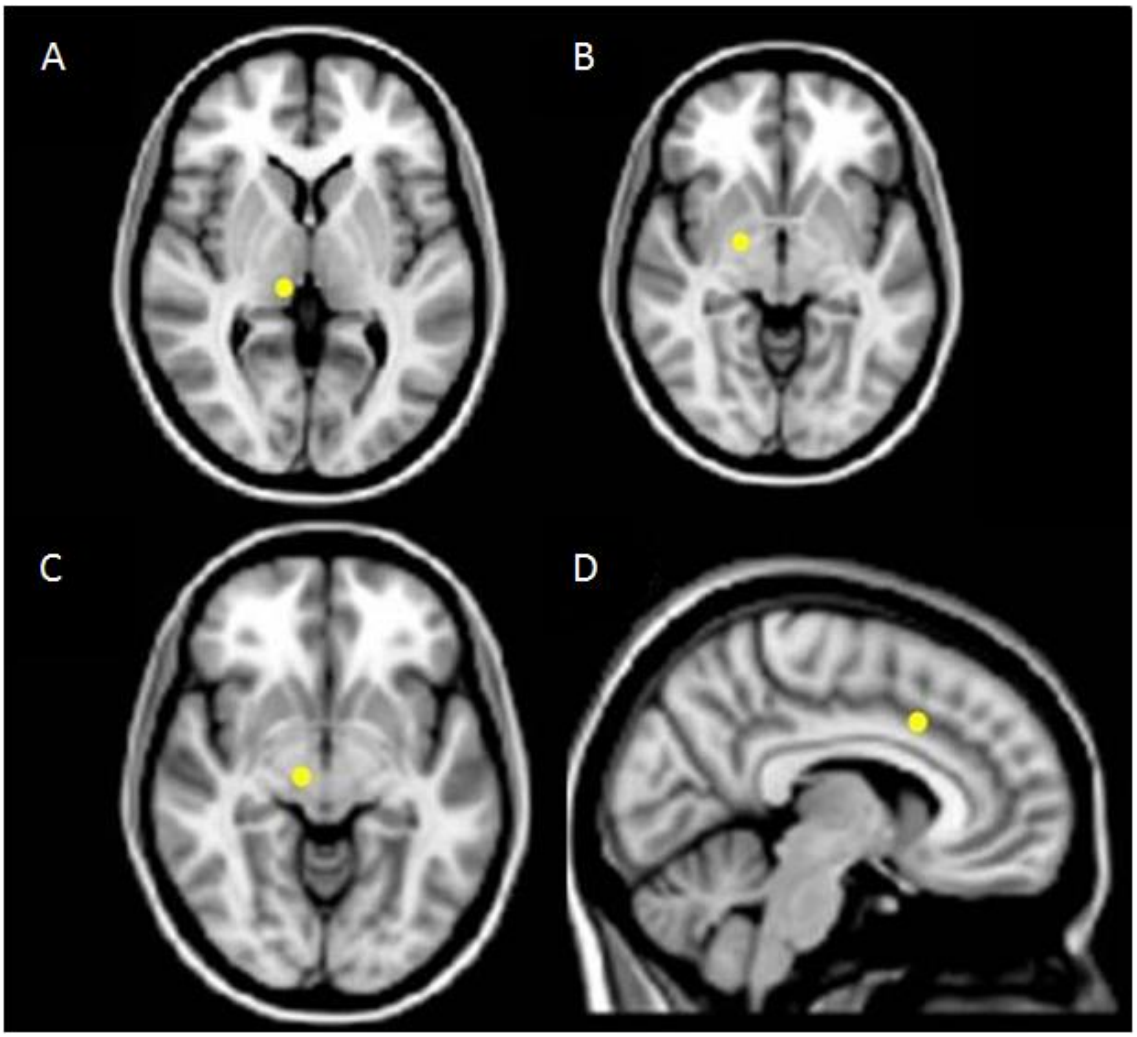

Figure 2.2 *– Post-operative images (post-operative CT scans fused to pre-operative MRI scans) showing target sites for electrodes being implanted in (A) the ventroposterolateral nucleus of the sensory thalamus, (B) the internal globus pallidus, (C) the subthalamic nucleus, and (D) the anterior cingulate cortex.*

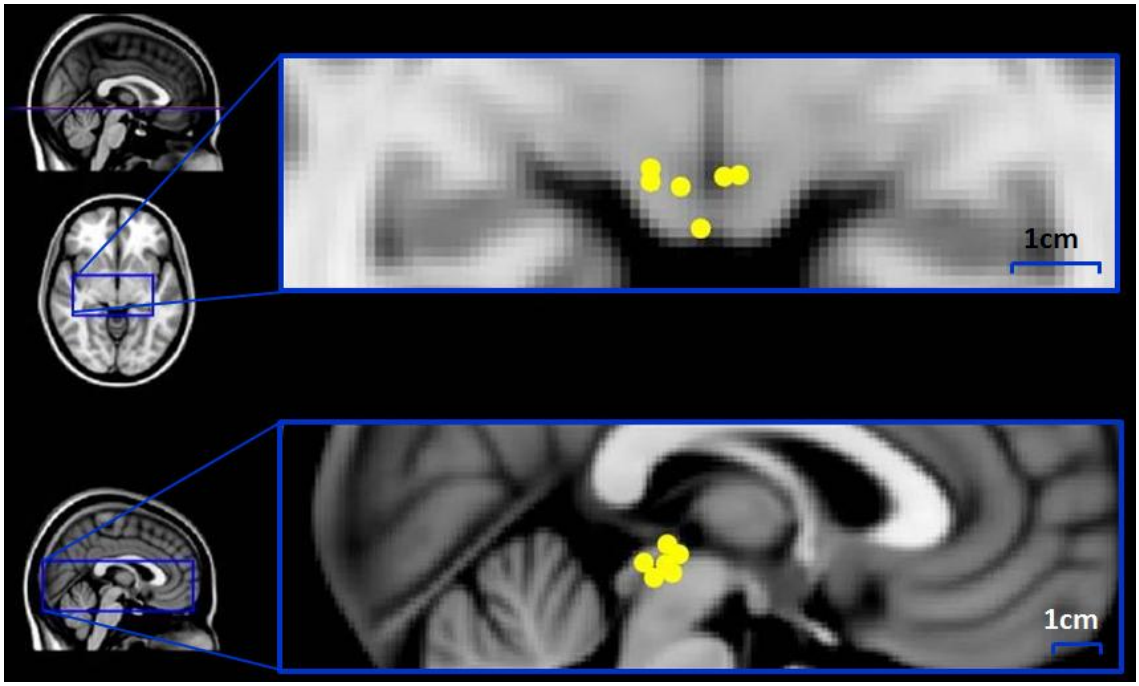

Figure 2.3 – *Post-operative image showing individual electrode locations in the transverse and sagittal planes for six periaqueductal grey patients to give an idea of inter-patient variability in electrode placement. Both scale bars represent 1 cm. Yellow dots represent the midpoints of each electrode.*

The subject's scalp is prepared with cetrimide and alcoholic chlorhexidine solution, and then injected with 20 ml of local anaesthetic. A curved incision is made over the coronal suture, followed by a 2.7 mm twist-drill craniostomy through the skull and dura (Fig. 2.4). A 1.8 mm diameter electrode with a 2.0 mm exposed tip (Radionics, Burlington, MA, USA) is then passed to the target. This electrode is replaced with a Medtronic 3387 electrode (Medtronic, Minneapolis, MN, USA), comprising of four 1.5 mm cylindrical contacts spaced 1.5 mm apart (Fig. 2.1A). At this point, intra-operative bipolar stimulation is carried out to establish the final position of the electrode. Stimulation is started 5 mm proximal to the target, after which the electrode is moved 2 mm at a time towards the target, until the best position is determined. Correct electrode location is identified in the periaqueductal grey/periventricular grey when analgesia is elicited by stimulation, accompanied by feelings of warmth and relaxation (Bittar *et al*, 2005). Correct positioning in the sensory thalamus is indicated by the induction of

paraesthesia in the area affected by chronic pain (Turnbull *et al*, 1980; Levy *et al*, 1987). Suppression of rigidity and bradykinesia is used as a guide for positioning subthalamic nucleus electrodes (Limousin *et al*, 1995). However, with the internal globus pallidus and the hypothalamus, therapeutic effects are not seen immediately upon stimulation (Gross *et al*, 1997; Vitek *et al*, 1998; Franzini *et al*, 2003). Therefore, when targeting these sites, the procedure is done under general anaesthetic.

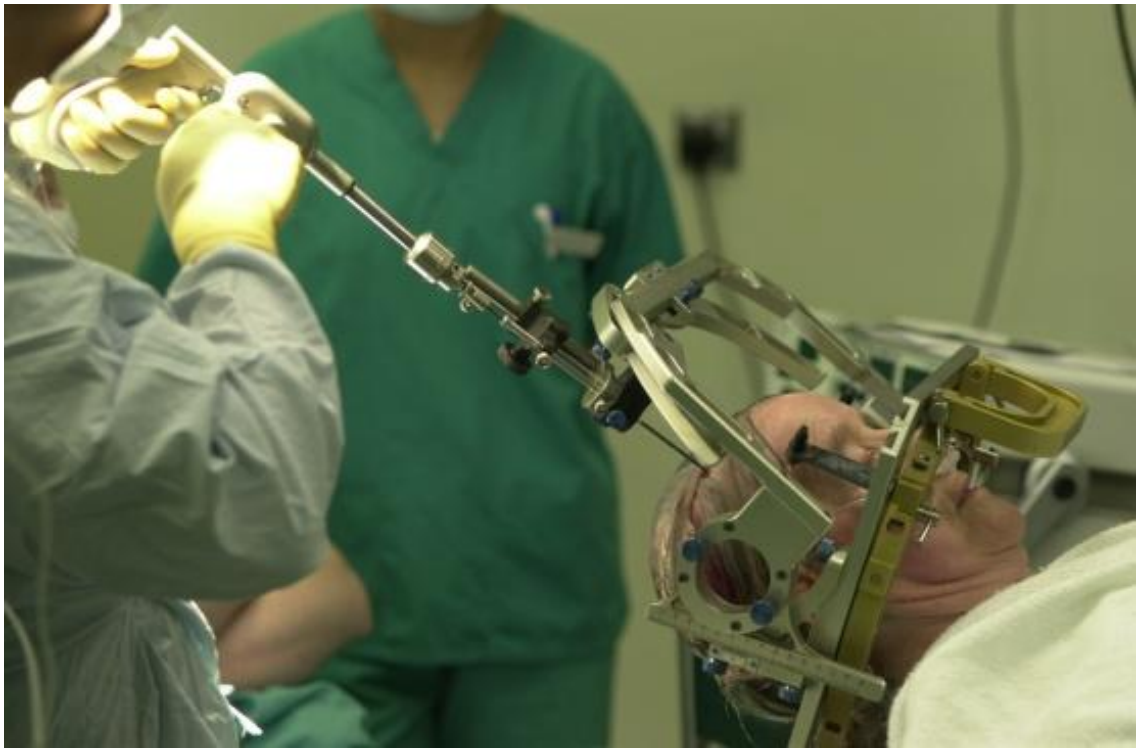

Figure 2.4 *– Photograph showing stage 1 of the deep brain stimulation surgical procedure involving the placement of the stimulating electrode via a 2.7 mm twist-drill craniostomy.*

Once in the correct position, the electrode is fixed onto the subject's skull with a titanium bioplate™ and connected to an external stimulator. The wounds can then be sutured. The electrodes are externalised for a week-long period of testing, in order to determine the optimal stimulation parameters. During this week, the electrodes can also be used to record neural activity from the target site. If the patient experiences good therapeutic benefit during the externalised period, the whole stimulation system can be internalised during stage 2 of the

DBS procedure. This happens under general anaesthetic and involves insertion of Medtronic extension leads and a Kinetra™ implantable pulse generator (Medtronic, Minneapolis, MN, USA), which is positioned in a subcutaneous pocket in the chest wall (Fig. 2.1B).

The experiments in Chapters 3, 4 and 5 took place during the week between stage 1 and stage 2 of the DBS procedure, whereas the experiments in Chapter 6 were conducted at any time after stage 1.

Experimental Measurements

Non-invasive continuous finger arterial blood pressure was measured with a Portapres (Finapres Medical Systems, Amsterdam, The Netherlands) (Fig. 2.5). The Portapres provides measurements based on the arterial volume-clamp method of Penaz and the physical criteria of Wesseling for the proper unloading of the finger arteries (Eckert and Horstkotte, 2002). The total finger arterial volume is measured (with an infrared plethysmograph built in to a finger cuff) when the 'internal pressure', i.e. the arterial pressure, equals the external pressure. Therefore, transmural pressure is zero and the artery wall is 'unloaded'. The artery is then 'volume-clamped' by continuous modulation of external pressure by the cuff, in parallel with the internal pressure; thus, the external pressure is constantly equal to the internal pressure and so can be recorded as a blood pressure waveform. The Portapres has a height correction unit to account for the hydrostatic height difference between the level of the heart and the level of the finger (Castiglioni *et al*, 1999). This consists of a tube filled with liquid, with a compliant plastic bag at the end attached to the finger cuff, and with a semiconductor pressure transducer fixed at heart-level. The transducer signal is added to the finger pressure signal in order to correct for any height difference. The final pressure signal was digitised at 4 kHz with 16-bit resolution (CED 1401 Mark II, Cambridge Electronic Design, Cambridge, UK) using Spike II software (version 6.0, Cambridge Electronic Design, Cambridge, UK).

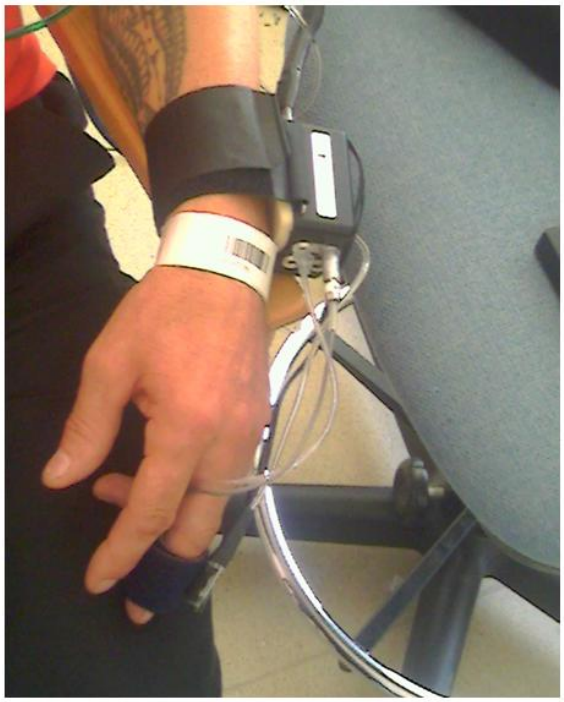

Figure 2.5 *– Photograph showing the Portapres (Finapres Medical Systems, Amsterdam, The Netherlands) in use.*

The Portapres has proved to be a valid method of measuring arterial blood pressure in deep brain stimulation patients. Green *et al* (2005) used this method to measure the arterial blood pressure changes in awake patients implanted with periventricular grey/periaqueductal grey electrodes, with the stimulation turned both on and off (Fig. 2.6).

R-R interval and heart rate were calculated from lead II electrocardiograms, which were recorded using disposable adhesive Ag/AgCl electrodes (H207PT, Kendall-LTP, MA, USA), amplified x1,000 (CED 1902, Cambridge Electronic Design, Cambridge, UK), and digitised using the same parameters that were used for blood pressure.

In Chapters 3, 4 and 5, local field potentials were recorded with bipolar configuration from the adjacent four circumferential contacts of each deep brain stimulating electrode. Data were only analysed from those contacts in which stimulation provided therapeutic benefit and relief from the symptoms of each subject; thus, increasing the likelihood that the neural activity

recorded was from the targeted site, and not the surrounding area. Signals were filtered at 0.5-500 Hz and amplified x10,000 (CED 1902, Cambridge Electronic Design, Cambridge, UK) and digitised at a rate of 4 kHz (CED 1401 Mark II, Cambridge Electronic Design, Cambridge, UK). The LFPs were displayed online and saved onto hard disk using Spike II (version 6.0, Cambridge Electronic Design, Cambridge, UK) (Fig. 2.7).

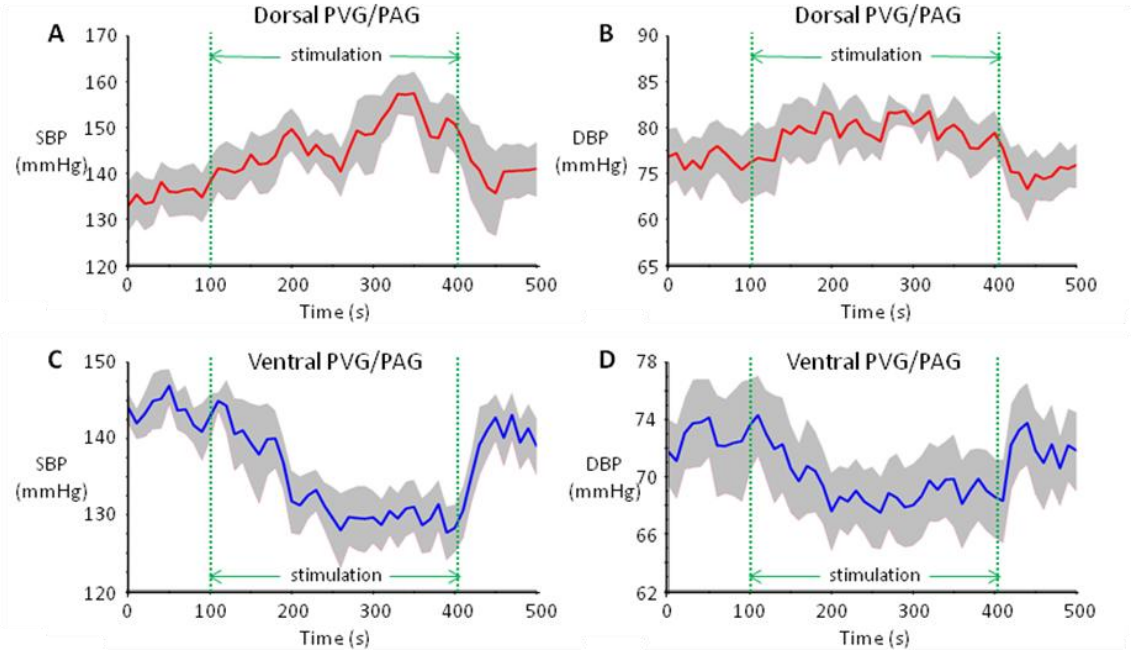

Figure 2.6 *– Arterial blood pressure response to periventricular grey/periaqueductal grey (PVG/PAG) stimulation measured with a Portapres (Finapres Medical Systems, Amsterdam, The Netherlands). (A & B) Mean changes in systolic blood pressure (SBP) and diastolic blood pressure (DBP) for six patients who had increased arterial blood pressure on stimulation of the dorsal PVG/PAG. (C & D) Mean changes in SBP and DBP for seven patients who had a reduction in arterial blood pressure on stimulation of the ventral PVG/PAG. [Grey area denotes ± 1 S.E.M.] Data re-drawn from Green et al (2005) – Neuroreport*

In Chapter 6, multi-unit efferent postganglionic muscle sympathetic nerve activity (MSNA) was recorded using an insulated tungsten microelectrode, with an uninsulated tip (1-5 µm diameter) (Vallbo *et al*, 1979) (Fig. 2.8). MSNA was recorded from the common peroneal nerve, which supplies the Peroneus longus and Peroneus brevis muscles which act to evert and plantar-flex the foot. The nerve was first located by palpation and transcutaneous

electrical stimulation with a custom-built 'pen' electrode. Once an appropriate site had been identified, the tungsten microelectrode was inserted posterior to the head of the fibula, into a muscle fascicle. A low-impedance reference electrode was then placed subcutaneously a few centimetres away from the recording electrode. When a muscle fascicle was entered, stimulation would produce fasciculations within the muscle. When recording from a muscle fascicle, pronounced activity could be induced by tapping against the muscle belly and by both passive joint movements and active contractions. There would be no response to slight tactile stimuli though, as that would have been indicative of a skin fascicle. Once the muscle fascicle was located, small adjustments were made in order to find a site where spontaneous pulse-synchronous sympathetic bursts could be recorded, with an adequate signal-to-noise ratio. It was important that the recorded bursts would increase during voluntary apnoea but would not respond to arousal stimuli. Neural activity was amplified (x50,000), filtered (bandpass, 0.7-2.0 kHz), and fed through a discriminator for audio-monitoring. The data were displayed online and saved onto hard disk using a computer-based data acquisition and analysis system (Fig. 2.9).

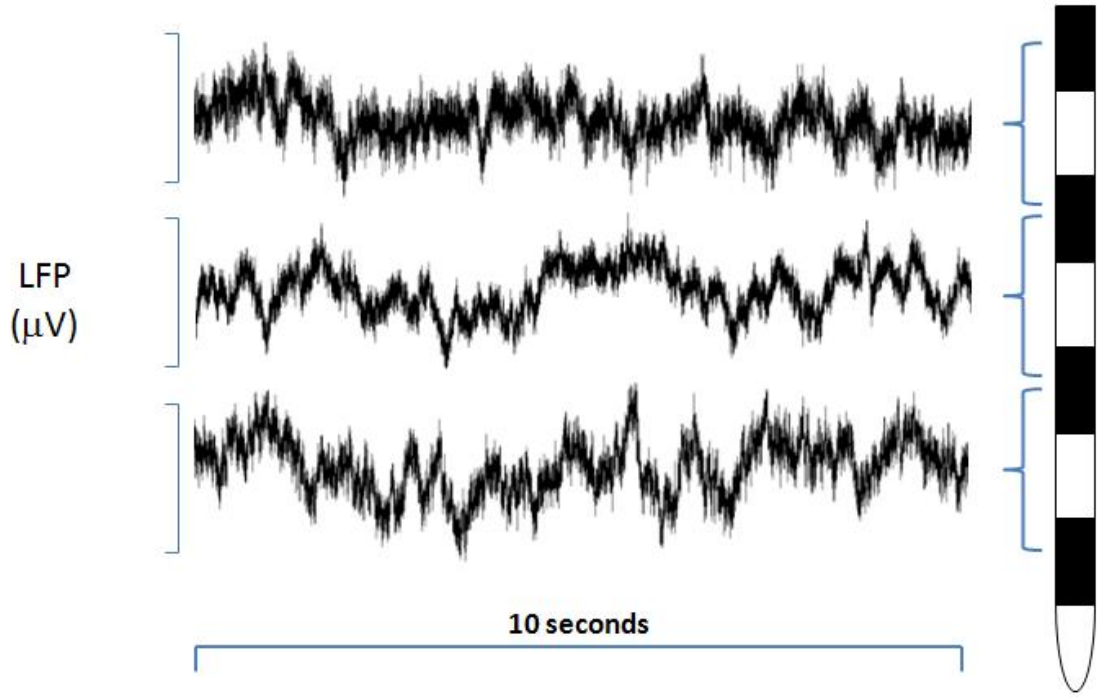

Figure 2.7 *– Diagram showing raw local field potential (LFP) data in terms of voltage (μV) against time (s), recorded with bipolar configuration and displayed using Spike II (version 6.0, Cambridge Electronic Design, Cambridge, UK).*

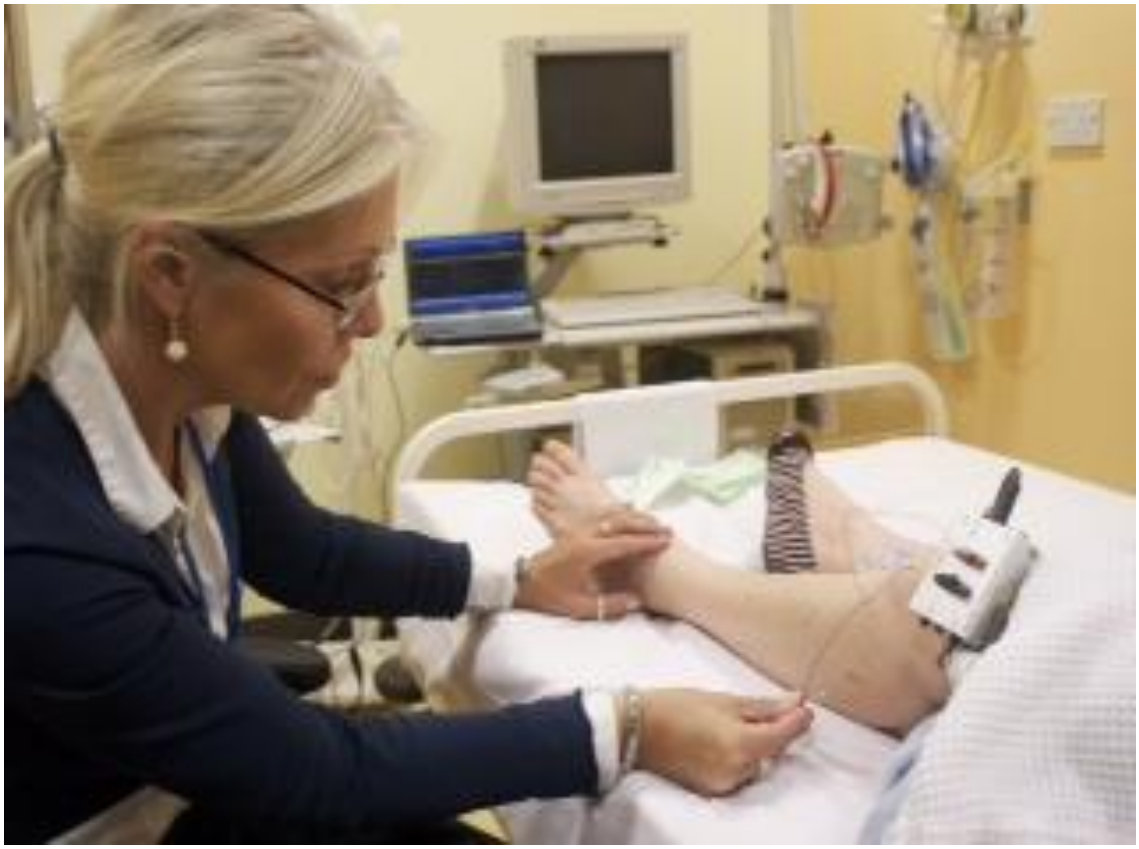

Figure 2.8 *– Photograph showing technique for recording muscle sympathetic nerve activity from the common peroneal nerve.*

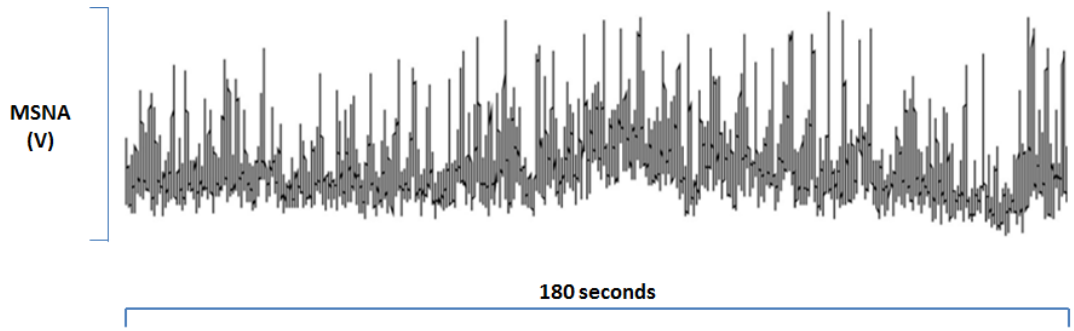

Figure 2.9 *– Voltage neurogram showing raw muscle sympathetic nerve activity (MSNA) data recorded from an insulated tungsten microelectrode in the common peroneal nerve.*

Data Analysis

In Chapters 3, 4 and 5, local field potentials (LFPs) were recorded from various brain nuclei. For each of the experiments, LFP data were split up into epochs of 30 seconds duration from each condition (e.g. 'rest', 'exercise', 'recovery', etc). In order to identify the fundamental spectral

frequencies of the recordings, each 30 s epoch was transformed from the time domain to the frequency domain, by using a digital spectrum analyser (Matlab, version 7.5, The MathWorks Inc., Natick, MA, USA) to apply a fast Fourier Transform algorithm offline (Fig. 2.10). The signals were re-sampled at a rate of 2500 Hz, and 50 Hz frequencies were filtered in order to exclude mains artifact. A 2 second Hann window was used to examine the signal. The area under each power spectrum for each condition was calculated for the following frequency bands: 4-8 Hz, 8-12 Hz, 12-25 Hz, 25-60 Hz, and 60-90 Hz (Fig. 2.11). It is common for LFPs to be divided into these frequency bands, which are defined by prominent surface features of the spectrum and by spectral factor analysis, and are believed to correlate with distinct behavioural states (Brazier *et al*, 1961; Shackman *et al*, 2010).

In chapter 6, muscle sympathetic nerve activity (MSNA) was recorded from the common peroneal nerve. For each of the experiments, the MSNA data were divided into periods when the stimulation was on and periods when the stimulation was off. Sympathetic neural bursts in each of these periods were identified during offline analysis by careful inspection of the morphology of every spike in the mean voltage neurogram. The amount of MSNA could then be expressed as burst frequency (bursts/minute) and burst incidence (bursts/100 heart beats). The strength of each burst was also measured in terms of mean voltage amplitude and surface area. The absolute strength of a burst is dependent on the proximity of the recording electrode. Therefore, in order to normalise the data, the area of the largest burst during each period was given a value of 100, and all other bursts were expressed as a proportion of this.

Mean arterial blood pressure was calculated offline from the blood pressure trace and heart rate from the ECG trace (Fig. 2.12), for the same time data segments used in either the LFP analysis or the MSNA analysis. Blood pressure variability and heart rate variability were also calculated. For statistical purposes, *n* always refers to the total number of patients – the

separate trials for each patient were averaged together, and the obtained average was used as a single value.

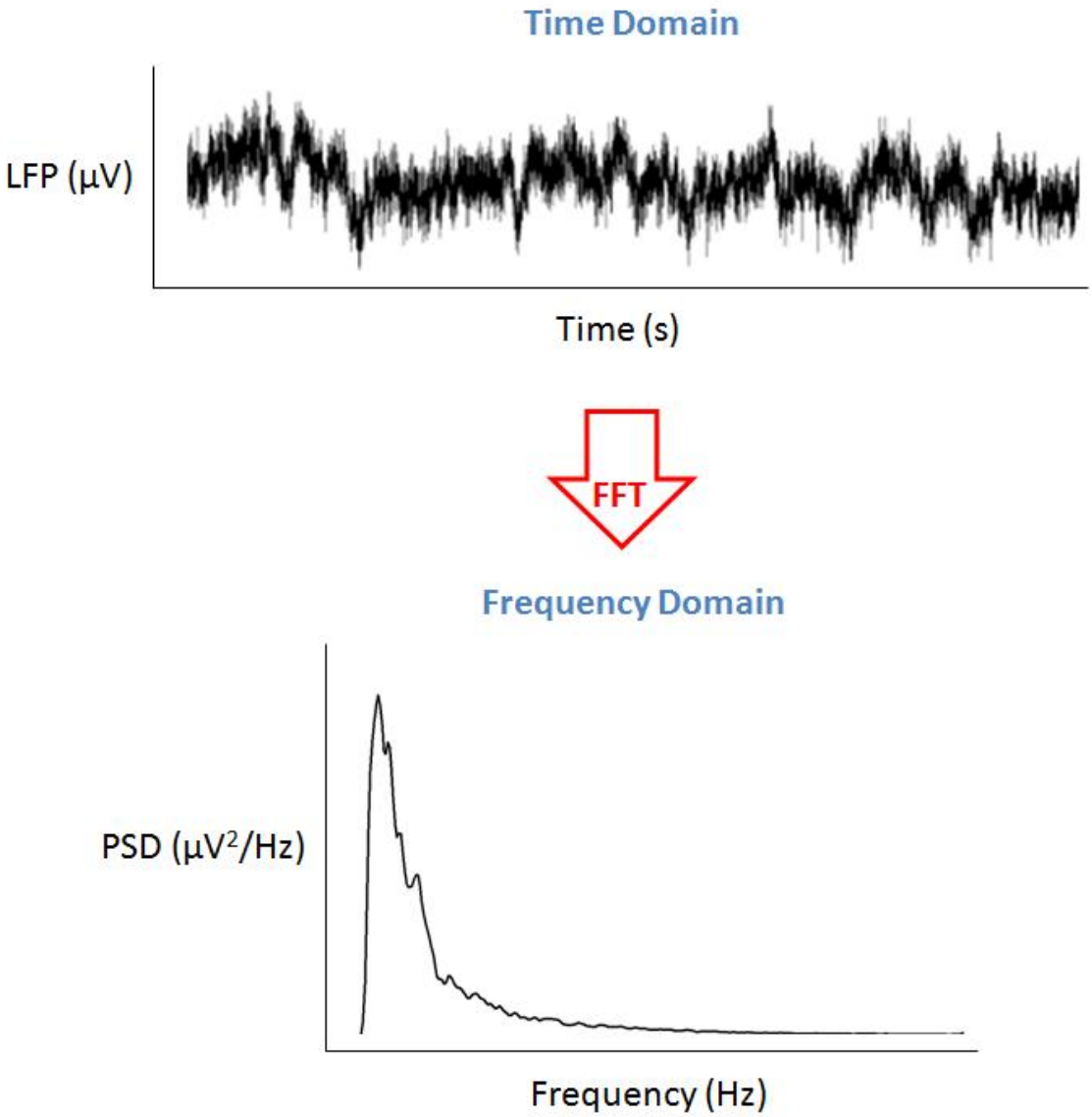

Figure 2.10 *– Diagram showing the transformation of the local field potential (LFP) data from the time domain to the frequency domain using a fast Fourier Transform (FFT) algorithm. This reveals the fundamental spectral frequencies of the recordings in terms of power spectral density (PSD).*

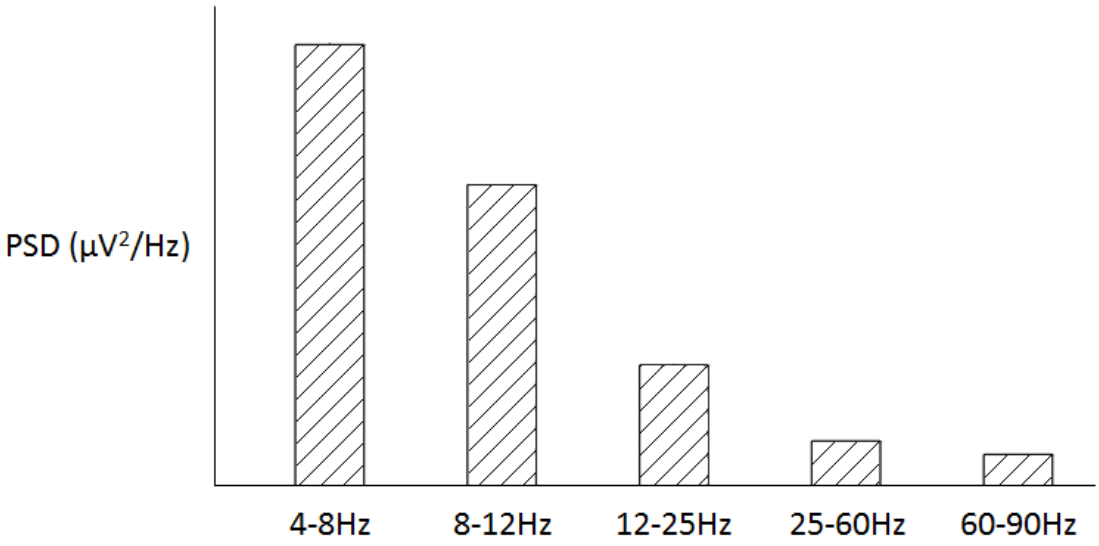

Figure 2.11 *– Diagram showing power spectral density (PSD) data from Fig. 2.10 split into specific frequency bands.*

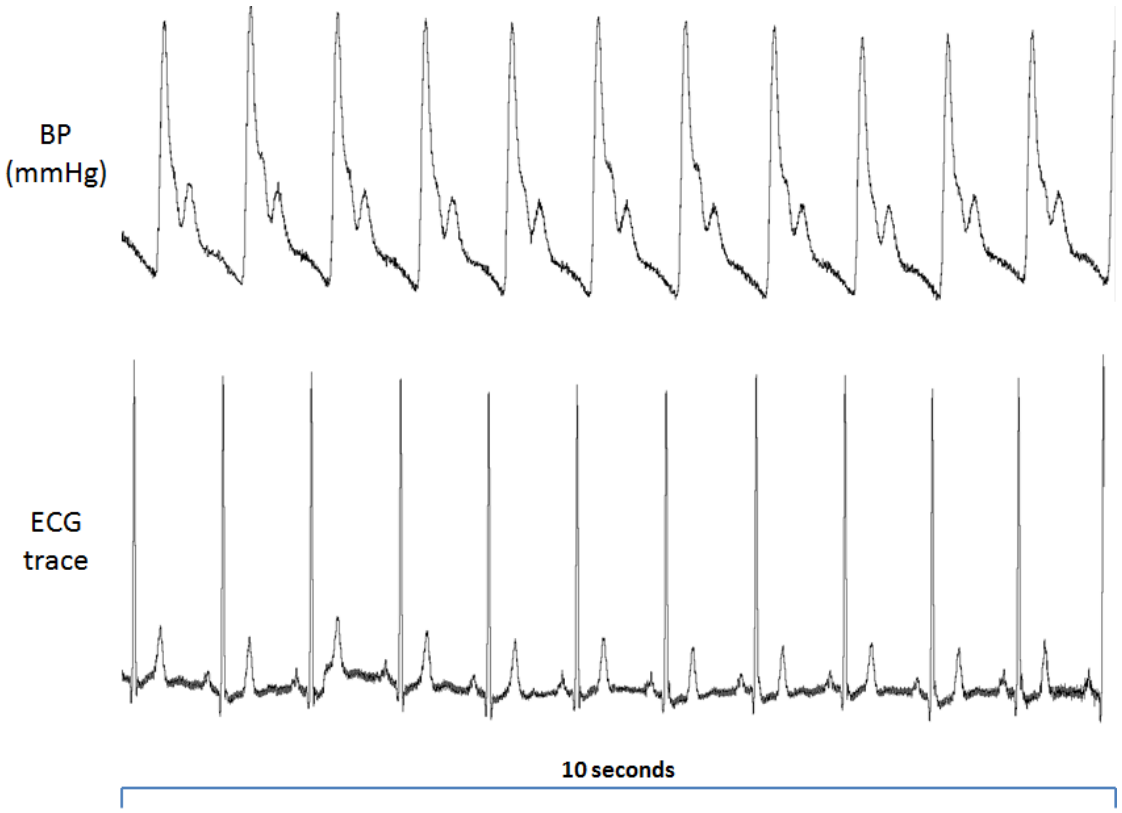

Figure 2.12 *– Diagram showing blood pressure (BP) trace and electrocardiogram (ECG) trace as displayed on Spike II (version 6.0, Cambridge Electronic Design, Cambridge, UK).*

Localisation of Electrodes

The periaqueductal grey (PAG) is composed of functionally distinct columns (as discussed in Chapter 1). Therefore, it was necessary to perform postoperative localisation on all the PAG electrodes to determine exactly which columns were being recorded from or stimulated. The magnetic resonance image (MRI) scans for each patient were viewed using the FMRIB Software Library (Smith *et al*, 2004; Woolrich *et al*, 2009) and rotated about the coronal plane, in order that the anterior and posterior commissures could be viewed in the same axial section. The mid-commissural point was calculated in Talairach space and given an X,Y,Z coordinate to be used as a reference for each electrode contact. The relative coordinates were calculated for both the electrode tip and the superior contact of each electrode, so that the angle of the electrode could also be taken into account. The position of each electrode was then mapped onto a schematic brain atlas (Mai *et al*, 1997), using basic trigonometry.

CHAPTER 3

Identifying Cardiovascular Neurocircuitry Involved In the Exercise Pressor Reflex in Humans Using Functional Neurosurgery

Introduction

Alam and Smirk (1937) were the first to submit experimental evidence to demonstrate that, in humans, the cardiovascular responses to exercise are partially mediated by a reflex response from exercising muscles. They arrested the circulation from the working muscles which caused maintenance of the elevated arterial blood pressure on cessation of exercise. This suggests that by-products produced from the contracting muscles were accumulating within the muscle, thereby stimulating its afferent fibres. Since this pioneering investigation, the 'metaboreflex' effect has been confirmed by many subsequent studies in humans, performing both static and dynamic exercise. For example, Freund *et al* (1979) showed that a sustained pressor response could be produced during total circulatory occlusion of both legs following cycle ergometry. Mark *et al* (1985) were also able to demonstrate a sustained pressor response, in addition to a sustained increase in muscle sympathetic nerve activity, during forearm ischaemia following handgrip exercise. Furthermore, Iellamo *et al* (1999) revealed the maintenance of increased arterial pressure during arrested leg circulation following static leg extension.

Coote *et al* (1971) provided direct evidence that this was a reflex effect by studying both anaesthetised and decerebrate cats. They stimulated the ventral roots supplying the hind limb muscles, which elicited increased arterial blood pressure. This effect was abolished upon sectioning the dorsal roots. Furthermore, direct current anodal block (which preferentially

affects large myelinated fibres) of the dorsal roots supplying exercising muscle had no effect on the cardiovascular responses produced by stimulation of the ventral roots. However, local anaesthetic block of the dorsal roots (which preferentially affects small myelinated and unmyelinated fibres) resulted in the cardiovascular responses to stimulation of the ventral roots being abolished (McCloskey and Mitchell, 1972).

Further evidence for this reflex is provided by studies in paralysed humans. Hobbs and Gandevia (1985) determined that spinal transection affects the cardiovascular response to exercise by asking paraplegic patients to attempt to contract their paralysed leg muscles. During these attempts, there was no change in either heart rate or blood pressure. However, the same patients demonstrated normal cardiovascular responses to handgrip contractions, suggesting that spinal cord pathways below the level of the lesion are necessary to produce a cardiovascular response to exercise. Additionally, epidural injection of anaesthetic in humans has been shown to abolish the post-exercise pressor response to muscle occlusion. Freund *et al* (1979) used bupivicaine injections into the peridural space at L4-L5, which either completely blocked or attenuated the pressor response to exercise-induced muscle ischaemia. Mitchell *et al* (1989) showed that the increases in mean arterial pressure and heart rate were diminished during contraction under epidural anaesthetic (lidocaine or bupivicaine administered epidurally at L3-L4) compared to the same relative contraction without anaesthetic. Fernandes *et al* (1990), using the same delivery of anaesthesia as Mitchell *et al* (1989), investigated the effects of anaesthesia on dynamic exercise, and concluded that the post-exercise ischaemic pressor response was attenuated with epidural anaesthesia.

It was originally established that the afferents of the reflex were group III nerve fibres (stimulated by mechanical effects of contraction) and group IV nerve fibres (stimulated by metabolic products of contraction) (Kaufman *et al*, 1983). Waldrop *et al* (1984) ruled out the involvement of group I and group II afferents by measuring the effects of intra-arterial doses

of succinylcholine on blood pressure, heart rate and the firing of muscle afferents during paralysis with gallamine triethiodide. Succinylcholine is a depolarising neuromuscular blocker which acts on nicotinic acetylcholine receptors. In non-paralysed cats, succinylcholine caused firing in all four muscle afferent groups, accompanied by increased blood pressure and heart rate. However, following paralysis, succinylcholine only stimulated group I and group II nerve afferents, and had no effect on cardiovascular parameters. Therefore, it was deemed unlikely that group I and group II muscle afferents contributed to the pressor reflex.

Tibes (1977) evoked dynamic exercise in the hind limb muscles of anaesthetised dogs with electrical stimulation of sciatic nerve branches. When group I and group II nerve fibres were blocked by cooling distally from the electrodes, the changes in cardiovascular parameters were only minimally affected. However, when a blocking temperature typical for the group III and group IV fibres was reached, the changes in cardiovascular parameters were abolished. Further evidence that the groups III and IV afferents are responsible for the reflex came from Crayton *et al* (1981), who injected capsaicin (a potent stimulator of unmyelinated fibres [Kaufman *et al*, 1982]) into the neurally-intact donor-perfused hind limb of an anaesthetised dog, and observed increases in mean aortic pressure, heart rate, cardiac output, and respiratory minute volume.

However, more recently, this distinct functional differentiation has been questioned. It has been shown that arterial infusions of potassium, lactic acid and prostaglandins are capable of stimulating equal percentages of the two groups of afferents (Rotto and Kaufman, 1988). Furthermore, the responsiveness of group III afferents can be affected by changes in the concentration of specific metabolites such as lactate (Sinoway *et al*, 1993), and conversely, studies have been conducted to show that metabolically-sensitive group IV afferents can be mechanically-sensitive too (Adreani *et al*, 1997).

The majority of research into the afferent pathways mediating the exercise pressor reflex has been conducted using animals. Using horseradish peroxidase staining, the groups III and IV afferents have been shown to synapse in the dorsal horn of the spinal cord in rats, cats and monkeys (Light and Perl, 1979; Craig and Mense, 1983; Mense and Craig, 1988), which serves as the first synapse site for the pressor reflex. Afferents from the gastrocnemius muscle in the rat have been shown to project primarily to Rexed's laminae I, II and V within the lumbar spinal cord and lamina VI within the rostral part of the sacral spinal cord (Panneton *et al*, 2005). Ascending projections from the dorsal horn then go on to activate medullary cells (Bauer *et al*, 1989). Both the rostral ventrolateral medulla (RVLM) and the caudal ventrolateral medulla (CVLM) are known to be crucial areas in modulating the reflex during exercise. Bauer *et al* (1989) observed that the reflex increase in arterial blood pressure evoked by muscle contraction could be significantly attenuated following bilateral injection of kynurenic acid (an excitatory amino acid [EAA] receptor antagonist) into the ventrolateral medulla. Injection of EAA receptor antagonists into the RVLM attenuates blood pressure and heart rate increases during static muscle contraction, whereas injection into the CVLM augments these responses (Ally, 1998).

The roles of supramedullary cortical areas in modulating the reflex have not been precisely ascertained. The subthalamic locomotor region in the posterior hypothalamus is believed to be a key integrating site of the cardiovascular responses to both muscle contraction and simulated exercise. Eldridge *et al* (1981) used unanaesthetised decorticate cats, which ran normally on a treadmill, to show that electrical stimulation of the subthalamic locomotor region resulted in locomotion, accompanied by increased arterial pressure and respiration. Cessation of the stimulation resulted in the end of locomotion and recovery of both arterial pressure and respiration back to pre-stimulation values. Moreover, contraction of the triceps surae muscle in anaesthetised cats by stimulation of the ventral roots supplying the muscle evokes an increase in the firing rate of the neurons in the subthalamic locomotor region.

Studies have suggested that the periaqueductal grey (PAG) could have a role in the exercise pressor reflex – muscle contraction has been shown to increase enkephalin release (Williams *et al*, 1992), increase neuropeptide Y release (Williams, 1996), and increase c-Fos activity (Li and Mitchell, 2000) within the cat PAG. Additionally, Iwamoto *et al* (1996) identified increased c-Fos activity in the rat PAG during dynamic treadmill exercise. Furthermore, the PAG is known to project to the medullary regions controlling blood pressure (Lovick, 1985; Carrive *et al*, 1988; Carrive *et al*, 1989) and also to higher cardiovascular centres, such as the hypothalamus (Horiuchi *et al*, 2009). Stimulation of the dorsal and lateral columns of the PAG in animals (Carrive and Bandler, 1991a; Lovick, 1992a) and the dorsal PAG/PVG (periventricular grey) in humans (Green *et al*, 2005) results in increased arterial blood pressure and heart rate. Stimulation of the ventral PAG/PVG, on the other hand, results in decreased arterial blood pressure (Green *et al*, 2005). Moreover, the PAG is considered to have a key role in the integration of the 'central command' component of the cardiovascular responses to exercise (Green *et al*, 2007; Green and Paterson, 2008).

The aim of this study was to investigate the neurocircuitry involved in the exercise pressor reflex; specifically, the subcortical structures that could have a role in the integration of the reflex. Local field potential recordings were made from specific nuclei in deep brain stimulation patients – these structures had been previously identified as cardiovascularly active in animals. The recordings were used to test the hypothesis that neural activity in particular subcortical structures corresponds to increases in arterial blood pressure when evoked by both actual exercise and stimulation of the pressor reflex with post-exercise muscle occlusion.

Methods

Thirty-six patients (21 male, 15 female), with a mean age of 54.5 years (range 31-69 years) were recruited for this study (Table 3.1). Six patients had electrodes implanted in the periaqueductal grey (PAG) for the treatment of chronic pain (mean age 52.7 years). A further eight patients had electrodes in the sensory thalamus, also for the treatment of chronic pain (mean age 52.8 years), either in the ventroposterolateral or ventroposteromedial nucleus for the treatment of limb pain or facial pain, respectively. Another eleven patients had electrodes in the subthalamic nucleus for the treatment of Parkinson's disease (mean age 58.9 years). One patient had an electrode in the inferior posterior hypothalamus for the treatment of cluster headaches (age 56 years). Six patients had electrodes in the internal globus pallidus for the treatment of generalised dystonia (mean age 53.5 years). Finally, four patients had electrodes in the anterior cingulate cortex for the treatment of chronic pain (mean age 50.0 years).

The experiments were conducted within the first week following stage 1 of the deep brain stimulation surgical procedure, while the electrodes were still externalised. For the entire duration of the experiment, the patients' stimulation was turned off. The protocol was as follows (Fig. 3.1): each patient was asked to sit comfortably and had a weight of 2 kg attached to their right wrist. Cardiovascular parameters and neural activity were recorded for a rest period of three minutes. After the rest period, the patient began exercising following an oral cue. This 'light' exercise task consisted of bicep curls at a rate of 30-60 per minute, according to each patient's fitness and capabilities. After two minutes of exercise, the patient was asked to stop exercising, and a blood pressure cuff around the exercised arm was immediately inflated to above systolic pressure (approximately 200 mmHg). The cuff was kept inflated for a two minute period, and then released. The patient was allowed a recovery period of one minute. The protocol was then repeated twice more, for a total of three sets of recordings, in

order to confirm the consistency of the response. If the response was consistent, the results were averaged together to give one set of results for each patient.

Table 3.1 *– Subject characteristics. PAG, periaqueductal grey; STN, subthalamic nucleus; GPi, internal globus pallidus; ACC, anterior cingulate cortex.*

Patient	*Age (years)*	*Sex*	*Diagnosis*	*DBS Electrode Location*
1	69	M	Chronic left arm pain from brachial plexus injury	PAG
2	51	M	Chronic right arm pain from brachial plexus injury	PAG
3	52	F	Chronic pain following stroke	PAG
4	54	M	Chronic neuropathic thumb & finger pain	PAG
5	31	M	Severe intractable left arm pain from brachial plexus injury	PAG
6	59	F	Right-sided anaesthesia dolorosa & neuropathic tongue pain	PAG
7	40	M	Right leg pain secondary to crush injury from industrial accident	Sensory Thalamus
8	69	M	Chronic left arm pain from brachial plexus injury	Sensory Thalamus
9	52	M	Chronic right arm pain from brachial plexus injury	Sensory Thalamus
10	52	F	Thalamic haemorrhage	Sensory Thalamus
11	54	M	Chronic neuropathic thumb & finger pain	Sensory Thalamus
12	65	F	Intractable atypical facial pain	Sensory Thalamus
13	31	M	Severe intractable left arm pain from brachial plexus injury	Sensory Thalamus
14	59	F	Right-sided anaesthesia dolorosa & neuropathic tongue pain	Sensory Thalamus
15	50	F	Parkinson's disease	STN
16	56	M	Parkinson's disease	STN
17	53	F	Parkinson's disease	STN
18	65	M	Parkinson's disease	STN
19	58	M	Parkinson's disease	STN
20	63	M	Parkinson's disease	STN
21	54	M	Parkinson's disease	STN
22	65	M	Parkinson's disease	STN
23	66	M	Parkinson's disease	STN
24	56	M	Parkinson's disease	STN
25	62	M	Parkinson's disease	STN
26	56	M	Cluster headaches	Hypothalamus
27	62	F	Generalised dystonia	GPi
28	58	F	Cervical dystonia	GPi
29	47	F	Cervical dystonia	GPi
30	53	F	Cervical dystonia	GPi
31	52	F	Generalised dystonia	GPi
32	49	F	Cervical dystonia	GPi
33	41	F	Chronic bilateral leg pain from spinal injury	ACC

34	49	M	Total body pain (brachial plexus injury & cervical myelopathy)	ACC
35	57	M	Chronic neuropathic pain	ACC
36	53	F	Chronic right leg pain from spinal injury	ACC

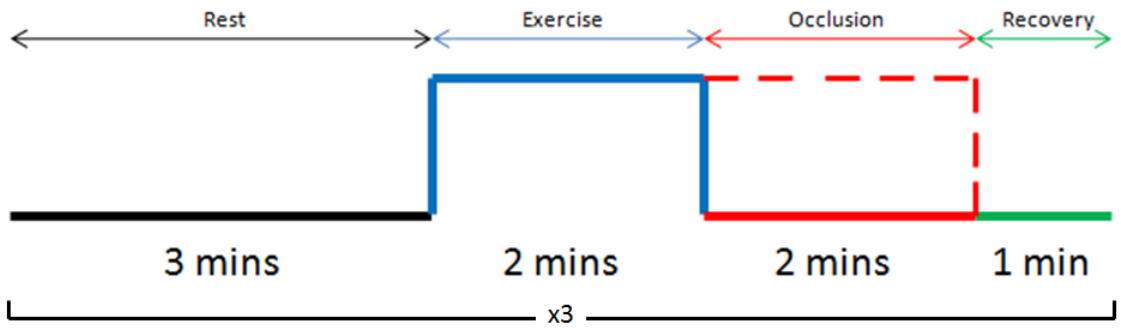

Figure 3.1 – *Protocol for the exercise pressor reflex experiment. The vertical axis represents the level of activity. The solid lines show the actual level of activity of the patient and the dotted lines represent the continued stimulation of the exercise pressor reflex, even though activity has stopped.*

The patients were also asked to perform three sets of a control experiment, in which the blood pressure cuff was inflated without prior exercise (Fig. 3.2). This was in order to determine whether or not any changes in neural activity that might have been observed during the period of cuff inflation were due to the sensation of the cuff inflation itself. Once more, if the responses were consistent across the three repeats, the results were averaged together to give one set of results per patient.

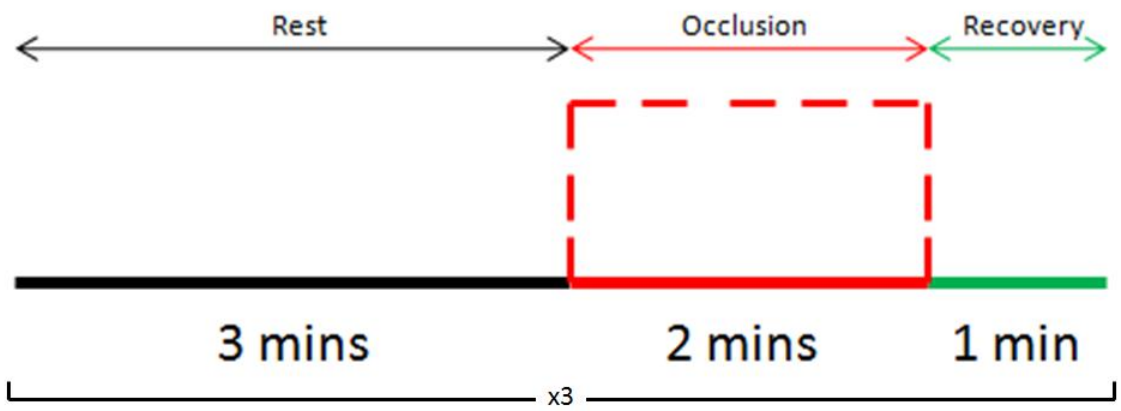

Figure 3.2 – *Protocol for the control experiment to determine whether neural activity might be due to the sensation of the occlusion. The vertical axis represents the level of activity. The solid lines represent the activity level of the patient and the dotted lines represent the potential changes in both neural and cardiovascular parameters during occlusion.*

Patients were asked to rate their levels of pain throughout the duration of the experiments using the Visual Analog Pain Severity Scale (VAPSS), in order to determine whether changes in neural activity could be due to the patients' pathology (for example, pain in PAG patients), as opposed to the neural responses to exercise. Data segments in which the VAPSS score changed were excluded from analysis.

Results

Cardiovascular Parameters

Out of the 36 patients who performed the experiment, 25 had successful blood pressure recordings from the Portapres. In the other eleven patients, the Portapres signal was lost during the experiment. Therefore, the data were not included. In all of the 25 patients from whom data were taken, mean arterial blood pressure (MABP) increased upon exercise, remained elevated during post-exercise occlusion, and returned to baseline within the recovery period. The MABP data for all of the patients were averaged together (Fig. 3.3). The average increase in MABP during exercise was 13.6 ± 3.3 mmHg ($P < 0.001$, $n = 25$), equivalent to an increase of 13.8%. During the post-exercise occlusion period, the average increase from rest in MABP was 11.1 ± 1.9 mmHg ($P < 0.001$, $n = 25$), equivalent to an increase of 11.3%. On recovery, there was an average decrease from rest of 1.2 ± 1.9 mmHg (equivalent to a 1.2% decrease). However, there was no significant difference between the initial rest period and the recovery period ($P = 0.372$, $n = 25$).

The changes in MABP were accompanied by analogous changes in systolic blood pressure (SBP) and diastolic blood pressure (DBP) (Fig. 3.4). The average increase in SBP during exercise was 31.4 ± 5.1 mmHg ($P < 0.001$, $n = 25$), equivalent to an increase of 23.8%. During the post-exercise occlusion period, the average increase from rest in SBP was 28.5 ± 2.6 mmHg ($P < 0.001$, $n = 25$), equivalent to an increase of 21.6%. On recovery there was an average increase from rest of 1.1 ± 2.2 mmHg (equivalent to a 0.8% increase). However, there was no significant difference between the initial rest period and the recovery period ($P = 0.725$, $n = 25$). The average increase in DBP during exercise was 4.7 ± 1.9 mmHg ($P = 0.043$, $n = 25$), equivalent to an increase of 5.8%. During the post-exercise occlusion period, the average increase from rest in DBP was 2.3 ± 1.2 mmHg (equivalent to an increase of 2.8%). However, this was not significant ($P = 0.158$, $n = 25$). On recovery there was an average decrease from rest of 2.3 ± 1.8 mmHg (equivalent to a 2.8% decrease), which was also insignificant ($P = 0.362$, $n = 25$).

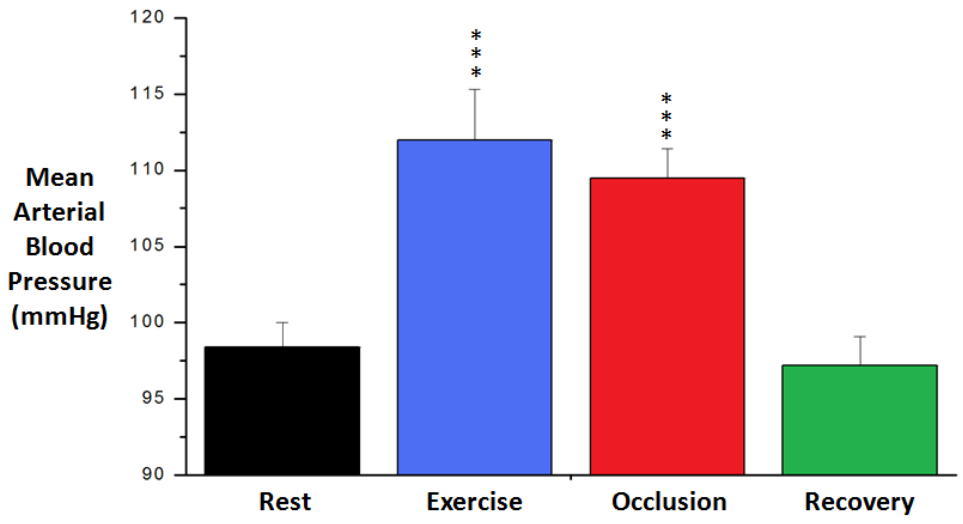

Figure 3.3 – *Graph showing significant increases in mean arterial blood pressure with exercise and post-exercise occlusion, compared to rest. n = 25, *** P < 0.001. Error bars represent standard error of the mean.*

All 36 patients who performed the experiment had a significantly decreased R-R interval during the exercise period, but not during the post-exercise occlusion or recovery periods. The R-R interval data for all 36 patients were averaged together (Fig. 3.5). The decrease from rest was 0.037 ± 0.014 s ($P < 0.001$, $n = 36$), equivalent to a decrease of 4.4%. During the post-exercise occlusion period there was an insignificant decrease from rest of 0.002 ± 0.033 s (equivalent to 0.2%, $P = 0.739$, $n = 36$), and an insignificant increase from rest of 0.002 ± 0.030 s (equivalent to 0.2%, $P = 0.681$, $n = 36$) during the recovery period.

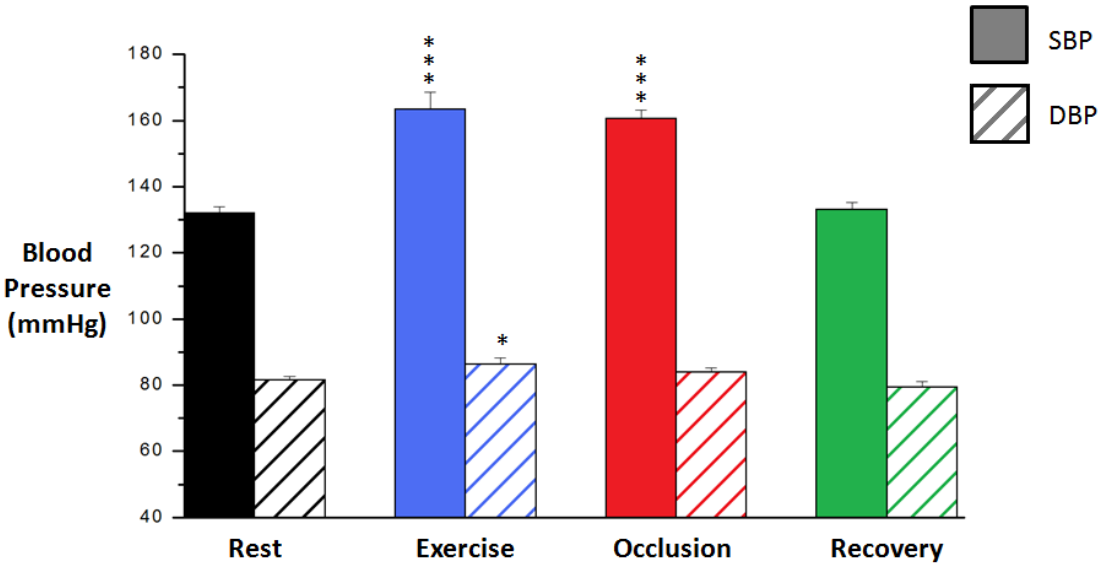

Figure 3.4 – *Graph showing significant increases in systolic blood pressure (SBP) with exercise and post-exercise occlusion, and in diastolic blood pressure (DBP) with exercise only, compared to rest. n = 25, * P < 0.05, *** P < 0.001. Error bars represent standard error of the mean.*

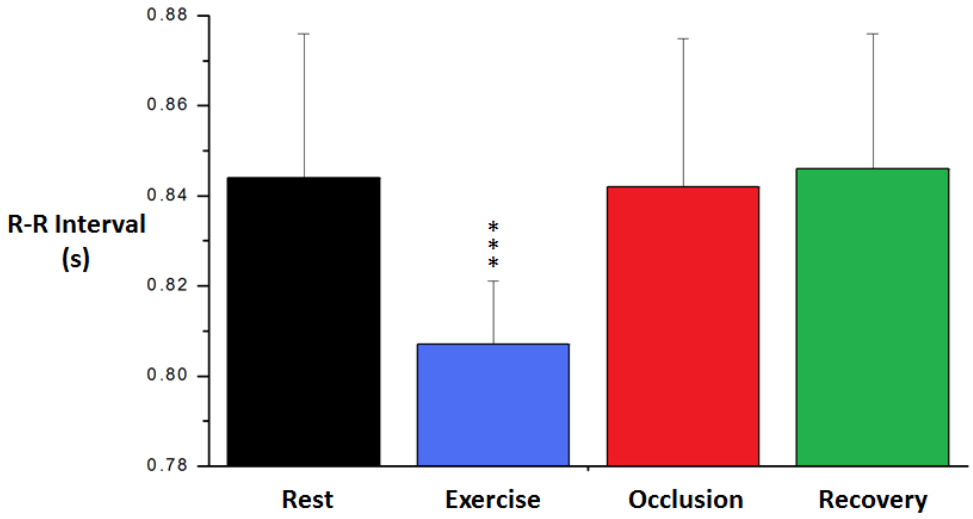

Figure 3.5 – *Graph showing a significant decrease in R-R interval (i.e. increase in heart rate) with exercise, compared to rest. n = 36, *** P < 0.001. Error bars represent standard error of the mean.*

Electrode Localisation

Due to the fact that the periaqueductal grey (PAG) is functionally opposite depending on location (i.e. there is a pressor region and a depressor region), it was imperative that the precise electrode locations were established. Fig. 3.6 shows the positions of the electrodes in the six PAG patients who performed the experiment, in both the transverse and sagittal planes. Fig. 3.7 shows a schematic diagram of these same six PAG electrodes so that the contacts on each electrode can be examined. Recordings were only made from those contacts that provided the patients with therapeutic benefit (i.e. pain relief). It is quite clear that all of these contacts were situated within the dorsal region of the PAG.

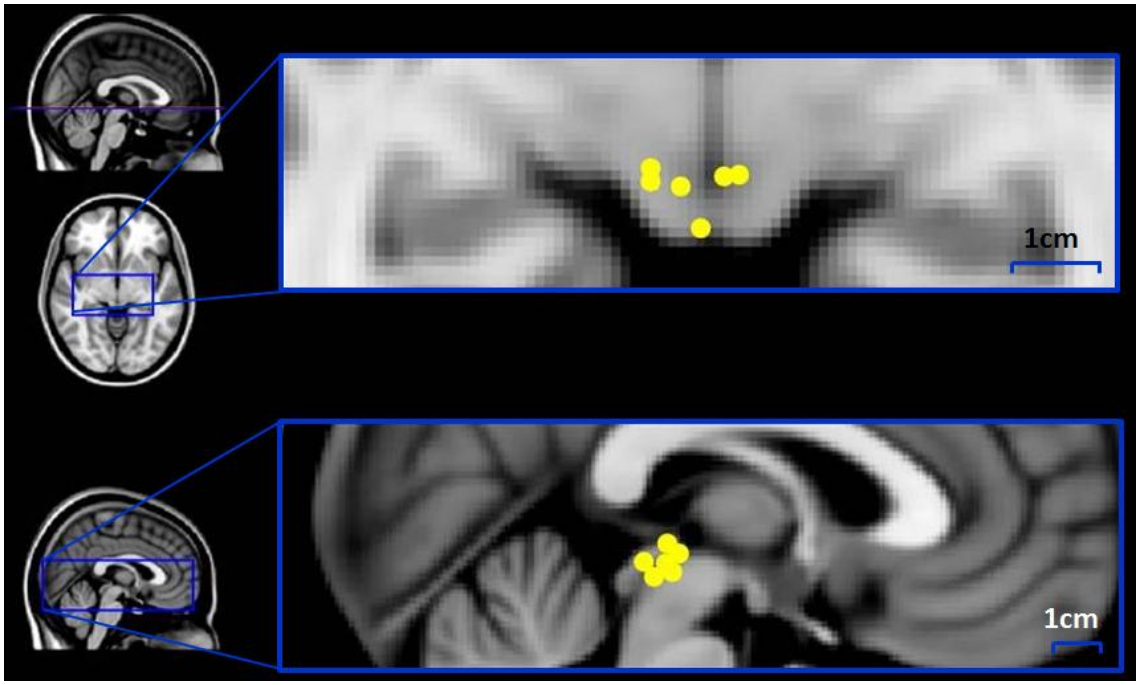

Figure 3.6 – *Post-operative image showing individual electrode locations in the transverse and sagittal planes for six periaqueductal grey patients. Both scale bars represent 1cm. Yellow dots represent the midpoints of each electrode.*

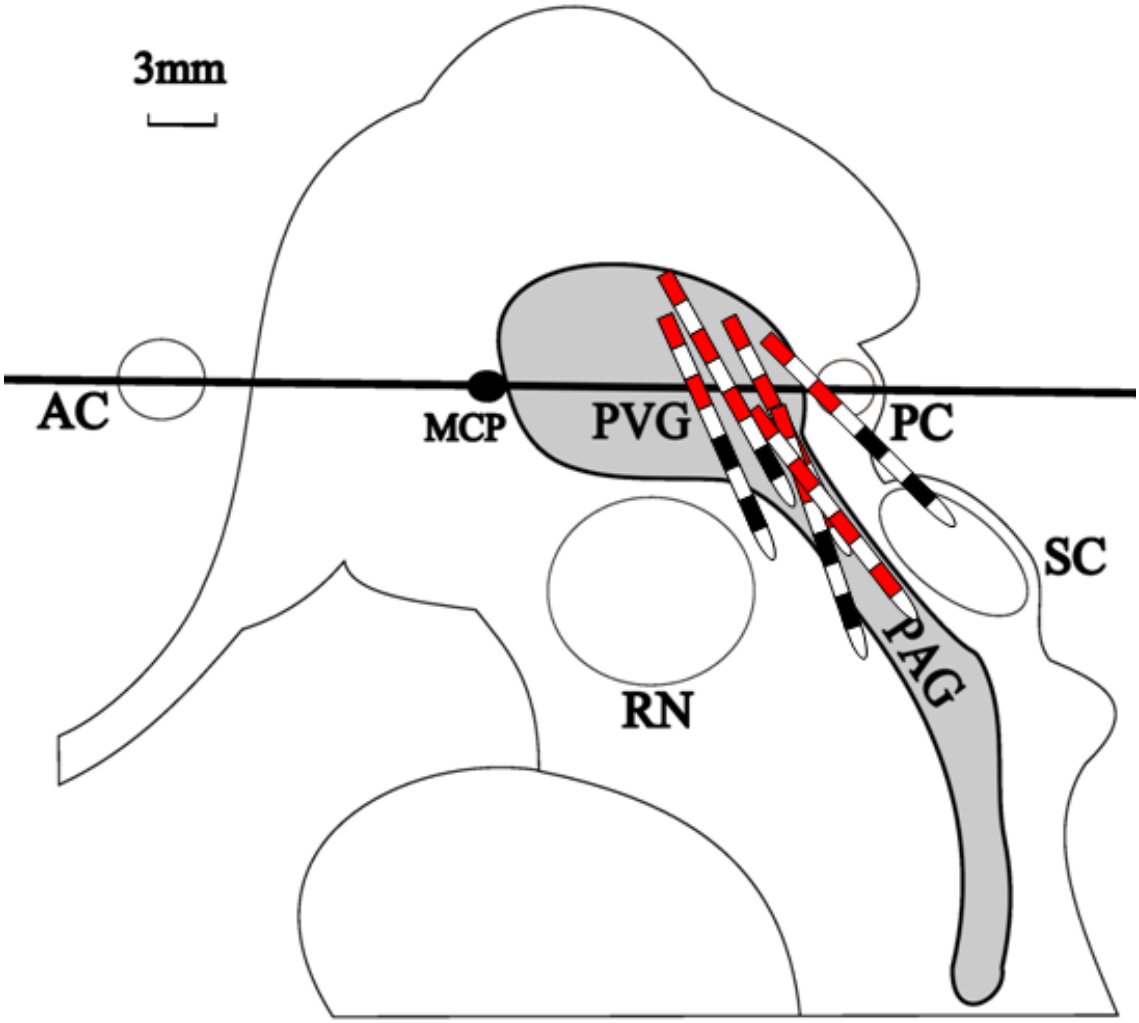

Figure 3.7 – *Schematic diagram in the sagittal plane showing the electrode locations for the six PAG patients who performed the experiment. The data presented in this study are recorded only from those contacts that provided therapeutic benefit – these were all within the dorsal aspect of the PVG/PAG (highlighted in red). AC, anterior commissure; MCP, mid-commissural point; PVG, periventricular grey; PC, posterior commissure; RN, red nucleus; PAG, periaqueductal grey; SC, superior colliculus.*

Local Field Potential Recordings from the Periaqueductal Grey

Fig. 3.8 shows the raw data from one of the periaqueductal grey (PAG) patients, showing a 10 second sample of the local field potential recordings from each condition of the protocol. Using ANOVA, a significant difference was revealed between the conditions of rest, exercise, post-exercise occlusion and recovery ($P < 0.05$) for each individual patient. Therefore, all the PAG data were averaged together (Fig. 3.9). Significant increases in neural activity occurred

during the post-exercise occlusion period, but not during the exercise period or the recovery period. These changes were seen in the lower frequency bands. In the 4-8 Hz band, post-exercise occlusion was associated with an increase in power spectral density (PSD) of 415.0 ± 172.3 μV^2/Hz (P = 0.002, *n* = 6), which is equivalent to a 20.8% increase. In the 8-12 Hz band, there was an increase in PSD of 236.3 ± 124.3 μV^2/Hz (P < 0.001, *n* = 6) during post-exercise occlusion, which is equivalent to a 29.6% increase. In the 12-25 Hz band, post-exercise occlusion was associated with an increase in PSD of 72.8 ± 23.3 μV^2/Hz (P < 0.001, *n* = 6), which is equivalent to a 30.4% increase.

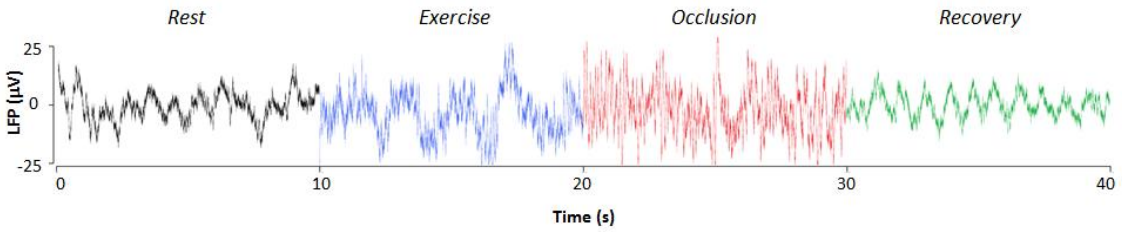

Figure 3.8 *– Raw data trace showing local field potential (LFP) recordings during each condition of the protocol from one of the periaqueductal grey patients.*

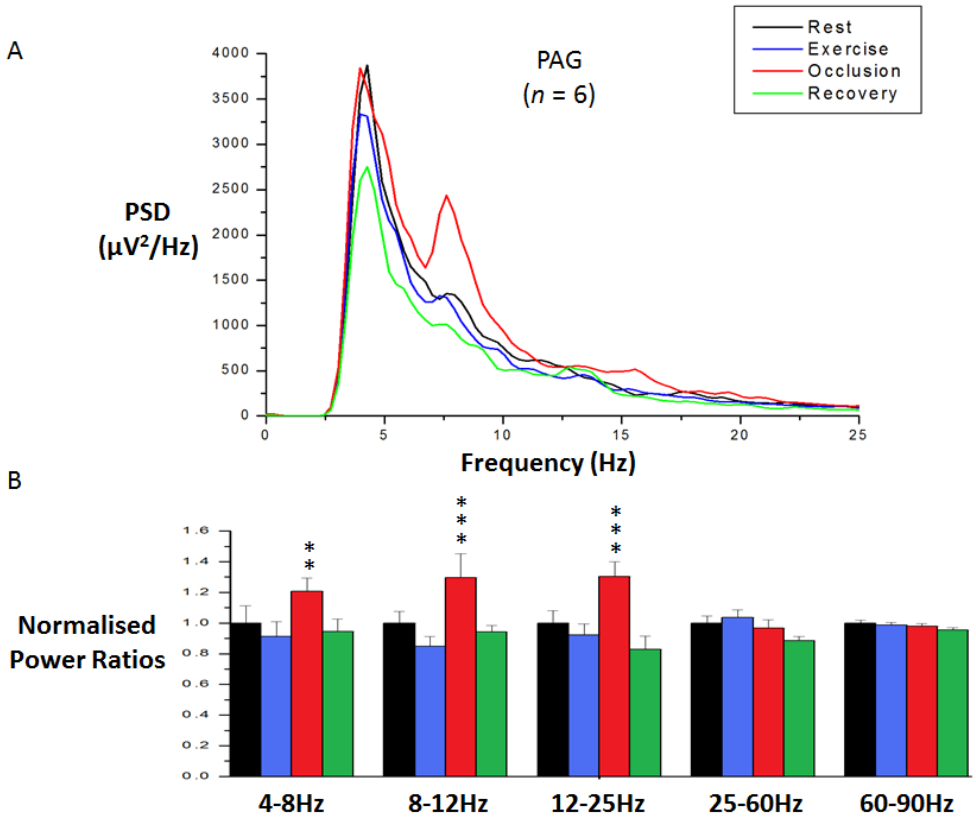

Figure 3.9 – *Graphs showing a significant increase in periaqueductal grey (PAG) neural activity during post-exercise occlusion, compared to rest. (A) Mean power spectral density (PSD) for all six patients. (B) Normalised spectral changes (rest = 1.0) divided into frequency bands, showing significant increases during post-exercise occlusion in the 4-8 Hz, 8-12 Hz and 12-25 Hz bands, compared to rest. n = 6, ** P < 0.01, *** P < 0.001. Error bars represent standard error of the mean.*

Local Field Potential Recordings from the Subthalamic Nucleus

ANOVA revealed a significant difference in neural activity between each test condition in the 12-25 Hz and 60-90 Hz frequency bands in each individual subthalamic nucleus (STN) patient. Therefore, I averaged the data from all eleven patients (Fig. 3.10). In contrast to the increased power spectral density (PSD) observed in the periaqueductal grey, I noted a decrease in PSD in the 12-25 Hz band during exercise and post-exercise occlusion. Exercise was associated with a decrease in PSD of 44.2 ± 1.8 $\mu V^2/Hz$ ($P < 0.001$, $n = 11$), which is equivalent to a decrease of 37.2%. Post-exercise occlusion in the same frequency band was associated with a decrease in PSD of 12.4 ± 3.7 $\mu V^2/Hz$ ($P < 0.001$, $n = 11$), which is equal to a 10.4% decrease. In the 60-90

Hz frequency band, there was a significant increase in PSD during exercise, but no change during post-exercise occlusion or recovery. During exercise, PSD increased by 4.8 ± 0.5 $\mu V^2/Hz$ ($P < 0.001$, $n = 11$), equivalent to a 27.1% increase.

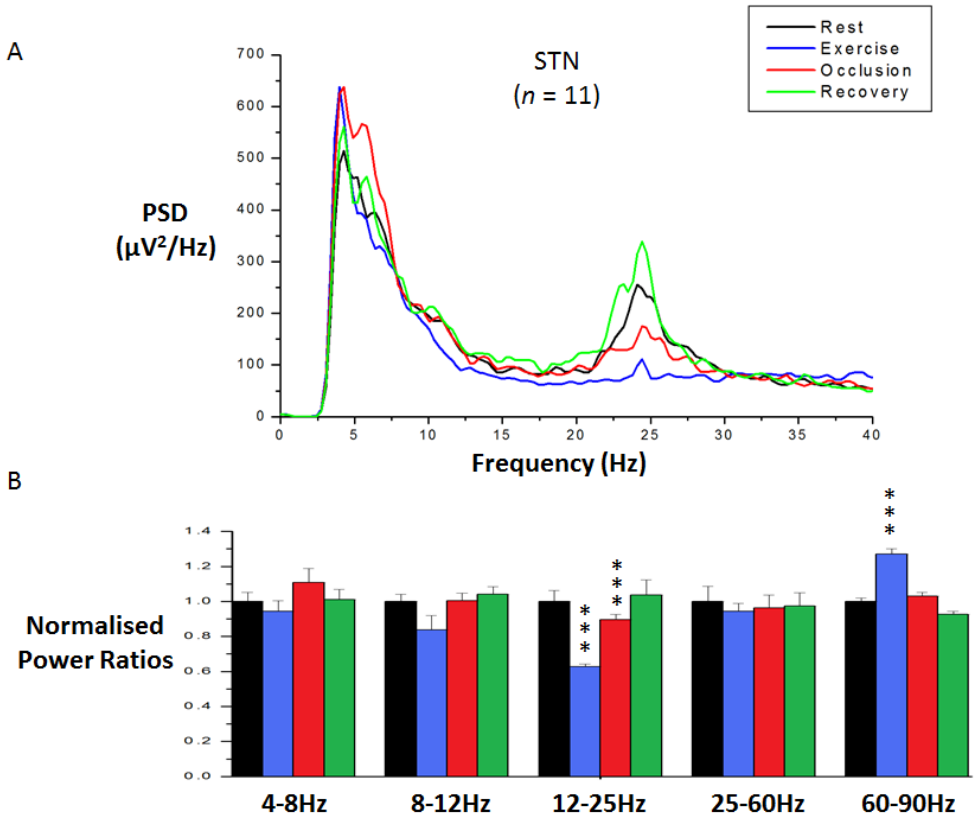

Figure 3.10 – *Graphs showing significant changes in subthalamic nucleus (STN) neural activity during exercise and post-exercise occlusion, compared to rest. (A) Mean power spectral density (PSD) for all eleven patients. (B) Normalised spectral changes (rest = 1.0) divided into frequency bands, showing significant decreases during exercise and post-exercise occlusion in the 12-25 Hz band, and a significant increase during exercise in the 60-90 Hz band, compared to rest. n = 11, *** P < 0.001. Error bars represent standard error of the mean.*

Local Field Potential Recordings from the Other Nuclei

Using ANOVA, it was shown that there were no significant differences among any of the conditions in any of the thalamus (Fig. 3.11), hypothalamus (Fig. 3.12), internal globus pallidus (GPi) (Fig. 3.13), and anterior cingulate cortex patients (Fig. 3.14). For the GPi patients, a peak in the power spectral density graphs was observed at approximately 25 Hz. However, this peak

was consistent across all the test conditions in all six GPi patients, thus it most likely represents the resting activity levels of the GPi.

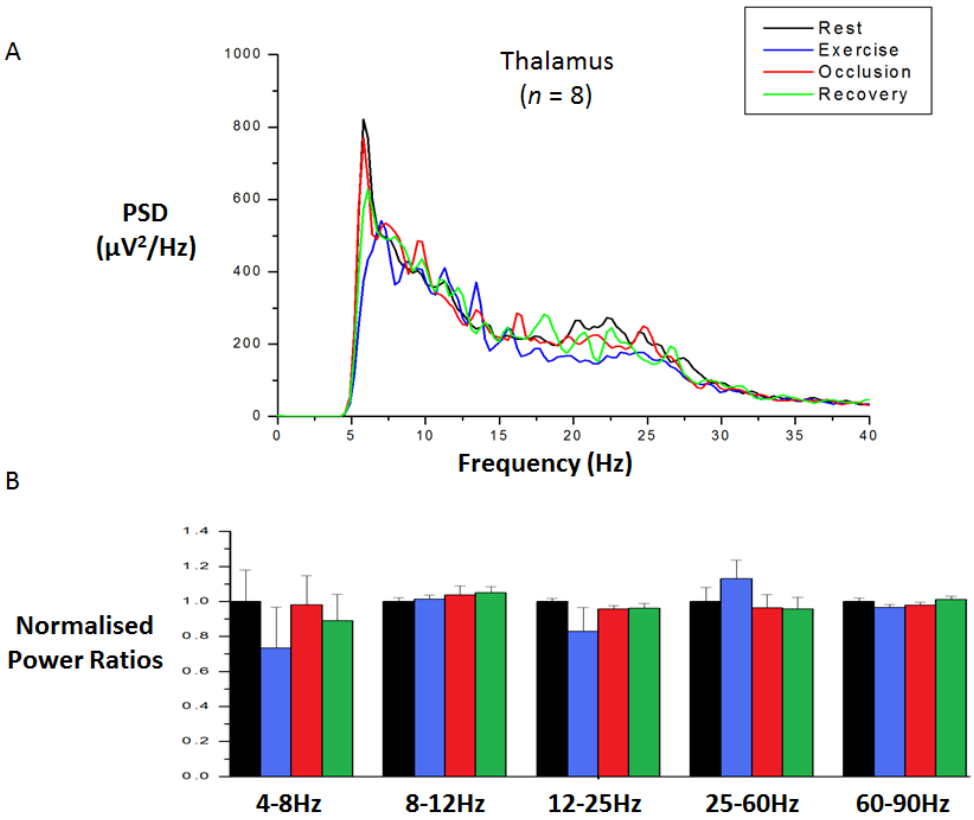

Figure 3.11 – *Graphs showing no changes in thalamic neural activity during exercise and post-exercise occlusion, compared to rest. (A) Mean power spectral density (PSD) for all eight patients. (B) Normalised spectral changes (rest = 1.0) divided into frequency bands, showing no significant differences compared to rest. n = 8. Error bars represent standard error of the mean.*

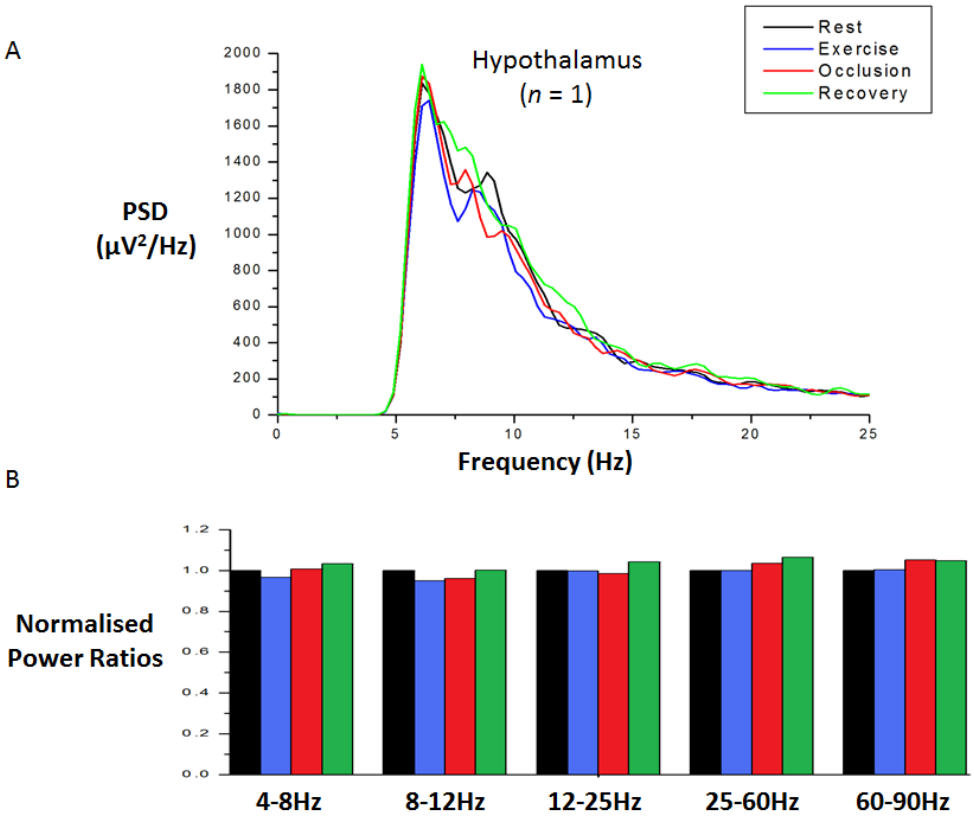

Figure 3.12 – *Graphs showing no changes in hypothalamic neural activity during exercise and post-exercise occlusion, compared to rest. (A) Mean power spectral density (PSD) for the hypothalamus patient. (B) Normalised spectral changes (rest = 1.0) divided into frequency bands. n = 1.*

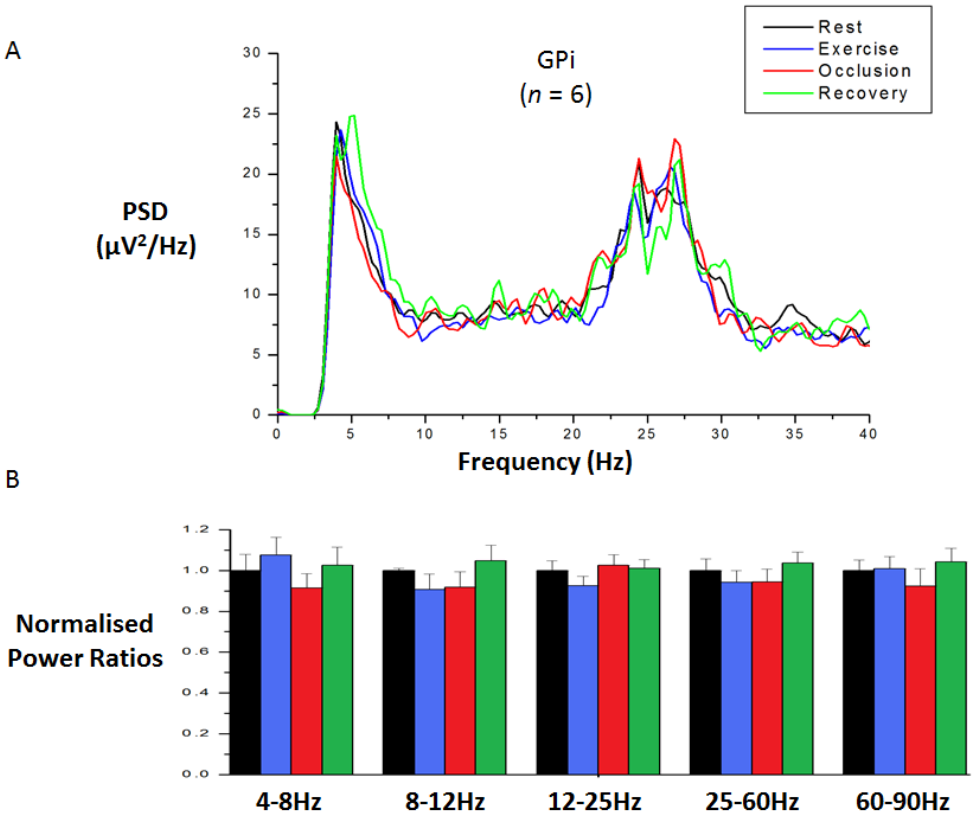

Figure 3.13 – *Graphs showing no changes in internal globus pallidus (GPi) neural activity during exercise and post-exercise occlusion, compared to rest. (A) Mean power spectral density (PSD) for all six patients. (B) Normalised spectral changes (rest = 1.0) divided into frequency bands, showing no significant differences compared to rest. n = 6. Error bars represent standard error of the mean.*

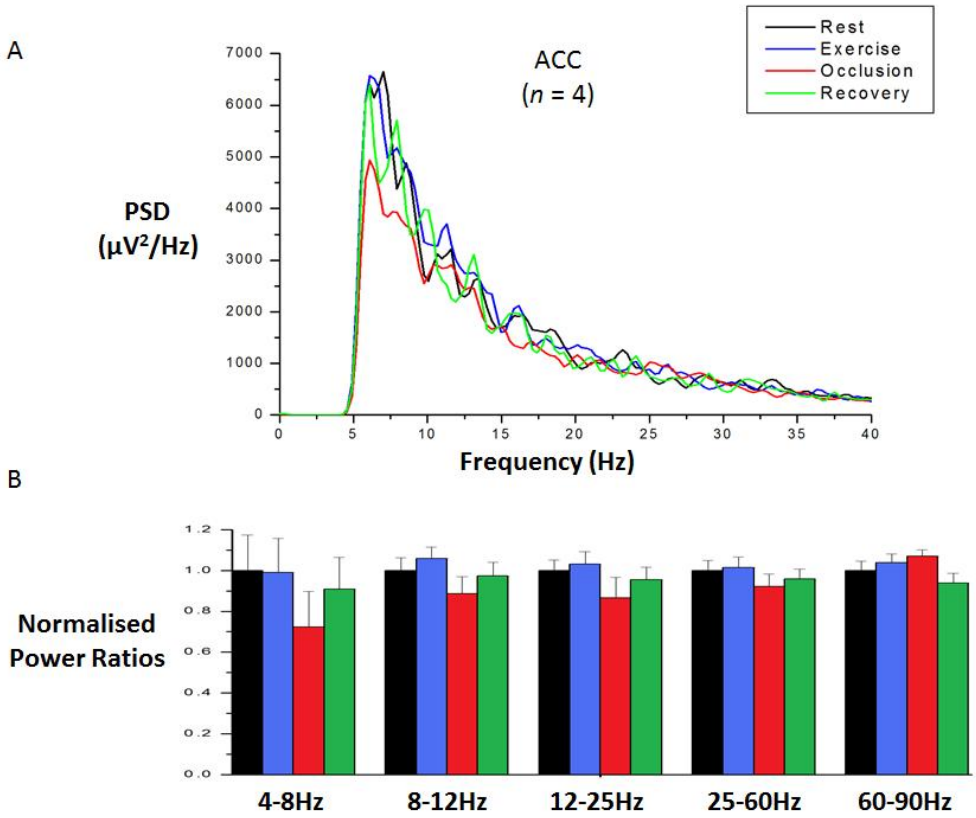

Figure 3.14 – *Graphs showing no changes in anterior cingulate cortex (ACC) neural activity during exercise and post-exercise occlusion, compared to rest. (A) Mean power spectral density (PSD) for all four patients. (B) Normalised spectral changes (rest = 1.0) divided into frequency bands, showing no significant differences compared to rest. n = 4. Error bars represent standard error of the mean.*

Cardiovascular Parameters and Local Field Potential Recordings from Control Experiment

I did not observe any significant differences among any of the conditions of the control experiment (occlusion without prior exercise) in any of the patients, either in terms of cardiovascular parameters (Figs. 3.15-3.17) or in terms of neural activity (Figs. 3.18-3.23).

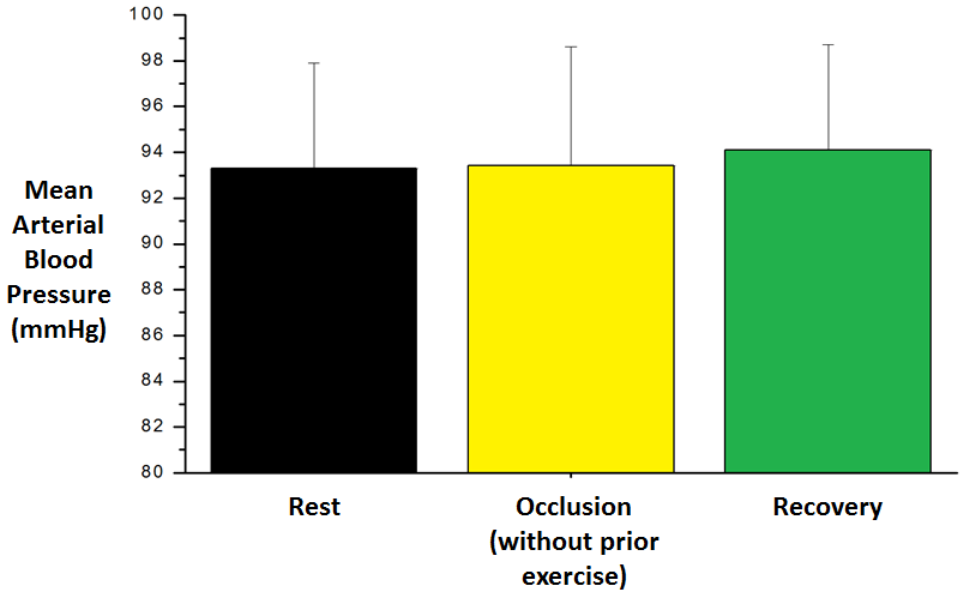

Figure 3.15 – *Graph showing no significant changes in mean arterial blood pressure during occlusion without prior exercise, compared to rest. n = 25. Error bars represent standard error of the mean.*

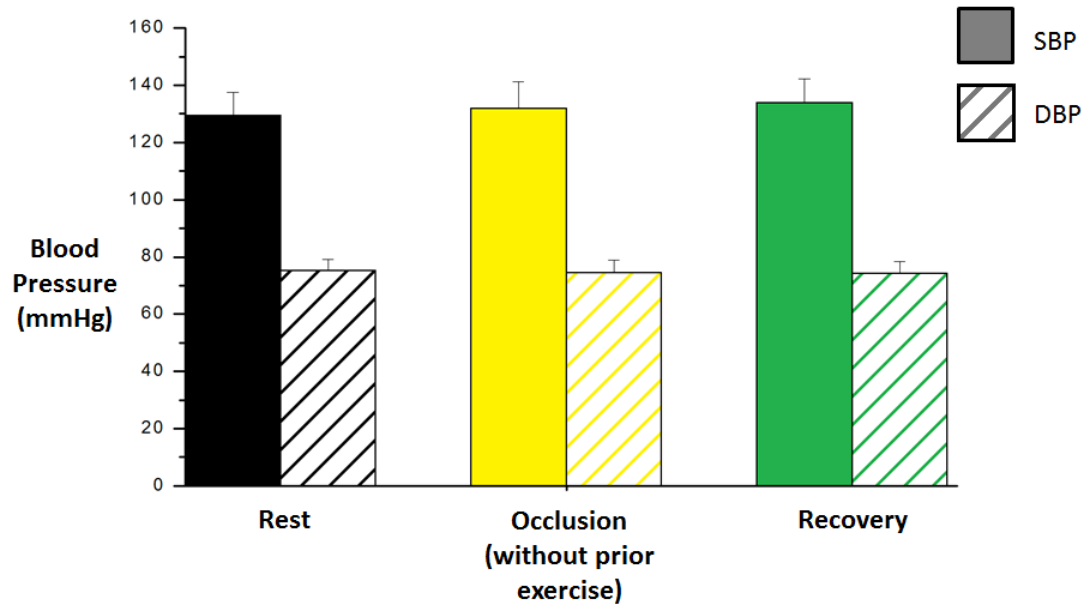

Figure 3.16 – *Graph showing no significant changes in systolic blood pressure (SBP) or diastolic blood pressure (DBP) during occlusion without prior exercise, compared to rest. n = 25. Error bars represent standard error of the mean.*

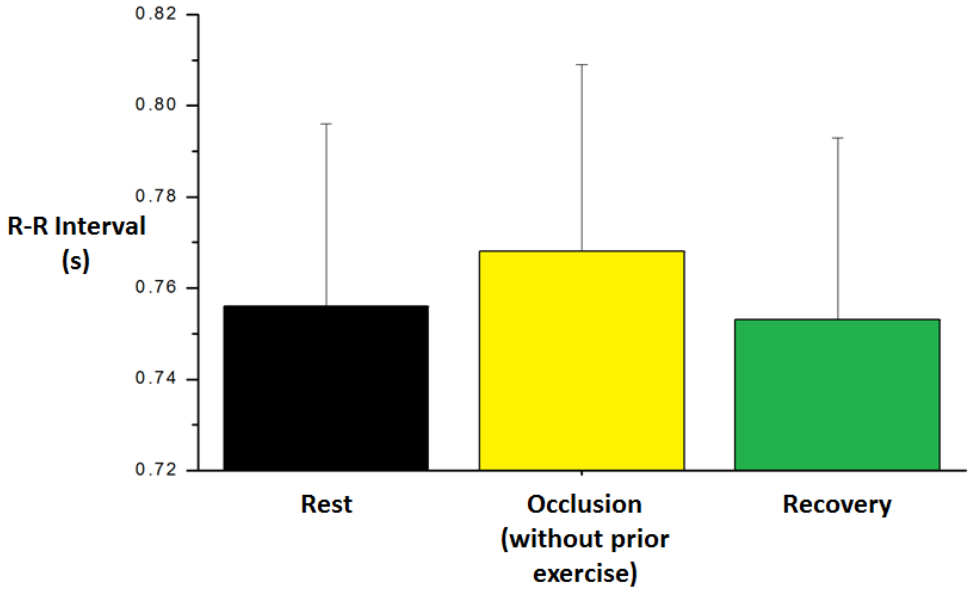

Figure 3.17 – *Graph showing no significant changes in R-R interval (i.e. no changes in heart rate) during occlusion without prior exercise, compared to rest. n = 36. Error bars represent standard error of the mean.*

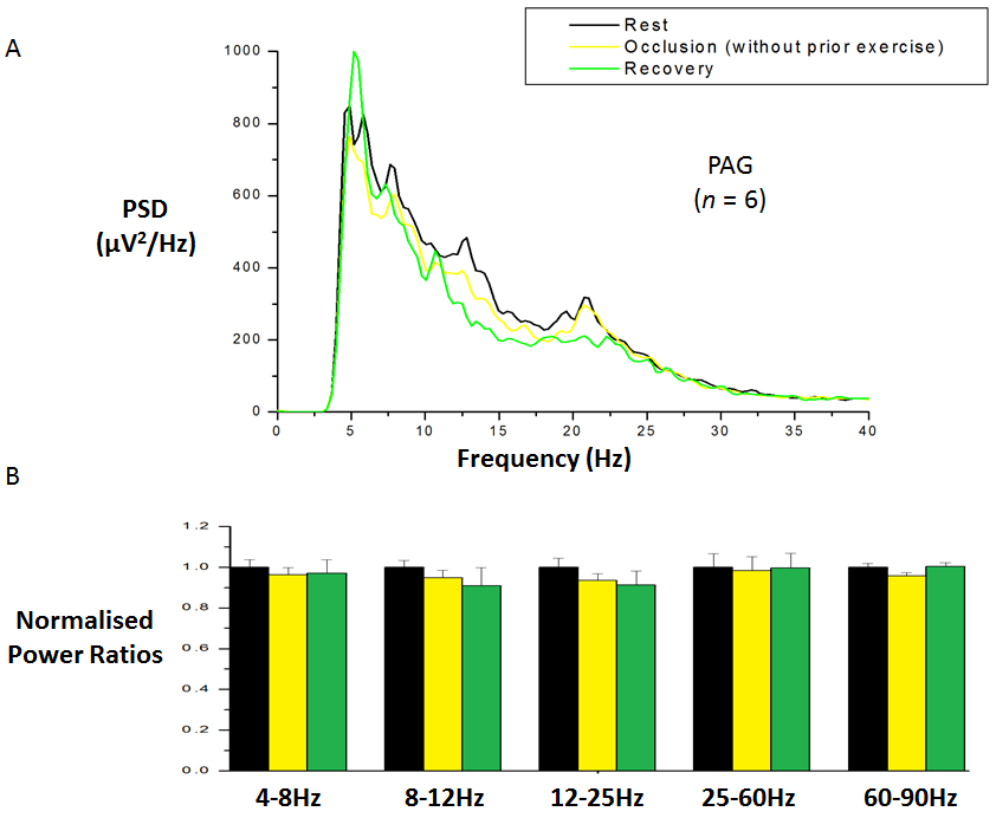

Figure 3.18 – *Graphs showing no significant changes in periaqueductal grey (PAG) neural activity during occlusion without prior exercise, compared to rest. (A) Mean power spectral density (PSD) for all six patients. (B) Normalised spectral changes (rest = 1.0) divided into frequency bands, showing no significant differences compared to rest. n = 6. Error bars represent standard error of the mean.*

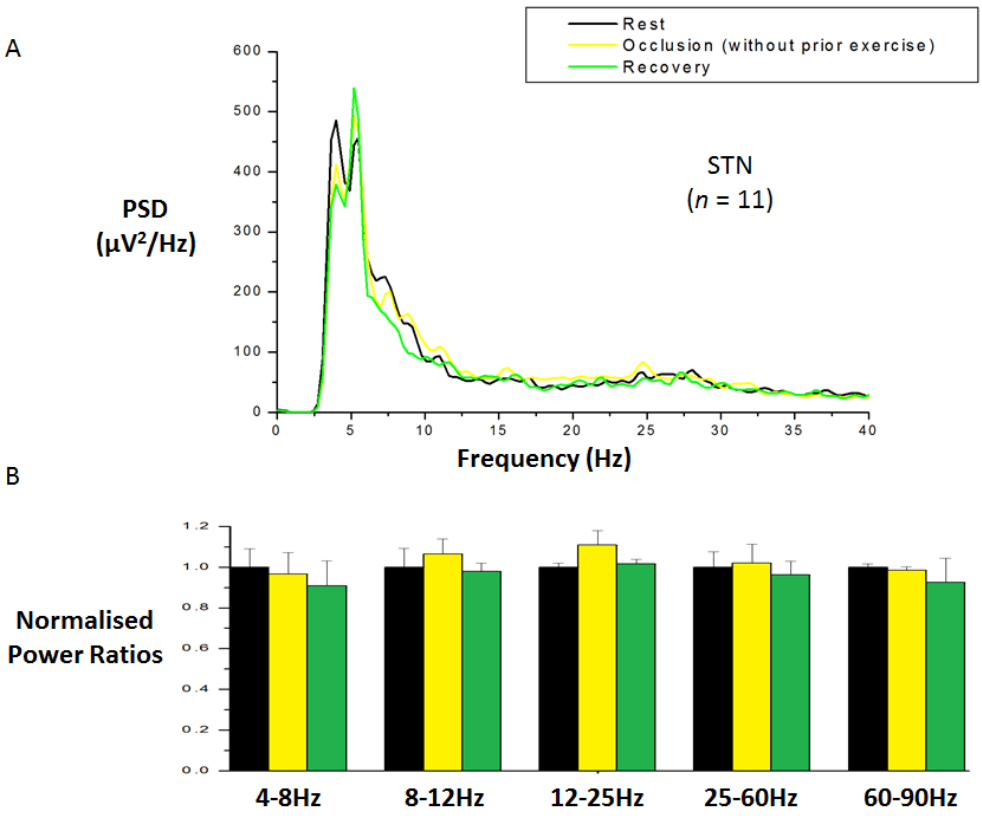

Figure 3.19 – *Graphs showing no significant changes in subthalamic nucleus (STN) neural activity during occlusion without prior exercise, compared to rest. (A) Mean power spectral density (PSD) for all eleven patients. (B) Normalised spectral changes (rest = 1.0) divided into frequency bands, showing no significant differences compared to rest. n = 11. Error bars represent standard error of the mean.*

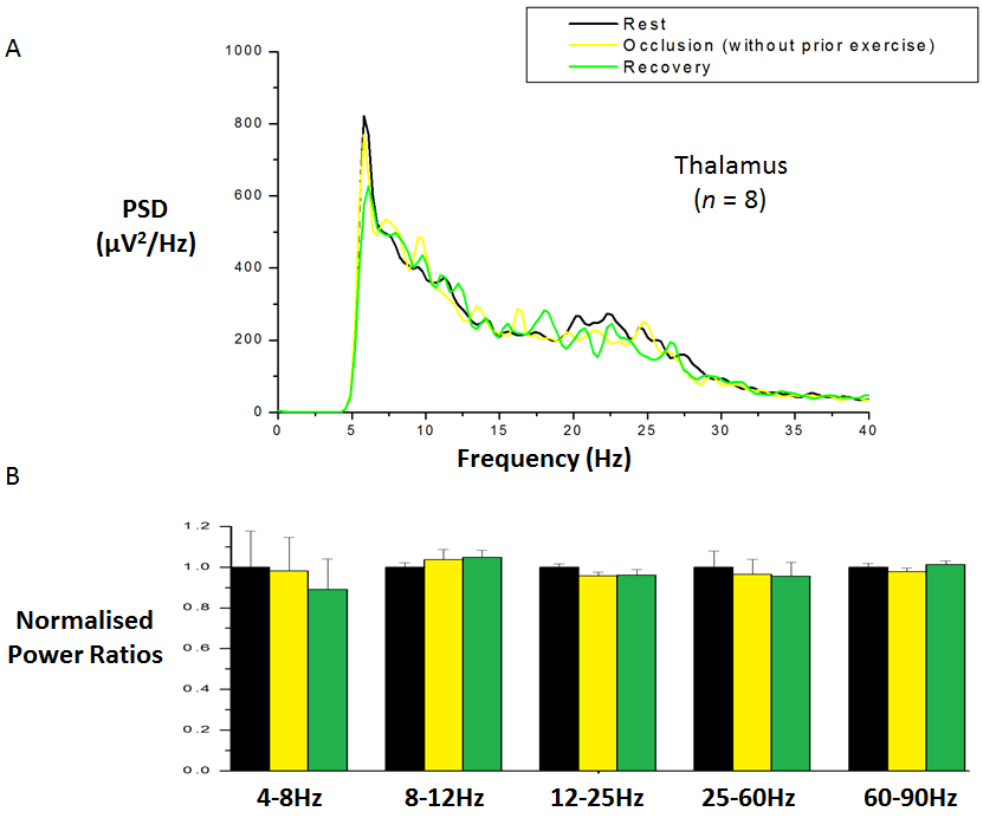

Figure 3.20 – *Graphs showing no significant changes in thalamic neural activity during occlusion without prior exercise, compared to rest. (A) Mean power spectral density (PSD) for all eight patients. (B) Normalised spectral changes (rest = 1.0) divided into frequency bands, showing no significant differences compared to rest. n = 8. Error bars represent standard error of the mean.*

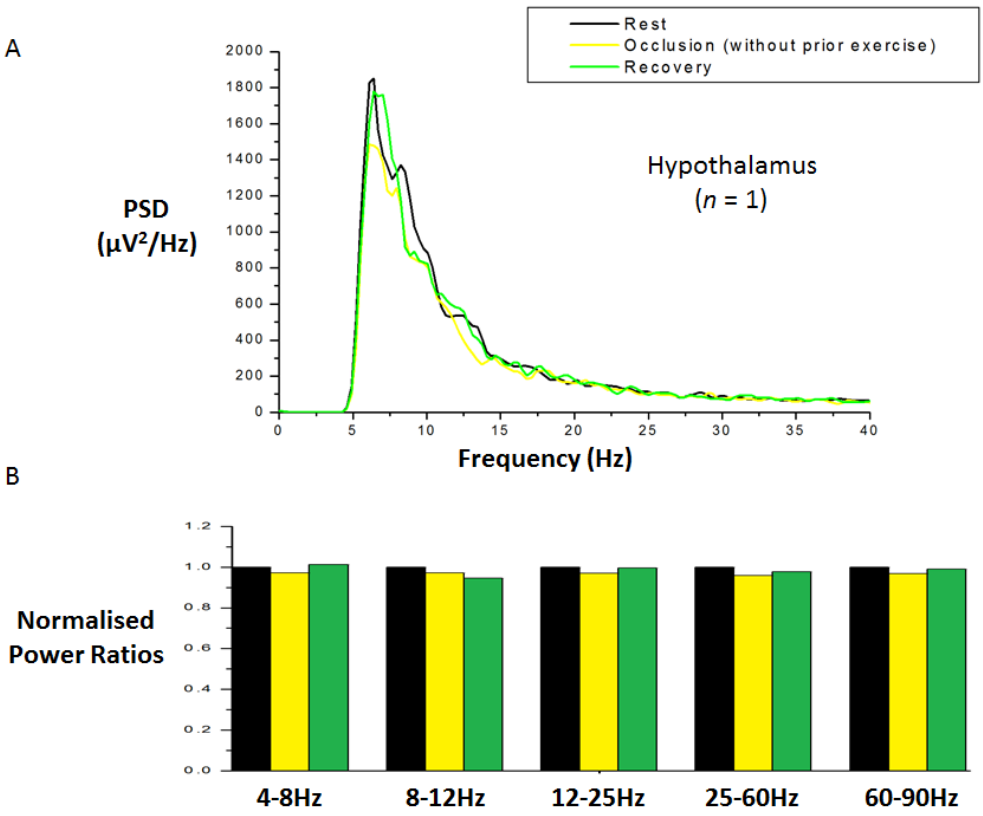

Figure 3.21 – *Graphs showing no significant changes in hypothalamic neural activity during occlusion without prior exercise, compared to rest. (A) Mean power spectral density (PSD) for the hypothalamus patient. (B) Normalised spectral changes (rest = 1.0) divided into frequency bands. n = 1.*

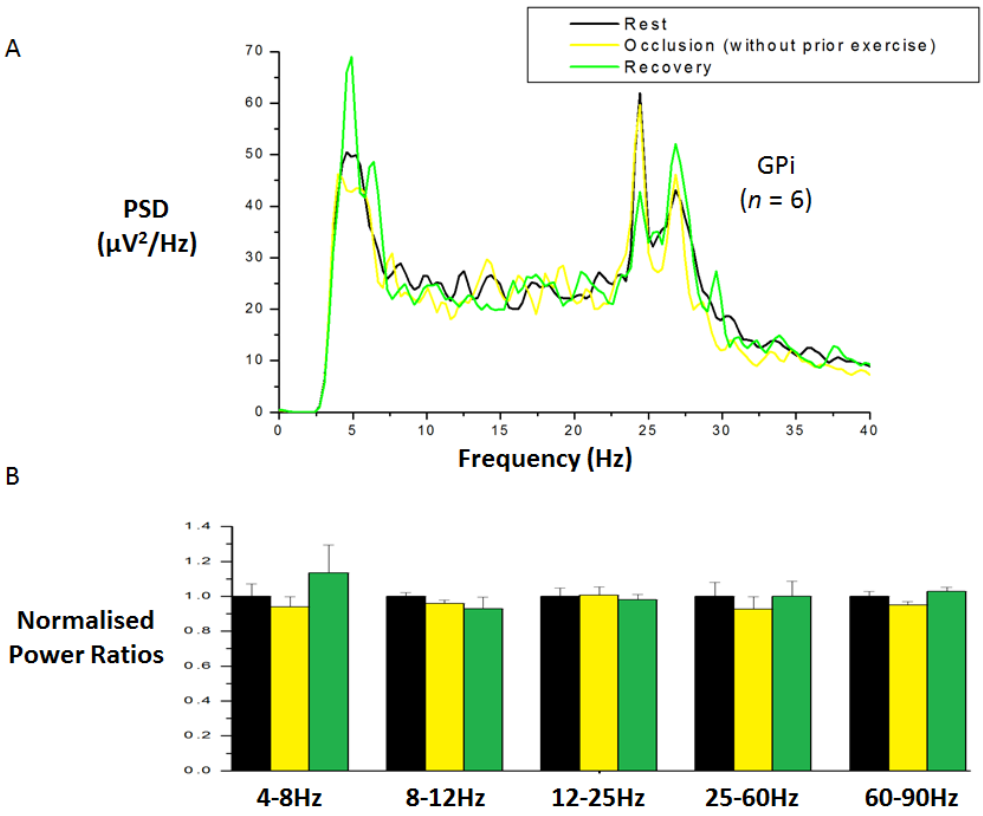

Figure 3.22 – *Graphs showing no significant changes in internal globus pallidus (GPi) neural activity during occlusion without prior exercise, compared to rest. (A) Mean power spectral density (PSD) for all six patients. (B) Normalised spectral changes (rest = 1.0) divided into frequency bands, showing no significant differences compared to rest. n = 6. Error bars represent standard error of the mean.*

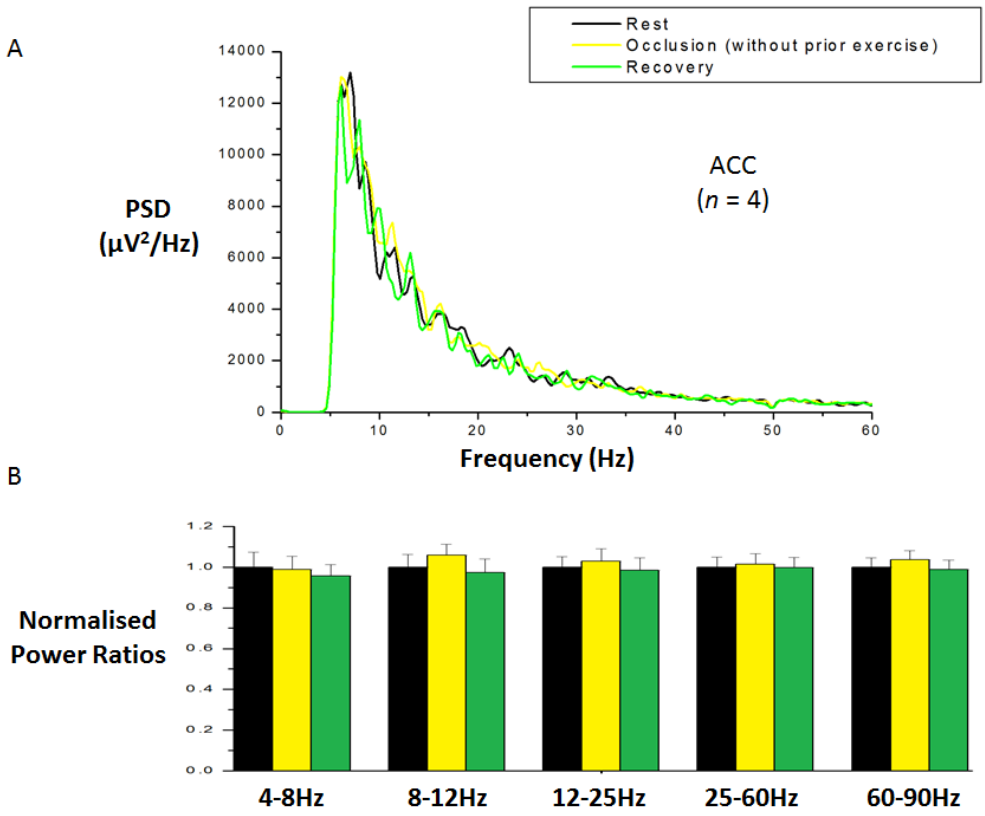

Figure 3.23 – *Graphs showing no significant changes in anterior cingulate cortex (ACC) neural activity during occlusion without prior exercise, compared to rest. (A) Mean power spectral density (PSD) for all four patients. (B) Normalised spectral changes (rest = 1.0) divided into frequency bands, showing no significant differences compared to rest. n = 4. Error bars represent standard error of the mean.*

Discussion

I have shown for the first time in humans that the exercise pressor reflex is associated with significantly increased neural activity in the dorsal periaqueductal grey (PAG), which is consistent with the hypothesis that the PAG is involved in the neurocircuitry of the reflex. The other sites that I investigated, which have been previously identified as cardiovascularly active in animals and in humans (Thornton *et al*, 2002), seem not to have a role in the integration of this reflex, as they are not activated during post-exercise occlusion. It is of note that the sensation of the cuff inflation itself does not correspond to a change in PAG activity, thus one

can be assured that the increase in activity seen during activation of the pressor reflex is not due to the actual method of occlusion.

Role of the Periaqueductal Grey in the Integration of the Exercise Pressor Reflex

My findings demonstrate a marked increase in neural activity in the PAG during post-exercise occlusion of the limb, across the 4-8 Hz, 8-12 Hz, and 12-25 Hz frequency bands. It should be noted that during the exercise period itself, the pressor reflex was probably not being activated, as the exercise was very light. This is exhibited by the fact that PAG activity did not increase during the 'light' exercise task, but only during the subsequent period of occlusion. The maintenance of the increase in arterial blood pressure is due to the retention of metabolites produced during exercise within the muscle. This occurs during post-exercise occlusion of the muscle, and would also occur during heavier exercise when the blood flow through the limb is insufficient to completely remove the newly formed metabolites. However, in this study, the blood flow through the limb during the exercise task would have been adequate, and the metabolites would have been removed before they could stimulate the group III and IV afferents to activate the reflex.

The PAG is recognised as a key neural structure for autonomic regulation, particularly for the cardiovascular changes that accompany integrated behavioural responses. It is a functionally heterogeneous structure divided into five columns, each of which is responsible for a distinct autonomic response. These columns are dorsomedial, dorsolateral, lateral, ventrolateral and ventromedial to the aqueduct. Stimulation of the ventral column of the PAG in rats is associated with decreased arterial blood pressure and analgesia (Johnson *et al*, 2004). In both cats and rats, microinjection of excitatory amino acids into the dorsolateral and lateral PAG columns elicits hypertension and tachycardia (Carrive *et al*, 1987). In contrast, excitation of the ventrolateral column elicits hypotension and bradycardia (Carrive and Bandler, 1991b).

Likewise, direct electrical stimulation of the dorsal PAG/PVG (periventricular grey) in humans evokes increased systolic blood pressure, whereas stimulation of the ventral PAG/PVG evokes decreased systolic blood pressure (Green *et al*, 2005).

Moreover, studies in animals have identified the PAG as having a role in the exercise pressor reflex itself. When the reflex is activated in rats performing dynamic treadmill exercise, c-Fos expression in PAG neurons increases (Iwamoto *et al*, 1996), and electrical stimulation of the ventral roots that supply the hind limb muscles in cats evokes increased PAG neuron discharge (Kramer *et al*, 1996). Muscle contraction in cats also increases the release of neuropeptide Y and enkephalin (Williams, 1996). When the results of this study are taken together with the well-recognised effects of excitation of the lateral PAG in animals and the effects of direct electrical stimulation of the dorsal PAG/PVG in humans, they offer strong evidence to suggest that the PAG is a key component of the neurocircuitry that is responsible for the integration of the exercise pressor reflex.

Williams and colleagues (Williams, 1985; Williams *et al*, 1987; Williams *et al*, 1992) proposed that the signal linking the muscle afferent pathway to the PAG was a catecholaminergic-opioidergic interaction, responsible for integrating the peripheral sensory traffic received from exercising muscle. Clonidine injected into the dorsolateral PAG in cats was shown to attenuate the muscle pressor reflex (Williams, 1985). This effect was prevented by naloxone, suggesting an interaction with the adrenergic-opioidergic system (Williams *et al*, 1987). The same group provided evidence to show increased levels of immunoreactive enkephalinergic substances in the dorsolateral PAG in cats made to perform fatiguing isometric contractions (Williams *et al*, 1992). This could provide an excitatory transmitter link, as it is well-recognised that the PAG projects to the classical cardiovascular medullary sites (Lovick, 1985; Carrive *et al*, 1989). Lesioning the PAG abolishes the increase in arterial blood pressure resulting from muscle

contraction (Williams *et al*, 1990). Likewise, lesioning the ventrolateral medulla in rats abolishes the cardiovascular responses evoked by stimulation of the dorsal PAG (Lovick, 1985).

Role of the Subthalamic Nucleus in the Integration of the Exercise Pressor Reflex

The decrease in activity of the subthalamic nucleus (STN) in the 12-25 Hz frequency band during exercise and post-exercise occlusion is consistent with evidence showing suppression in STN activity following warning and 'go' cues (Kuhn *et al*, 2004; Green *et al*, 2007). The increase in STN activity during exercise in the 60-90 Hz band is also consistent with what Green *et al* (2007) observed when they asked subjects to perform bouts of cycle ergometry. However, there was no change in STN activity in the 60-90 Hz band during activation of the exercise pressor reflex (i.e. during post-exercise occlusion). The decrease in STN activity during exercise in the 12-25 Hz frequency band suggests that there is a release of the inhibitory drive on the cardiovascular nuclei which receive projections from the STN, resulting in an increase in heart rate and arterial blood pressure.

Stimulation of the STN (depolarising block) in humans results in increased arterial blood pressure, increased heart rate, and facilitation of movement (Thornton *et al*, 2002). Although the STN is recognised as a cardiovascularly active area, the data suggest that it is not a major integrating site of the exercise pressor reflex itself. The decrease in STN activity during exercise in the 12-25 Hz frequency band could potentially be due to the 'central command component' of the cardiovascular response to exercise, and the increase in activity in the 60-90 Hz band during exercise could be due to the locomotion during the exercise itself (discussed in Chapter 5).

Limitations

The results of this study pose the question: do changes in power spectral density directly translate into neural activity changes? Local field potentials (LFPs) are thought to be a consequence of local synchronous neuronal population activity, rather than isolated spikes or asynchronous activity (Mitzdorf, 1985; Rasch *et al*, 2009). Therefore, the increase in periaqueductal grey (PAG) activity, as measured in terms of LFPs during the exercise pressor reflex, is likely to reflect an increase in network size or network synchrony (Logothetis *et al*, 2001; Katzner *et al*, 2009; Kelly *et al*, 2010).

It could be debated that one cannot be sure whether the increase in PAG neural activity is causal to the exercise pressor reflex, compensatory to the reflex, or purely coincidental due to perceptual aspects of the exercise task. However, it is highly unlikely that the activity is purely coincidental, due to the fact that the increase in activity was only observed during occlusion following an exercise period, and never observed during occlusion without prior exercise. There is also evidence to oppose the idea that the increase in activity was a compensatory response to the exercise pressor reflex – Williams *et al* (2000) demonstrated in cats that increasing arterial blood pressure with phenylephrine had no effect on c-Fos immunoreactivity in the PAG. However, it did increase immunoreactivity in other cardiovascularly active brainstem areas. On the other hand, Murphy *et al* (1995) reported that both phenylephrine and nitroprusside elicited Fos expression in the PAG. Nevertheless, the increase in PAG activity demonstrated in this study was only observed during the post-exercise occlusion period, and not during the exercise period itself, even though the blood pressure increase was greater during the exercise period than during the post-exercise occlusion period. Thus, it is very unlikely that the PAG activity increase is secondary to the arterial blood pressure increase. Furthermore, in humans, direct electrical stimulation of the dorsal PAG/PVG (periventricular grey) is known to cause an increase in arterial blood pressure (Green *et al*, 2005).

It could also be argued that the changes in activity that I observed in the PAG could be related to anxiety, fear or a 'stress' response (Nashold *et al*, 1969). However, none of these reactions were observed in any of my patients during the experiments. A further limitation to be considered is that I was working with a patient model with underlying pathologies. Even though patients with PAG electrodes have an idiopathic presentation of pain, there is no indication that the PAG, or even the autonomic nervous system, are dysfunctional in these subjects. Due to the nature of the study, I was also limited in terms of the specific nuclei that I could record from, as the sites that I investigated were targeted on the basis of best therapeutic outcome given the pathology of each subject. Even so, the areas that I was able to investigate have been clearly described in animal models as being cardiovascularly active.

Compared to the size of some of the neural sites that were targeted, the deep brain stimulating electrodes were quite large, thus it was difficult to be entirely accurate about the exact location of the electrodes without histology. Another possible limitation was that I could have been recording activity from axons of passage, as opposed to the PAG neurons themselves. However, the electrodes were implanted by neurosurgeons using very precise stereotactic coordinates. For the PAG electrodes, I conducted postoperative localisation analysis to further verify their locations within the dorsal region of the PAG.

Lastly, the particular exercise task that was undertaken by the subjects and its fairly low intensity could possibly have underestimated the complete range of the increase in power that was potentially available from the PAG. The exercise task was purposely designed to be of low intensity as the majority of subjects did not feel capable of performing high intensity exercise tasks so soon after their surgery.

Conclusion

In conclusion, using direct neurophysiological recordings, this study provides the first direct evidence to suggest that the dorsal PAG is a key component of the neurocircuitry responsible for integrating the exercise pressor reflex in humans.

CHAPTER 4

Do Changes in Exercise Intensity Affect Neurocircuitry Involved In the Exercise Pressor Reflex?

Introduction

Cardiovascular Responses to Increased Exercise Intensity

It is known that during dynamic exercise cardiovascular responses increase with the intensity of the exercise task. When Alam and Smirk (1937) proposed that the exercise pressor reflex was partially responsible for the cardiovascular responses to exercise, they also observed that the extent of the resulting increase in blood pressure depended on the amount of work carried out. The subjects in their study were asked to raise and lower a weight using their forearm muscles. The number of muscular efforts and the distance which the weight was lifted was kept constant. However, the weight to be lifted varied between 0.5 kg and 5 kg. As the weight increased, so did the extent of the arterial blood pressure increase. Coote *et al* (1971) used anaesthetised cats to demonstrate that tetanic contractions of the hind limb muscles, elicited by stimulation of the ventral roots, caused an increase in arterial blood pressure, and that with tetani of different intensities, the magnitude of the pressor response increased as the tension increased. Strange *et al* (1993) also demonstrated this direct relationship between exercise intensity and cardiovascular response in humans. Not only did they show a graded increase in blood pressure to exercise intensity, but also in heart rate, cardiac output and systemic vascular conductance.

Gandevia *et al* (1993) studied artificially ventilated human subjects who had undergone total neuromuscular blockade. During paralysis, they noted marked increases in arterial blood pressure and heart rate during attempted isometric contractions of the arm, leg and trunk

muscles. When the subjects attempted handgrip contractions, the increases in mean arterial pressure and heart rate were comparable to those observed during actual handgrip contractions. It was found that these increases in cardiovascular parameters are graded according to the intensity of the contraction. If this is the case for the central command component of the cardiovascular responses to exercise, it follows that the exercise pressor reflex could also be graded to exercise intensity.

Wiles *et al* (2008) asked human subjects to perform incremental isometric exercise tests involving seated double-leg knee extensions. They calculated each subject's maximum voluntary contraction and determined corresponding peak electromyographic activity. The exercise test ranged from 10%-30% of the peak activity. Linear relationships were observed between the percentage of peak activity and heart rate, and also between percentage of peak activity and systolic blood pressure. Bailey *et al* (2008) examined brain activity in humans during a graded exercise task. Exercise intensity was steadily increased while electroencephalography was measured from different sites on the scalp. They observed a significant increase in brain activity above 200 W that continued through until the post-exercise period.

Cardiovascular Responses to Ischaemic Exercise

It is also known that the cardiovascular response to exercise is greater when the arterial supply to exercising muscles is occluded compared to exercise under normal blood flow conditions (Mitchell, 1985), suggesting that the activity of the nerve afferents originating in the exercising muscle is increased during ischaemic exercise compared to non-ischaemic exercise. Bessou and Laporte, in 1958, recorded action potentials from non-myelinated (group IV) afferent nerve fibres in cats and showed that a considerable number of them were only activated by ischaemic contractions (*see* Mense and Stahnke, 1983). Coote *et al* (1971) further

showed that contraction of the hind limb muscles resulted in an increase in arterial blood pressure, and that this pressor response was potentiated by occluding the blood circulation through the exercising muscles. Not only has the potentiating effect of ischaemia been shown in anaesthetised animals, but it has also been shown in humans (Alam and Smirk, 1937; McCloskey and Mitchell, 1972).

Remote Ischaemic Preconditioning

When the blood supply to tissues or organs in the body is occluded (e.g. during myocardial infarction), the resulting lack of oxygen can eventually lead to cell death. In order to prevent this and limit the size of the infarct, it is vital to re-establish the blood flow and 'reperfuse' the tissue. However, the reperfusion of ischaemic tissue can be equally damaging to the myocardium as the ischaemia itself (Grace, 1994). In the context of myocardial infarction, this phenomenon is known as 'lethal myocardial reperfusion injury' (Murry *et al*, 1986).

The term 'ischaemic preconditioning' was coined by Murry *et al* in 1986. They used a canine model of myocardial infarction to demonstrate that multiple brief ischaemic episodes prior to a sustained ischaemic insult provided a protective effect on the heart against reperfusion injury, by significantly limiting the size of infarcts. Schott *et al* (1990) used a porcine model, and demonstrated that preconditioning had the same cardio-protective effect following a prolonged period of ischaemia. Ischaemic preconditioning has also been shown to result in improved ventricular wall motion following an ischaemic insult in rabbits (Cohen *et al*, 1991) and in rats (Yellon *et al*, 1992).

Although ischaemic preconditioning proved to be successful in limiting damage to the myocardium following sustained ischaemia and reperfusion, the method would not have been viable in a clinical scenario as the procedure would have had to have been highly invasive in order to access a major coronary artery. The experiments of Przyklenk *et al* (1993) were

paramount in being able to translate ischaemic preconditioning into clinical practice. They subjected the circumflex coronary artery of anaesthetised dogs to the ischaemic preconditioning stimulus, and found that remote virgin myocardium supplied by the left anterior descending artery was also protected against reperfusion injury. Their experiments were the first to explore the potential of preconditioning from a remote arterial location not directly supplying the myocardial tissue. Birnbaum *et al* (1997) demonstrated that myocardial infarct size was reduced following preconditioning of the hind limb skeletal muscle in anaesthetised rabbits. Gho *et al* (1996) observed that preconditioning of both the anterior mesenteric artery and the left renal artery in rats offered myocardial protection against reperfusion injury. This has become known as 'remote ischaemic preconditioning' (RIPC).

RIPC was introduced into clinical practice by Kharbanda *et al* (2002). They were able to demonstrate reduced endothelial reperfusion injury following a prolonged period of ischaemia in the forearms of humans who had had their contralateral forearms preconditioned, compared to the forearms of humans who had had no preconditioning. Additionally, they used a porcine model to demonstrate that preconditioning the lower limb could provide cardio-protection following sustained occlusion and reperfusion of the left anterior descending artery. Clinical trials of RIPC induced by inflation and deflation of a cuff around the upper or lower limb have revealed a significant reduction in myocardial injury during cardiac surgery in both adults (Hausenloy *et al*, 2007) and children (Cheung *et al*, 2006).

The pathway by which the signal from the remote preconditioned tissue is carried to the myocardium remains undetermined. There is evidence to support the existence of both a humoral pathway and a neurogenic pathway (Kharbanda *et al*, 2009; Lim *et al*, 2010). In 1999, Dickson *et al* collected effluent from donor rabbit hearts during RIPC. They found that when this effluent was transfused to acceptor rabbit hearts that had not been preconditioned (even remotely), there was a decrease in mean infarct size following sustained ischaemia, compared

to when using control donor hearts or control acceptor hearts. This suggested that the remote protection was initiated by a humoral mechanism. There has also been evidence that this cardioprotective effect is transferable across species (Shimizu *et al*, 2009).

On the other hand, studies using autonomic ganglion blockers have provided evidence for a neurogenic pathway. Gho *et al* (1996) used anaesthetised rats to show that the cardioprotective effect of remote preconditioning of anterior mesenteric artery could be blocked on application of hexamethonium. Similar results, again using a rat model, were demonstrated by Wolfrum *et al* (2002), and by Loukogeorgakis *et al* (2005) in humans using Trimetaphan as a ganglion blocker. Adenosine (Liem *et al*, 2002) and bradykinin (Schoemaker *et al*, 2000) have both been implicated as having a role in initiating the neurogenic pathway, as both successfully induced a cardioprotective effect in rats when infused into the mesenteric artery. In both cases, this effect was abolished by pre-treatment with hexamethonium.

The involvement of a neurogenic pathway in carrying the RIPC signal implies that central neurocircuitry could be involved in its mechanism. The exercise pressor reflex can be induced by a state of ischaemia in skeletal muscle, equivalent to the effects of inflating and deflating a cuff around a limb, i.e. RIPC. It is possible that the neurocircuitry involved in mediating the exercise pressor reflex could also be involved in the transduction of the RIPC signal.

The aim of the experiments in this chapter were two-fold: (1) to investigate whether the changes in the cardiovascular neurocircuitry that occur during the exercise pressor reflex are graded to exercise intensity, and (2) to establish whether specific cardiovascular sites in the brain have a role in the transduction of the RIPC stimulus from remote tissue to the myocardium. Local field potentials were recorded from specific nuclei (which had previously been identified as cardiovascularly active) in deep brain stimulation patients. The recordings were used to test the hypotheses that (1) neural activity in the periaqueductal grey is graded to increases in exercise intensity and corresponding increases in blood pressure, and (2) neural

activity in particular subcortical structures corresponds to the cardioprotection offered following preconditioning of the upper limb.

Methods

Twenty-four patients (18 male, 16 female), with a mean age of 53.9 years (range 31-71 years) were recruited for this study. Ten of these patients (6 male, 4 female, mean age 53.0 years) performed the increased intensity exercise protocol (Table 4.1). Three patients had electrodes implanted in the periaqueductal grey (PAG) for the treatment of chronic pain (mean age 53.0 years), a further three patients had electrodes in the sensory thalamus, also for the treatment of chronic pain (mean age 43.3 years), another two patients had electrodes in the subthalamic nucleus (STN) for the treatment of Parkinson's disease (mean age 65.0 years), and two patients had electrodes in the internal globus pallidus for the treatment of generalised dystonia (mean age 55.5 years). Five patients in total performed the ischaemic exercise protocol (3 male, 2 female, mean age 55.6 years) (Table 4.2). Three of these patients had electrodes implanted in the PAG (mean age 56.3 years), and two patients had electrodes in the sensory thalamus (mean age 54.5 years). Nine patients were recruited to perform the remote ischaemic preconditioning (RIPC) protocol (9 male, mean age 54.0 years) (Table 4.3). Two of these patients had electrodes implanted in the PAG (mean age 58.5 years), a further three patients had electrodes in the sensory thalamus (mean age 59.7 years), and four patients had electrodes in the STN (mean age 47.5 years).

The experiments were conducted within the first week following stage 1 of the deep brain stimulation surgical procedure, while the electrodes were still externalised. For the entire duration of the experiments, the patients' stimulation was turned off. The increased intensity exercise protocol was as follows (Fig. 4.1): each patient was asked to sit comfortably and had a weight of 2 kg attached to their right wrist. For the first part of the protocol, cardiovascular

parameters and neural activity were recorded for a rest period of three minutes. After the rest period, the patient began exercising following an oral cue. The exercise task consisted of bicep curls at a rate of 30-60 per minute, according to each patient's fitness and capabilities. After two minutes, the patient was asked to stop exercising, and a blood pressure cuff around the exercised arm was immediately inflated to above systolic pressure (approximately 200 mmHg). The cuff was kept inflated for a two minute period, and then released. The patient was allowed a recovery period of one minute. The protocol was then repeated twice more, for a total of three sets of recordings, in order to confirm the consistency of the response. For the second part of the protocol, the previous protocol was repeated three times, except with 4 kg of weight attached to the patient's wrist. If responses were consistent for each weight, the data were averaged together to give two sets of results for each patient (one set of results for 2 kg exercise and one set of results for 4 kg exercise).

Table 4.1 – *Subject characteristics for increased intensity exercise pressor reflex experiments. PAG, periaqueductal grey; STN, subthalamic nucleus; GPi, internal globus pallidus.*

Patient	***Age (years)***	***Sex***	***Diagnosis***	***DBS Electrode Location***
1	69	M	Chronic left arm pain from brachial plexus injury	PAG
2	31	M	Severe intractable left arm pain from brachial plexus injury	PAG
3	59	F	Right-sided anaesthesia dolorosa & neuropathic tongue pain	PAG
4	40	M	Right leg pain secondary to crush injury from industrial accident	Sensory Thalamus
5	31	M	Severe intractable left arm pain from brachial plexus injury	Sensory Thalamus
6	59	F	Right-sided anaesthesia dolorosa & neuropathic tongue pain	Sensory Thalamus
7	63	M	Parkinson's disease	STN
8	67	M	Parkinson's disease	STN
9	58	F	Cervical dystonia	GPi
10	53	F	Cervical dystonia	GPi

The patients were also asked to perform three sets of a control experiment, in which the blood pressure cuff was inflated without prior exercise (Fig. 4.2). This was in order to determine whether any changes in neural activity that might be observed during the period of cuff

inflation were not due to the sensation of the cuff inflation itself. If the responses were consistent across the three repeats, the results were averaged together to give one set of results per patient.

Table 4.2 – *Subject characteristics for ischaemic exercise pressor reflex experiments. PAG, periaqueductal grey.*

Patient	***Age (years)***	***Sex***	***Diagnosis***	***DBS Electrode Location***
1	62	M	Chronic pain following stroke	PAG
2	59	F	Right-sided anaesthesia dolorosa & neuropathic tongue pain	PAG
3	48	M	Chronic left arm pain from brachial plexus injury	PAG
4	50	M	Chronic pain following stroke	Sensory Thalamus
5	59	F	Right-sided anaesthesia dolorosa & neuropathic tongue pain	Sensory Thalamus

Table 4.3 – *Subject characteristics for remote ischaemic preconditioning experiments. PAG, periaqueductal grey; STN, subthalamic nucleus.*

Patient	***Age (years)***	***Sex***	***Diagnosis***	***DBS Electrode Location***
1	46	M	Phantom limb pain in amputated left arm	PAG
2	71	M	Chronic right-sided pain following vertebral artery dissection	PAG
3	62	M	Central pain syndrome following intra-cerebral bleed	Sensory Thalamus
4	46	M	Phantom limb pain in amputated left arm	Sensory Thalamus
5	71	M	Chronic right-sided pain following vertebral artery dissection	Sensory Thalamus
6	55	M	Parkinson's disease	STN
7	44	M	Parkinson's disease	STN
8	51	M	Parkinson's disease	STN
9	40	M	Parkinson's disease	STN

The ischaemic exercise protocol was as follows (Fig. 4.3): each patient was asked to sit comfortably and had a weight of 2 kg attached to their right wrist. Cardiovascular parameters and neural activity were recorded for a rest period of three minutes. After the rest period, the patient began exercising following an oral cue. The exercise task was the same as that described above (bicep curls). After two minutes of exercise, a blood pressure cuff was inflated around the exercising arm to above systolic pressure, and the patient was asked to *continue*

exercising for a further two minutes. After this, the cuff was released and the patient was allowed to rest for a recovery period of one minute. The protocol was then repeated twice more, for a total of three sets of recordings. If the response was consistent, the results were averaged together to give one set of results for each patient.

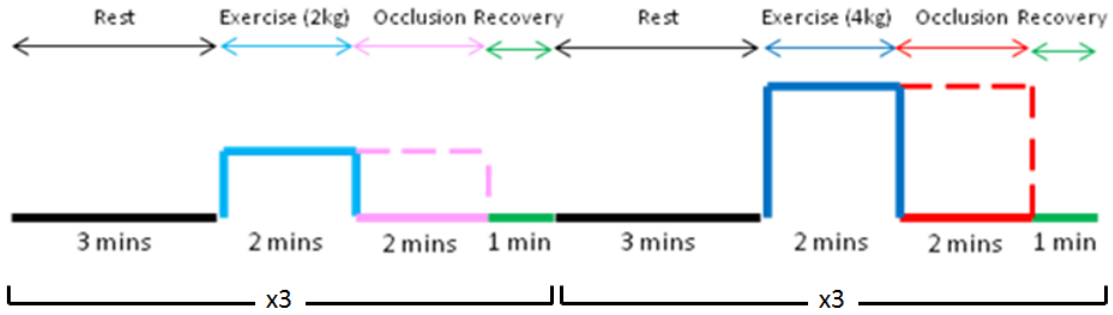

Figure 4.1 – *Protocol for increased intensity exercise experiment. The vertical axis represents the level of activity. The solid lines show the actual level of activity of the patient and the dotted lines represent the continued stimulation of the exercise pressor reflex, even though activity has stopped.*

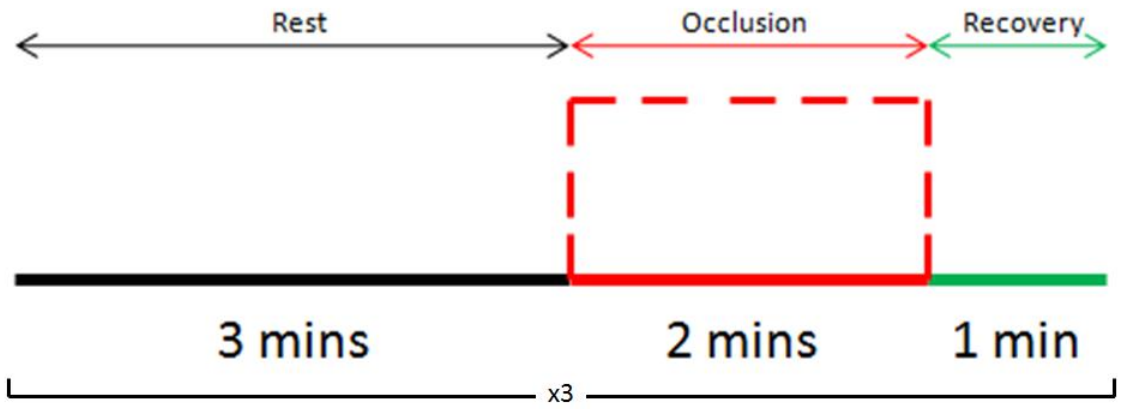

Figure 4.2 – *Protocol for the control experiment to determine whether neural activity might be due to the sensation of the occlusion. The vertical axis represents the level of activity. The solid lines represent the activity level of the patient and the dotted lines represent the potential changes in both neural and cardiovascular parameters during occlusion.*

These patients were also asked to perform three sets of the control experiment, in which the blood pressure cuff was inflated without prior exercise (Fig. 4.2).

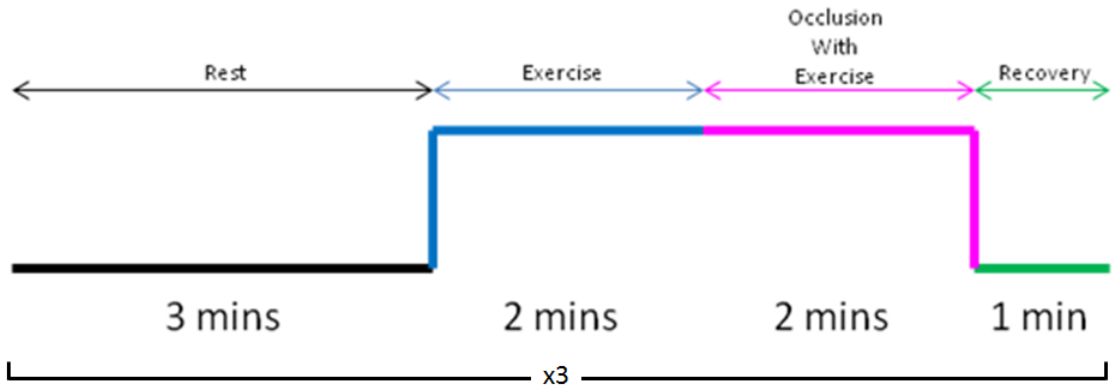

Figure 4.3 – *Protocol for the ischaemic exercise experiment. The vertical axis represents the level of activity. The solid lines show the level of activity of the patient.*

The RIPC protocol was as follows (Fig. 4.4): each patient was asked to sit comfortably and had a weight of 2 kg attached to their right wrist. Cardiovascular parameters and neural activity were recorded for a rest period of five minutes. After the rest period, the patient began exercising following an oral cue. The patient was asked to perform the same exercise task as that described above (two minutes of bicep curls). The patient was asked to perform this task a total of three times, with a one minute recovery period between each exercise period. A blood pressure cuff was then inflated around the right upper arm to above systolic pressure for five minutes, in order to cause ischaemia. After this, the cuff was released, and five minutes of reperfusion followed. This ischaemia-reperfusion was repeated three more times, and constituted the RIPC stimulus. The patient was then asked to exercise again for three two-minute periods, each separated by one minute of recovery time.

All patients who participated in any of the three protocols were asked to rate their levels of pain throughout the duration of the experiments using the Visual Analog Pain Severity Scale (VAPSS), in order to determine whether changes in neural activity could be due to the patients' pathology (for example, pain in PAG patients), as opposed to the neural responses to exercise. Data segments in which the VAPSS score changed were then excluded from analysis.

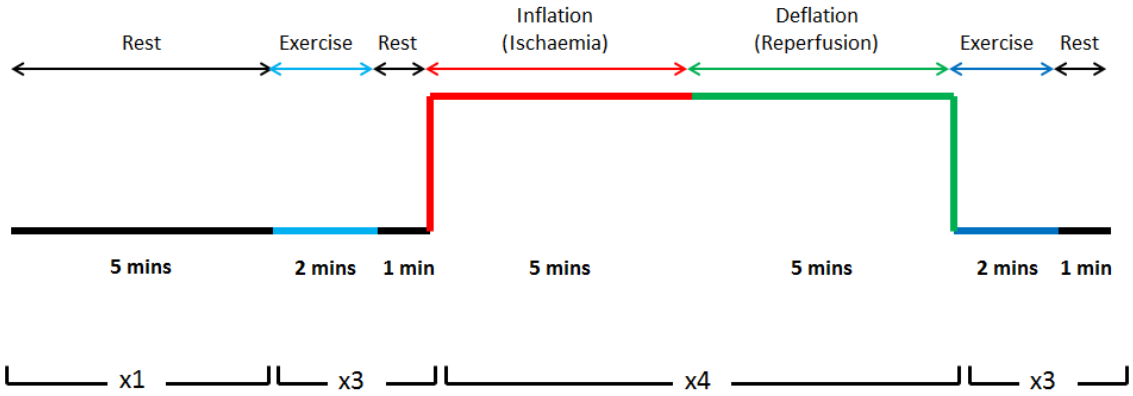

Figure 4.4 – *Protocol for the remote ischaemic preconditioning experiment. The raised lines indicate the ischaemic preconditioning stimulus.*

Results

Increased Intensity Exercise Protocol

Cardiovascular Parameters

In all of the ten patients from whom data were measured, mean arterial blood pressure (MABP) increased upon exercise, remained elevated during post-exercise occlusion, and returned to baseline within the recovery period, regardless of whether 2 kg exercise or 4 kg exercise was being performed. Furthermore, in all patients, MABP increased further during the 4 kg exercise compared to the 2 kg exercise. The data for all of the patients were averaged together (Fig. 4.5). The average increase in MABP during 2 kg exercise was 17.0 ± 3.6 mmHg ($P < 0.001$, $n = 10$), equivalent to an increase of 18.2%. During the post-exercise occlusion period following the 2 kg exercise, the average increase from rest in MABP was 12.3 ± 3.1 mmHg ($P < 0.001$, $n = 10$), equivalent to an increase of 13.2%. On recovery, there was an average increase from rest of 1.2 ± 1.0 mmHg (equivalent to a 1.2% increase). However, there was no significant difference between the initial rest period and the recovery period ($P = 0.248$, $n = 10$). The average increase in MABP during 4 kg exercise was 22.5 ± 3.0 mmHg ($P < 0.001$, $n = 10$), equivalent to an increase of 24.1%. During the post-exercise occlusion period following the 4

kg exercise, the average increase from rest in MABP was 16.7 ± 8.4 mmHg (P < 0.001, *n* = 10), equivalent to an increase of 17.9%. On recovery, there was an average increase from rest of 1.0 ± 0.8 mmHg (equivalent to a 1.1% increase) and, once again, there was no significant difference between the initial rest period and the recovery period (P = 0.612, *n* = 10).

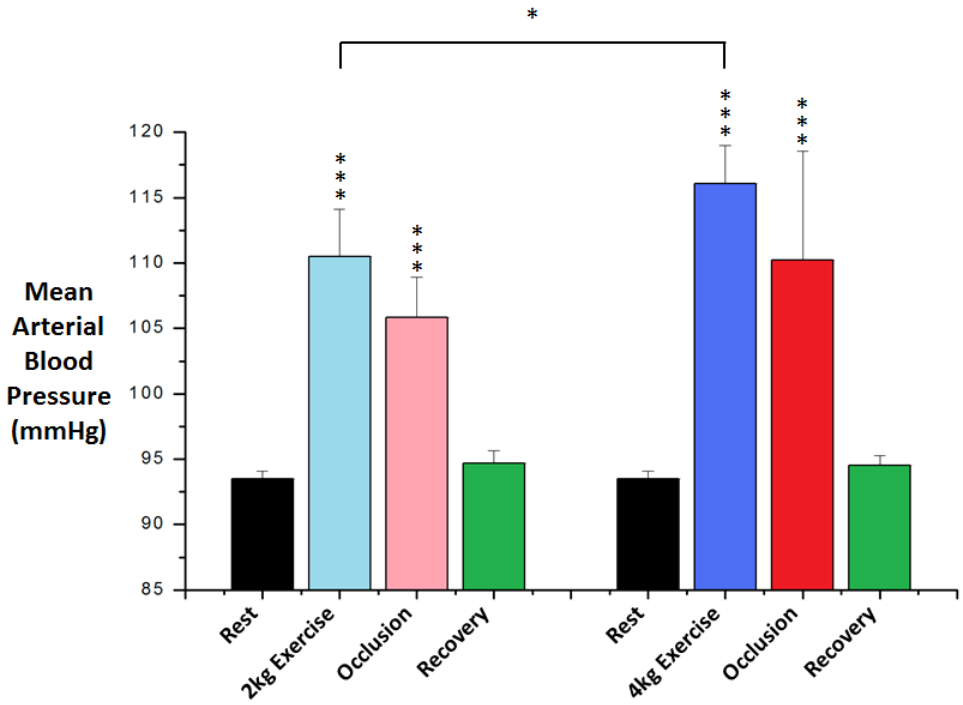

Figure 4.5 *– Graph showing significant increases in mean arterial blood pressure with 2 kg exercise, 4 kg exercise and both corresponding periods of post-exercise occlusion, compared to rest. There is also a significant difference between mean arterial blood pressure with 2 kg exercise and mean arterial blood pressure with 4 kg exercise. n = 10, * P < 0.05, *** P < 0.001. Error bars represent standard error of the mean.*

The changes in MABP were accompanied by analogous changes in systolic blood pressure (SBP) and diastolic blood pressure (DBP) (Fig. 4.6). The average increase in SBP during 2 kg exercise was 25.3 ± 3.7 mmHg (P < 0.001, *n* = 10), equivalent to an increase of 19.7%. During post-exercise occlusion following 2 kg exercise, the average increase from rest in SBP was 15.1 ± 2.1 mmHg (P < 0.001, *n* = 10), equivalent to an increase of 11.7%. On recovery there was an average increase from rest of 4.0 ± 5.0 mmHg (equivalent to a 3.2% increase). However, there

was no significant difference between the initial rest period and the recovery period (P = 0.476, *n* = 10). The average increase in SBP during 4 kg exercise was 28.9 ± 4.7 mmHg (P < 0.001, *n* = 10), equivalent to an increase of 22.2%. During post-exercise occlusion following 4 kg exercise, the average increase from rest in SBP was 19.3 ± 5.1 mmHg (P < 0.001, *n* = 10), equivalent to an increase of 14.9%. On recovery there was an average increase from rest of 8.6 ± 7.6 mmHg (equivalent to a 6.6% increase). However, there was no significant difference between the initial rest period and the recovery period (P = 0.172, *n* = 10). The average increase in DBP during 2 kg exercise was 8.4 ± 1.7 mmHg (P < 0.001, *n* = 10), equivalent to an increase of 10.3%. During post-exercise occlusion following 2 kg exercise, the average increase from rest in DBP was 1.9 ± 1.2 mmHg (equivalent to an increase of 2.3%). However, this was not significant (P = 0.077, *n* = 10). On recovery there was an average increase from rest of 0.8 ± 1.2 mmHg (equivalent to a 1.0% increase), which was also insignificant (P = 0.858, *n* = 10). The average increase in DBP during 4 kg exercise was 10.9 ± 1.7 mmHg (P < 0.001, *n* = 10), equivalent to an increase of 13.3%. During post-exercise occlusion following 4 kg exercise, the average increase from rest in DBP was 7.1 ± 2.7 mmHg (P < 0.001, *n* = 10), equivalent to an increase of 8.7%. On recovery there was an average increase from rest of 1.0 ± 0.5 mmHg (equivalent to a 1.3% increase). However, this was not significant (P = 0.657, *n* = 10).

All ten patients who performed the experiment had a significantly decreased R-R interval during the exercise period, but not during the post-exercise occlusion or recovery periods. The R-R interval data for all ten patients were averaged together (Fig. 4.7). The decrease from rest during 2 kg exercise was 0.037 ± 0.006 s (P < 0.001, *n* = 10), equivalent to a decrease of 4.1%. During the post-exercise occlusion period following 2 kg exercise, there was an insignificant decrease from rest of 0.000 ± 0.005 s (equivalent to 0.0%, P = 0.873, *n* = 10), and an insignificant increase from rest of 0.006 ± 0.006 s (equivalent to 0.7%, P = 0.378, *n* = 10) during the recovery period. The decrease from rest during 4 kg exercise was 0.044 ± 0.003 s (P < 0.001, *n* = 10), equivalent to a decrease of 4.9%. During the post-exercise occlusion period

following 4 kg exercise, there was an insignificant decrease from rest of 0.009 ± 0.010 s (equivalent to 1.0%, P = 0.495, *n* = 10), and an insignificant decrease from rest of 0.004 ± 0.008 s (equivalent to 0.4%, P = 0.691, *n* = 10) during the recovery period.

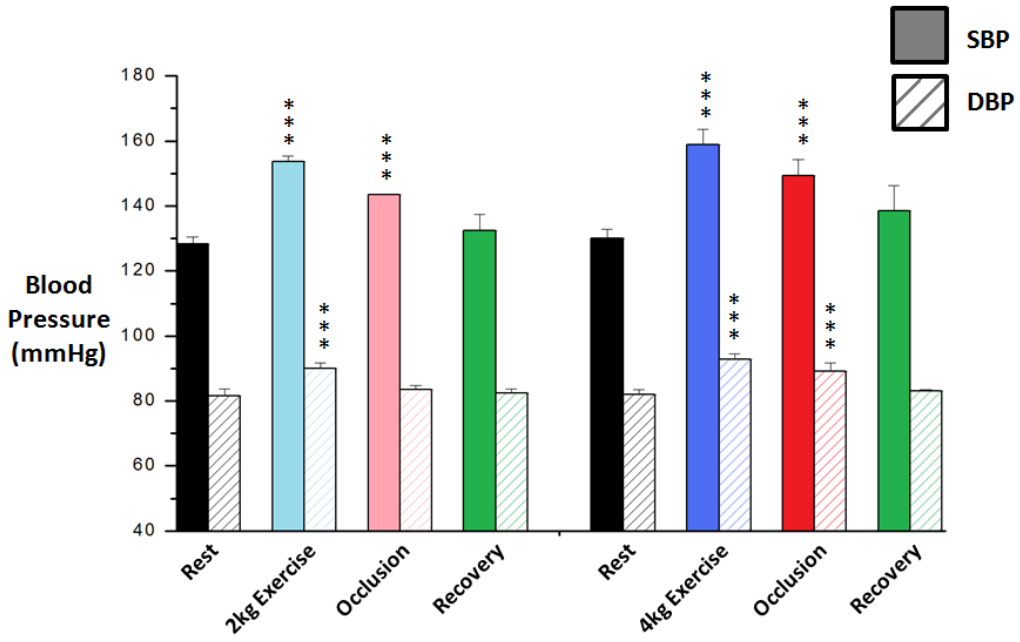

Figure 4.6 – *Graph showing significant increases in systolic blood pressure (SBP) with 2 kg exercise, 4 kg exercise and both corresponding periods of post-exercise occlusion, and in diastolic blood pressure (DBP) with 2 kg exercise, 4 kg exercise and the period of post-exercise occlusion following 4 kg exercise, compared to rest. n = 10, *** P < 0.001. Error bars represent standard error of the mean.*

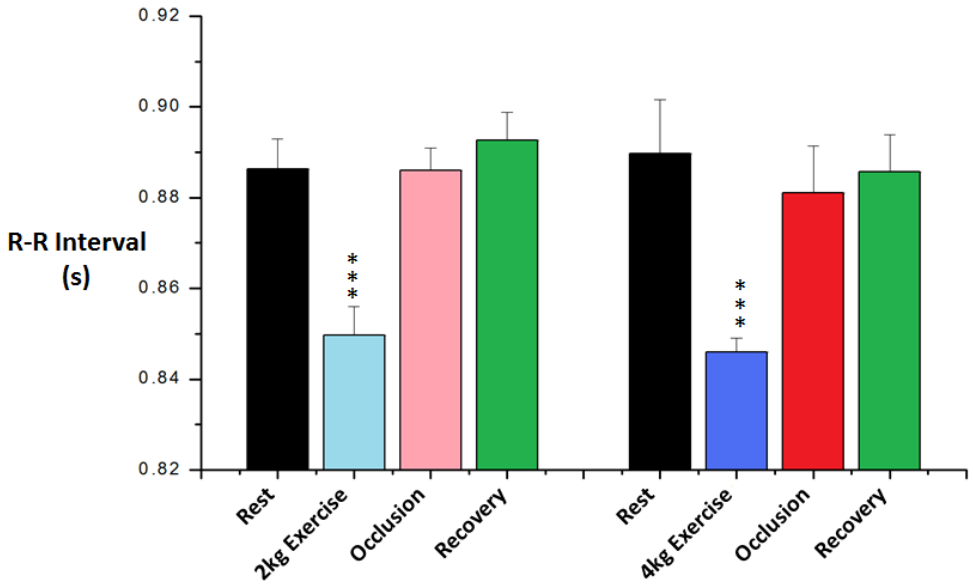

Figure 4.7 – *Graph showing a significant decrease in R-R interval (i.e. increase in heart rate) with both 2 kg exercise and 4 kg exercise, compared to rest. n = 10, *** P < 0.001. Error bars represent standard error of the mean.*

Electrode Localisation

It was important to establish the precise electrode locations of those electrodes in the periaqueductal grey (PAG), due to it being functionally opposite depending on location (i.e. there is a pressor region and a depressor region). Fig. 4.8 shows the positions of the electrodes in the three PAG patients who performed the experiment, in both the transverse and coronal planes. Fig. 4.9 shows a schematic diagram of these same three PAG electrodes so that the contacts on each electrode can be examined. Recordings were only made from those contacts that provided the patients with therapeutic benefit (i.e. pain relief). All of these contacts were situated within the dorsal region of the PAG.

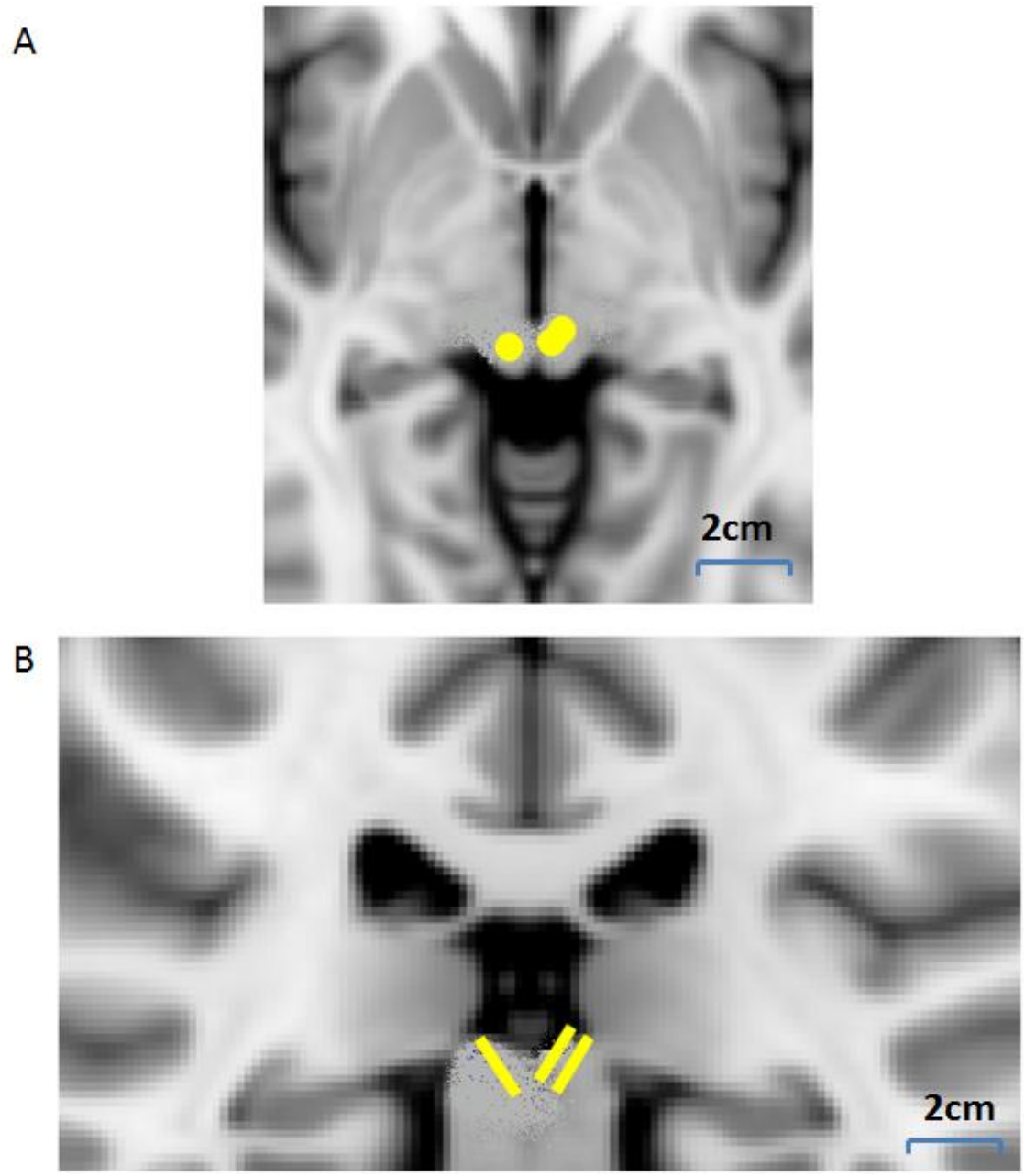

Figure 4.8 – *Post-operative image showing individual electrode locations in the transverse (A) and coronal (B) planes for three periaqueductal grey patients. Both scale bars represent 2 cm. Yellow dots represent the midpoints of each electrode. Yellow rectangles represent entire length of each electrode.*

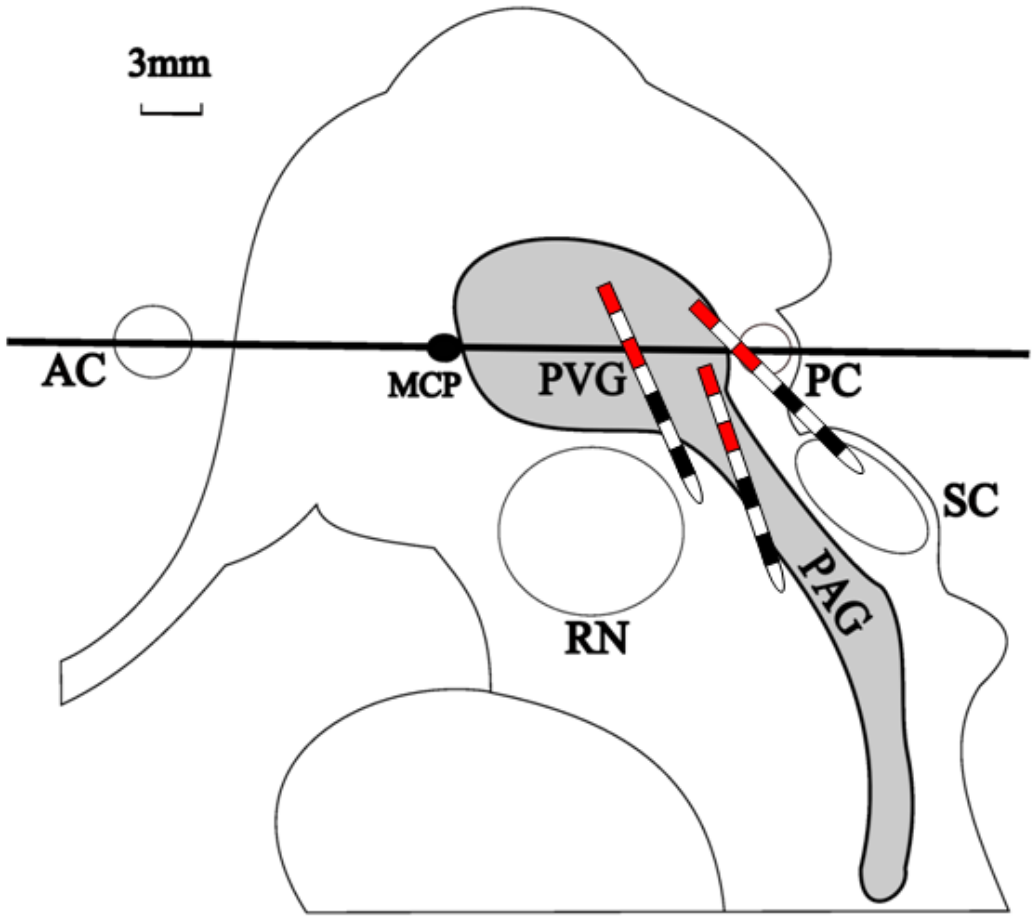

Figure 4.9 – *Schematic diagram in the sagittal plane showing electrode locations for three PAG patients who performed the experiment. The data presented in this study are recorded only from those contacts that provided therapeutic benefit – these were all within the dorsal aspect of the PVG/PAG (highlighted in red). AC, anterior commissure; MCP, mid-commissural point; PVG, periventricular grey; PC, posterior commissure; RN, red nucleus; PAG, periaqueductal grey; SC, superior colliculus.*

Local Field Potential Recordings from the Periaqueductal Grey

Using ANOVA, I revealed a significant difference between the conditions of rest, 2 kg exercise/4 kg exercise, post-exercise occlusion and recovery ($P < 0.05$) for each individual patient. Therefore, I averaged all the periaqueductal grey (PAG) data together (Fig. 4.10). With 2 kg exercise, significant increases in neural activity occurred during the following post-exercise occlusion period, but not during the exercise period itself or the subsequent recovery period. These changes were seen in the lower frequency bands. In the 4-8 Hz band, post-

exercise occlusion following 2 kg exercise was associated with an increase in power spectral density (PSD) of 314.6 ± 73.3 μV^2/Hz (P = 0.025, *n* = 3), which is equivalent to a 23.5% increase. In the 8-12 Hz band, there was an increase in PSD of 296.1 ± 95.7 μV^2/Hz (P < 0.001, *n* = 3) during post-exercise occlusion following 2 kg exercise, which is equivalent to a 38.0% increase. With 4 kg exercise, significant increases in neural activity occurred during the 4 kg exercise period itself and during the following period of post-exercise occlusion. In the 4-8 Hz band, post-exercise occlusion following 4 kg exercise was associated with an increase in PSD of 337.4 ± 72.1 μV^2/Hz (P < 0.001, *n* = 3), which is equivalent to a 24.1% increase. In the 8-12 Hz band, post-exercise occlusion following 4 kg exercise was associated with an increase in PSD of 485.8 ± 114.9 μV^2/Hz (P < 0.001, *n* = 3), which is equivalent to a 62.6% increase. In the 12-25 Hz band, there was an increase in PSD of 72.2 ± 45.0 μV^2/Hz (P = 0.002, *n* = 3) during the 4 kg exercise period itself, which is equivalent to a 28.5% increase, and an increase of 41.3 ± 14.7 μV^2/Hz (P = 0.004, *n* = 3) during the subsequent period of post-exercise occlusion – equivalent to an increase of 16.3%.

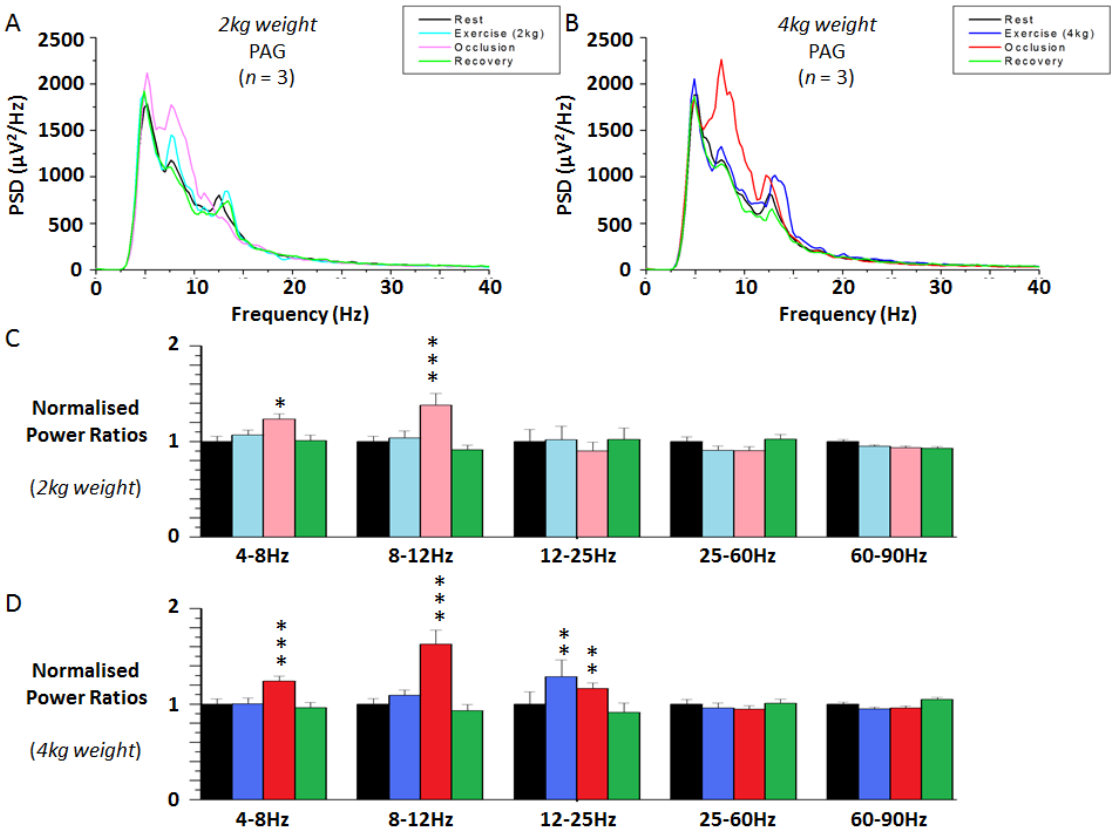

Figure 4.10 – *Graphs showing a significant increase in periaqueductal grey (PAG) neural activity during 4 kg exercise and post-exercise occlusion following both 2 kg and 4 kg exercise, compared to rest. (A) Mean power spectral density (PSD) for all three patients performing 2 kg exercise. (B) Mean PSD for all three patients performing 4 kg exercise. (C) Normalised spectral changes (rest = 1.0) divided into frequency bands, showing significant increases during post-exercise occlusion following 2 kg exercise in the 4-8 Hz and 8-12 Hz bands, compared to rest. (D) Normalised spectral changes (rest = 1.0) divided into frequency bands, showing significant increases during 4 kg exercise in the 12-25 Hz band and during post-exercise occlusion following 4 kg exercise in the 4-8 Hz, 8-12 Hz and 12-25 Hz bands, compared to rest. n = 3, * P < 0.05, ** P < 0.01, *** P < 0.001. Error bars represent standard error of the mean.*

Local Field Potential Recordings from the Subthalamic Nucleus

ANOVA revealed a significant difference in neural activity between each test condition in one of the subthalamic nucleus (STN) patients (Fig. 4.11), but not in the other (Fig. 4.12). For the STN patient in whom there were significant changes in neural activity, there was found to be a decrease in power spectral density (PSD) in the 4-8 Hz and 8-12 Hz bands during 2 kg exercise, 4 kg exercise and post-exercise occlusion following 4 kg exercise; there were no changes from

rest during the post-exercise occlusion following 2 kg exercise or the recovery periods. 2 kg exercise was associated with a decrease in PSD of 127.6 ± 17.4 μV^2/Hz ($P < 0.001$) (equivalent to a decrease of 43.2%) in the 4-8 Hz band, and a decrease of 45.8 ± 5.3 μV^2/Hz ($P < 0.001$) (equivalent to a decrease of 37.5%) in the 8-12 Hz band. 4 kg exercise was associated with a decrease in PSD of 120.4 ± 11.6 μV^2/Hz ($P < 0.001$) (equivalent to a 38.1% decrease) in the 4-8 Hz band, and a decrease of 13.4 ± 4.0 μV^2/Hz ($P = 0.006$) (equivalent to a 12.8% decrease) in the 8-12 Hz band. During the period of post-exercise occlusion following 4 kg exercise, there was a decrease in PSD of 130.5 ± 14.7 μV^2/Hz ($P < 0.001$) (which is equal to a decrease of 41.3%) in the 4-8 Hz band, and a decrease of 14.1 ± 4.9 μV^2/Hz ($P = 0.004$) (which is equal to a decrease of 13.5%) in the 8-12 Hz band.

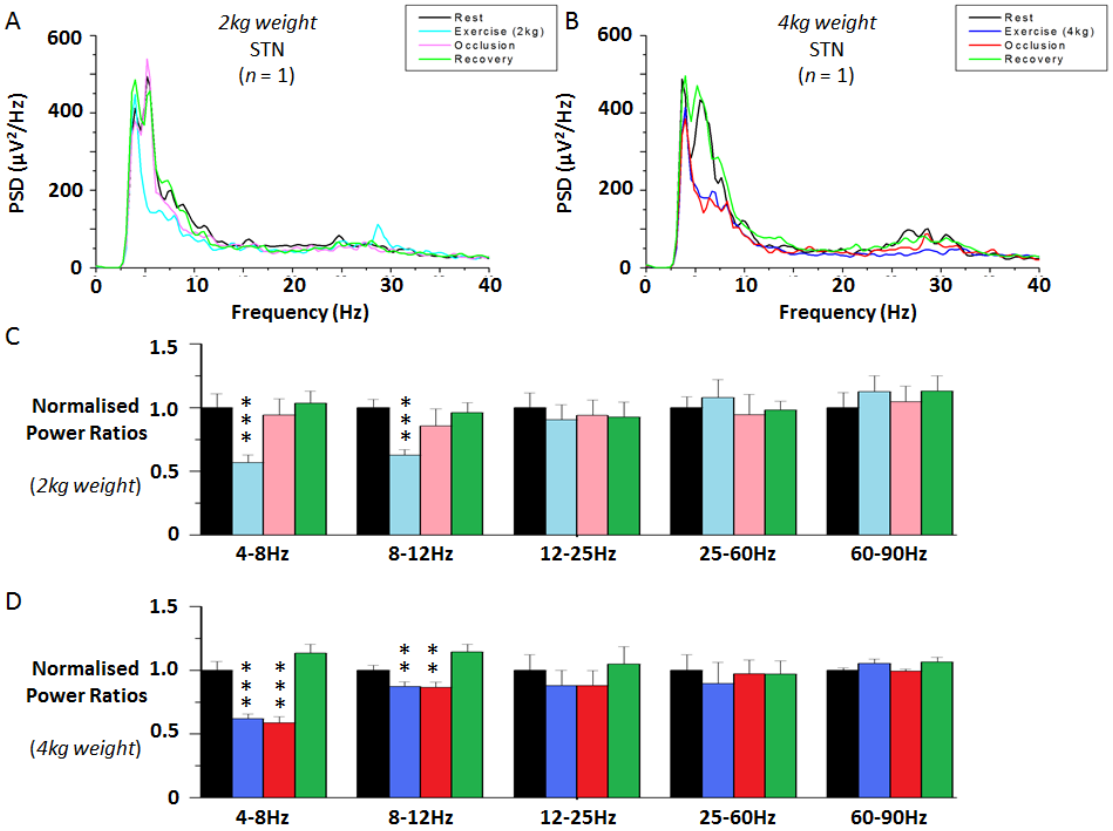

Figure 4.11 *– Graphs showing a significant decrease in subthalamic nucleus (STN) neural activity during both 2 kg and 4 kg exercise and post-exercise occlusion following 4 kg exercise, compared to rest. (A) Mean power spectral density (PSD) for the patient performing 2 kg exercise. (B) Mean PSD for the patient performing 4 kg exercise. (C) Normalised spectral changes (rest = 1.0) divided into frequency bands, showing significant decreases during 2 kg exercise in the 4-8 Hz and 8-12 Hz bands, compared to rest. (D) Normalised spectral changes (rest = 1.0) divided into frequency bands, showing significant decreases during 4 kg exercise and the following period of post-exercise occlusion in the 4-8 Hz and 8-12 Hz bands, compared to rest. n = 1, ** P < 0.01, *** P < 0.001 (significance was calculated using ANOVA on several data points collected from the patient). Error bars represent standard error of the mean.*

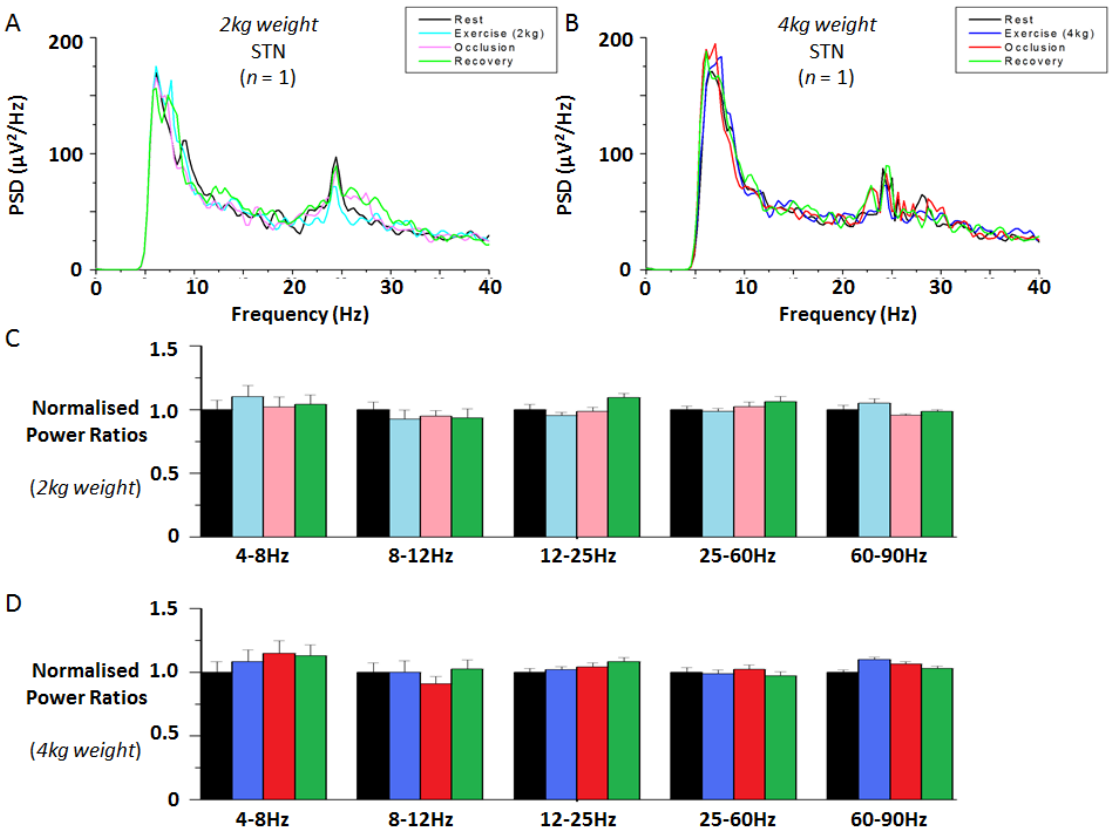

Figure 4.12 – *Graphs showing no changes in subthalamic nucleus (STN) neural activity during either of the exercise periods or during the subsequent post-exercise occlusion periods, compared to rest. (A) Mean power spectral density (PSD) for the patient performing 2 kg exercise. (B) Mean PSD for the patient performing 4 kg exercise. (C) Normalised spectral changes (rest = 1.0) divided into frequency bands, showing no significant differences in 2 kg exercise or post-exercise occlusion, compared to rest. (D) Normalised spectral changes (rest = 1.0) divided into frequency bands, showing no significant differences in 4 kg exercise or post-exercise occlusion, compared to rest. n = 1. Error bars represent standard error of the mean.*

Local Field Potential Recordings from the Other Nuclei

Using ANOVA, I showed that there were no significant differences among any of the conditions in any of the thalamus (Fig. 4.13) and internal globus pallidus (GPi) patients (Fig. 4.14). As discussed in Chapter 3, with the GPi patients, a peak was observed in the power spectral density graphs at approximately 25 Hz, which was thought to represent its resting activity levels as it was consistent across all the test conditions in both patients.

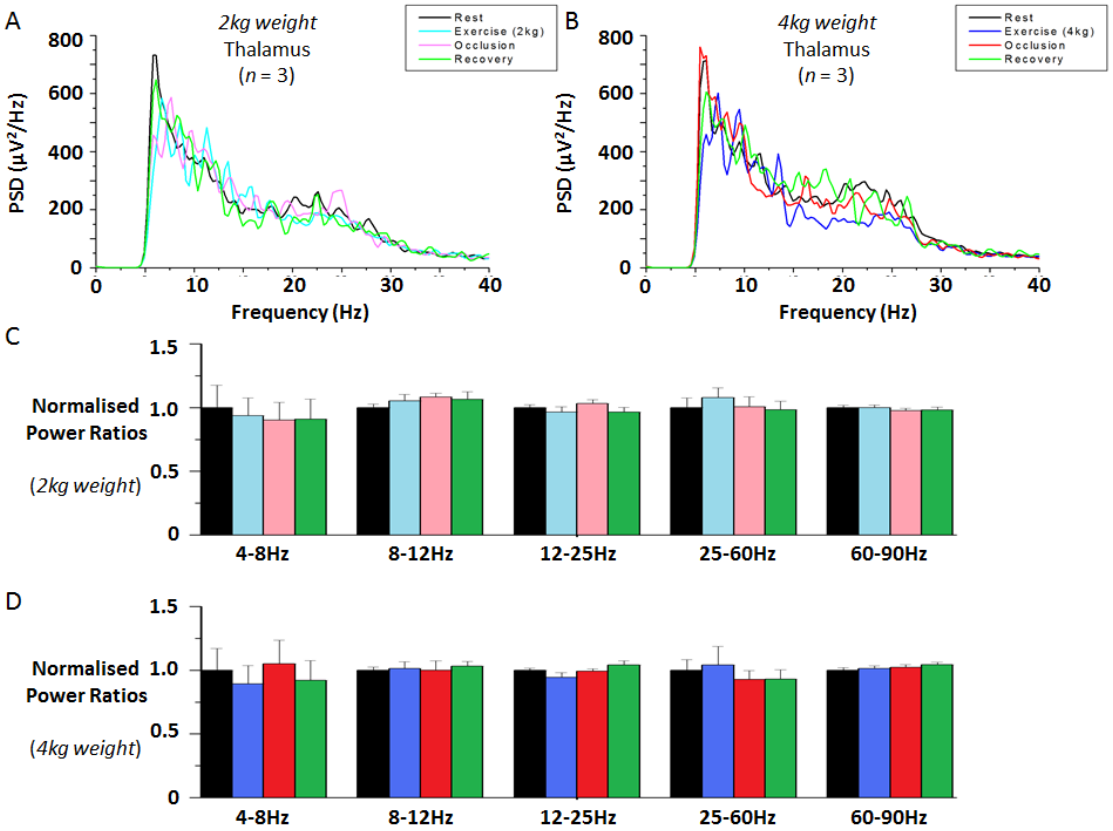

Figure 4.13 – *Graphs showing no changes in thalamus neural activity during either of the exercise periods or during the subsequent post-exercise occlusion periods, compared to rest. (A) Mean power spectral density (PSD) for the patients performing 2 kg exercise. (B) Mean PSD for the patients performing 4 kg exercise. (C) Normalised spectral changes (rest = 1.0) divided into frequency bands, showing no significant differences in 2 kg exercise or post-exercise occlusion, compared to rest. (D) Normalised spectral changes (rest = 1.0) divided into frequency bands, showing no significant differences in 4 kg exercise or post-exercise occlusion, compared to rest. n = 3. Error bars represent standard error of the mean.*

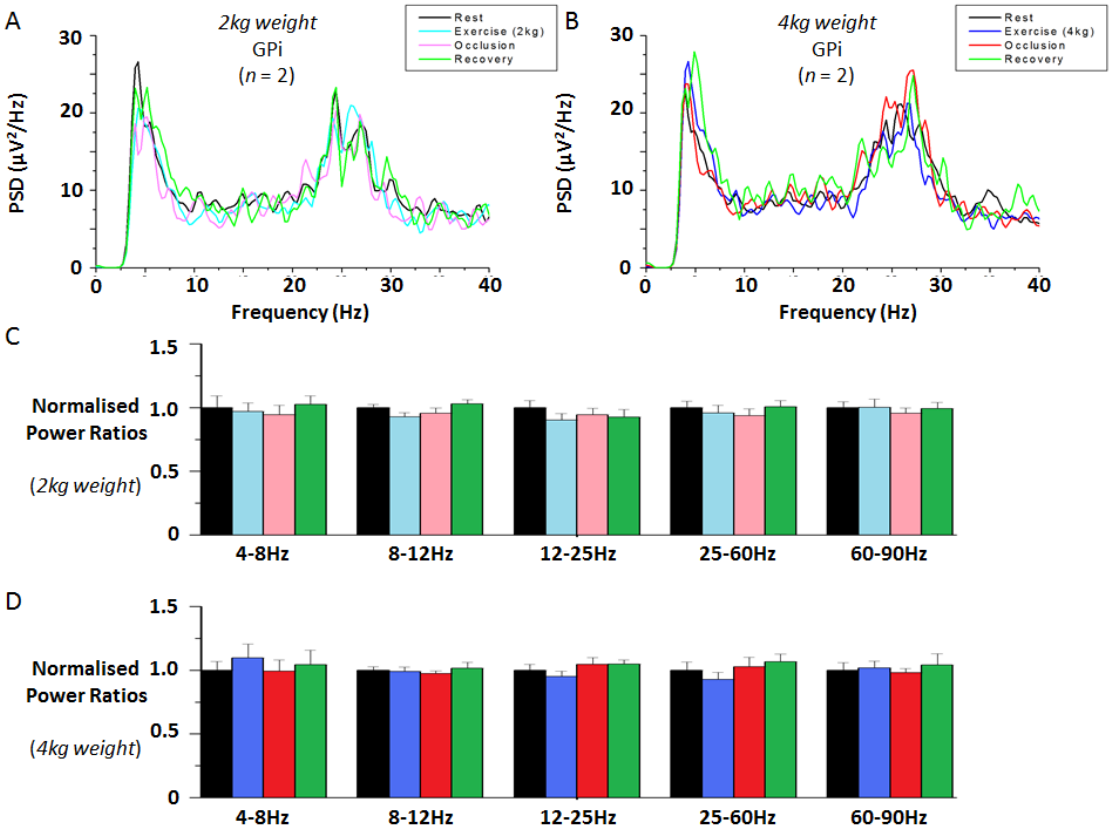

Figure 4.14 – *Graphs showing no changes in internal globus pallidus (GPi) neural activity during either of the exercise periods or during the subsequent post-exercise occlusion periods, compared to rest. (A) Mean power spectral density (PSD) for the patients performing 2 kg exercise. (B) Mean PSD for the patients performing 4 kg exercise. (C) Normalised spectral changes (rest = 1.0) divided into frequency bands, showing no significant differences in 2 kg exercise or post-exercise occlusion, compared to rest. (D) Normalised spectral changes (rest = 1.0) divided into frequency bands, showing no significant differences in 4 kg exercise or post-exercise occlusion, compared to rest. n = 2. Error bars represent standard error of the mean.*

Cardiovascular Parameters and Local Field Potential Recordings from Control Experiment

I did not observe any significant differences among any of the conditions of the control experiment (occlusion without prior exercise) in any of the patients, either in terms of cardiovascular parameters (Figs. 4.15-4.17) or in terms of neural activity (Figs. 4.18-4.21).

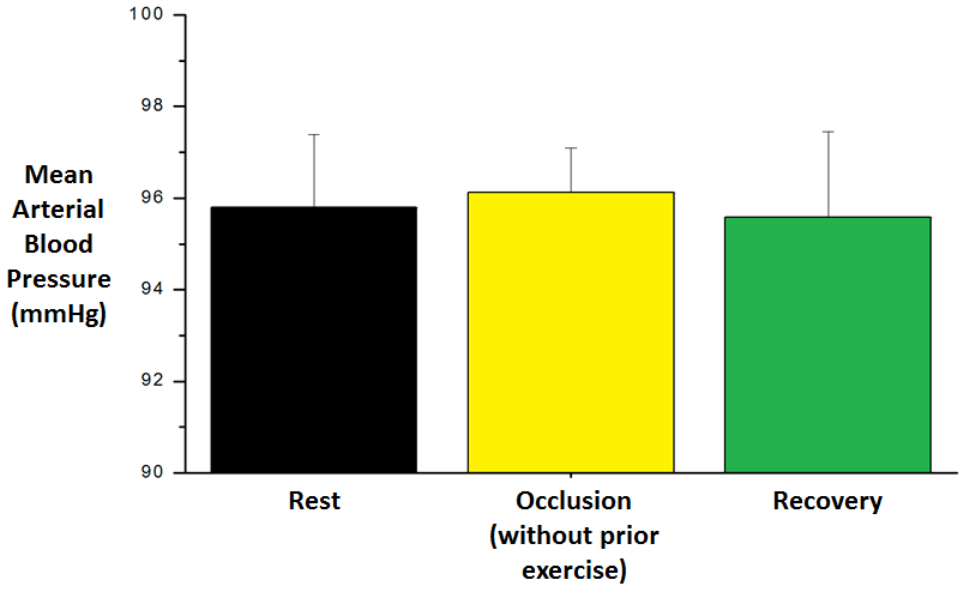

Figure 4.15 *– Graph showing no significant changes in mean arterial blood pressure during occlusion without prior exercise, compared to rest. n = 10. Error bars represent standard error of the mean.*

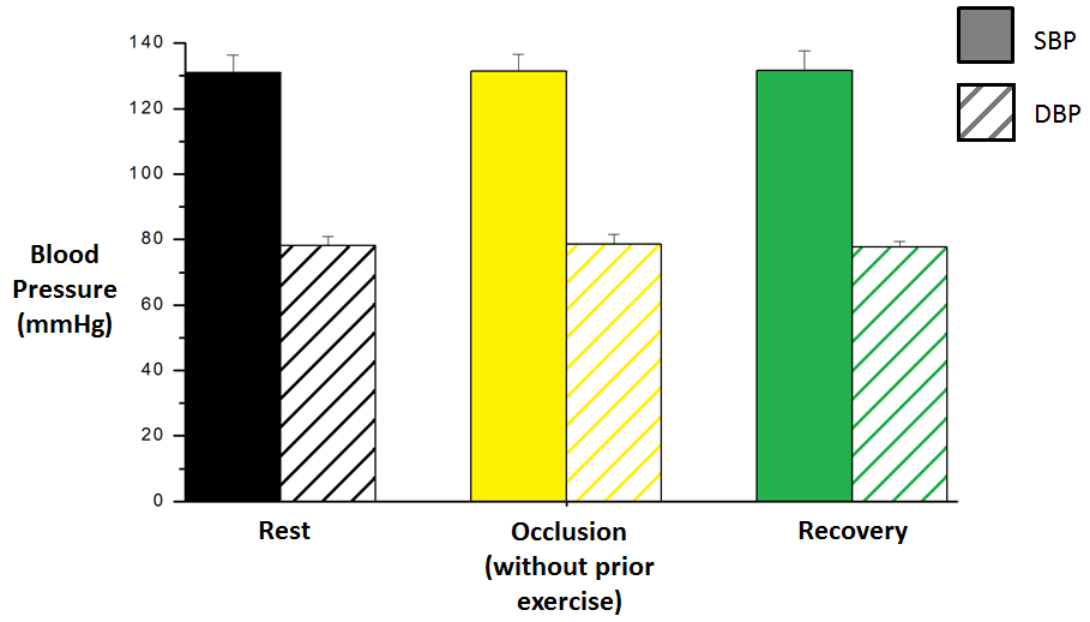

Figure 4.16 *– Graph showing no significant changes in systolic blood pressure (SBP) or diastolic blood pressure (DBP) during occlusion without prior exercise, compared to rest. n = 10. Error bars represent standard error of the mean.*

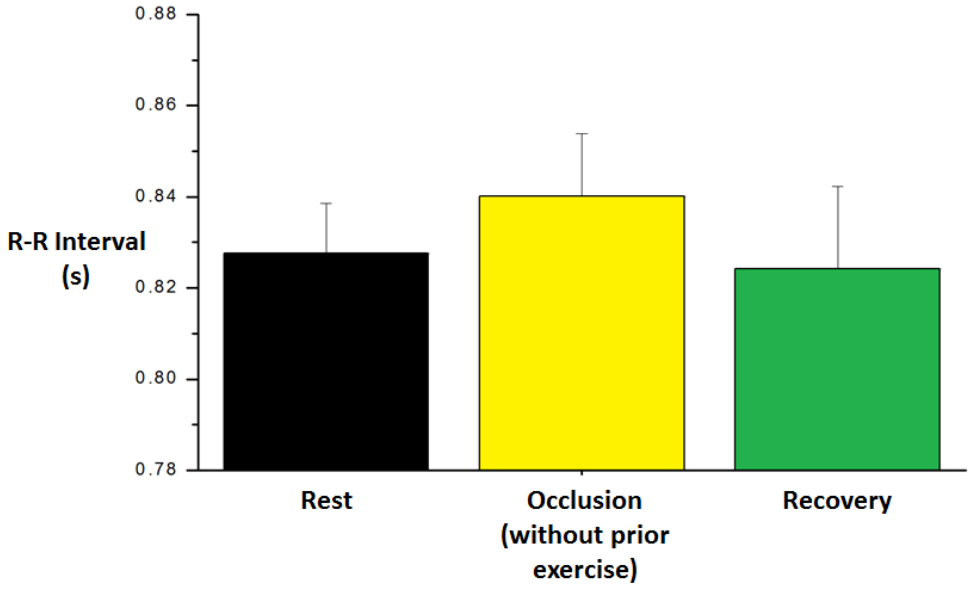

Figure 4.17 *– Graph showing no significant changes in R-R interval (i.e. no changes in heart rate) during occlusion without prior exercise, compared to rest. n = 10. Error bars represent standard error of the mean.*

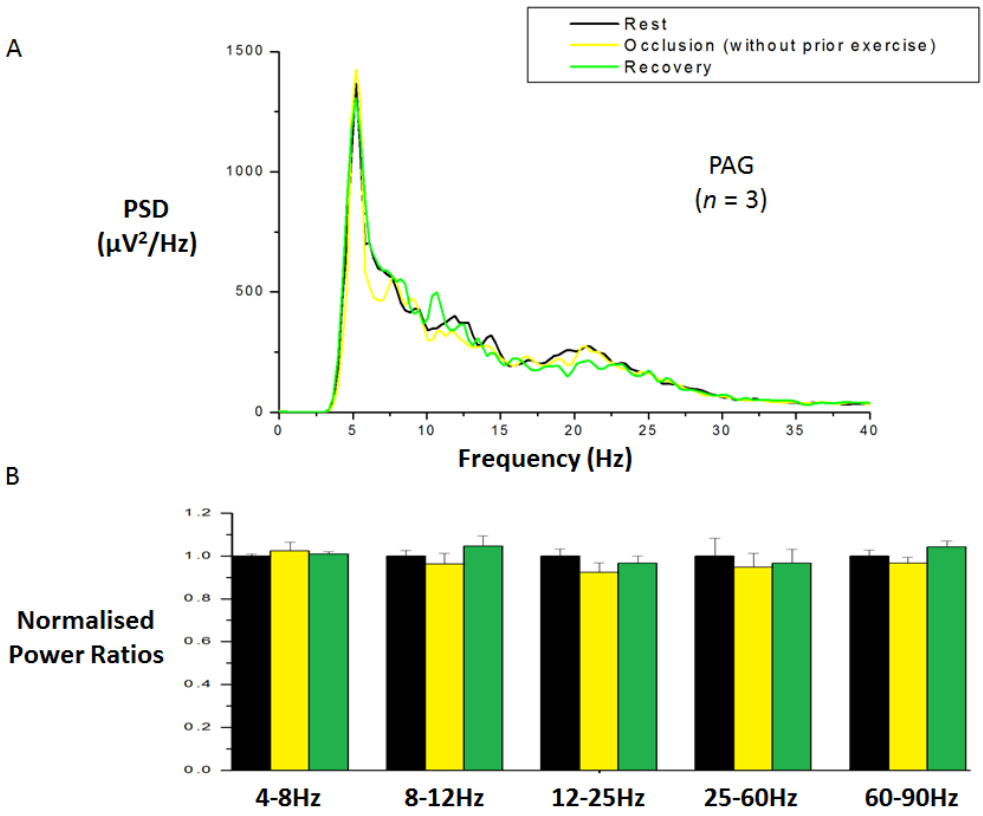

Figure 4.18 – *Graphs showing no significant changes in periaqueductal grey (PAG) neural activity during occlusion without prior exercise, compared to rest. (A) Mean power spectral density (PSD) for all three patients. (B) Normalised spectral changes (rest = 1.0) divided into frequency bands, showing no significant differences compared to rest. n = 3. Error bars represent standard error of the mean.*

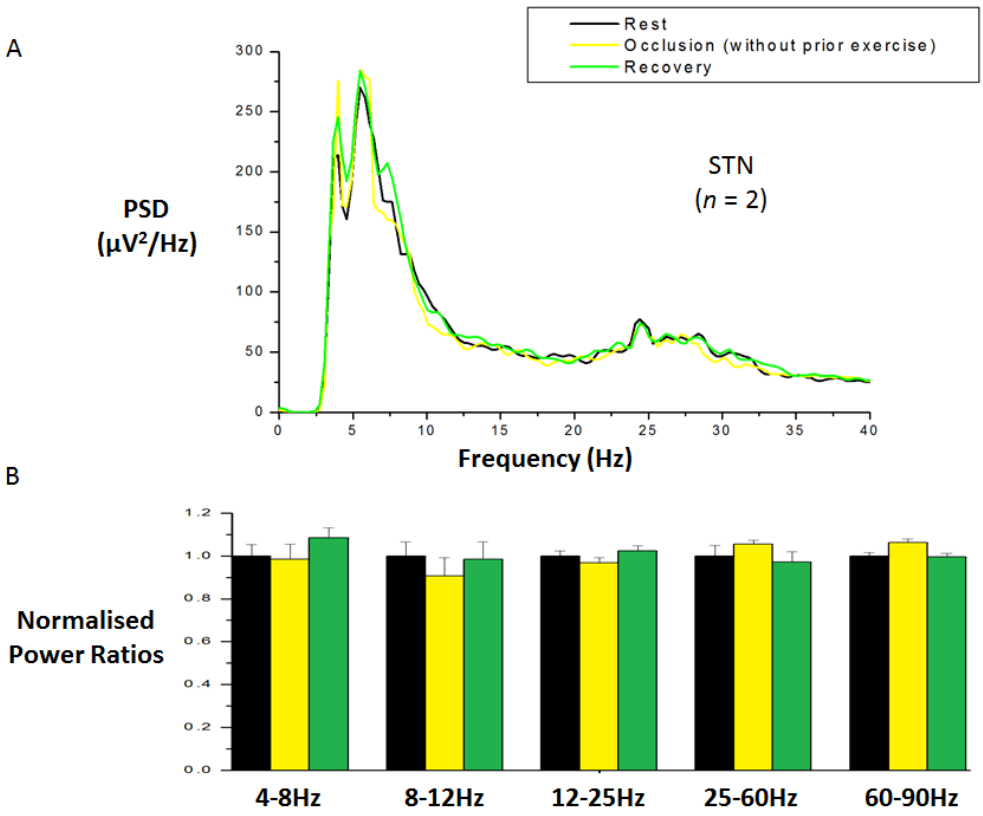

Figure 4.19 – *Graphs showing no significant changes in subthalamic nucleus (STN) neural activity during occlusion without prior exercise, compared to rest. (A) Mean power spectral density (PSD) for both patients. (B) Normalised spectral changes (rest = 1.0) divided into frequency bands, showing no significant differences compared to rest. n = 2. Error bars represent standard error of the mean.*

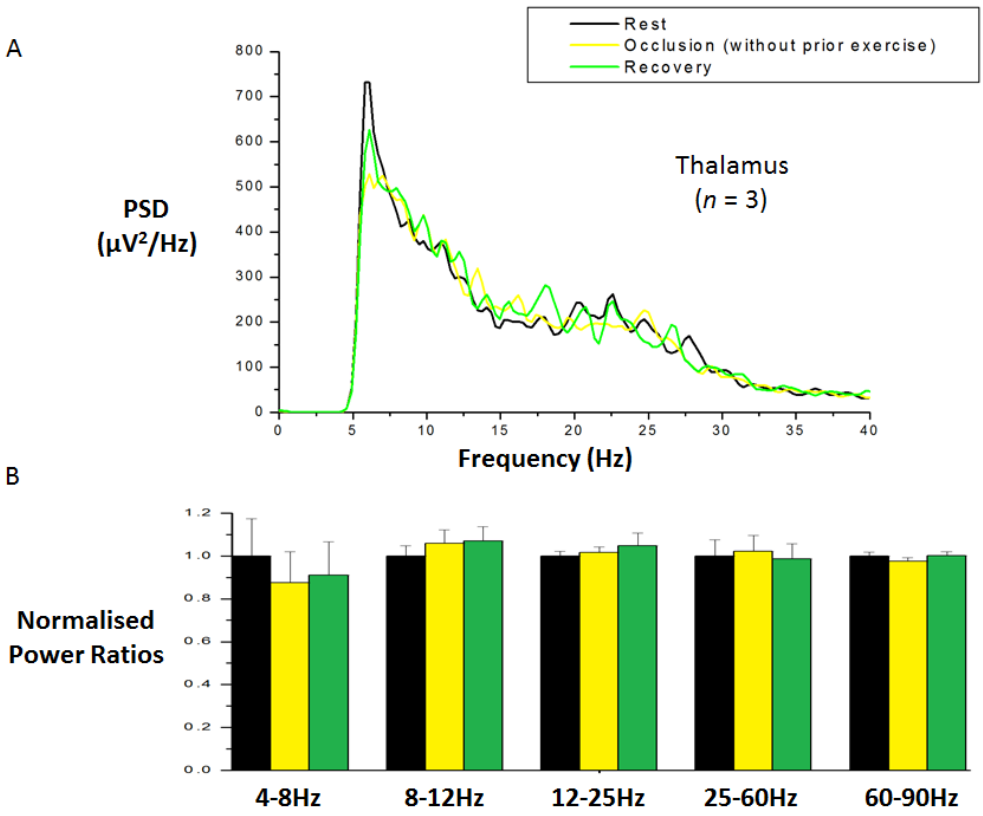

Figure 4.20 – *Graphs showing no significant changes in thalamic neural activity during occlusion without prior exercise, compared to rest. (A) Mean power spectral density (PSD) for all three patients. (B) Normalised spectral changes (rest = 1.0) divided into frequency bands, showing no significant differences compared to rest. n = 3. Error bars represent standard error of the mean.*

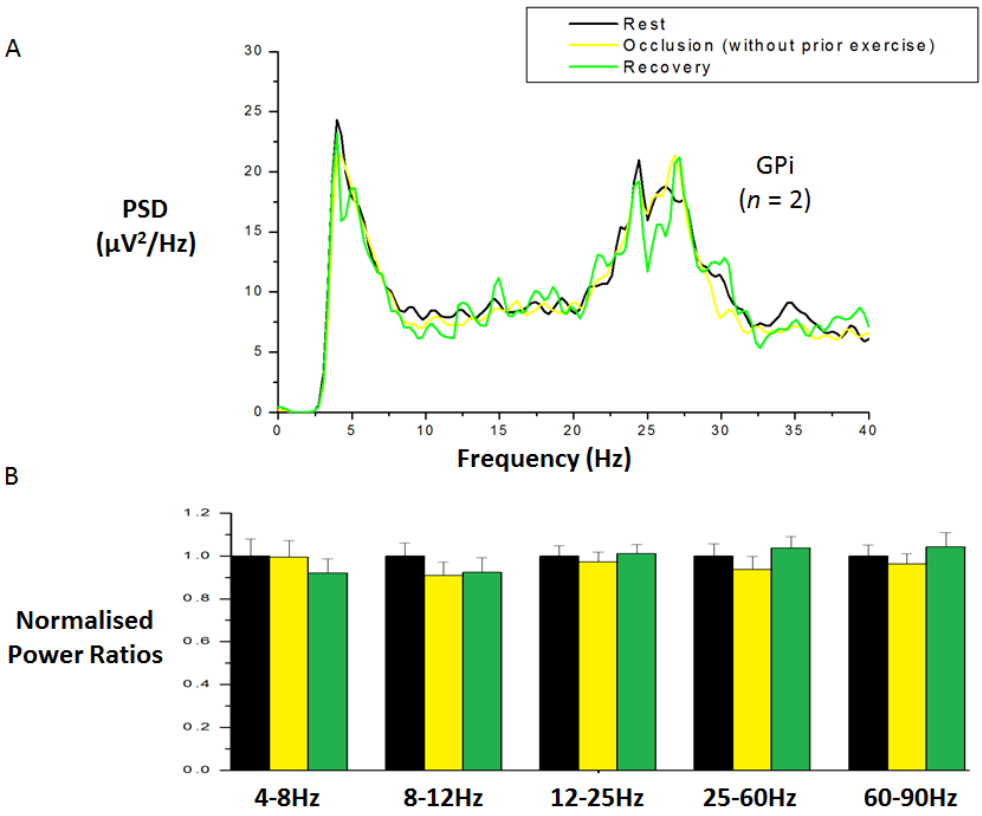

Figure 4.21 – *Graphs showing no significant changes in internal globus pallidus (GPi) neural activity during occlusion without prior exercise, compared to rest. (A) Mean power spectral density (PSD) for both patients. (B) Normalised spectral changes (rest = 1.0) divided into frequency bands, showing no significant differences compared to rest. n = 2. Error bars represent standard error of the mean.*

Ischaemic Exercise Protocol

Cardiovascular Parameters

In the five patients from whom data were measured, mean arterial blood pressure (MABP) increased during exercise, then increased further during exercise with occlusion, and subsequently returned to baseline within the recovery period. The data for all of the patients were averaged together (Fig. 4.22). The average increase in MABP during exercise was 11.2 ± 3.4 mmHg ($P = 0.009$, $n = 5$), equivalent to an increase of 13.1%. During the subsequent period of occlusion with continuing exercise, the average increase from rest in MABP was 15.2 ± 4.1 mmHg ($P < 0.001$, $n = 5$), equivalent to an increase of 17.8%. On recovery, there was an

average increase from rest of 1.3 ± 6.1 mmHg (equivalent to a 1.5% increase). However, there was no significant difference between the initial rest period and the recovery period (P = 0.628, *n* = 5).

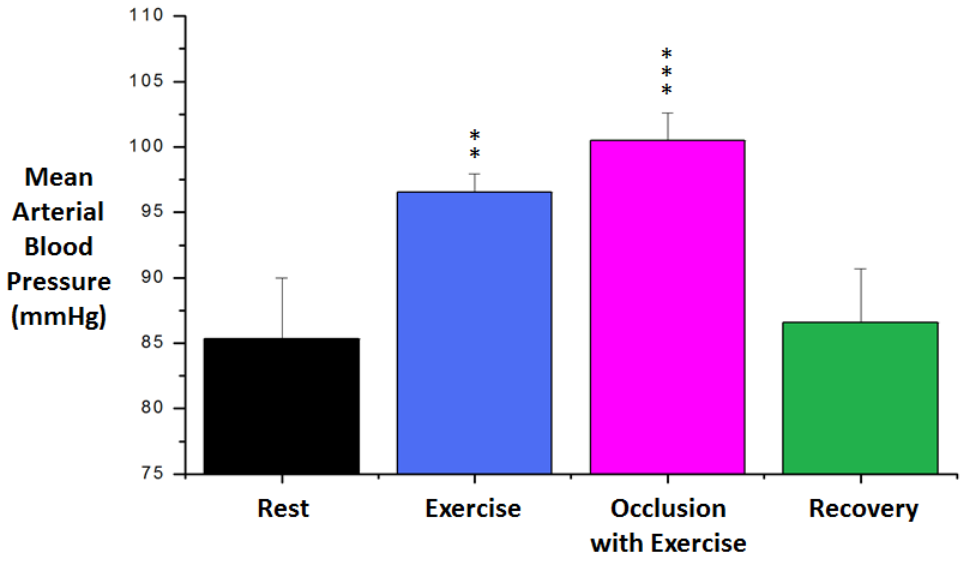

Figure 4.22 – *Graph showing significant increases in mean arterial blood pressure with exercise and occlusion with continuing exercise, compared to rest. n = 5, ** P < 0.01, *** P < 0.001. Error bars represent standard error of the mean.*

The changes in MABP were accompanied by analogous changes in systolic blood pressure (SBP) and diastolic blood pressure (DBP) (Fig. 4.23). The average increase in SBP during exercise was 11.7 ± 3.5 mmHg (P < 0.001, *n* = 5), equivalent to an increase of 8.3%. During the occlusion period with continuing exercise, the average increase from rest in SBP was 17.4 ± 4.5 mmHg (P < 0.001, *n* = 5), equivalent to an increase of 12.3%. On recovery there was an average decrease from rest of 0.1 ± 2.9 mmHg (equivalent to a 0.1% decrease). However, there was no significant difference between the initial rest period and the recovery period (P = 0.549, *n* = 5). The average increase in DBP during exercise was 3.4 ± 1.7 mmHg (P = 0.037, *n* = 5), equivalent to an increase of 4.6%. During the occlusion period with continuing exercise, the average increase from rest in DBP was 6.9 ± 2.7 mmHg (P < 0.001, *n* = 5), equivalent to an

increase of 9.2%. On recovery there was an average decrease from rest of 1.1 ± 1.8 mmHg (equivalent to a 1.4% decrease). However, this decrease was insignificant (P = 0.628, *n* = 5).

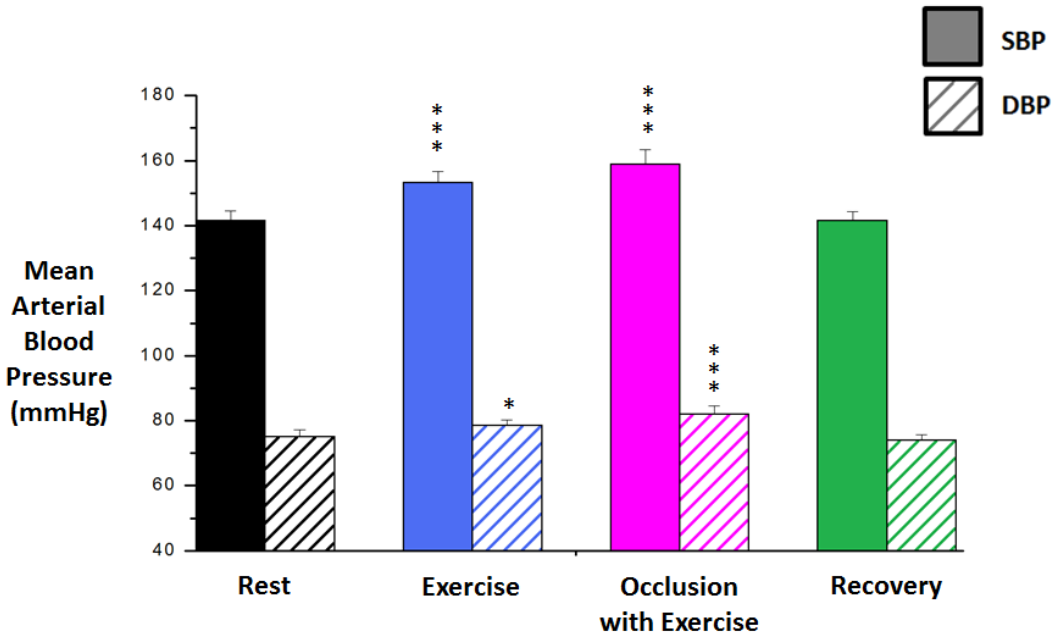

Figure 4.23 – *Graph showing significant increases in both systolic blood pressure (SBP) and diastolic blood pressure (DBP) with exercise and occlusion with continuing exercise, compared to rest. n = 5, * P < 0.05, *** P < 0.001. Error bars represent standard error of the mean.*

All five of the patients who performed the experiment had a significantly decreased R-R interval during the exercise period and during the period of occlusion with continuing exercise, but not during the recovery period. The R-R interval data for all five patients were averaged together (Fig. 4.24). The decrease from rest during exercise was 0.036 ± 0.009 s (P < 0.001, *n* = 5), equivalent to a decrease of 4.1%. During the period of occlusion with continuing exercise, there was a decrease from rest of 0.048 ± 0.009 s (P < 0.001, *n* = 5), equivalent to a 5.5% decrease. There was an insignificant decrease from rest of 0.006 ± 0.010 s (equivalent to a decrease of 0.6%) during the recovery period (P = 0.655, *n* = 5).

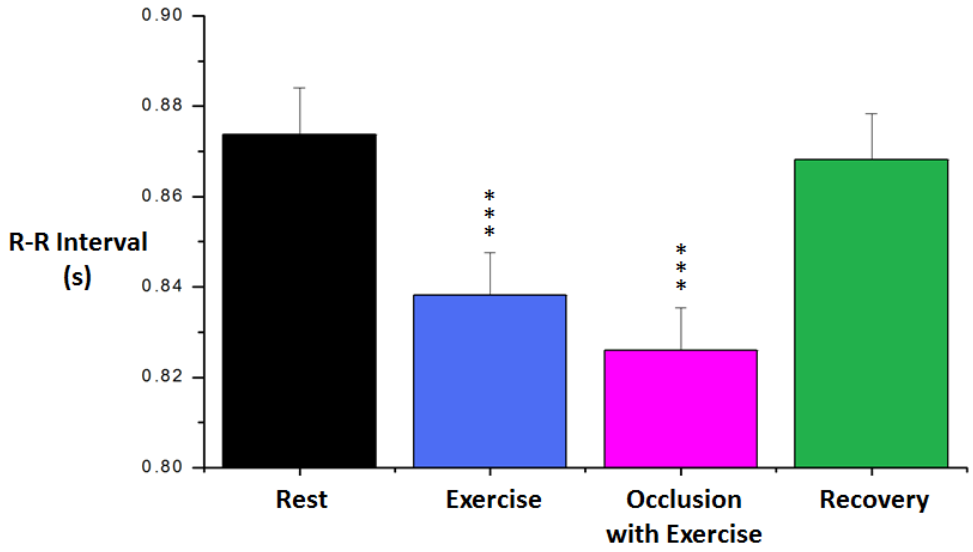

Figure 4.24 – *Graph showing a significant decrease in R-R interval (i.e. increase in heart rate) during exercise and occlusion with continuing exercise, compared to rest. n = 5, *** P < 0.001. Error bars represent standard error of the mean.*

Electrode Localisation

Fig. 4.25 shows the positions of the electrodes in the three PAG patients who performed the experiment, in both the transverse and coronal planes. Fig. 4.26 shows a schematic diagram of these same three PAG electrodes so that the contacts on each electrode can be examined. Recordings were only made from those contacts that provided the patients with therapeutic benefit (i.e. pain relief). All of these contacts were located within the dorsal region of the PAG.

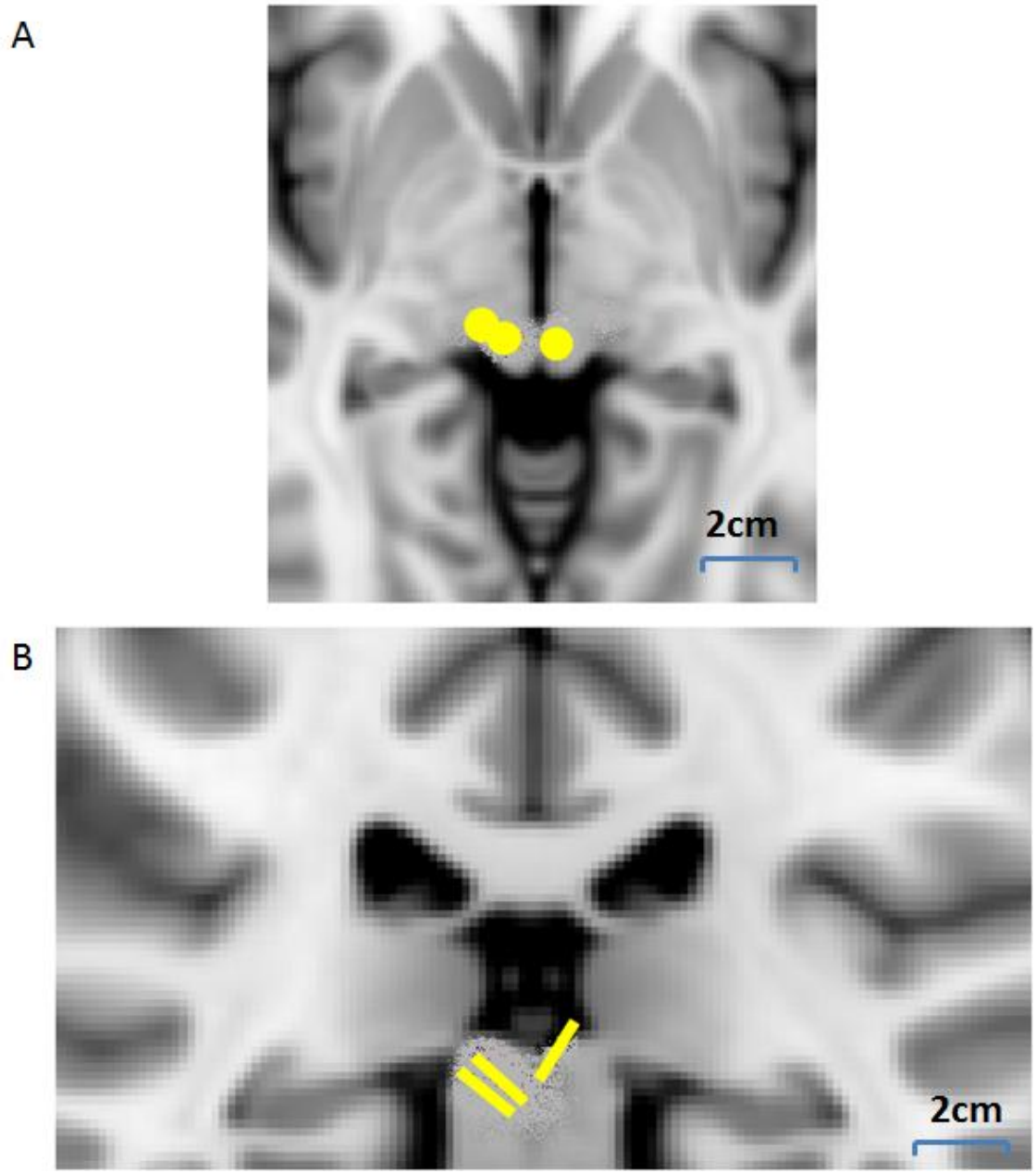

Figure 4.25 – *Post-operative image showing individual electrode locations in the transverse (A) and coronal (B) planes for three periaqueductal grey patients. Both scale bars represent 2 cm. Yellow dots represent the midpoints of each electrode. Yellow rectangles represent entire length of each electrode.*

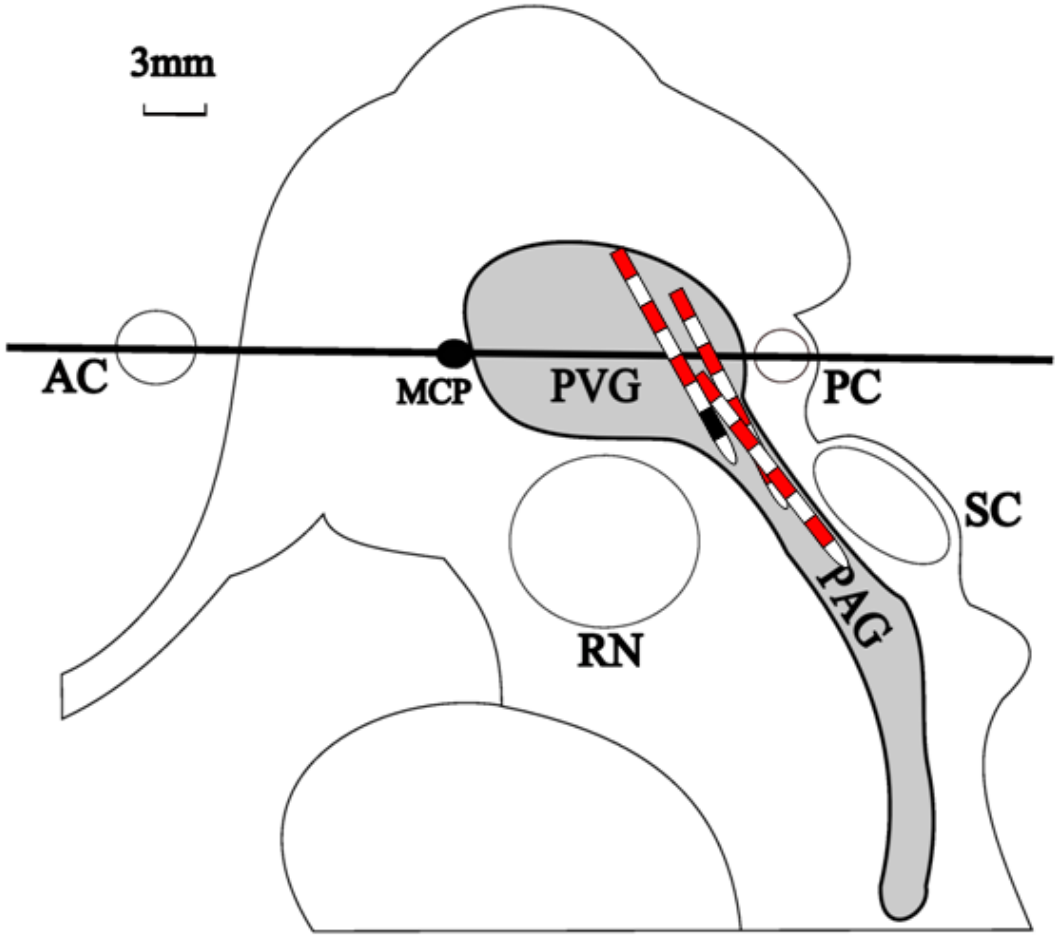

Figure 4.26 – *Schematic diagram in the sagittal plane showing electrode locations for three PAG patients who performed the experiment. The data presented in this study are recorded only from those contacts that provided therapeutic benefit – these were all within the dorsal aspect of the PVG/PAG (highlighted in red). AC, anterior commissure; MCP, mid-commissural point; PVG, periventricular grey; PC, posterior commissure; RN, red nucleus; PAG, periaqueductal grey; SC, superior colliculus.*

Local Field Potential Recordings from the Periaqueductal Grey

Using ANOVA, a significant difference was revealed between the conditions of rest, exercise, occlusion with continuing exercise, and recovery ($P < 0.05$) for each individual patient. Therefore, all of the periaqueductal grey (PAG) data were averaged together (Fig. 4.27). Significant increases in neural activity occurred during both exercise and occlusion with continuing exercise, but not during the recovery period. These changes were seen in the lower frequency bands. Exercise was associated with an increase in power spectral density (PSD) in

the 4-8 Hz band of 5232.6 ± 2820.8 $\mu V^2/Hz$ (P = 0.023, *n* = 3), which is equivalent to a 29.9% increase. Additionally in the 4-8 Hz band, occlusion with continuing exercise was associated with an increase in PSD of 7192.8 ± 3118.8 $\mu V^2/Hz$ (P < 0.001, *n* = 3), which is equivalent to a 41.0% increase. In the 8-12 Hz band, there was an increase in PSD of 3848.0 ± 1273.5 $\mu V^2/Hz$ (P < 0.001, *n* = 3) during occlusion with continuing exercise, which is equivalent to a 39.6% increase. In the 12-25 Hz band, occlusion with continuing exercise was associated with an increase in PSD of 1472.1 ± 461.6 $\mu V^2/Hz$ (P < 0.001, *n* = 3), which is equivalent to an increase of 41.0%.

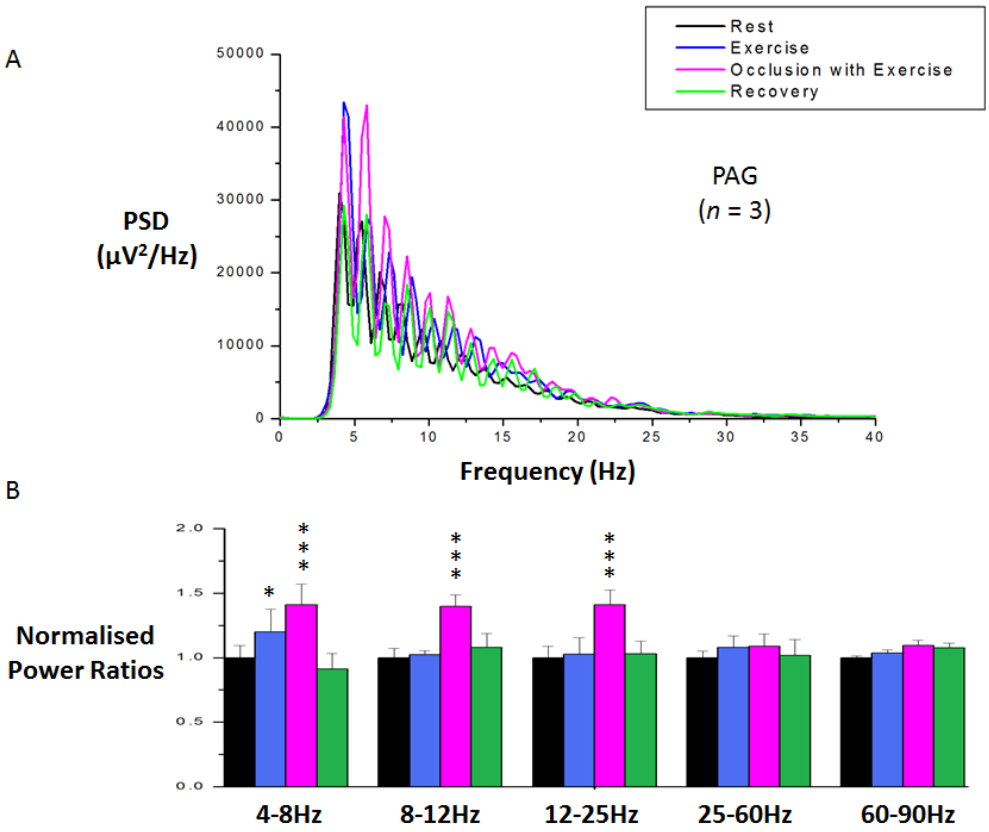

Figure 4.27 – *Graphs showing a significant increase in periaqueductal grey (PAG) neural activity during exercise and occlusion with continuing exercise, compared to rest. (A) Mean power spectral density (PSD) for the three patients. (B) Normalised spectral changes (rest = 1.0) divided into frequency bands, showing significant increases during exercise in the 4-8 Hz band, and during occlusion with continuing exercise in the 4-8 Hz, 8-12 Hz and 12-25 Hz bands, compared to rest. n = 3, * P < 0.05, *** P < 0.001. Error bars represent standard error of the mean.*

Local Field Potential Recordings from the Other Nuclei

Using ANOVA, it was shown that there were no significant differences among any of the conditions in either of the thalamus patients (Fig. 4.28).

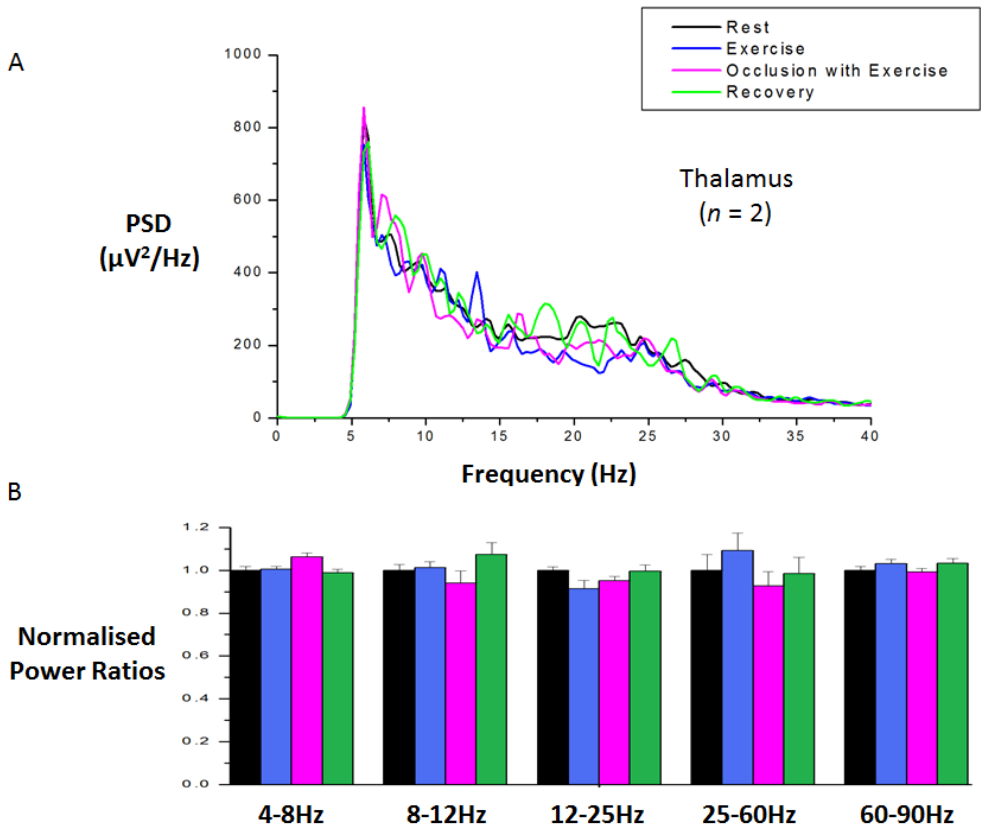

Figure 4.28 – *Graphs showing no changes in thalamic neural activity during exercise and occlusion with continuing exercise, compared to rest. (A) Mean power spectral density (PSD) for both patients. (B) Normalised spectral changes (rest = 1.0) divided into frequency bands, showing no significant differences compared to rest. n = 2. Error bars represent standard error of the mean.*

Cardiovascular Parameters and Local Field Potential Recordings from Control Experiment

No significant differences were observed among any of the conditions of the control experiment (occlusion without prior exercise) in any of the patients, either in terms of cardiovascular parameters (Figs. 4.29-4.31) or in terms of neural activity (Figs. 4.32-4.33).

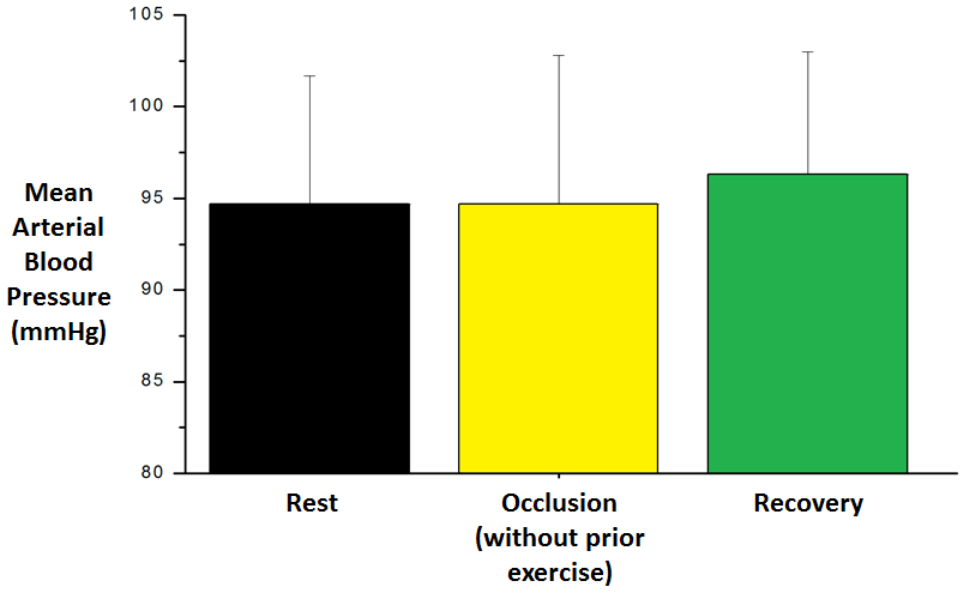

Figure 4.29 – *Graph showing no significant changes in mean arterial blood pressure during occlusion without prior exercise, compared to rest. n = 5. Error bars represent standard error of the mean.*

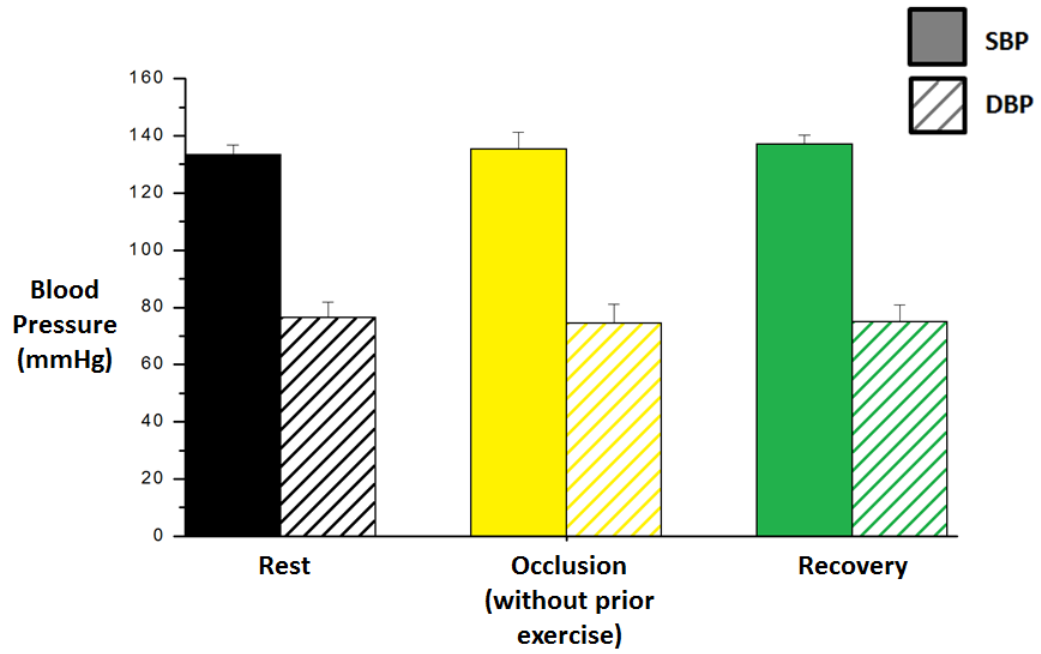

Figure 4.30 – *Graph showing no significant changes in systolic blood pressure (SBP) or diastolic blood pressure (DBP) during occlusion without prior exercise, compared to rest. n = 5. Error bars represent standard error of the mean.*

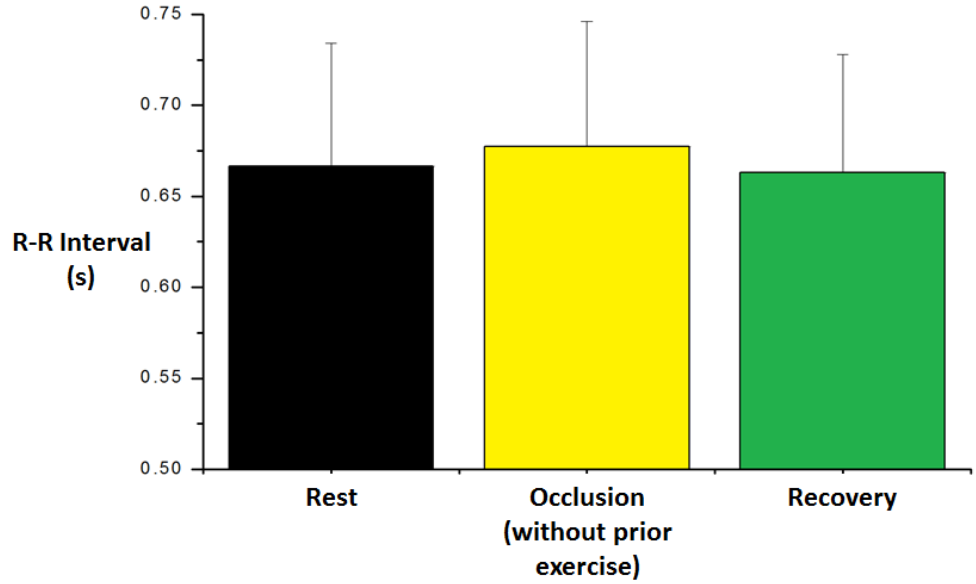

Figure 4.31 – *Graph showing no significant changes in R-R interval (i.e. no changes in heart rate) during occlusion without prior exercise, compared to rest. n = 5. Error bars represent standard error of the mean.*

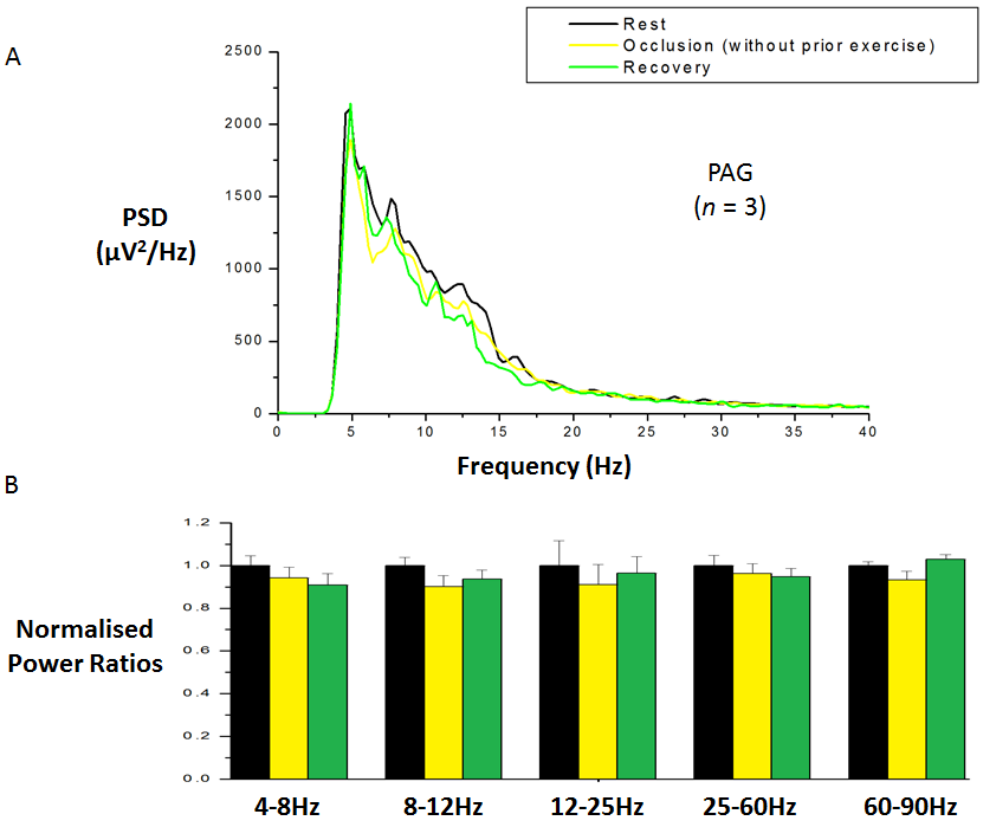

Figure 4.32 – *Graphs showing no significant changes in periaqueductal grey (PAG) neural activity during occlusion without prior exercise, compared to rest. (A) Mean power spectral density (PSD) for all three patients. (B) Normalised spectral changes (rest = 1.0) divided into frequency bands, showing no significant differences compared to rest. n = 3. Error bars represent standard error of the mean.*

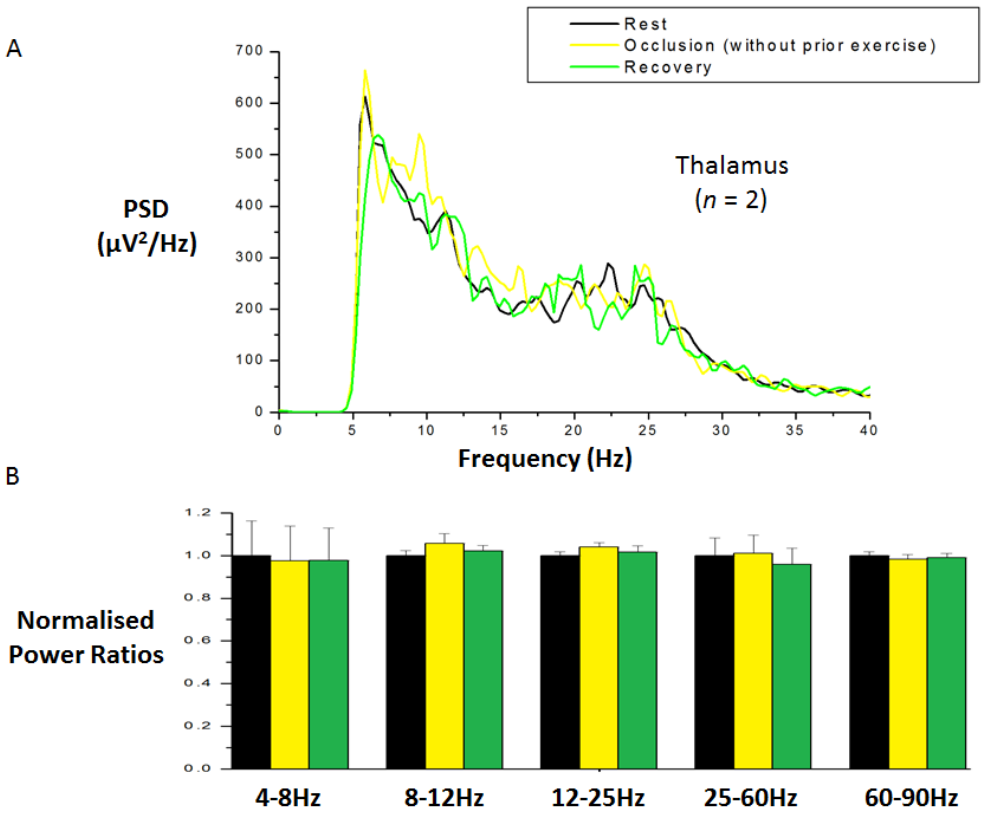

Figure 4.33 – *Graphs showing no significant changes in thalamic neural activity during occlusion without prior exercise, compared to rest. (A) Mean power spectral density (PSD) for both patients. (B) Normalised spectral changes (rest = 1.0) divided into frequency bands, showing no significant differences compared to rest. n = 2. Error bars represent standard error of the mean.*

Remote Ischaemic Preconditioning Protocol

Cardiovascular Parameters

In all nine of the patients from whom data were taken, mean arterial blood pressure (MABP) increased during exercise before the remote ischaemic preconditioning (RIPC) stimulus. However, after the RIPC stimulus, the resting blood pressure was increased in all patients compared to resting blood pressure before the stimulus. Exercise following the stimulus did not cause a significant increase in blood pressure compared to this new resting baseline. The MABP data for all of the patients were averaged together (Fig. 4.34). The average increase in MABP during exercise before the RIPC stimulus was 7.4 ± 2.5 mmHg ($P < 0.001$, $n = 9$),

equivalent to an increase of 8.0%. After the RIPC stimulus, the average increase in MABP during exercise was 2.8 ± 2.2 mmHg (equivalent to a 2.6% increase), which was not significant (P = 0.134, *n* = 9). The baseline resting MABP after the RIPC stimulus increased by 14.3 ± 2.4 mmHg (P < 0.001, *n* = 9) compared to the baseline resting MABP before the stimulus, which is equivalent to an increase of 15.4%. During the RIPC stimulus itself, MABP gradually fell and then increased towards the final (fourth) period of cuff inflation in all patients – these data were also averaged together (Fig. 4.35).

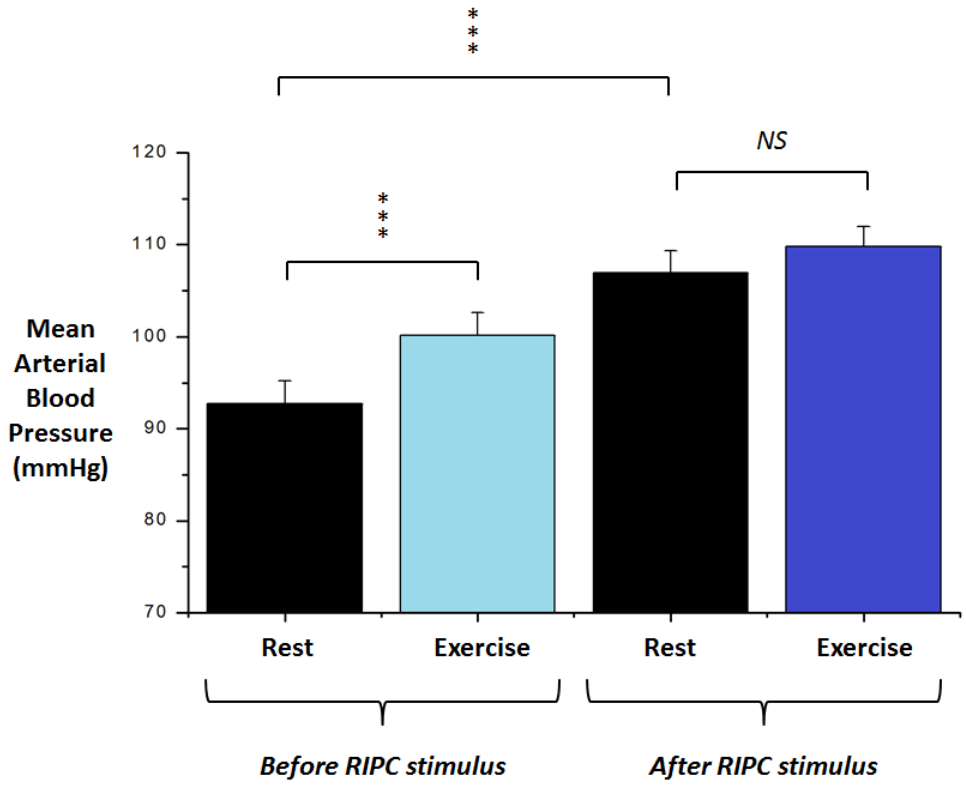

Figure 4.34 – *Graph showing a significant increase in mean arterial blood pressure (MABP) during exercise compared to rest before the remote ischaemic preconditioning (RIPC) stimulus, and a non-significant (NS) increase in MABP during exercise compared to rest after the RIPC stimulus. Resting MABP after the RIPC stimulus is significantly elevated compared to resting MABP before the RIPC stimulus. n = 9, *** P < 0.001. Error bars represent standard error of the mean.*

The changes in MABP were accompanied by analogous changes in systolic blood pressure (SBP) and diastolic blood pressure (DBP) (Fig. 4.36). The average increase in SBP during

exercise before the RIPC stimulus was 11.5 ± 4.2 mmHg (P < 0.001, *n* = 9), equivalent to an increase of 9.3%. After the RIPC stimulus, the average increase in SBP during exercise was 3.2 ± 2.3 mmHg (equivalent to a 2.3% increase), which was not significant (P = 0.165, *n* = 9). The baseline resting SBP after the RIPC stimulus increased by 14.2 ± 2.0 mmHg (P < 0.001, *n* = 9) compared to the baseline resting SBP before the stimulus, which is equivalent to an increase of 11.5%. The average increase in DBP during exercise before the RIPC stimulus was 2.0 ± 5.1 mmHg (equivalent to an increase of 2.6%), which was not significant (P = 0.225, *n* = 9). After the RIPC stimulus, the average increase in DBP during exercise was 0.4 ± 3.3 mmHg (equivalent to a 0.4% increase), which was also not significant (P = 0.393, *n* = 9). The baseline resting DBP after the RIPC stimulus increased by 13.7 ± 2.4 mmHg (P < 0.001, *n* = 9) compared to the baseline resting DBP before the stimulus, which is equivalent to an increase of 17.6%. During the RIPC stimulus itself, both SBP and DBP gradually fell and then increased towards the final period of cuff inflation in all patients – these data were also averaged together (Fig. 4.37).

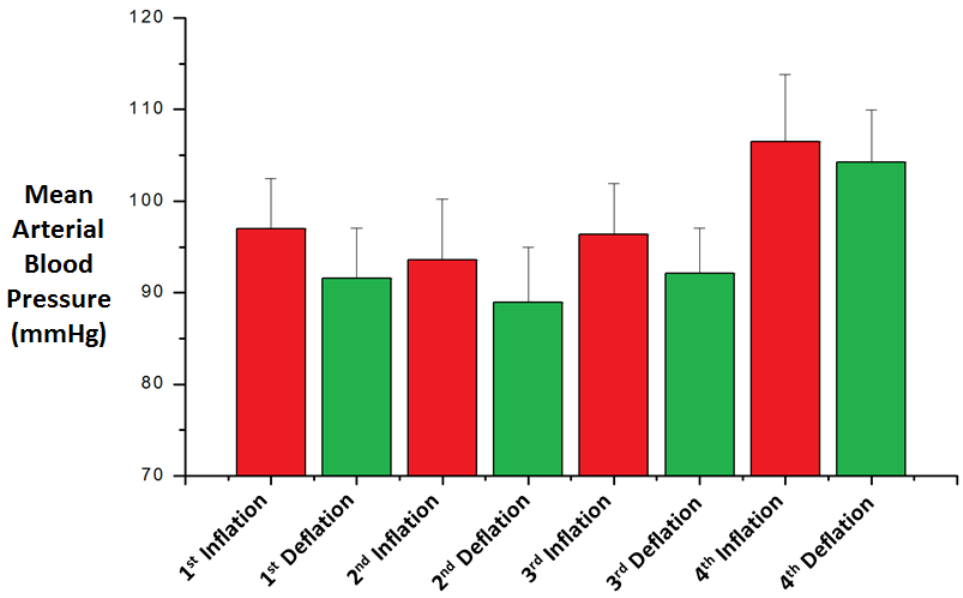

Figure 4.35 – *Graph showing mean arterial blood pressure gradually falling during the remote ischaemic preconditioning (RIPC) stimulus, and then increasing towards the end of the stimulus. n = 9. Error bars represent standard error of the mean.*

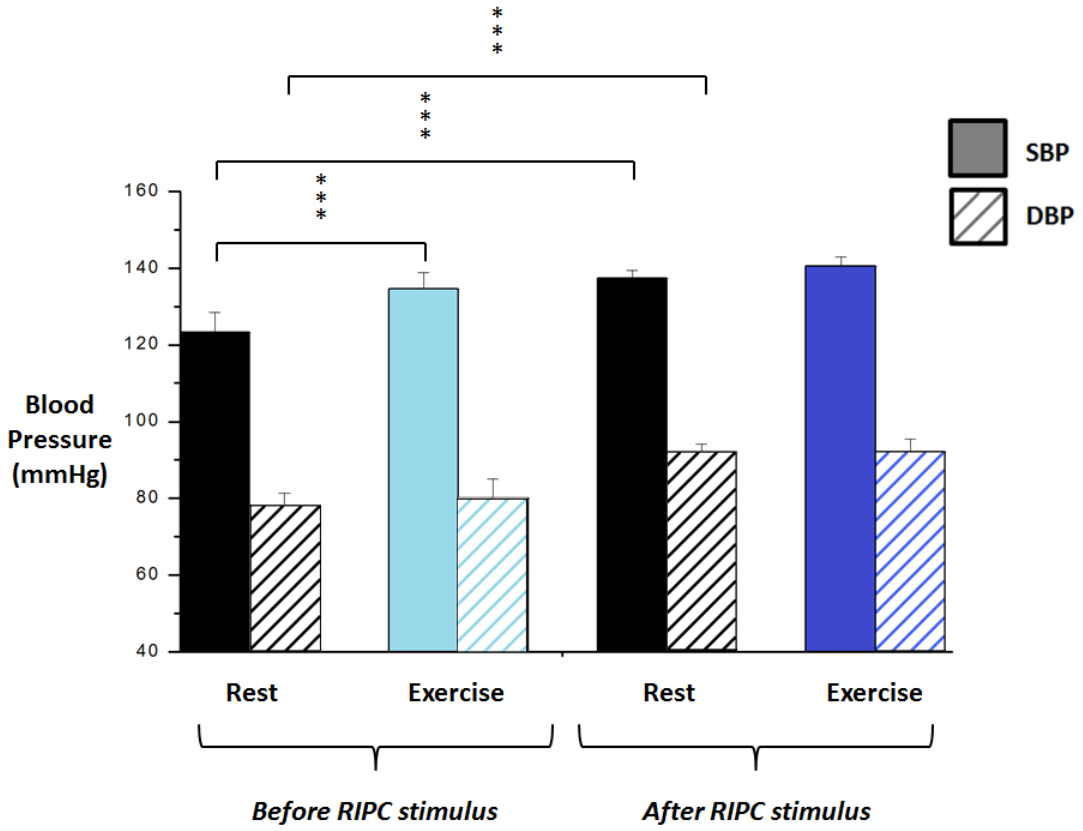

Figure 4.36 – *Graph showing a significant increase in systolic blood pressure (SBP) during exercise compared to rest before the remote ischaemic preconditioning (RIPC) stimulus, and a non-significant increase in SBP during exercise compared to rest after the RIPC stimulus. Resting SBP and diastolic blood pressure (DBP) after the RIPC stimulus are both significantly elevated compared to resting SBP and DBP before the RIPC stimulus. n = 9, *** P < 0.001. Error bars represent standard error of the mean.*

All nine of the patients who performed the experiment had a significantly decreased R-R interval during exercise before the RIPC stimulus. However, after the stimulus, the resting R-R interval was significantly increased in all patients compared to the resting R-R interval before the stimulus. Exercise following the stimulus did not cause a significant decrease in R-R interval compared to this new resting baseline. The R-R interval data for all nine patients were averaged together (Fig. 4.38). The decrease from rest during exercise before the RIPC stimulus was 0.055 ± 0.021 s ($P < 0.001$, $n = 9$), equivalent to a decrease of 7.2%. After the RIPC stimulus, the decrease from rest during exercise was 0.027 ± 0.020 s (equivalent to a 3.3%

decrease), which was not significant (P = 0.077, *n* = 9). The baseline resting R-R interval after the stimulus increased by 0.051 ± 0.021 s (P = 0.023, *n* = 9) compared to the baseline resting R-R interval before the stimulus, which is equivalent to an increase of 6.7%. During the RIPC stimulus itself, the R-R interval gradually increased – these data were also averaged together (Fig. 4.39).

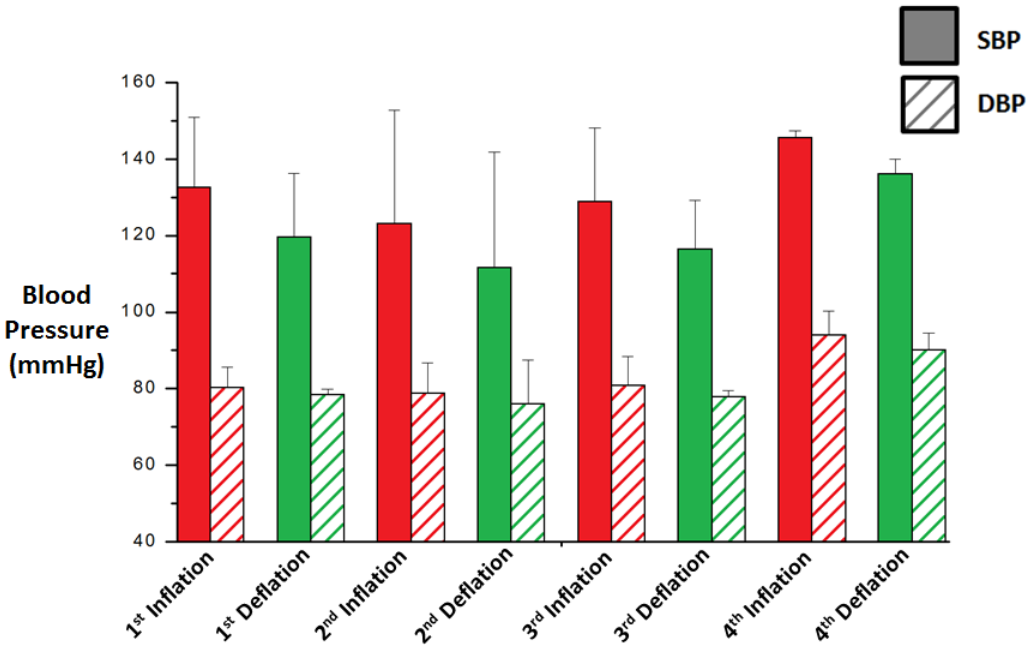

Figure 4.37 – *Graph showing both systolic blood pressure (SBP) and diastolic blood pressure (DBP) gradually falling during the remote ischaemic preconditioning (RIPC) stimulus, and then increasing towards the end of the stimulus. n = 9. Error bars represent standard error of the mean.*

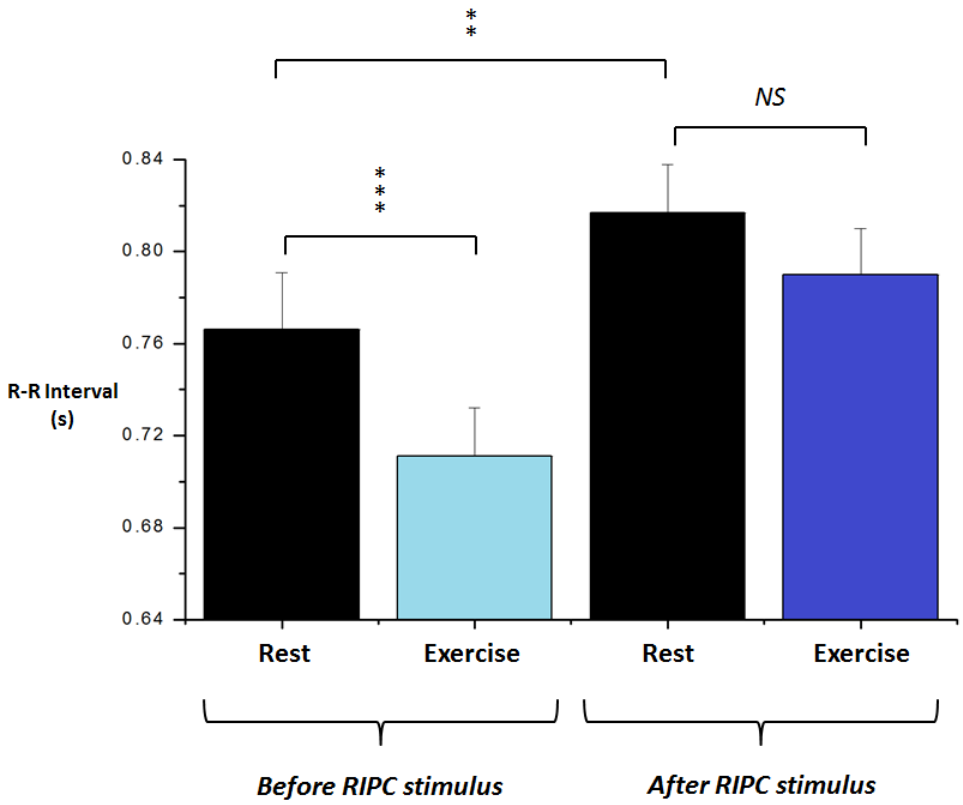

Figure 4.38 – *Graph showing a significant decrease in R-R interval (i.e. an increase in heart rate) during exercise compared to rest before the remote ischaemic preconditioning (RIPC) stimulus, and a non-significant (NS) decrease in R-R interval during exercise compared to rest after the RIPC stimulus. The resting R-R interval after the RIPC stimulus is significantly increased (i.e. resting heart rate is decreased) compared to the resting R-R interval before the RIPC stimulus. n = 9, ** P < 0.01, *** P < 0.001. Error bars represent standard error of the mean.*

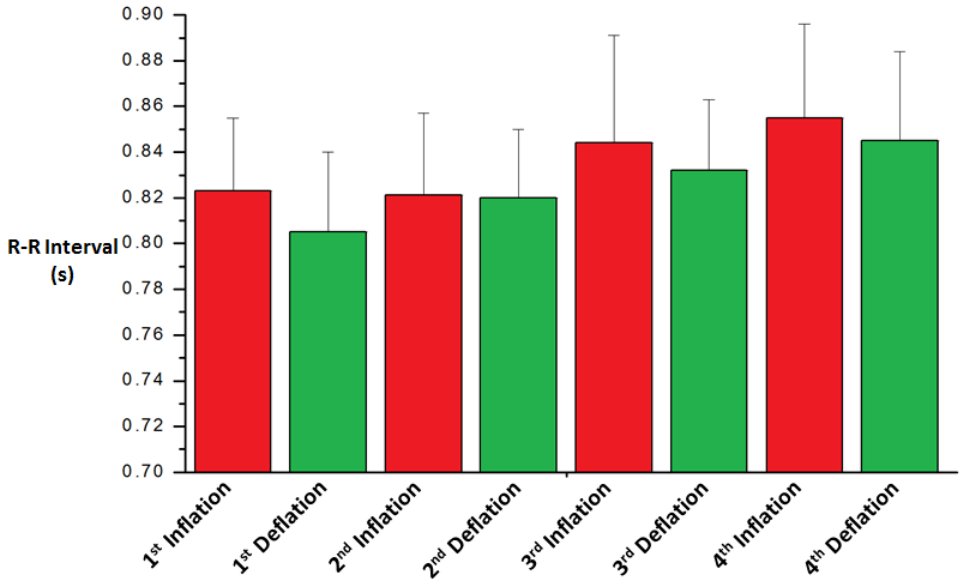

Figure 4.39 – *Graph showing R-R interval gradually increasing (i.e. heart rate gradually falling) during the remote ischaemic preconditioning (RIPC) stimulus. n = 9. Error bars represent standard error of the mean.*

Electrode Localisation

Fig. 4.40 shows the positions of the electrodes in the two periaqueductal grey (PAG) patients who performed the experiment, in both the transverse and coronal planes. Fig. 4.41 shows a schematic diagram of these same two PAG electrodes so that the contacts on each electrode can be examined. Recordings were only made from those contacts that provided the patients with therapeutic benefit (i.e. pain relief). All of these contacts were located within the dorsal region of the PAG.

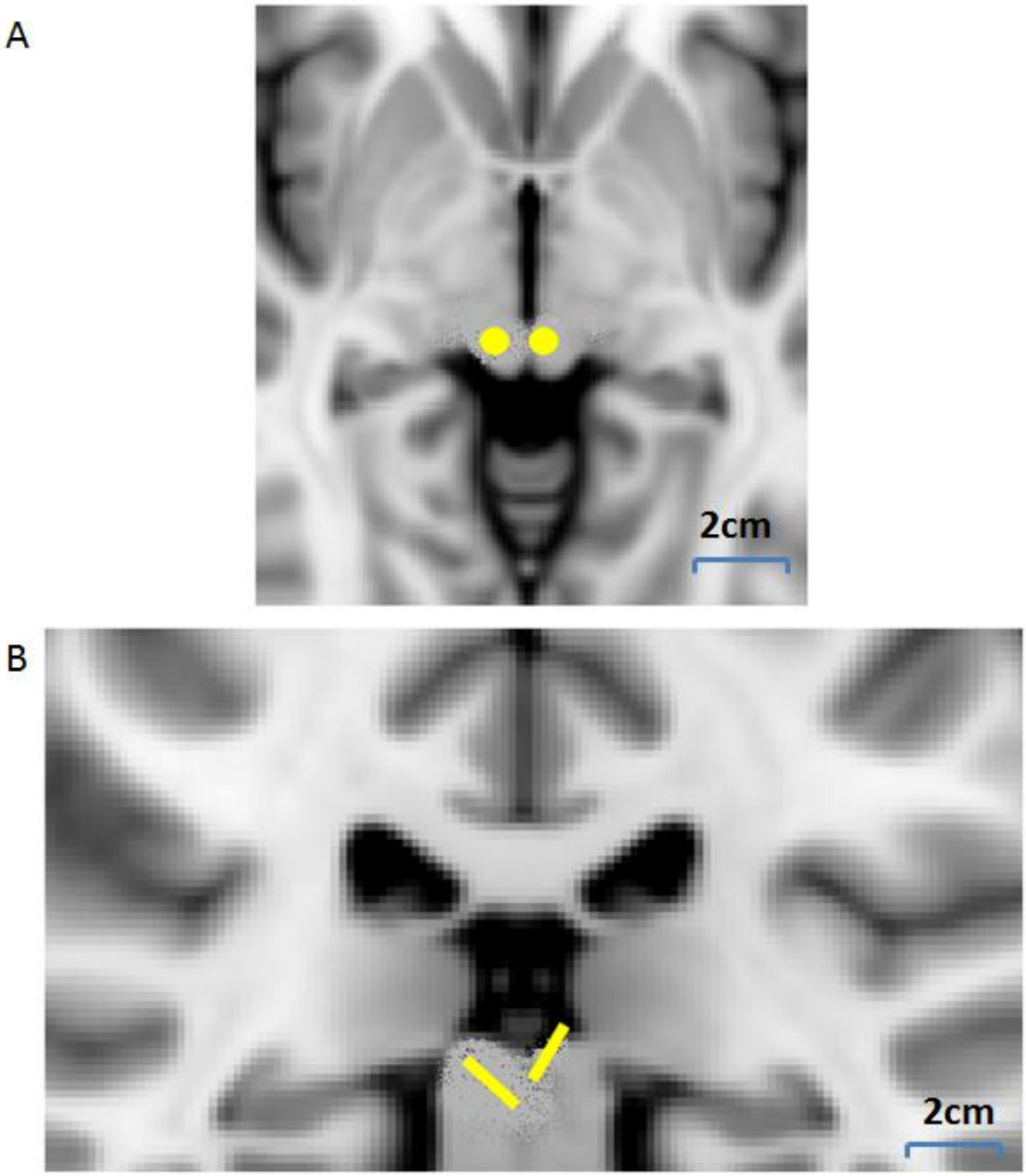

Figure 4.40 - *Post-operative image showing individual electrode locations in the transverse (A) and coronal (B) planes for two periaqueductal grey patients. Both scale bars represent 2 cm. Yellow dots represent the midpoints of each electrode. Yellow rectangles represent entire length of each electrode.*

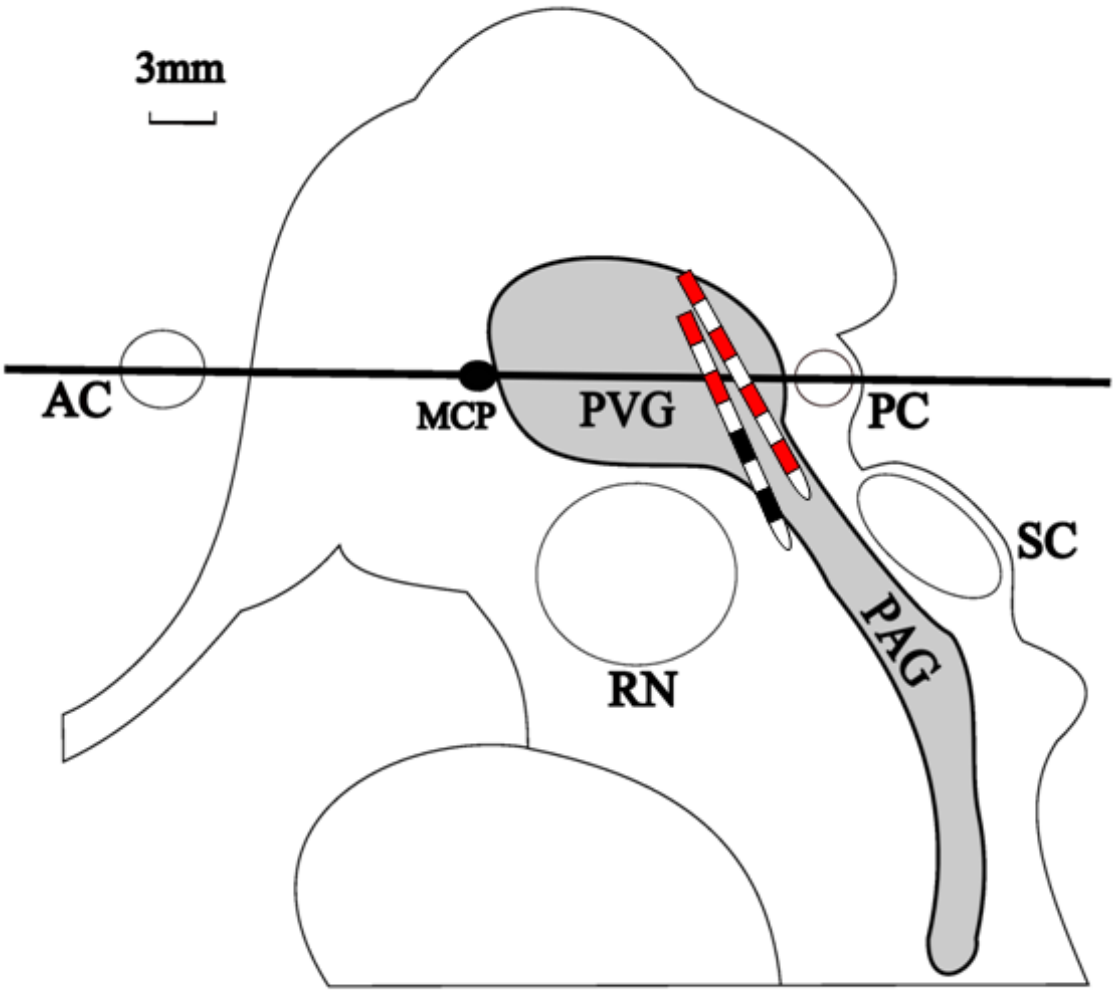

Figure 4.41 – *Schematic diagram in the sagittal plane showing electrode locations for two PAG patients who performed the experiment. The data presented in this study are recorded only from those contacts that provided therapeutic benefit – these were all within the dorsal aspect of the PVG/PAG (highlighted in red). AC, anterior commissure; MCP, mid-commissural point; PVG, periventricular grey; PC, posterior commissure; RN, red nucleus; PAG, periaqueductal grey; SC, superior colliculus.*

Local Field Potential Recordings from the Subthalamic Nucleus

Using ANOVA, a significant difference was revealed between the conditions of exercise and rest before the remote ischaemic preconditioning (RIPC) stimulus and exercise and rest after the RIPC stimulus ($P < 0.05$) for each individual patient. Therefore, all the subthalamic nucleus (STN) data were averaged together (Fig. 4.42). Significant decreases in STN neural activity

occurred during exercise performed before the RIPC stimulus. However, increases in STN neural activity were observed during exercise performed after the stimulus. In the 4-8 Hz band, exercise before RIPC was associated with a decrease in power spectral density (PSD) of 124.1 ± 79.5 μV^2/Hz (P = 0.041, *n* = 4), which is equivalent to a 20.1% decrease. In the 8-12 Hz band, there was a decrease in PSD of 45.0 ± 9.0 μV^2/Hz (P < 0.001, *n* = 4) during exercise before RIPC, which is equivalent to a 20.9% decrease. In the 12-25 Hz band, exercise before RIPC was associated with a decrease in PSD of 25.7 ± 2.2 μV^2/Hz (P < 0.001, *n* = 4), which is equivalent to a decrease of 31.6%. During exercise after RIPC, there were significant increases across all the frequency bands. In the 4-8 Hz band, exercise after RIPC was associated with an increase in PSD of 961.7 ± 236.8 μV^2/Hz (P < 0.001, *n* = 4), equivalent to a 204.6% increase. In the 8-12 Hz band, there was an increase in PSD of 328.7 ± 34.8 μV^2/Hz (P < 0.001, *n* = 4) during exercise after RIPC, equivalent to a 188.8% increase. In the 12-25 Hz band, exercise after RIPC was associated with an increase in PSD of 172.1 ± 12.0 μV^2/Hz (P < 0.001, *n* = 4), equivalent to an increase of 291.5%. In the 25-60 Hz band, there was an increase in PSD of 55.0 ± 2.7 μV^2/Hz (P < 0.001, *n* = 4) during exercise after RIPC, equivalent to a 173.3% increase. Finally, in the 60-90 Hz band, exercise after RIPC was associated with an increase in PSD of 22.7 ± 1.0 μV^2/Hz (P < 0.001, *n* = 4), equivalent to an increase of 161.1%.

Furthermore, a significant decrease was observed in STN neural activity at rest after the RIPC stimulus compared to before the stimulus (Fig. 4.43). In the 4-8 Hz band, rest after RIPC was associated with a decrease in PSD of 147.1 ± 54.2 μV^2/Hz (P = 0.002, *n* = 4), equivalent to a 23.8% decrease. In the 8-12 Hz band, there was a decrease in PSD of 40.9 ± 14.2 μV^2/Hz (P < 0.001, *n* = 4) during rest after RIPC, equivalent to a 19.0% decrease. In the 12-25 Hz band, rest after RIPC was associated with a decrease in PSD of 22.3 ± 3.7 μV^2/Hz (P < 0.001, *n* = 4), equivalent to a decrease of 27.4%.

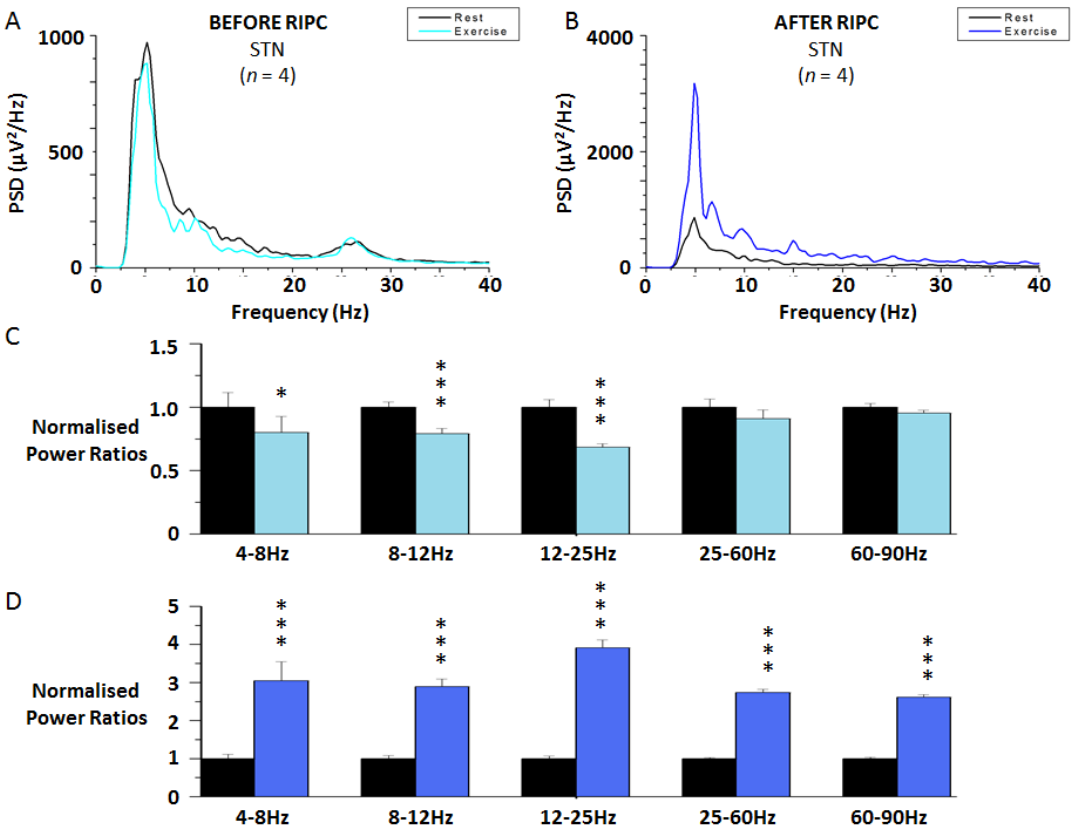

Figure 4.42 – *Graphs showing significant changes in subthalamic nucleus (STN) neural activity during exercise both before and after the remote ischaemic preconditioning (RIPC) stimulus, compared to rest. (A) Mean power spectral density (PSD) for all four patients performing exercise before the RIPC stimulus. (B) Mean PSD for all four patients performing exercise after the RIPC stimulus. (C) Normalised spectral changes (rest = 1.0) divided into frequency bands, showing significant decreases during exercise before RIPC in the 4-8 Hz, 8-12 Hz and 12-25 Hz bands, compared to rest. (D) Normalised spectral changes (rest = 1.0) divided into frequency bands, showing significant increases during exercise after RIPC in all frequency bands, compared to rest. n = 4, * P < 0.05, *** P < 0.001. Error bars represent standard error of the mean.*

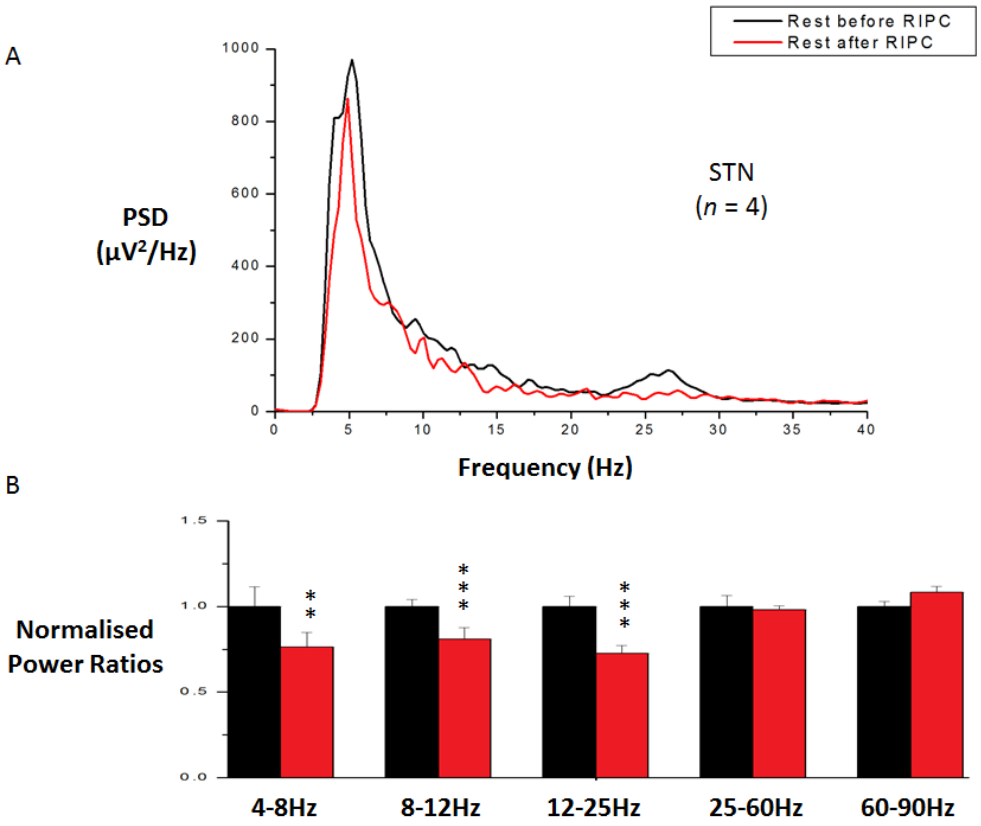

Figure 4.43 – *Graphs showing a significant decrease in subthalamic nucleus (STN) neural activity at rest after the remote ischaemic preconditioning (RIPC) stimulus, compared to rest before the stimulus. (A) Mean power spectral density (PSD) for the four STN patients. (B) Normalised spectral changes (rest = 1.0) divided into frequency bands, showing significant decreases at rest after RIPC in the 4-8 Hz, 8-12 Hz and 12-25 Hz bands, compared to rest before RIPC. n = 4, ** P < 0.01, *** P < 0.001. Error bars represent standard error of the mean.*

Local Field Potential Recordings from the Other Nuclei

Using ANOVA, there were no significant differences found among any of the conditions in any of the periaqueductal grey (PAG) (Figs. 4.44-4.45) or thalamus patients (Figs. 4.46-4.47).

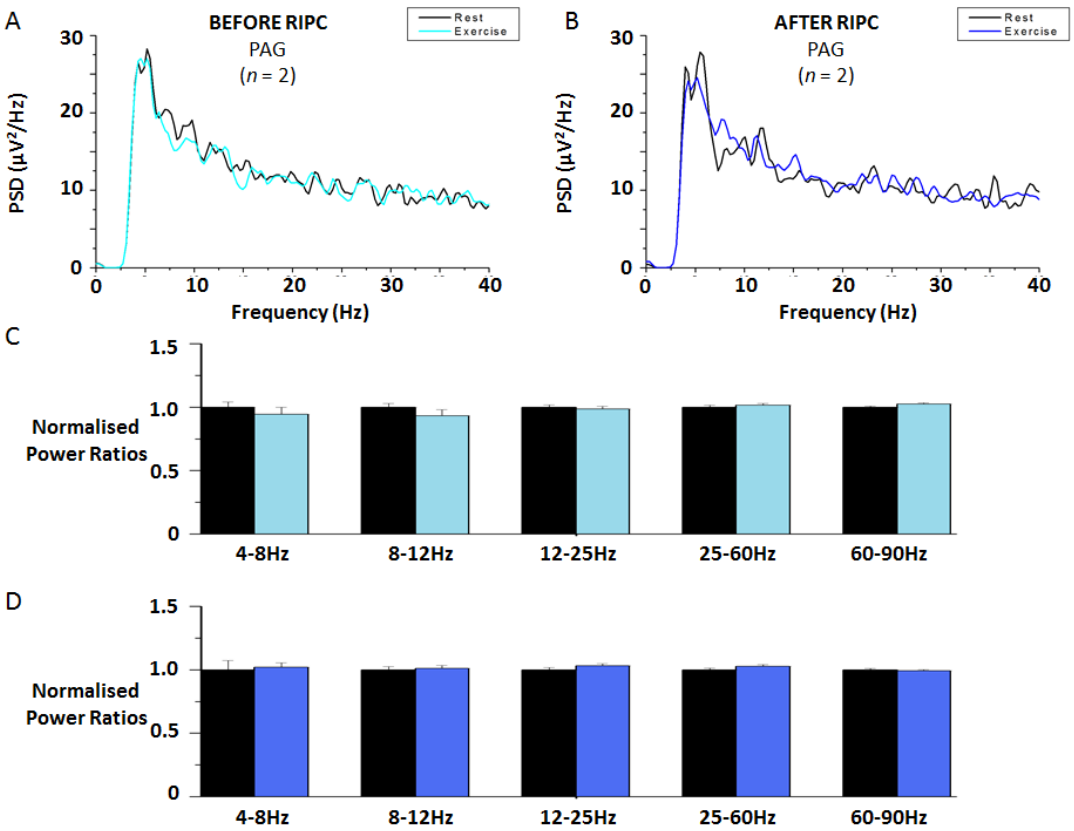

Figure 4.44 – *Graphs showing no significant changes in periaqueductal grey (PAG) neural activity following the remote ischaemic preconditioning (RIPC) stimulus. (A) Mean power spectral density (PSD) for both patients performing exercise before the RIPC stimulus. (B) Mean PSD for both patients performing exercise after the RIPC stimulus. (C) Normalised spectral changes (rest = 1.0) divided into frequency bands, showing no significant differences in exercise before RIPC, compared to rest. (D) Normalised spectral changes (rest = 1.0) divided into frequency bands, showing no significant differences in exercise after RIPC, compared to rest. n = 2. Error bars represent standard error of the mean.*

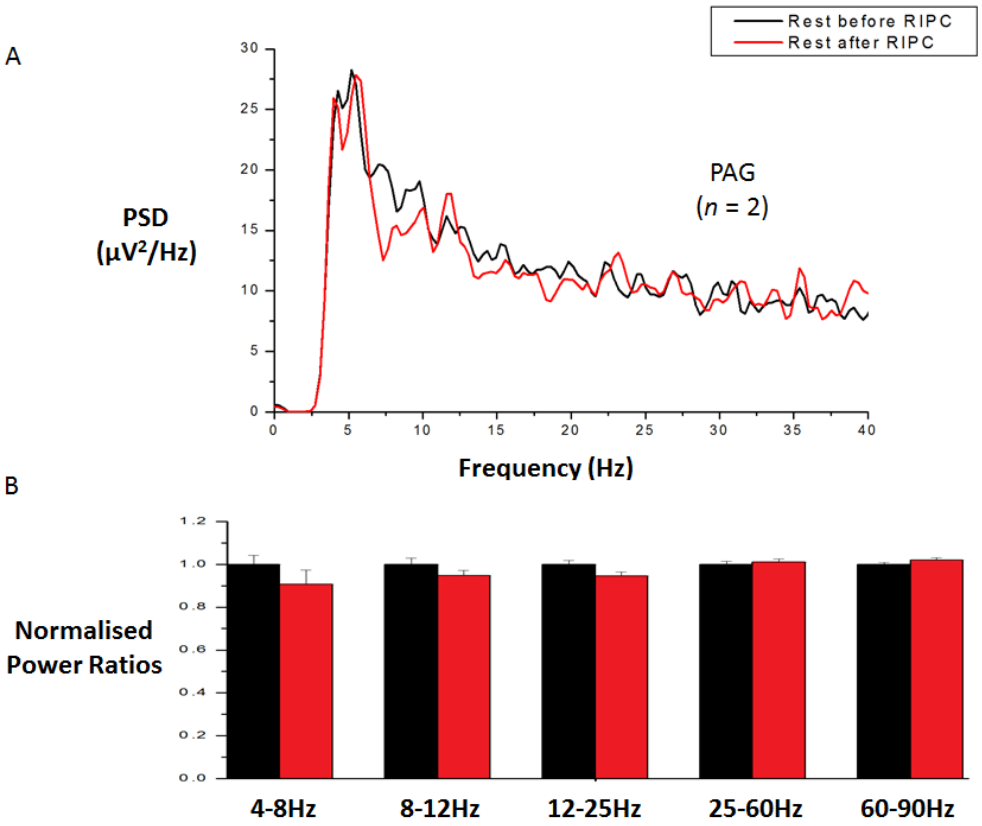

Figure 4.45 – *Graphs showing no significant changes in periaqueductal grey (PAG) neural activity following the remote ischaemic preconditioning (RIPC) stimulus. (A) Mean power spectral density (PSD) for both patients. (B) Normalised spectral changes (rest = 1.0) divided into frequency bands, showing no significant differences at rest after RIPC compared to rest before RIPC. n = 2. Error bars represent standard error of the mean.*

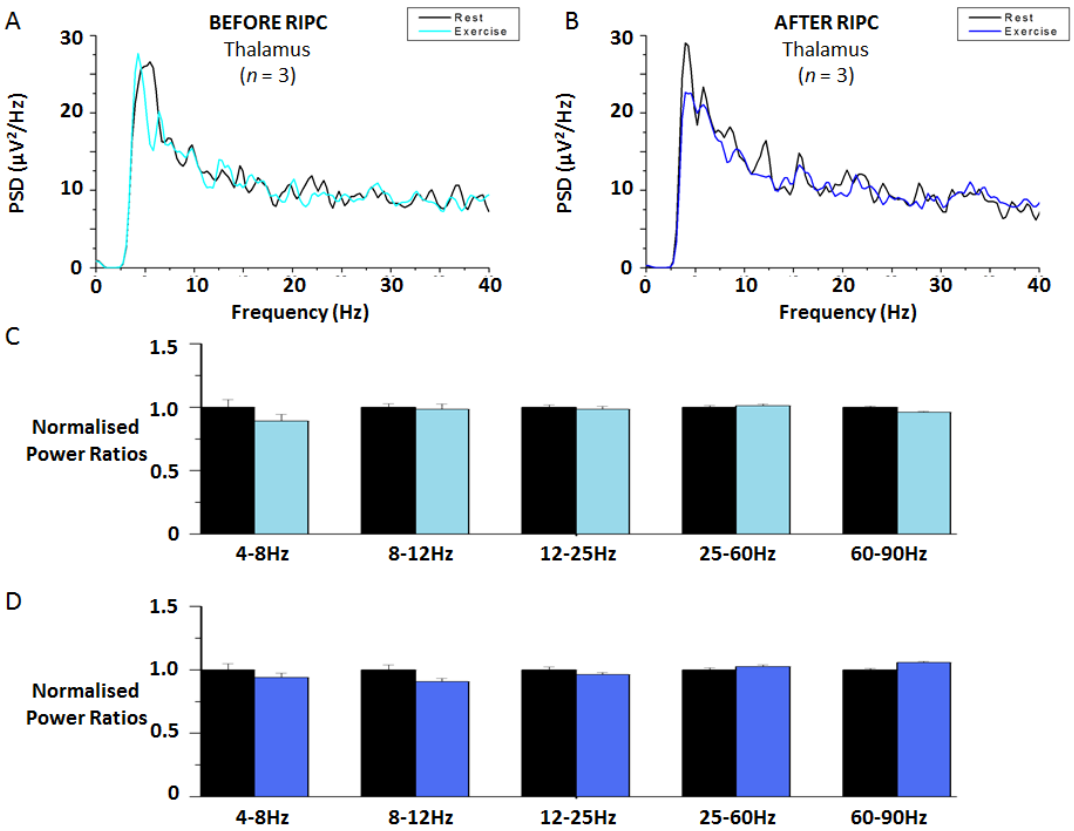

Figure 4.46 – *Graphs showing no significant changes in thalamic neural activity following the remote ischaemic preconditioning (RIPC) stimulus. (A) Mean power spectral density (PSD) for all three patients performing exercise before the RIPC stimulus. (B) Mean PSD for all three patients performing exercise after the RIPC stimulus. (C) Normalised spectral changes (rest = 1.0) divided into frequency bands, showing no significant differences in exercise before RIPC, compared to rest. (D) Normalised spectral changes (rest = 1.0) divided into frequency bands, showing no significant differences in exercise after RIPC, compared to rest. n = 3. Error bars represent standard error of the mean.*

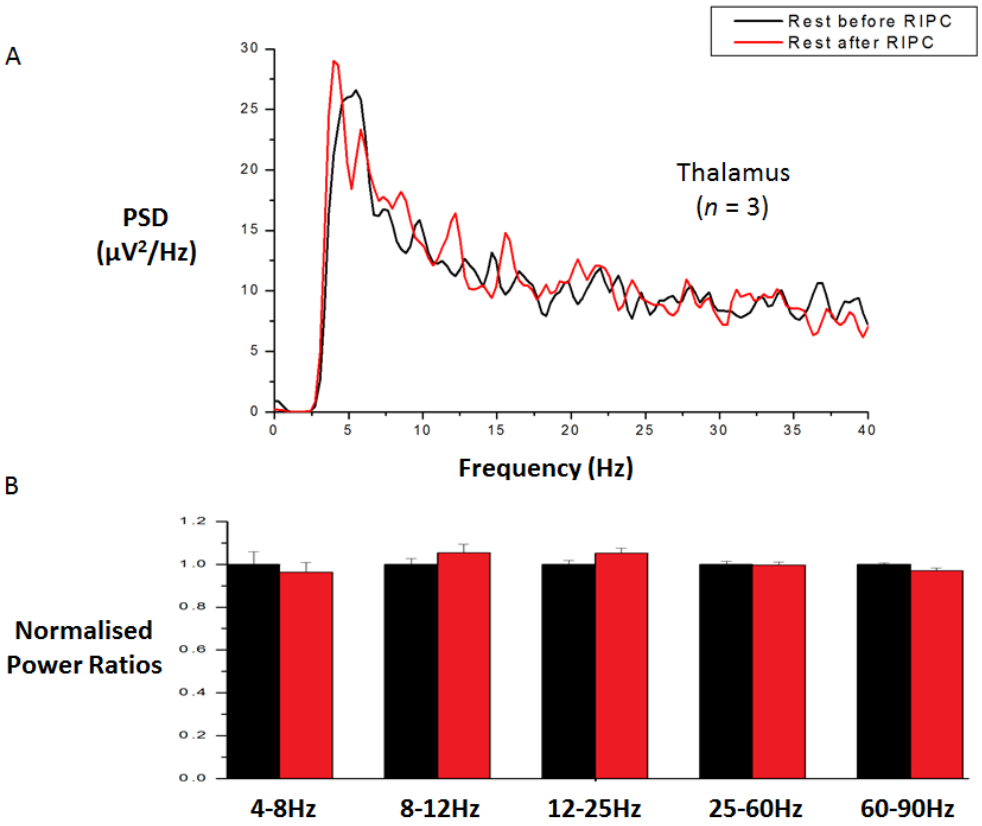

Figure 4.47 – *Graphs showing no significant changes in thalamic neural activity following the remote ischaemic preconditioning (RIPC) stimulus. (A) Mean power spectral density (PSD) for all three patients. (B) Normalised spectral changes (rest = 1.0) divided into frequency bands, showing no significant differences at rest after RIPC compared to rest before RIPC. n = 3. Error bars represent standard error of the mean.*

Discussion

The findings presented in this chapter are consistent with the hypothesis that neural activity in the periaqueductal grey (PAG) is graded to increases in exercise intensity and corresponding increases in arterial blood pressure. The other sites that were investigated (the subthalamic nucleus [STN], the thalamus and the internal globus pallidus) appear not to be involved in the integration of the reflex, despite having been previously identified as cardiovascularly active in both animals and humans (Eldridge *et al*, 1981; Thornton *et al*, 2002), as discussed in Chapter 3. It should once again be noted that the sensation of the cuff inflation itself does not correspond to a change in PAG activity. Another finding that I have been able to demonstrate

in this chapter is that neural activity in the STN (but not in the PAG or the thalamus) appears to correspond to the cardiovascular changes evoked by the remote ischaemic preconditioning stimulus performed on the upper limb in humans.

Role of the Periaqueductal Grey in the Integration of the Exercise Pressor Reflex at Varying Exercise Intensities and During Ischaemic Exercise

I have once again shown that there is a significant increase in neural activity in the periaqueductal grey (PAG) during post-exercise occlusion of the limb in the lower frequency bands (4-8 Hz and 8-12 Hz). However, in this chapter I have also been able to demonstrate that when the intensity of the exercise is increased, the increase in PAG neural activity (in terms of absolute power spectral density [PSD] values) also increases, along with corresponding increases in arterial blood pressure. Wiles *et al* (2008) have previously demonstrated linear relationships between exercise intensity and both systolic blood pressure and heart rate. Although I have not been able to demonstrate a linear relationship between exercise intensity and cardiovascular parameters per se, I have been able to show that increased exercise intensity results in a further increase of arterial blood pressure and heart rate from rest. An explanation for this discrepancy could be that the patients in the Wiles *et al* (2008) study were asked to perform isometric exercise tasks of different intensities using a large muscle mass, whereas in my experiments the patients were asked to perform dynamic exercise tasks of different intensities using a smaller muscle mass. It is known that during dynamic exercise, systolic blood pressure (SBP) increases and diastolic blood pressure (DBP) remains relatively unchanged, whereas during static exercise, both SBP and DBP increase. This could explain why I did not observe an exact linear relationship between exercise intensity and cardiovascular parameters, whereas Wiles *et al* (2008) did.

Past research also shows that when exercise intensity is increased, neural activity increases accordingly. Kakizaki *et al* (1988) investigated the effects of bicycle exercise on neural activity, and demonstrated that occipital EEG amplitude increased as workload increased. Bailey *et al* (2008) observed significant increases in EEG activity with increasing exercise on a recumbent cycle ergometer. I have not only shown increasing PAG activity corresponding to increasing exercise intensity, but also that the increase in neural activity appears to be more widespread across the frequency bands. This pattern is comparable to the results of Green *et al* (2007), whose protocol demanded a much higher intensity of exercise from their patients, who were asked to perform cycle ergometry, as opposed to the small muscle mass exercise required of the patients in my experiments. They observed significantly increased PAG activity even in the 25-60 Hz and 60-90 Hz frequency bands. Therefore, increased effort and higher drive seem to be associated with increased PAG neural activity over a broader spectrum of frequencies.

Furthermore, at an increased intensity of exercise (bicep curls with 4kg of weight), the pressor reflex was being activated during the exercise period itself – this was evidenced by the significant elevation of PSD during 4 kg exercise in the 12-25 Hz band. During lower intensity exercise (bicep curls with 2 kg of weight), the pressor reflex was not activated during exercise, but only during the following period of post-exercise occlusion. However, with higher intensity exercise, the blood flow through the limb would have been insufficient to completely remove the metabolites produced during exercise. Therefore, the group III and IV nerve afferents within the muscles would have been stimulated, even without occlusion, thereby activating the pressor reflex.

In addition, during ischaemic exercise, neural activity in the PAG is also significantly increased in terms of absolute PSD values, again with corresponding increases in arterial blood pressure. The patterns of activity of fine muscle afferents during ischaemic contractions compared to normal contractions with the same developed tension have been studied by Kaufman *et al*

(1984). They observed that group III and IV nerve afferents within exercising muscle in cats were stimulated more by ischaemic exercise compared to normal exercise, when the tension developed by both was the same. This finding is mirrored in my results – ischaemic exercise results in increased stimulation of group III and IV nerve endings which results in increased PAG neural activity compared to normal exercise. Thus, it appears that the PAG could be responsible for the enhanced cardiovascular response that was observed.

It has already been established that the PAG plays an important role in autonomic regulation. Stimulation of the dorsolateral and lateral areas in animals has been shown to produce tachycardia and hypertension (Carrive *et al*, 1987) and, conversely, stimulation of the ventrolateral column results in bradycardia and hypotension (Carrive and Bandler, 1991b). Likewise, in humans, stimulation of the dorsal area produces hypertension, and stimulation of the ventral area results in hypotension (Green *et al*, 2005). When the results from this chapter and the previous chapter are taken together with the recognised effects of stimulation of the dorsal PAG in humans and the dorsolateral and lateral PAG in animals, they strongly suggest that the PAG is a key structure within the neurocircuitry that integrates and modulates the exercise pressor reflex.

Remote Ischaemic Preconditioning

I have shown that the remote ischaemic preconditioning (RIPC) stimulus appears to 'reset' the resting arterial blood pressure to a higher basal level in humans, and following the stimulus, exercise no longer causes a significant increase in arterial blood pressure. Conversely, the RIPC stimulus appears to 'reset' the resting heart rate to a lower basal level, and after the stimulus, exercise no longer causes a significant increase in heart rate. I have also provided evidence to support the hypothesis that these modulations in the cardiovascular responses to exercise could be mediated by the subthalamic nucleus (STN).

Role of the Subthalamic Nucleus in the Integration of the Remote Ischaemic Preconditioning Stimulus

The results of the remote ischaemic preconditioning (RIPC) experiments indicate that the subthalamic nucleus (STN) could be a key structure of the neurogenic pathway of the RIPC signal. Prior to the stimulus, STN neural activity decreased during exercise, as previously observed in Chapter 3. This is consistent with data showing decreased STN activity during exercise following warning and 'go' cues (Kuhn *et al*, 2004; Green *et al*, 2007). The decrease in STN activity that was observed during exercise before the RIPC stimulus is indicative of a release of the inhibitory drive on the cardiovascular nuclei which receive projections from the STN, resulting in increased arterial blood pressure and heart rate. After the RIPC stimulus, the STN neural activity at rest was significantly decreased compared to its resting activity before the stimulus. This was reflected in the blood pressure recordings – arterial blood pressure was higher during rest after the stimulus compared to before the stimulus, due to the release of the inhibitory drive on the nuclei receiving STN projections.

This drop in neural activity could represent an event-related desynchronisation caused by a decrease in synchrony of populations of local neurons (Pfurtscheller and Lopes da Silva, 1999). Levy *et al* (2002) proposed that decreases in STN neural activity observed during voluntary movement are altered by the cortical input to the STN. With regards to RIPC, the stimulus itself could be causing a modulation of the input to the STN (in terms of decreased synchrony), thereby modifying its output.

Interestingly, during exercise following the RIPC stimulus, STN neural activity was seen to increase. This suggests that the inhibitory drive on the cardiovascular nuclei receiving projections from the STN is heightened during periods of exercise following preconditioning, which is mirrored by the fact that during exercise after RIPC, there is no longer a significant

increase in arterial blood pressure and heart rate. It appears that the RIPC stimulus somehow reverses the response of the STN to exercise in order to maintain its inhibitory effect over the cardiovascular nuclei to which it projects, thereby resulting in arterial blood pressure and heart rate remaining unchanged compared to rest.

The STN is considered to be a cardiovascularly active area, as there is evidence to support its involvement in the parallel activation of the cardiovascular and locomotor systems. Stimulation of the STN in both freely moving and anaesthetised cats results in significantly increased arterial blood pressure and heart rate (Angyan and Angyan, 1999b). STN stimulation caused significant cardiovascular changes in anaesthetised cats, despite the absence of visible locomotor activity, which suggests that the STN is directly involved in integrating cardiovascular function. Additionally, it indicates that the cardiovascular responses to stimulation of the STN are not secondary to electrically elicited movement. Smith *et al* (1960) showed that stimulation of the dorsal area of the STN in dogs evoked cardiovascular responses comparable to those which resulted from volitional exercise. Eldridge *et al* (1981) stimulated the subthalamic locomotor region in unanaesthetised decorticate cats and demonstrated that this area drove both cardiovascular and locomotor activity. High frequency stimulation of the STN in humans (equivalent to depolarising block) results in increased arterial blood pressure, increased heart rate and facilitation of movement (Thornton *et al*, 2002). The results from this study, taken together with the evidence from both humans and animals, suggest that the STN is an important aspect of the circuitry underpinning the cardiovascular responses to exercise, and could potentially be a key structure in the neurogenic signalling pathway of the RIPC stimulus.

Limitations

The limitations of these experiments overlap considerably with those put forward in Chapter 3. Once more, the question can be posed of whether the changes in power spectral density (PSD) directly translate into changes in neural activity. As local field potentials are considered to be due to local synchronous neuronal population activity (Mitzdorf, 1985; Rasch *et al*, 2009), increases in PSD are thought to be a reflection of increases in network synchrony or size (Logothetis *et al*, 2001; Katzner *et al*, 2009; Kelly *et al*, 2010).

For the varied intensity exercise protocol and the ischaemic exercise protocol, there is a chance that the increased periaqueductal grey (PAG) neural activity might not be causal to the pressor reflex, but instead be compensatory to the reflex, or simply a coincidence. It is extremely unlikely to be a coincidence, particularly as the increase in PAG neural activity was only observed during exercise, post-exercise occlusion, or occlusion with continuing exercise – there was never any increase in PAG activity during occlusion without prior exercise. With regards to the increase in neural activity being compensatory to the pressor reflex, it has been shown in cats that increasing arterial blood pressure with phenylephrine does not alter c-Fos immunoreactivity within the PAG, whereas it did have an effect in other cardiovascularly active areas in the brainstem (Williams *et al*, 2000). Additionally, direct electrical stimulation of the dorsal PAG in humans causes an increase in arterial blood pressure (Green *et al*, 2005), and I have shown here that the magnitude of the reflex and PAG neural activity are graded to the intensity of the exercise task.

A further limitation for all of the experiments in this chapter is the underlying pathology in the patient model. Although there is no indication that the PAG is dysfunctional in the patients suffering from chronic pain, it is known that the subthalamic nucleus (STN) is affected in patients suffering from Parkinson's disease. This makes it difficult to translate my findings to healthy humans. Furthermore, the specific nuclei studied in these experiments were limited,

as only sites that provided therapeutic benefit to the patient could be recorded from. Nevertheless, the nuclei examined have all been identified in animal models as cardiovascularly active. In addition, without histological data, the precise location of the electrodes within the various nuclei can only be estimated, despite their careful placement using stereotactic coordinates.

For the remote ischaemic preconditioning (RIPC) protocol, a major limitation lay in the fact that it was not known whether the RIPC stimulus had actually been successful and the heart had been preconditioned. Further studies with DBS patients based on the human endothelial model of RIPC (Loukogeorgakis *et al*, 2005) would be valuable in determining whether the stimulus has actually worked. Finally, the RIPC stimulus is likely to have a wide range of effects on multiple neural structures. Even though the STN was the only nucleus to show changes in activity in this set of experiments, it would be imprudent to assume that it is the only nucleus to be a part of, or necessarily essential to, the neurogenic pathway of the RIPC stimulus.

Conclusion

This chapter has resulted in two conclusions:

(1) Using direct neurophysiological recordings, this study provides evidence to suggest that the dorsal PAG is a key component of the neurocircuitry responsible for integrating the exercise pressor reflex in humans, and its activity is directly graded to exercise intensity.

(2) This study – the first of its kind to attempt to establish the neurocircuitry involved in preconditioning – provides evidence to suggest that the STN is a key component of the neurocircuitry involved in the neurogenic pathway of RIPC.

CHAPTER 5

Identifying Cardiovascular Neurocircuitry Involved During Changes in Central Command during Isometric Exercise at Constant Muscle Tension Using Muscle Vibration

Introduction

It was Zuntz and Geppert (1886) who first suggested that a signal originating from higher brain centres was responsible for initiating the cardiorespiratory responses to exercise. This concept was later introduced as 'cortical irradiation' by Krogh and Lindhard (1913), who proposed that neural impulses from the brain controlled cardiorespiratory parameters in a 'top-down' manner in order to meet the anticipated metabolic demands of working muscle. They were able to demonstrate in humans, that at the start of exercise, cardiorespiratory parameters, such as heart rate, arterial blood pressure and pulmonary ventilation, were influenced by the subject's perception of the exercise task. They showed that the initial cardiorespiratory response to exercise anticipated each subject's perceived work rate. It was proposed that the mechanism controlling this was a sudden increase in the excitability of the cardiorespiratory centres in the brainstem, induced by 'irradiation' of impulses from the motor cortex. This cortically-initiated feed-forward regulatory response is now referred to as 'central command' (Goodwin *et al*, 1972).

In 1965, Asmussen *et al* used intravenous injections of tubocurarine to induce partial neuromuscular blockade, in order to study the influence of central command on the responses to exercise in humans performing cycle ergometry. When muscle strength was reduced by partial paralysis, they found that there was an exaggerated ventilatory response despite the intensity level of the dynamic exercise task remaining unchanged.

In the 1980s, Eldridge *et al* (1981; 1985) examined the relationship between respiration and locomotion in unanaesthetised decorticate cats; this animal model had been shown to move normally when placed on treadmills. Their experimental design allowed the influence of feedback pathways to be eliminated, as the cats were able to move both spontaneously and during electrical stimulation of the subthalamic locomotor region in the brain. They noted an increase in both respiratory rate and arterial blood pressure before the onset of the treadmill exercise, and once exercise had stopped, they observed a rapid decrease in respiratory rate. Additionally, it was observed that both arterial blood pressure and respiratory rate increased proportionately according to the intensity of the exercise task. In paralysed cats, electrical stimulation of the subthalamic locomotor region caused 'fictive' locomotion, which was also preceded by increased arterial blood pressure and respiratory rate. The findings of Eldridge *et al* (1981; 1985) provided evidence to support the theory that a neural signal originating above the cardiorespiratory centres of the medulla could be responsible for both locomotion and the increase in cardiorespiratory parameters associated with it, without the need for feedback from working muscles. These studies provided compelling support for the role of midbrain circuits (sub-cortical control) in the cardiorespiratory response to exercise.

Gandevia *et al* (1993) further investigated the central command response in artificially ventilated human subjects who had undergone total neuromuscular blockade. Whilst paralysed, it was noted that there was a marked increase in both arterial blood pressure and heart rate during attempted isometric contractions of the arm, leg and trunk muscle groups. The increases in mean arterial blood pressure and heart rate during attempted handgrip contractions were comparable to the increases observed during actual handgrip contractions. It was noted that these changes in cardiovascular parameters were graded in proportion to the intensity of muscle contraction. It is clear that these responses could not have been part of a regulatory feedback pathway, as the subjects had undergone total neuromuscular blockade and were paralysed. Evidently, neural signals originating from the cortex can trigger activation

of sympathetic outflow to both the heart and the appropriate vascular beds (Eldridge *et al*, 1981; Eldridge *et al*, 1985; Gandevia *et al*, 1993).

It was formerly thought that the central command response of the cardiorespiratory system was closely associated with the parallel feedforward motor system. However, in 2006, Williamson *et al* proposed that central command actually involves the simultaneous activation of two distinct pathways – one pathway influencing central motor control, and the other pathway influencing central cardiorespiratory control. Studies in which the subject's perception of an exercise task appears to determine their cardiovascular response (as opposed to the exercise task itself) provides evidence for this, such as those conducted by Thornton *et al* (2001) and Williamson *et al* (2001). Both of these groups used the hypnotic suggestion of exercise in order to uncouple central command from peripheral feedback. Thornton *et al* (2001) demonstrated, in hypnotically induced human subjects, that during the imagination of a heavy exercise task (uphill cycling), heart rate and ventilation both increased, whereas imagination of free-wheeling downhill had no effect on either. They also used positron emission tomography (PET) to identify several neural correlates that were active during the imagination of exercise which are known to be coupled to cardiorespiratory centres. It was shown that the right dorsolateral prefrontal cortex, the right premotor area, the superolateral sensorimotor areas, the supplementary motor areas, the thalamus and the cerebellum were all active during the imagination of exercise. During volitional hyperventilation to match the respiratory rate caused by imagination of exercise, the lateral sensorimotor cortical areas and the supplementary motor areas were active. This is indicative of a component of the respiratory response to exercise being activated by a behavioural response, without any afferent motor feedback. Williamson *et al* (2001) used single-photon-emission computed tomography to obtain comparable results, again with hypnotically induced human subjects, and showed that increases in perceived effort during constant-load exercise could elevate the cardiorespiratory responses to imagined exercise.

The precise neurocircuitry responsible for integrating the central command response has not yet been firmly established. However, there are several target areas that have thus far been investigated and putatively shown to be involved. Fink *et al* (1995) used PET to measure regional cerebral blood flow in order to highlight neural sites active during and immediately following an exercise task. They asked human subjects to perform a one-legged exercise task, and identified a role in central command for the primary motor cortex, along with the premotor and supplementary motor areas. As discussed earlier, these same areas are activated when ventilation increases during imagination of an exercise task without the movement of the exercise task itself (Thornton *et al*, 2001). Additionally, Thornton *et al* demonstrated an increase in neural activity in the dorsolateral prefrontal cortex, which is an area thought to be responsible for storing motor tasks based on working memory. This area could provide a site from which behavioural or learnt components of the cardiorespiratory response to exercise are initiated, allowing more accurate anticipation of the metabolic demands required for an upcoming exercise task. Furthermore, Williamson *et al* (2001) proposed a role for the insular cortex, which has projections to cardiac vagal motor neurons, in influencing the increase in heart rate associated with the imagination of exercise.

Although higher cortical sites have been investigated with regards to their roles in setting the central command response, the part played by midbrain nuclei in driving both motor activity and cardiorespiratory activity is unclear. Smith *et al* (1960) stereotaxically stimulated distinct areas of the brain in dogs in order to identify sites that might be involved in cardiorespiratory control. They demonstrated that stimulation of the periventricular grey area around the third ventricle and of the H_1 and H_2 fields of Forel resulted in the same magnitude of cardiorespiratory responses to that resulting from dynamic treadmill exercise. Direct electrical stimulation of the hypothalamus, the basal ganglia and the mesencephalic locomotor region in decorticate animals has been shown to drive motor activity alongside cardiorespiratory

responses comparable to those in response to volitional exercise (Smith *et al*, 1960; Eldridge *et al*, 1981; Eldridge *et al*, 1985).

Thornton *et al* (2002) used direct electrical stimulation of various basal ganglia nuclei in awake humans to demonstrate that the subthalamic nucleus (STN) and the thalamus can drive an increase in both arterial blood pressure and heart rate, without any peripheral feedback from muscle activity. It has also been shown that direct electrical stimulation of the periaqueductal grey (PAG) area in humans results in marked increases or decreases in arterial blood pressure; the direction of the blood pressure response is dependent on whether stimulation occurs in the dorsal or ventral part of the PAG (Green *et al*, 2005).

In 2007, Green *et al* tested the hypothesis that activity recorded from subcortical neural structures in humans is directly linked to changes in cardiorespiratory parameters, such as heart rate, arterial blood pressure and ventilation, in response to both anticipation of an exercise task and the actual exercise task itself. They used the paradigm of Krogh and Lindhard (1913) to uncouple peripheral feedback from the exercise. The subjects tested all had deep brain stimulating electrodes chronically implanted within different neural sites. Green *et al* (2007) found that anticipation of exercise is associated with increased cardiorespiratory parameters, and is also correlated with increased PAG activity. On the other hand, STN activity decreased, suggesting a release of the inhibitory drive on the cardiovascular nuclei receiving projections from the STN, thereby causing the increases in cardiorespiratory parameters. During actual exercise, both PAG and STN neural activity increased. Their results provided direct neurophysiological evidence that both of these structures in humans have a role in the central command response to exercise.

I decided to use the paradigm from an experiment by Goodwin *et al* (1972) to investigate the neurocircuitry involved during changes in central command whilst performing sustained isometric exercise. Goodwin *et al* (1972) designed a series of experiments to demonstrate

whether the command signals descending from higher neural control centres to working muscle provide an element of cardiorespiratory control. They applied a vibration stimulus to the biceps tendon of humans holding sustained isometric contractions with either their biceps muscle or their triceps muscle. Vibration is known to be a strong stimulus to muscle spindle primary afferents in animals (Brown *et al*, 1967) and is thought to act via these same afferents to cause a tonic vibration reflex in humans; it can be used to reflexly obtain tension in a muscle without a central command signal (De Gail *et al*, 1966). In the Goodwin *et al* (1972) study, vibration was used to either assist or inhibit a voluntary isometric contraction. On contraction of the biceps muscle, the activation of primary afferents of the biceps muscle spindles via vibration provided a degree of reflex excitation. Therefore, less central command than usual was necessary to hold a given tension. On the other hand, during contraction of the triceps muscle, vibration of the primary afferents of its antagonist muscle spindles (the biceps spindles) provided a degree of reflex inhibition. Therefore, more central command was necessary to hold a given tension. Thus, they were able to investigate the cardiovascular responses to an isometric effort during varying degrees of central command. They observed that blood pressure and heart rate both increase during an isometric effort. This increase was greater when the central command was increased, and lessened when the central command was decreased, which led to the conclusion that there is 'irradiation' of the cardiovascular control centres by descending central command signals during voluntary isometric muscle contractions in humans.

The aim of my study was to investigate the neurocircuitry involved in central command using muscle vibration; specifically, during changes in central command during isometric exercise at constant muscle tension. Local field potential recordings were made from specific nuclei in deep brain stimulation patients – these structures had previously been identified as cardiovascularly active in animals. The recordings were used to test the hypothesis that neural

activity in particular subcortical structures corresponds to changes in arterial blood pressure and heart rate in response to an isometric effort during varying degrees of central command.

Methods

Seventeen patients (15 male, 2 female), with a mean age of 50.8 years (range 30-71 years) were recruited for this study (Table 5.1). Five patients had electrodes implanted in the periaqueductal grey (PAG) for the treatment of chronic pain (mean age 48.6 years). A further six patients had electrodes in the sensory thalamus, also for the treatment of chronic pain (mean age 50.8 years), either in the ventroposterolateral or ventroposteromedial nucleus for the treatment of limb pain or facial pain, respectively. Another six patients had electrodes in the subthalamic nucleus for the treatment of Parkinson's disease (mean age 52.7 years).

Table 5.1 – *Subject characteristics for central command experiments. PAG, periaqueductal grey; STN, subthalamic nucleus.*

Patient	***Age (years)***	***Sex***	***Diagnosis***	***DBS Electrode Location***
1	30	M	Chronic left-sided atypical facial pain	PAG
2	50	M	Chronic right arm pain from brachial plexus injury	PAG
3	46	M	Phantom limb pain in amputated left arm	PAG
4	71	M	Chronic right-sided pain following vertebral artery dissection	PAG
5	46	F	Right-sided pain (internal capsule clot after temporal lobectomy)	PAG
6	30	M	Chronic left-sided atypical facial pain	Sensory Thalamus
7	50	M	Chronic right arm pain from brachial plexus injury	Sensory Thalamus
8	62	M	Central pain syndrome following intra-cerebral bleed	Sensory Thalamus
9	46	M	Phantom limb pain in amputated left arm	Sensory Thalamus
10	71	M	Chronic right-sided pain following vertebral artery dissection	Sensory Thalamus
11	46	F	Right-sided pain (internal capsule clot after temporal lobectomy)	Sensory Thalamus
12	55	M	Parkinson's disease	STN
13	51	M	Parkinson's disease	STN
14	63	M	Parkinson's disease	STN
15	63	M	Parkinson's disease	STN
16	44	M	Parkinson's disease	STN
17	40	M	Parkinson's disease	STN

The experiments were conducted within the first week following stage 1 of the deep brain stimulation surgical procedure, while the electrodes were still externalised. For the entire duration of the experiment, the patients' stimulation was turned off.

Using the Goodwin study as a paradigm (Goodwin *et al*, 1972), I varied the central command required for a certain isometric contraction; specifically, 50% of each subject's maximum voluntary biceps contraction, held for two minutes. Although tension can be reflexly produced in muscle, without central command, by vibration of primary afferents of the muscle spindles, the tension produced is only about 10% of the maximum voluntary contraction. Cardiovascular responses to isometric exercise are seen most clearly at tensions greater than 10% of the maximum (Lind *et al*, 1966). Therefore, I decided to add a component of voluntary contraction to the reflex contraction. Each subject was shown a digital display of the tension they were achieving, and were instructed to hold 50% of their maximum voluntary biceps contraction.

I used the same model of physiotherapy vibrator (Vibratory Massager, Pifco Ltd) as Goodwin *et al* (1972) oscillating at a frequency of 100 Hz, and applied it to the tendon of either the exercising biceps muscle or its antagonist triceps muscle, in order to alter the central command required to produce a constant tension. For example, during vibration of the biceps tendon, if the subject holds a tension of 50% of their maximum voluntary biceps contraction, some of this would be reflexly achieved. Therefore, the central command required to hold the contraction would only be equivalent to about 30-40% of their maximum (Fig. 5.1). On the other hand, during vibration of the triceps tendon (the antagonist muscle), disynaptic inhibition of the active muscle motor neurons is produced. This means that more central command is necessary to produce the required tension (Fig. 5.2).

I made sure that the reflex inhibition provided by vibration of the triceps muscle tendon was not accompanied by contraction of the triceps muscle itself by palpating the muscle. Goodwin

et al (1972) found that as little as 2% of the maximum voluntary contraction could be reliably detected by palpation.

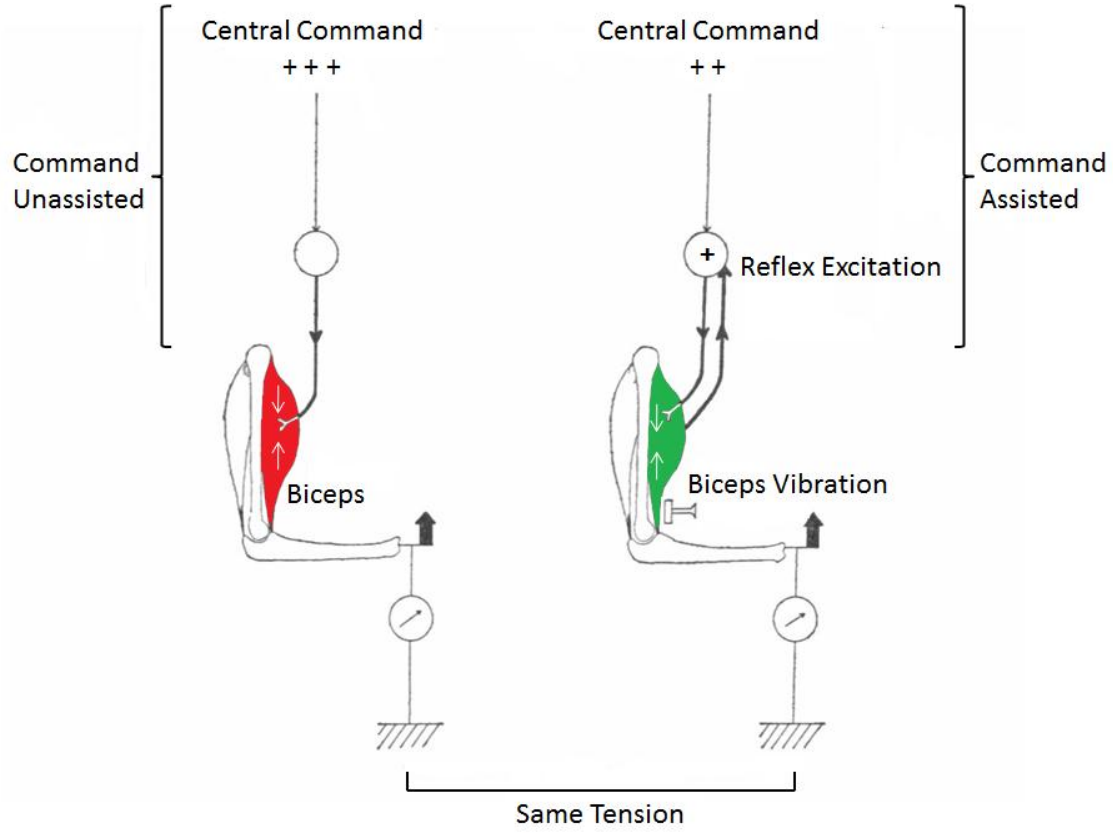

Figure 5.1 *– Diagram showing application of the vibration stimulus to the biceps tendon during a biceps contraction resulting in an element of reflex excitation so that less central command is required to achieve a given tension.*

The protocol was as follows (Figs. 5.3-5.6): each patient was asked to sit comfortably, with their elbows resting on the arms of the chair. One of their wrists was bound to the end of the arm of the chair with a strap connected to a strain gauge. Isometric contractions of the biceps muscle in the right arm were usually investigated, unless a specific preference for the left arm was stated by the patient. The experiment was divided into four sections.

In Section 1 of the experiment (Fig. 5.3), cardiovascular parameters and neural activity were recorded for a rest period of five minutes. The patient's maximum voluntary contraction (MVC) was then measured, by asking them to pull upwards against the strain gauge as hard as

they could for 30 seconds; the absolute value of this maximum contraction was displayed in Newtons on a digital screen in front of the patient. The patient was then allowed to rest.

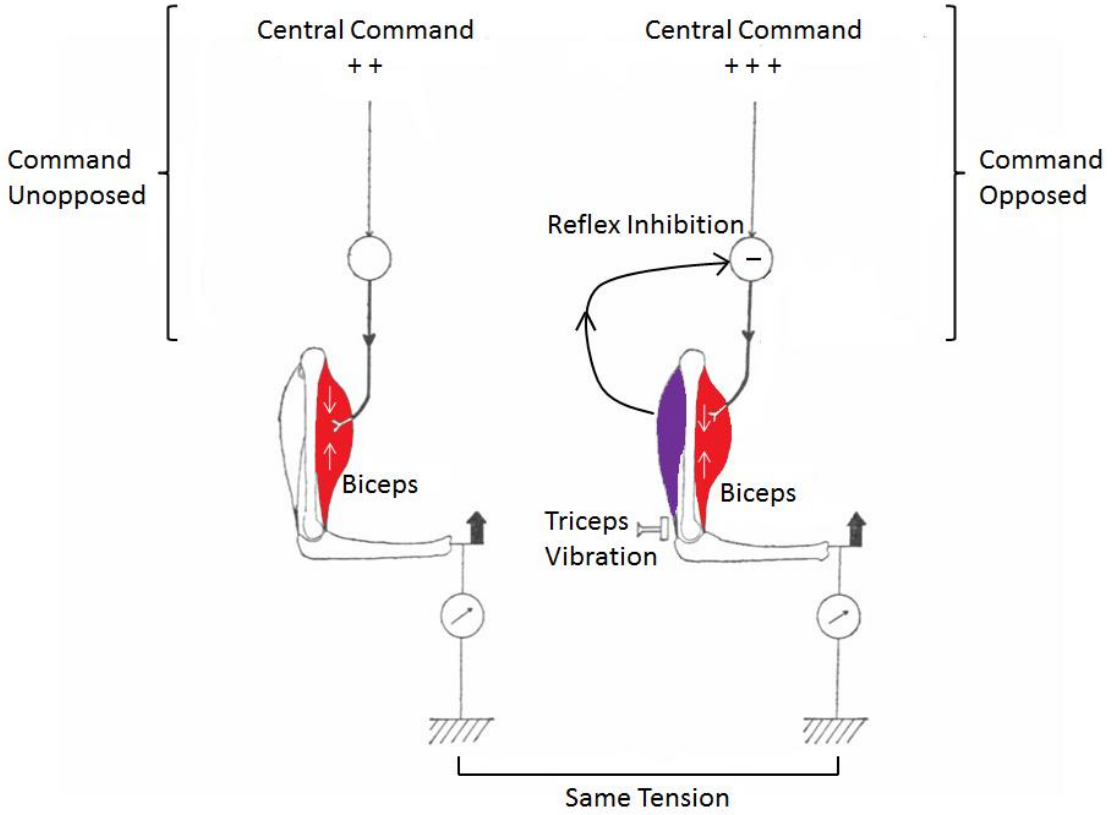

Figure 5.2 – *Diagram showing application of the vibration stimulus to the triceps tendon during a biceps contraction resulting in an element of reflex inhibition so that more central command is required to achieve a given tension.*

Section 2 of the experiment (Fig. 5.4) began with the patient holding 50% of their previously established MVC for two minutes. They were then allowed to rest for five minutes. After the rest period, the patient was instructed to hold 50% of their MVC for two minutes, this time with the vibration stimulus held against their triceps tendon, followed by another five minute rest period. Then the patient was asked to hold 50% of their MVC for two minutes again, but with no vibration. This was followed by a five minute rest period.

Section 3 of the experiment (Fig. 5.5) began with the patient holding 50% of their MVC for two minutes, with no vibration. This was followed by a five minute rest period. The patient was

then instructed to hold 50% of their MVC for two minutes, this time with the vibration stimulus held against their biceps tendon, followed by a five minute rest period. Finally, the patient was asked to hold 50% of their MVC for two minutes, but with no vibration. This was followed by another five minute rest period.

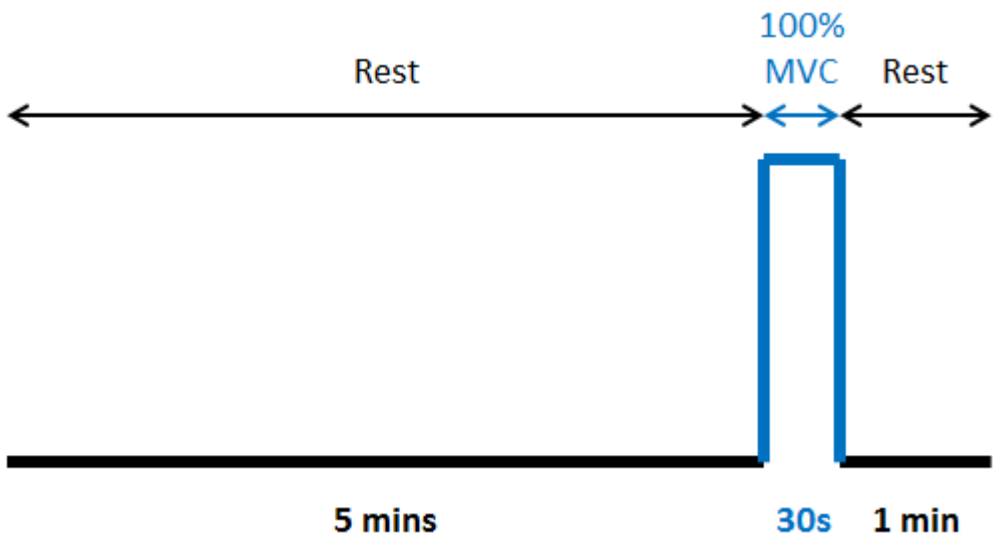

Figure 5.3 – *Section 1 of the protocol for the central command experiment. The vertical axis represents the level of activity. The raised line indicates contraction at 100% MVC (maximum voluntary contraction).*

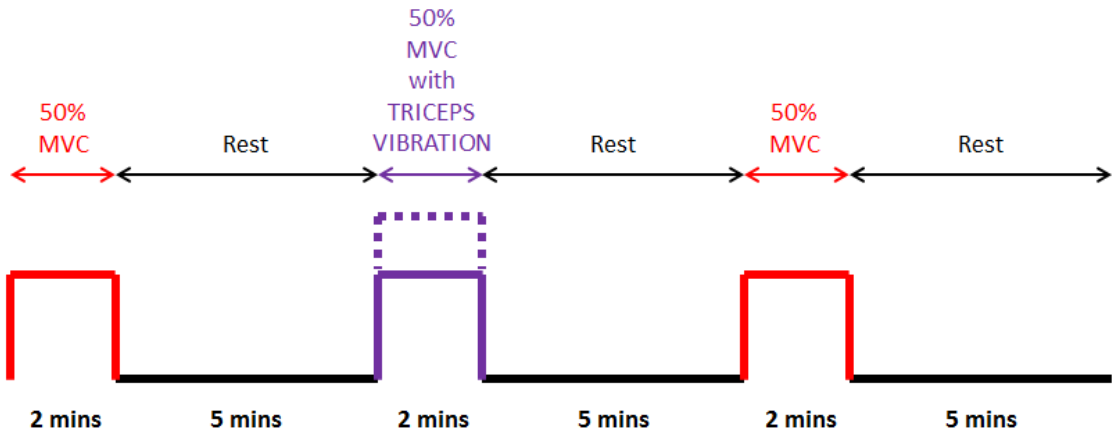

Figure 5.4 – *Section 2 of the protocol for the central command experiment. The vertical axis represents the level of activity. The raised lines indicate contraction at 50% MVC (maximum voluntary contraction). The dotted line indicates the subject's perception of the force required to hold the contraction.*

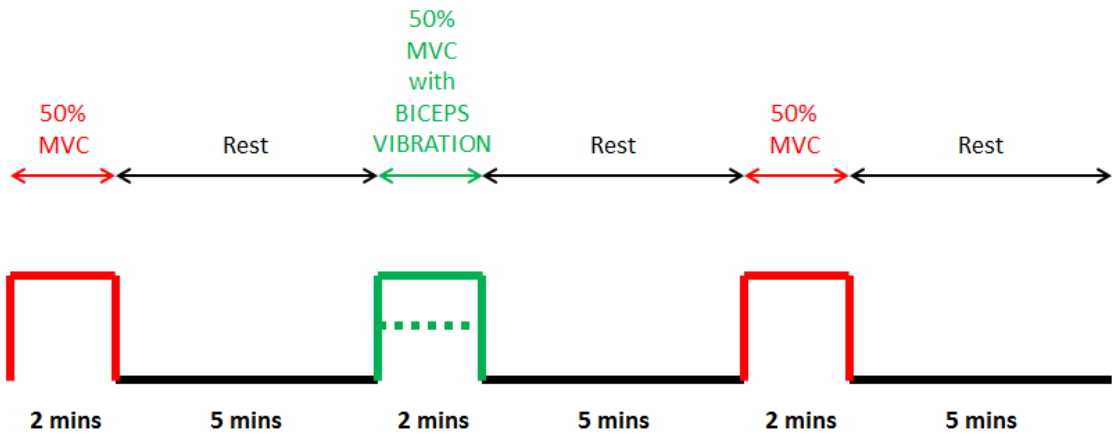

Figure 5.5 – *Section 3 of the protocol for the central command experiment. The vertical axis represents the level of activity. The raised lines indicate contraction at 50% MVC (maximum voluntary contraction). The dotted line indicates the subject's perception of the force required to hold the contraction.*

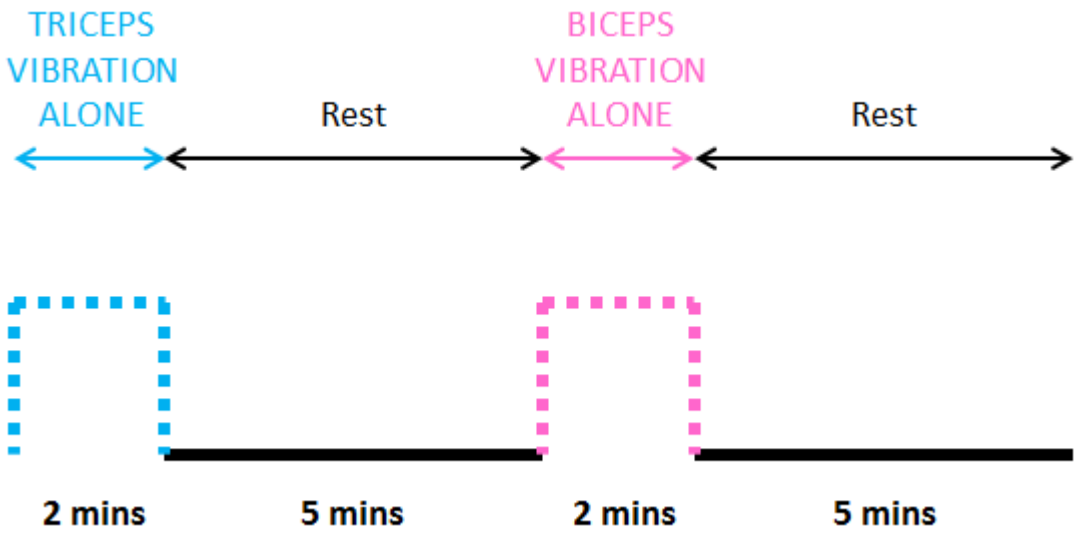

Figure 5.6 – *Section 4 of the protocol for the central command experiment. The vertical axis represents the level of activity. The dotted lines indicate vibration of the stated tendons without any voluntary contractions from the subject.*

Section 4 of the experiment (Fig. 5.6) was a control experiment. The patient was asked to sit at rest (i.e. no voluntary contraction) while the vibration stimulus was placed against their triceps tendon for two minutes. After a five minute rest period, the vibration stimulus was placed

against their biceps tendon for two minutes, again with no voluntary contraction from the patient. This was in order to determine whether any changes in neural activity that might have been observed during the contractions with the vibration stimulus were not due to the sensation of the vibration itself.

During contractions, the wrist was pulled directly upwards from the strain gauge, and the wrist was rotated so that the plane of the hand was vertical. The subjects were specifically instructed to try to confine their efforts to the biceps muscle, and to avoid changing their leverage by using shoulder and trunk movements. The subjects were also asked to keep the tip of the elbow firmly in contact with the arm of the chair throughout the contraction periods.

Patients were asked to rate their levels of pain throughout the duration of the experiments using the Visual Analog Pain Severity Scale (VAPSS), in order to determine whether changes in neural activity could be due to the patients' pathology (for example, pain in PAG patients), as opposed to the neural responses to exercise. Data segments in which the VAPSS score changed were excluded from analysis.

Results

Cardiovascular Parameters

In all of the 17 patients in whom data were measured, mean arterial blood pressure (MABP) increased from resting levels during isometric contractions, both with the vibration stimulus and without. Furthermore, in all patients, MABP increased further during biceps contractions with triceps tendon vibration compared to biceps contractions with no vibration. Similarly, in all patients, the increase in MABP was smaller during biceps contractions with biceps tendon vibration compared to biceps contractions with no vibration. The data for all of the patients were averaged together (Figs. 5.7-5.8). In Section 2 of the experiment (Fig. 5.7), the average

increase from rest in MABP during isometric biceps contraction with no vibration was 14.6 ± 3.2 mmHg ($P < 0.001$, $n = 17$), equivalent to an increase of 15.0%. During the isometric biceps contraction with vibration of the triceps tendon, the average increase from rest in MABP was 20.4 ± 2.7 mmHg ($P < 0.001$, $n = 17$), equivalent to an increase of 20.8%. There was also a significant difference in MABP between contraction with no vibration and contraction with triceps vibration ($P = 0.008$, $n = 17$). In Section 3 of the experiment (Fig. 5.8), the average increase from rest in MABP during isometric biceps contraction with no vibration was 14.8 ± 2.9 mmHg ($P < 0.001$, $n = 17$), equivalent to an increase of 15.1%. During isometric biceps contraction with vibration of the biceps tendon, the average increase from rest in MABP was 9.2 ± 2.6 mmHg ($P < 0.001$, $n = 17$), equivalent to an increase of 9.3%. There was also a significant difference in MABP between contraction with no vibration and contraction with biceps vibration ($P = 0.035$, $n = 17$).

The changes in MABP were accompanied by analogous changes in systolic blood pressure (SBP) and diastolic blood pressure (DBP) (Figs. 5.9-5.10). In Section 2 of the experiment (Fig. 5.9), the average increase from rest in SBP during isometric biceps contraction with no vibration was 16.8 ± 5.0 mmHg ($P < 0.001$, $n = 17$), equivalent to an increase of 12.5%. During the isometric biceps contraction with vibration of the triceps tendon, the average increase from rest in SBP was 21.8 ± 5.7 mmHg ($P < 0.001$, $n = 17$), equivalent to an increase of 16.2%. There was also a significant difference in SBP between contraction with no vibration and contraction with triceps vibration ($P = 0.013$, $n = 17$). In Section 3 of the experiment (Fig. 5.10), the average increase from rest in SBP during isometric biceps contraction with no vibration was 11.5 ± 3.2 mmHg ($P < 0.001$, $n = 17$), equivalent to an increase of 8.7%. During isometric biceps contraction with vibration of the biceps tendon, the average increase from rest in SBP was 10.9 ± 2.5 mmHg ($P < 0.001$, $n = 17$), equivalent to an increase of 8.2%. There was no significant difference in SBP between contraction with no vibration and contraction with biceps vibration ($P = 0.844$, $n = 17$). In Section 2 of the experiment (Fig. 5.9), the average

increase from rest in DBP during isometric biceps contraction with no vibration was 11.7 ± 2.4 mmHg ($P < 0.001$, $n = 17$), equivalent to an increase of 14.4%. During the isometric biceps contraction with vibration of the triceps tendon, the average increase from rest in DBP was 16.8 ± 3.9 mmHg ($P < 0.001$, $n = 17$), equivalent to an increase of 20.7%. There was also a significant difference in DBP between contraction with no vibration and contraction with triceps vibration ($P = 0.041$, $n = 17$). In Section 3 of the experiment (Fig. 5.10), the average increase from rest in DBP during isometric biceps contraction with no vibration was 16.8 ± 3.3 mmHg ($P < 0.001$, $n = 17$), equivalent to an increase of 20.7%. During isometric biceps contraction with vibration of the biceps tendon, the average increase from rest in DBP was 12.3 ± 3.5 mmHg ($P < 0.001$, $n = 17$), equivalent to an increase of 15.2%. There was no significant difference in DBP between contraction with no vibration and contraction with biceps vibration ($P = 0.286$, $n = 17$).

All 17 patients who performed the experiment had a significantly decreased R-R interval compared to rest during isometric contractions, both with the vibration stimulus and without. The R-R interval data for all 17 patients were averaged together (Figs. 5.11-5.12). In Section 2 of the experiment (Fig. 5.11), the average decrease in R-R interval from rest during isometric biceps contraction with no vibration was 0.043 ± 0.020 s ($P < 0.001$, $n = 17$), equivalent to a decrease of 5.6%. During the isometric biceps contraction with vibration of the triceps tendon, the average decrease in R-R interval from rest was 0.061 ± 0.028 s ($P < 0.001$, $n = 17$), equivalent to a decrease of 8.0%. There was no significant difference in R-R interval between contraction with no vibration and contraction with triceps vibration ($P = 0.796$, $n = 17$). In Section 3 of the experiment (Fig. 5.12), the average decrease in R-R interval from rest during isometric biceps contraction with no vibration was 0.035 ± 0.018 s ($P < 0.001$, $n = 17$), equivalent to a decrease of 4.6%. During isometric biceps contraction with vibration of the biceps tendon, the average decrease in R-R interval from rest was 0.031 ± 0.027 s ($P = 0.029$, $n = 17$), equivalent to a decrease of 4.1%. There was no significant difference in R-R interval

between contraction with no vibration and contraction with biceps vibration (P = 0.340, *n* = 17).

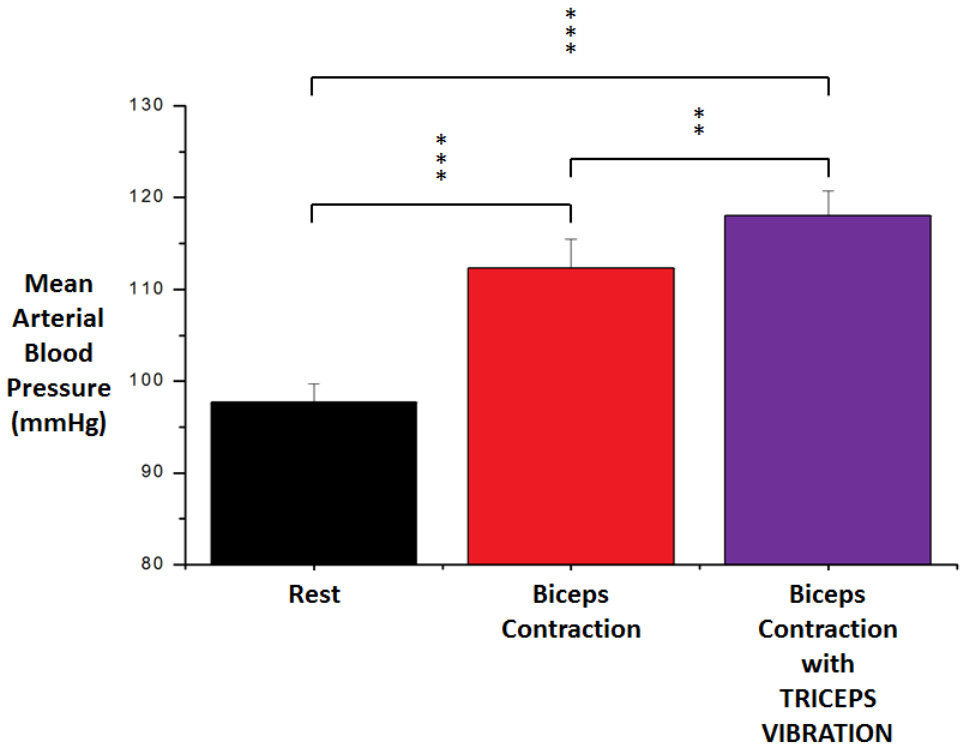

Figure 5.7 *– Graph showing significant increases in mean arterial blood pressure during both biceps contraction (with no vibration) and biceps contraction with triceps vibration, compared to rest. There is also a significant increase in mean arterial blood pressure during biceps contraction with triceps vibration compared to biceps contraction (with no vibration). ** P < 0.01, *** P < 0.001, n = 17. Error bars represent standard error of the mean.*

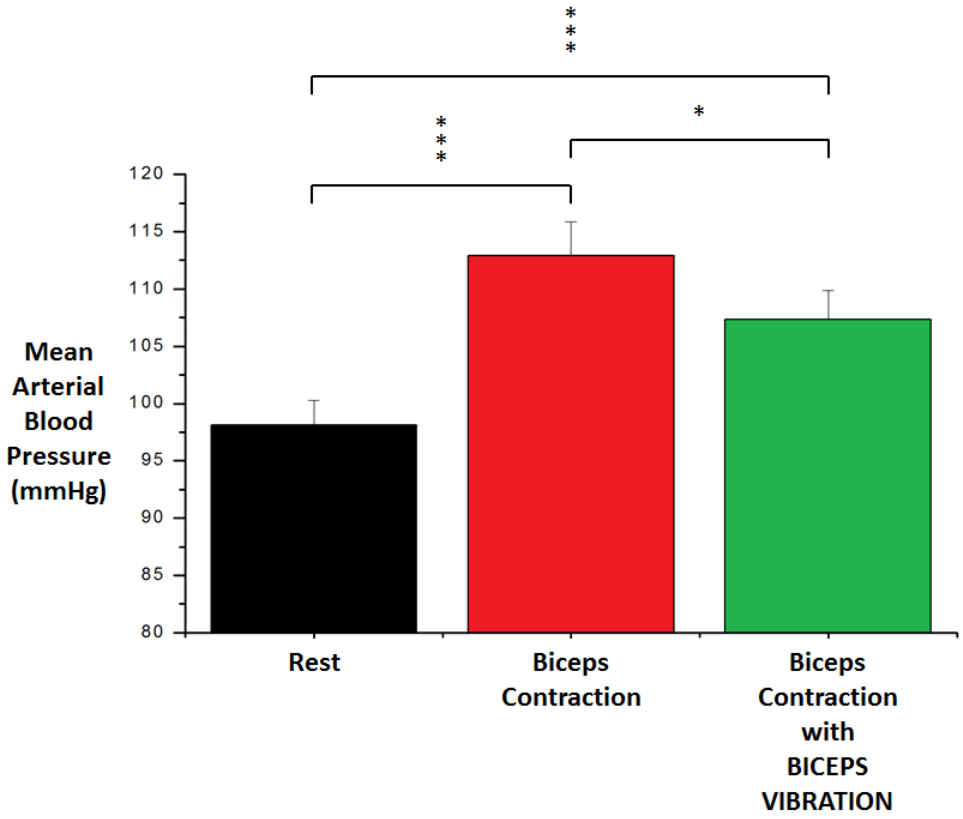

Figure 5.8 – *Graph showing significant increases in mean arterial blood pressure during both biceps contraction (with no vibration) and biceps contraction with biceps vibration, compared to rest. There is also a significant decrease in mean arterial blood pressure during biceps contraction with biceps vibration compared to biceps contraction (with no vibration). * P < 0.05, *** P < 0.001, n = 17. Error bars represent standard error of the mean.*

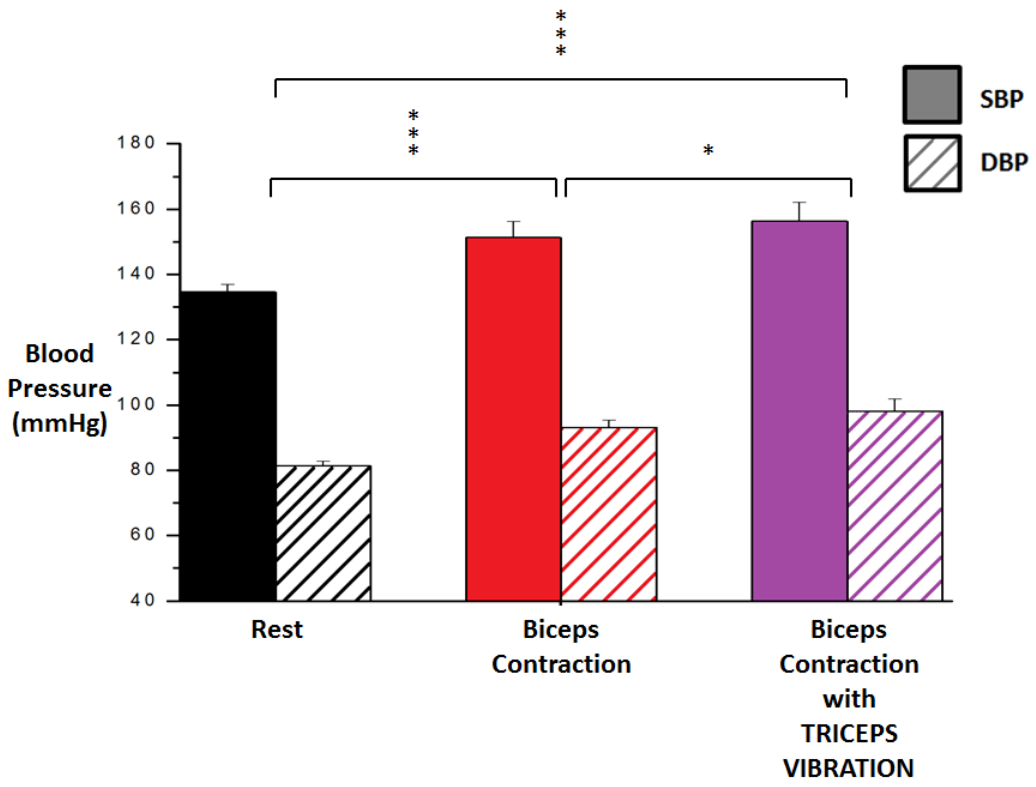

Figure 5.9 – *Graph showing significant increases in systolic blood pressure (SBP) and diastolic blood pressure (DBP) during both biceps contraction (with no vibration) and biceps contraction with triceps vibration, compared to rest. There are also significant increases in both SBP and DBP during biceps contraction with triceps vibration compared to biceps contraction (with no vibration). n = 17, * P < 0.05, *** P < 0.001. Error bars represent standard error of the mean.*

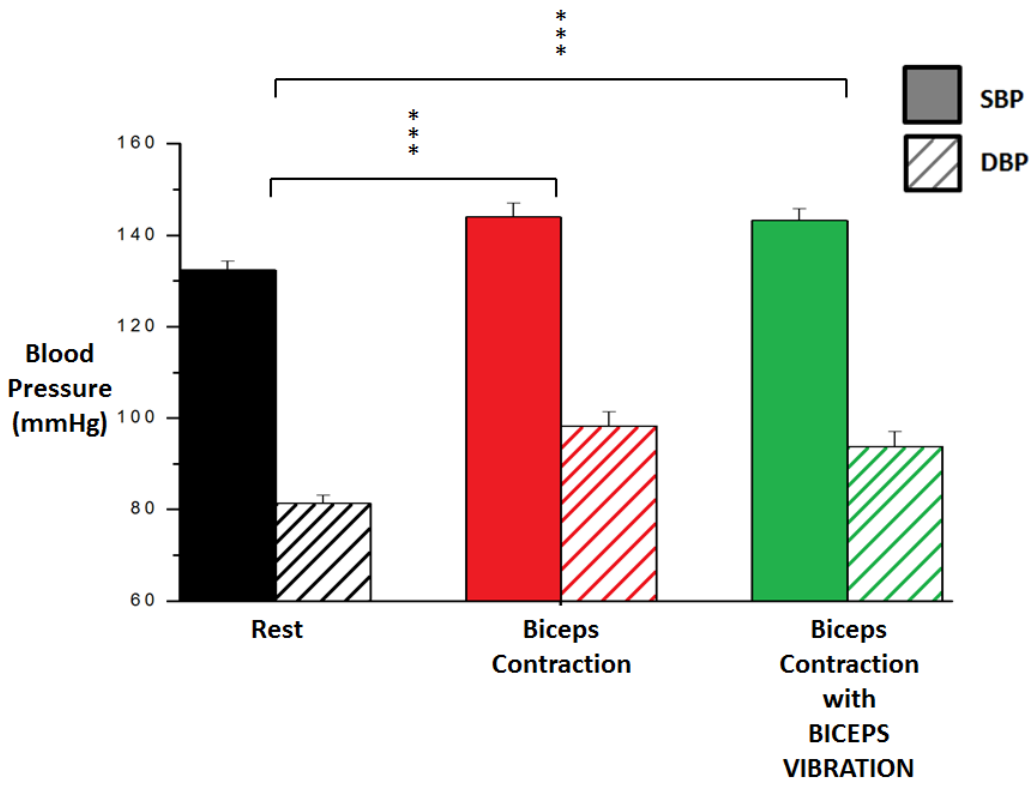

Figure 5.10 *– Graph showing significant increases in systolic blood pressure (SBP) and diastolic blood pressure (DBP) during both biceps contraction (with no vibration) and biceps contraction with biceps vibration, compared to rest. There are no significant differences in SBP or DBP during biceps contraction with biceps vibration compared to biceps contraction (with no vibration). n = 17, *** P < 0.001. Error bars represent standard error of the mean.*

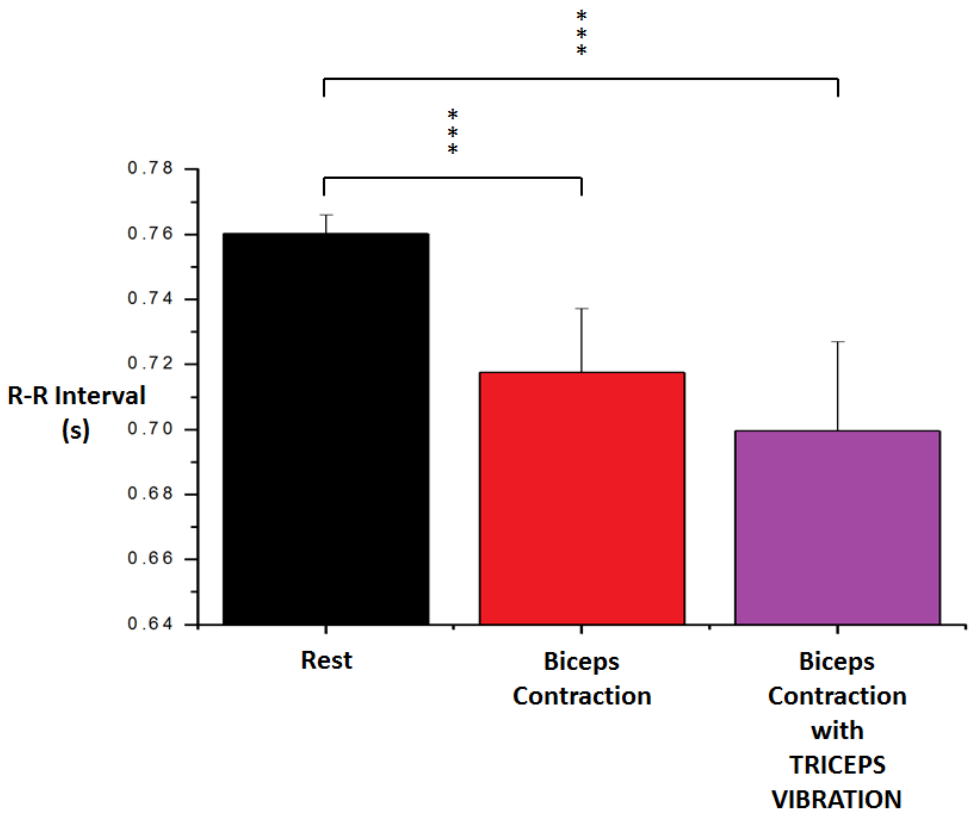

Figure 5.11 – *Graph showing significant decreases in R-R interval (i.e. increases in heart rate) during both biceps contraction (with no vibration) and biceps contraction with triceps vibration, compared to rest. There is no significant decrease in R-R interval during biceps contraction with triceps vibration compared to biceps contraction (with no vibration). *** P < 0.001, n = 17. Error bars represent standard error of the mean.*

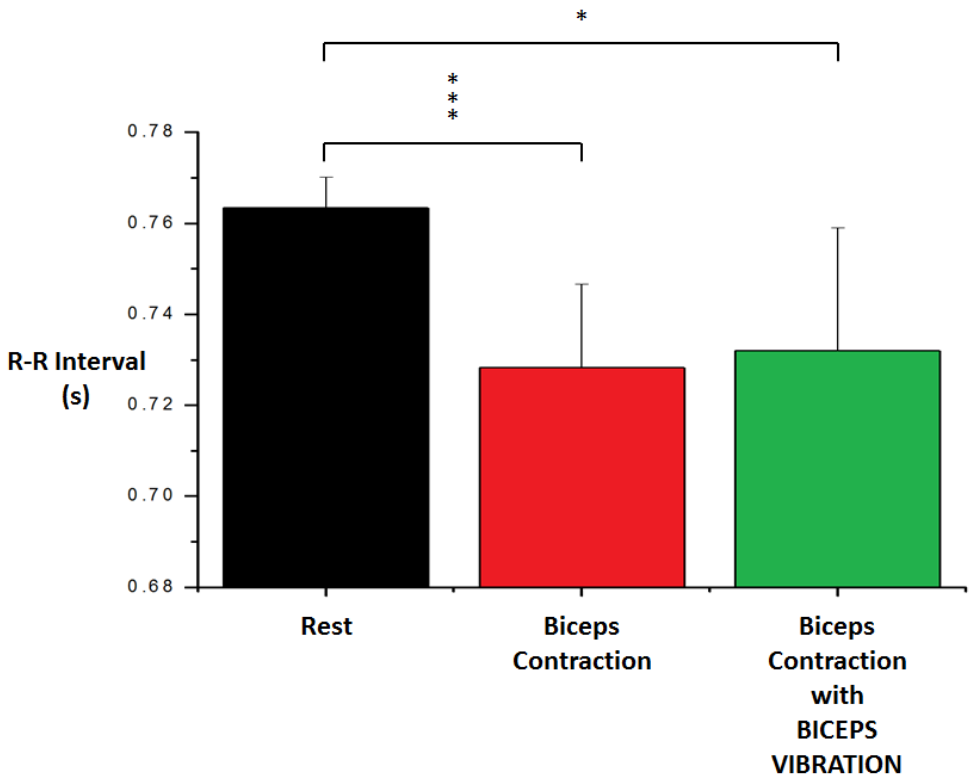

Figure 5.12 – *Graph showing significant decreases in R-R interval (i.e. increases in heart rate) during both biceps contraction (with no vibration) and biceps contraction with biceps vibration, compared to rest. There is no significant decrease in R-R interval during biceps contraction with biceps vibration compared to biceps contraction (with no vibration). * P < 0.05, *** P < 0.001, n = 17. Error bars represent standard error of the mean.*

Electrode Localisation

As the cardiovascular response from the periaqueductal grey (PAG) is functionally opposite depending on which columns are active, it was vital to establish the precise locations of each electrode. Fig. 5.13 shows the positions of the electrodes in the five PAG patients who performed the experiment, in both the transverse and coronal planes. Fig. 5.14 shows a schematic diagram of these same five PAG electrodes so that the contacts on each electrode can be examined. Recordings were only made from those contacts that provided the patients with therapeutic benefit (i.e. pain relief). These contacts were all within the dorsal region of the PAG.

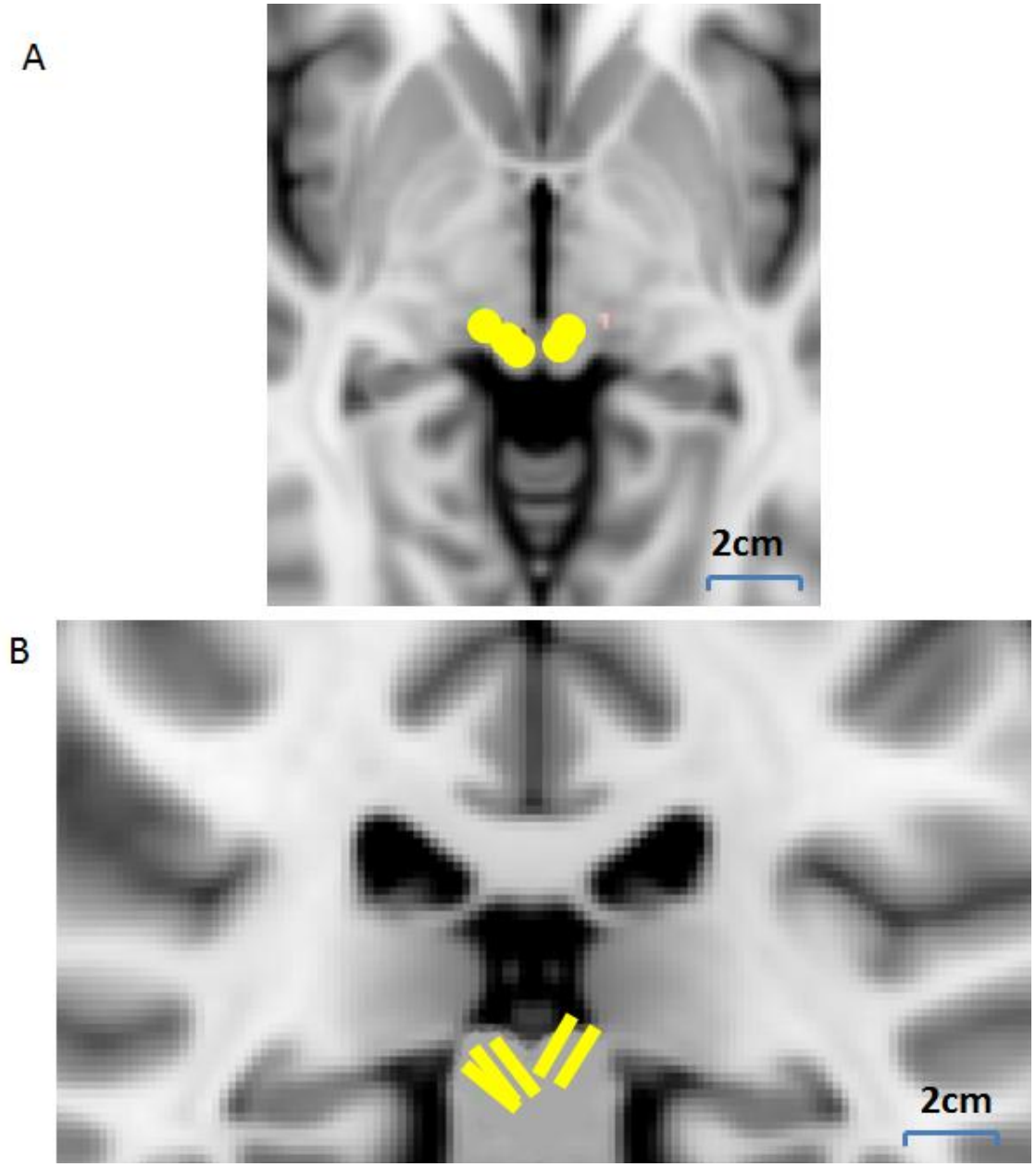

Figure 5.13 – *Post-operative image showing individual electrode locations in the transverse (A) and coronal (B) planes for five periaqueductal grey patients. Both scale bars represent 2 cm. Yellow dots represent the midpoints of each electrode. Yellow rectangles represent entire length of each electrode.*

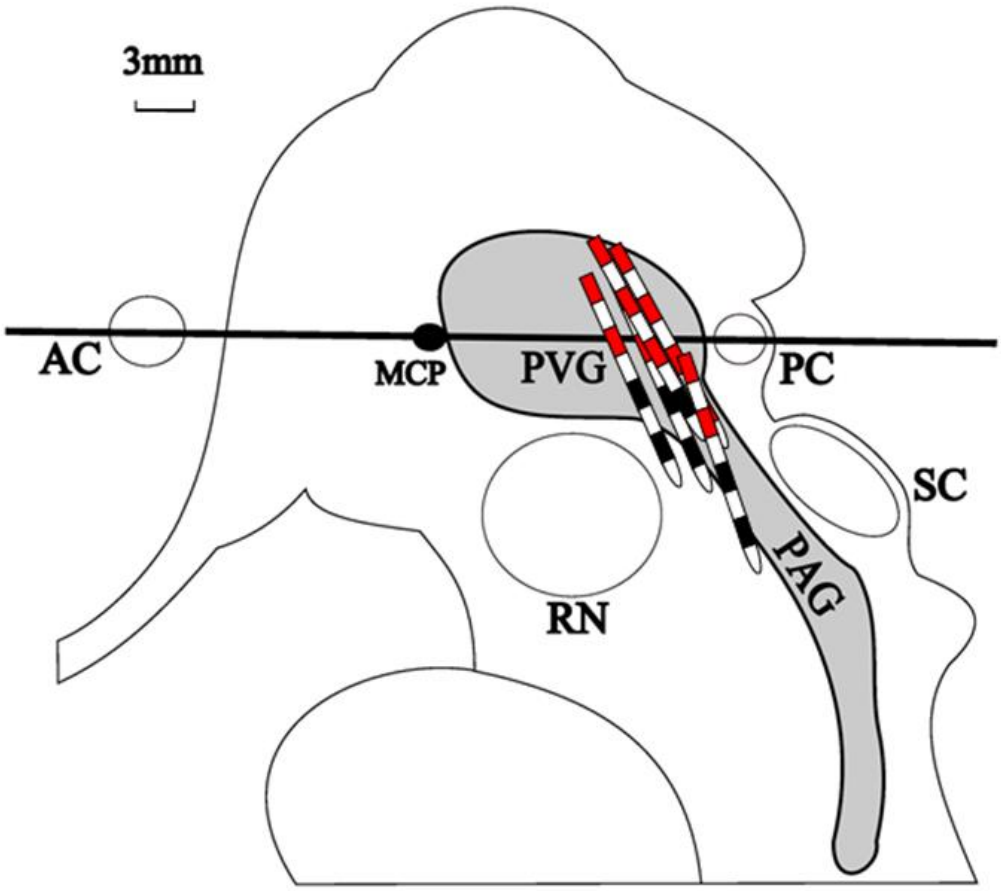

Figure 5.14 – *Schematic diagram in the sagittal plane showing electrode locations for five PAG patients who performed the experiment. The data presented in this study are recorded only from those contacts that provided therapeutic benefit – these were all within the dorsal aspect of the PVG/PAG (highlighted in red). AC, anterior commissure; MCP, mid-commissural point; PVG, periventricular grey; PC, posterior commissure; RN, red nucleus; PAG, periaqueductal grey; SC, superior colliculus.*

Local Field Potential Recordings from the Subthalamic Nucleus

Using ANOVA, a significant difference was revealed between the conditions of rest, contraction (with no vibration), contraction with triceps vibration and contraction with biceps vibration ($P < 0.05$) for each individual patient. Therefore, all the subthalamic nucleus (STN) data were averaged together (Figs. 5.15-5.16). In Section 2 of the experiment (Fig. 5.15), significant decreases in neural activity occurred during isometric biceps contraction with no vibration and during isometric biceps contraction with triceps vibration. In the 4-8 Hz band,

biceps contraction with no vibration was associated with a decrease in power spectral density (PSD) of 8.3 ± 2.1 $\mu V^2/Hz$ ($P < 0.001$, $n = 6$), which is equivalent to a 20.7% decrease. Biceps contraction with triceps vibration was associated with a decrease in PSD of 14.2 ± 1.8 $\mu V^2/Hz$ ($P < 0.001$, $n = 6$), which is equivalent to a 35.1% decrease. In the 8-12 Hz band, there was a decrease in PSD of 1.2 ± 0.6 $\mu V^2/Hz$ ($P = 0.025$, $n = 6$) during biceps contraction with no vibration, which is equivalent to a 6.3% decrease. There was a decrease in PSD of 3.8 ± 0.4 $\mu V^2/Hz$ ($P < 0.001$, $n = 6$) during biceps contraction with triceps vibration, which is equivalent to a 20.0% decrease. In the 12-25 Hz band, biceps contraction with no vibration was associated with a decrease in PSD of 1.6 ± 0.2 $\mu V^2/Hz$ ($P < 0.001$, $n = 6$), which is equivalent to a decrease of 12.2%. Biceps contraction with triceps vibration was associated with a decrease in PSD of 2.2 ± 0.2 $\mu V^2/Hz$ ($P < 0.001$, $n = 6$), which is equivalent to a decrease of 17.0%. In Section 3 of the experiment (Fig. 5.16), significant decreases in neural activity occurred during isometric biceps contraction with no vibration and during isometric biceps contraction with biceps vibration. In the 4-8 Hz band, biceps contraction with no vibration was associated with a decrease in PSD of 14.7 ± 1.9 $\mu V^2/Hz$ ($P < 0.001$, $n = 6$), which is equivalent to a 36.4% decrease. Biceps contraction with biceps vibration was associated with a decrease in PSD of 5.0 ± 2.3 $\mu V^2/Hz$ ($P = 0.018$, $n = 6$), which is equivalent to a 12.3% decrease. In the 8-12 Hz band, there was a decrease in PSD of 4.1 ± 0.6 $\mu V^2/Hz$ ($P < 0.001$, $n = 6$) during biceps contraction with no vibration, which is equivalent to a 21.1% decrease. There was a decrease in PSD of 1.7 ± 0.9 $\mu V^2/Hz$ ($P = 0.040$, $n = 6$) during biceps contraction with biceps vibration, which is equivalent to an 8.8% decrease. In the 12-25 Hz band, biceps contraction with no vibration was associated with a decrease in PSD of 3.1 ± 0.2 $\mu V^2/Hz$ ($P < 0.001$, $n = 6$), which is equivalent to a decrease of 23.2%. Biceps contraction with biceps vibration was associated with a decrease in PSD of 1.7 ± 0.2 $\mu V^2/Hz$ ($P < 0.001$, $n = 6$), which is equivalent to a decrease of 13.2%.

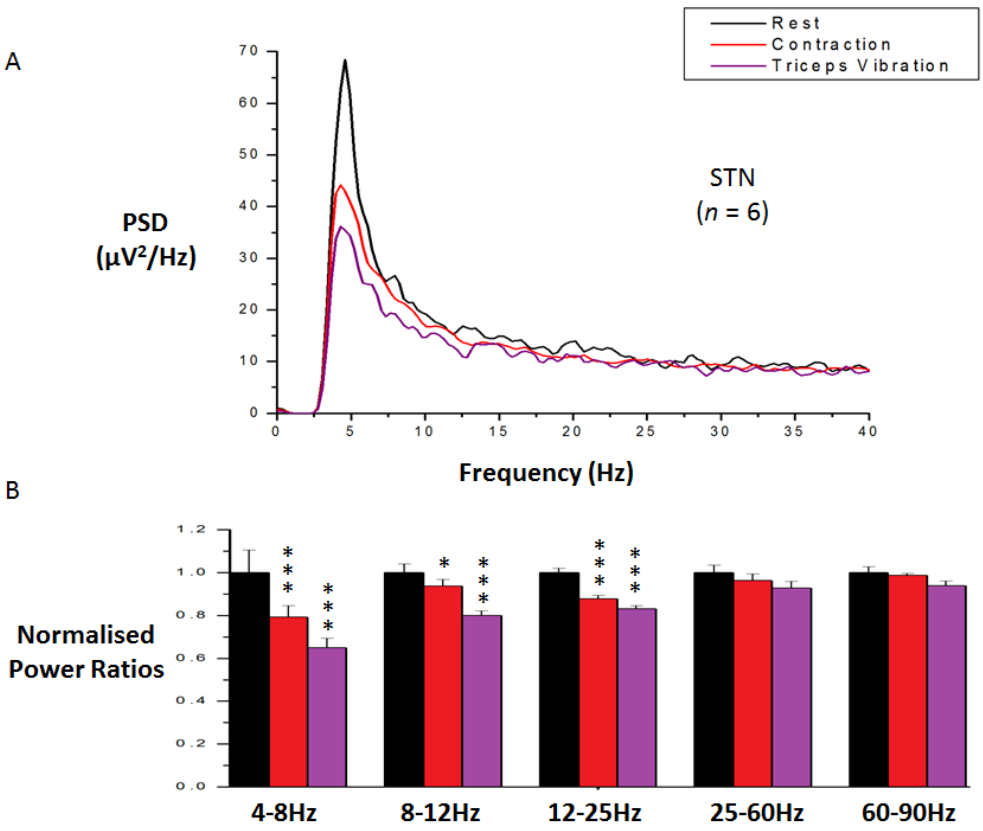

Figure 5.15 – *Graphs showing a significant decrease in subthalamic nucleus (STN) neural activity during both biceps contraction (with no vibration) and biceps contraction with triceps vibration, compared to rest. (A) Mean power spectral density (PSD) for all six patients. (B) Normalised spectral changes (rest = 1.0) divided into frequency bands, showing significant decreases during both biceps contraction and biceps contraction with triceps vibration in the 4-8 Hz, 8-12 Hz and 12-25 Hz bands, compared to rest. n = 6, * P < 0.05, *** P < 0.001. Error bars represent standard error of the mean.*

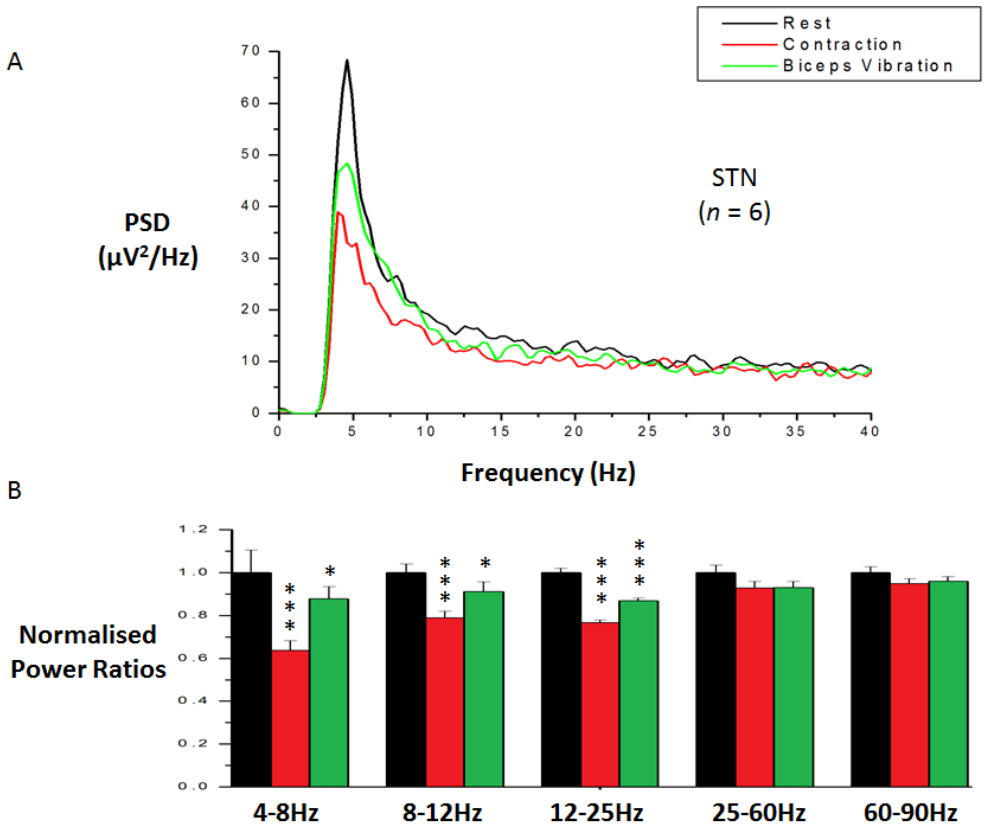

Figure 5.16 – *Graphs showing a significant decrease in subthalamic nucleus (STN) neural activity during both biceps contraction (with no vibration) and biceps contraction with biceps vibration, compared to rest. (A) Mean power spectral density (PSD) for all six patients. (B) Normalised spectral changes (rest = 1.0) divided into frequency bands, showing significant decreases during both biceps contraction and biceps contraction with biceps vibration in the 4-8 Hz, 8-12 Hz and 12-25 Hz bands, compared to rest. n = 6, * P < 0.05, *** P < 0.001. Error bars represent standard error of the mean.*

Local Field Potential Recordings from the Periaqueductal Grey

ANOVA revealed a significant difference in neural activity between each test condition in the lower frequency bands in each individual periaqueductal grey (PAG) patient. Therefore, the data from all five patients were averaged together (Figs. 5.17-5.18). In contrast to the decreased power spectral density (PSD) observed in the subthalamic nucleus, increased PSD was noted in the 4-8 Hz, 8-12 Hz and 12-25 Hz frequency bands during periods of muscle contraction, both with the vibration stimulus and without. In Section 2 of the experiment (Fig. 5.17), significant increases in neural activity occurred during isometric biceps contraction with

no vibration and during isometric biceps contraction with triceps vibration. In the 4-8 Hz band, biceps contraction with no vibration was associated with an increase in PSD of 339.1 ± 66.9 μV^2/Hz ($P < 0.001$, $n = 5$), which is equivalent to a 25.2% increase. Biceps contraction with triceps vibration was associated with an increase in PSD of 539.6 ± 134.5 μV^2/Hz ($P < 0.001$, $n = 5$), which is equivalent to a 40.2% increase. In the 8-12 Hz band, there was an increase in PSD of 192.2 ± 128.9 μV^2/Hz ($P = 0.014$, $n = 5$) during biceps contraction with no vibration, which is equivalent to a 23.5% increase. In the 12-25 Hz band, biceps contraction with no vibration was associated with an increase in PSD of 55.7 ± 12.1 μV^2/Hz ($P < 0.001$, $n = 5$), which is equivalent to an increase of 27.2%. Biceps contraction with triceps vibration was associated with an increase in PSD of 40.1 ± 13.0 μV^2/Hz ($P < 0.001$, $n = 5$), which is equivalent to an increase of 19.6%. In Section 3 of the experiment (Fig. 5.18), significant increases in neural activity occurred during isometric biceps contraction with no vibration and during isometric biceps contraction with biceps vibration. In the 4-8 Hz band, biceps contraction with no vibration was associated with an increase in PSD of 181.7 ± 65.9 μV^2/Hz ($P = 0.007$, $n = 5$), which is equivalent to a 13.5% increase. Biceps contraction with biceps vibration was associated with an increase in PSD of 91.6 ± 75.5 μV^2/Hz ($P = 0.042$, $n = 5$), which is equivalent to a 6.8% increase. In the 8-12 Hz band, there was an increase in PSD of 132.5 ± 45.5 μV^2/Hz ($P = 0.003$, $n = 5$) during biceps contraction with no vibration, which is equivalent to a 16.2% increase. In the 12-25 Hz band, biceps contraction with no vibration was associated with an increase in PSD of 28.5 ± 12.9 μV^2/Hz ($P < 0.001$, $n = 5$), which is equivalent to an increase of 13.9%. Biceps contraction with biceps vibration was associated with an increase in PSD of 27.2 ± 11.8 μV^2/Hz ($P < 0.001$, $n = 5$), which is equivalent to an increase of 13.3%.

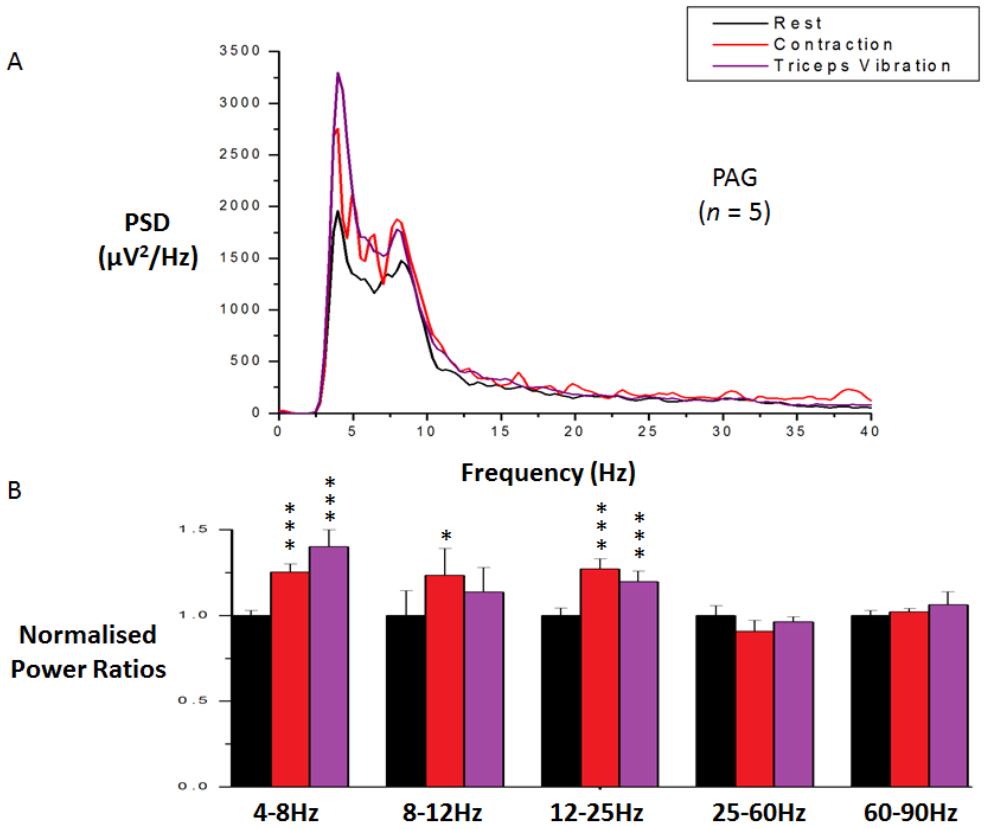

Figure 5.17 – *Graphs showing a significant increase in periaqueductal grey (PAG) neural activity during both biceps contraction (with no vibration) and biceps contraction with triceps vibration, compared to rest. (A) Mean power spectral density (PSD) for all five patients. (B) Normalised spectral changes (rest = 1.0) divided into frequency bands, showing significant increases during both biceps contraction and biceps contraction with triceps vibration in the 4-8 Hz, 8-12 Hz and 12-25 Hz bands, compared to rest. n = 5, * P < 0.05, *** P < 0.001. Error bars represent standard error of the mean.*

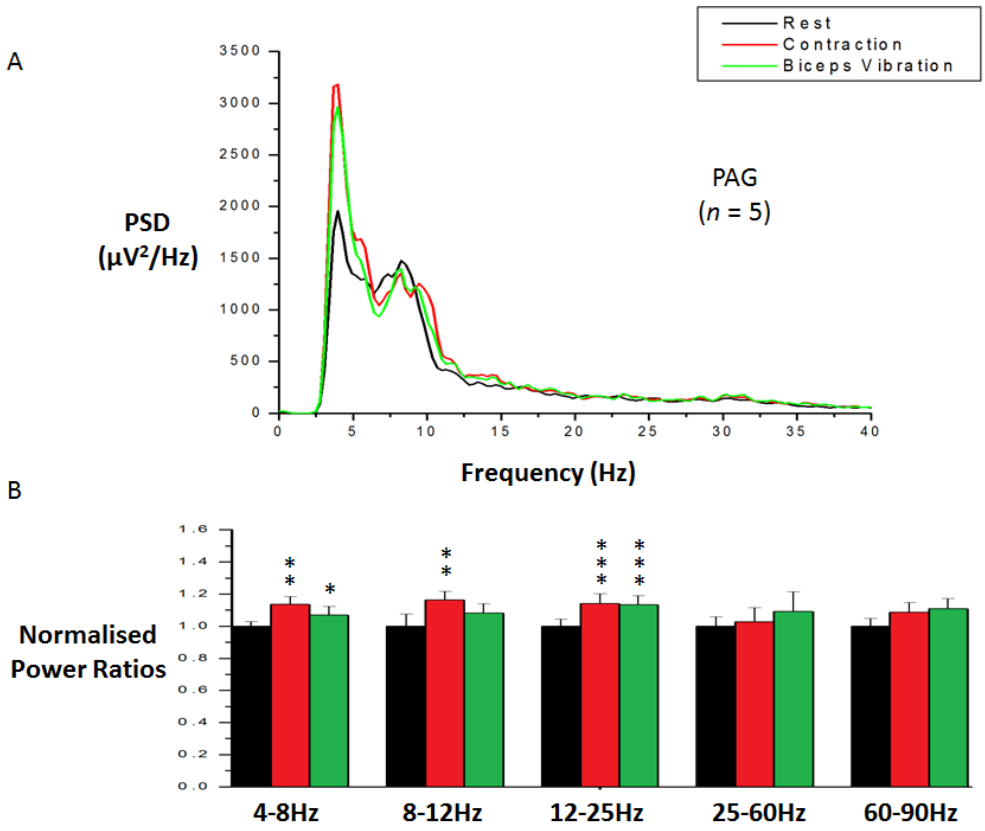

Figure 5.18 – *Graphs showing a significant increase in periaqueductal grey (PAG) neural activity during both biceps contraction (with no vibration) and biceps contraction with biceps vibration, compared to rest. (A) Mean power spectral density (PSD) for all five patients. (B) Normalised spectral changes (rest = 1.0) divided into frequency bands, showing significant increases during both biceps contraction and biceps contraction with biceps vibration in the 4-8 Hz, 8-12 Hz and 12-25 Hz bands, compared to rest. n = 5, * P < 0.05, ** P < 0.01, *** P < 0.001. Error bars represent standard error of the mean.*

Local Field Potential Recordings from the Other Nuclei

Using ANOVA, it was shown that there were no significant differences among any of the conditions in any of the sensory thalamus patients (Figs. 5.19-5.20).

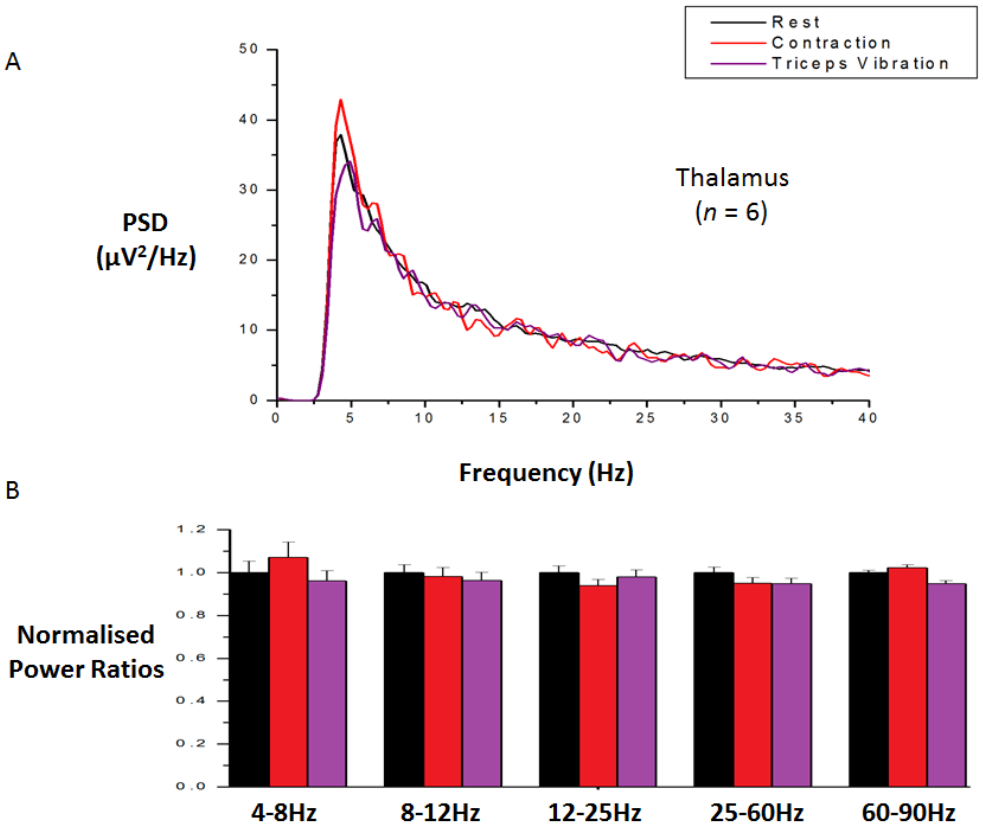

Figure 5.19 – *Graphs showing no changes in thalamic neural activity during biceps contraction (with no vibration) and during biceps contraction with triceps vibration, compared to rest. (A) Mean power spectral density (PSD) for all six patients. (B) Normalised spectral changes (rest = 1.0) divided into frequency bands, showing no significant differences compared to rest. n = 6. Error bars represent standard error of the mean.*

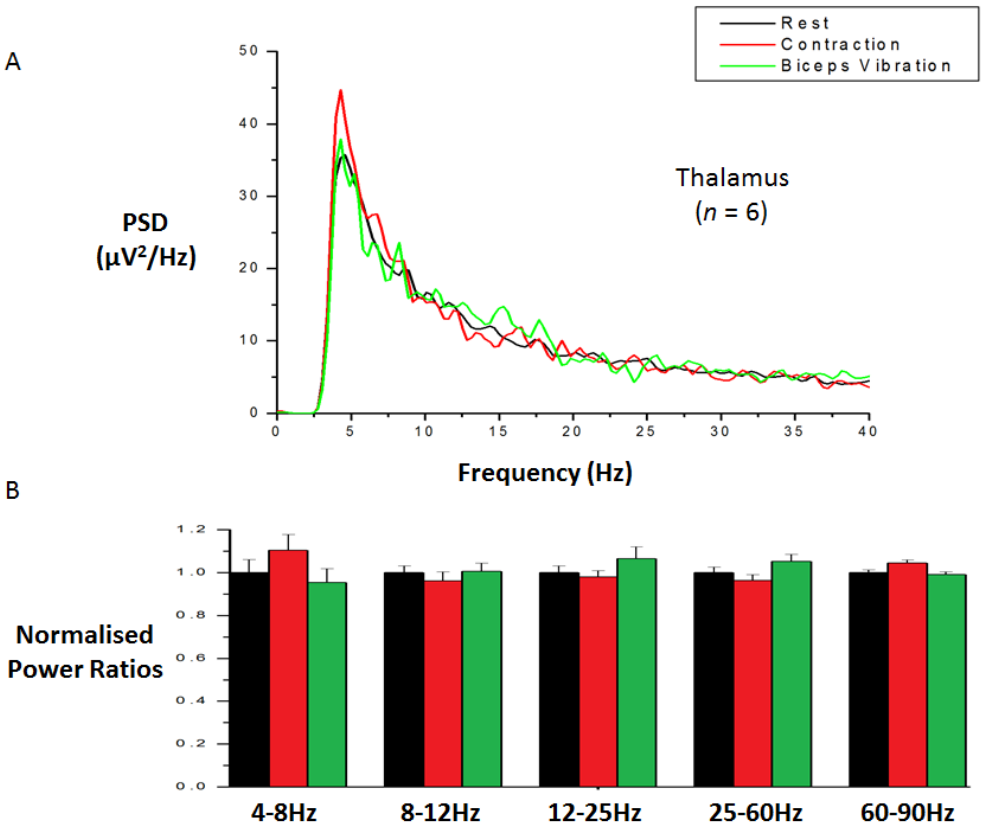

Figure 5.20 – *Graphs showing no changes in thalamic neural activity during biceps contraction (with no vibration) and during biceps contraction with biceps vibration, compared to rest. (A) Mean power spectral density (PSD) for all six patients. (B) Normalised spectral changes (rest = 1.0) divided into frequency bands, showing no significant differences compared to rest. n = 6. Error bars represent standard error of the mean.*

Cardiovascular Parameters and Local Field Potential Recordings from Control Experiment (Section 4)

There were no significant differences among any of the conditions of Section 4 of the experiment (i.e. the control experiment of vibration without contraction) in any of the patients, either in terms of cardiovascular parameters (Figs. 5.21-5.23) or in terms of neural activity (Figs. 5.24-5.26).

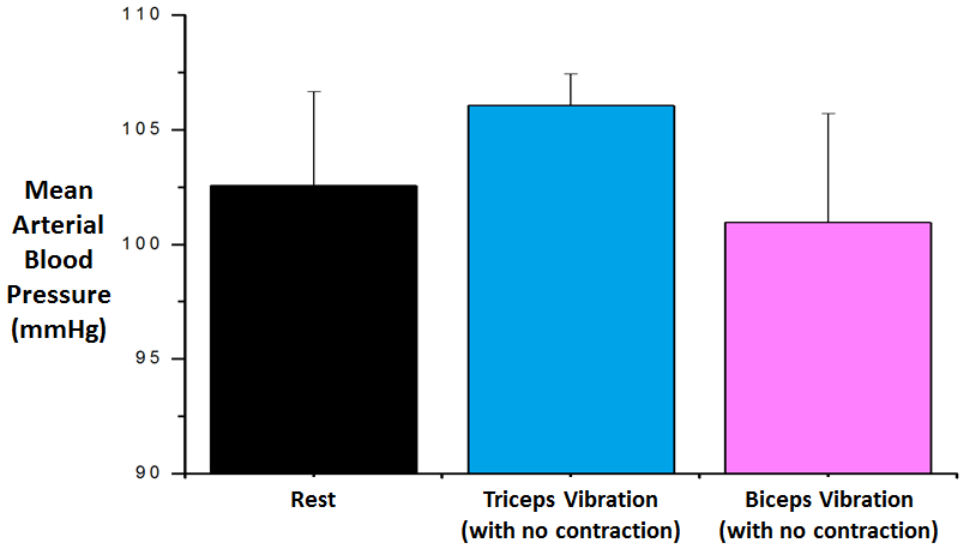

Figure 5.21 – *Graph showing no significant changes in mean arterial blood pressure either during triceps vibration without contraction or during biceps vibration without contraction, compared to rest. n = 17. Error bars represent standard error of the mean.*

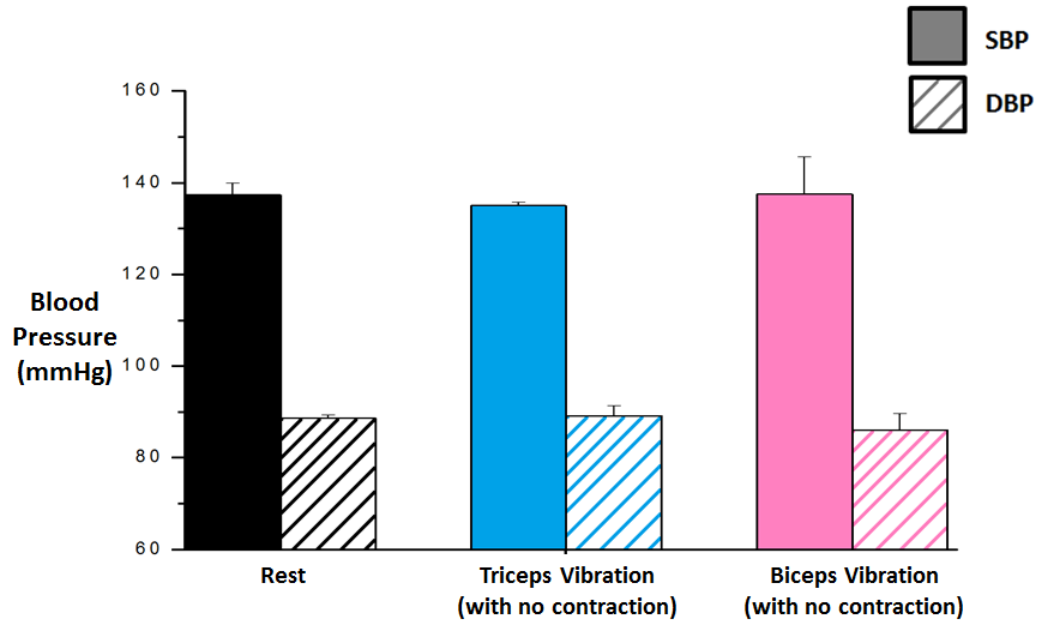

Figure 5.22 – *Graph showing no significant changes in systolic blood pressure (SBP) or diastolic blood pressure (DBP) either during triceps vibration without contraction or during biceps vibration without contraction, compared to rest. n = 17. Error bars represent standard error of the mean.*

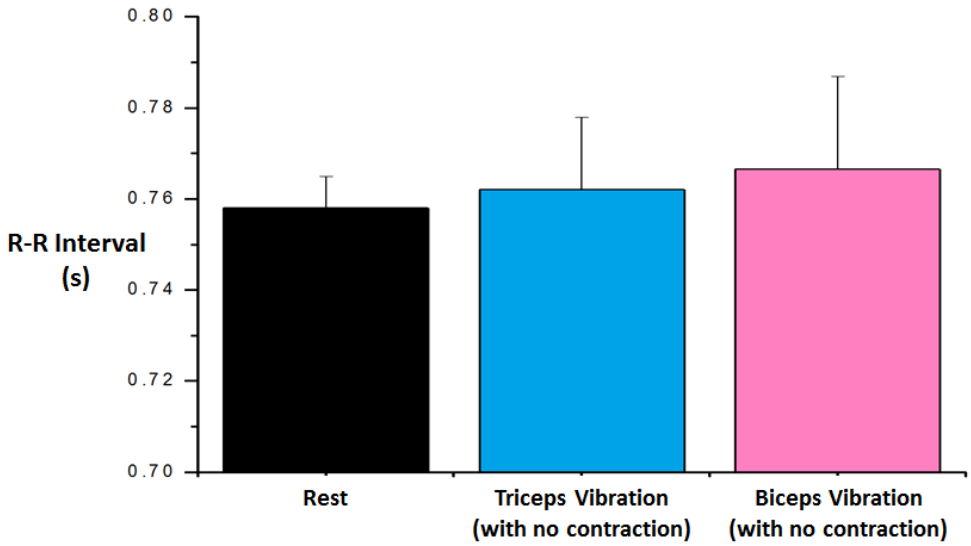

Figure 5.23 – *Graph showing no significant changes in R-R interval (i.e. no changes in heart rate) either during triceps vibration without contraction or during biceps vibration without contraction, compared to rest. n = 17. Error bars represent standard error of the mean.*

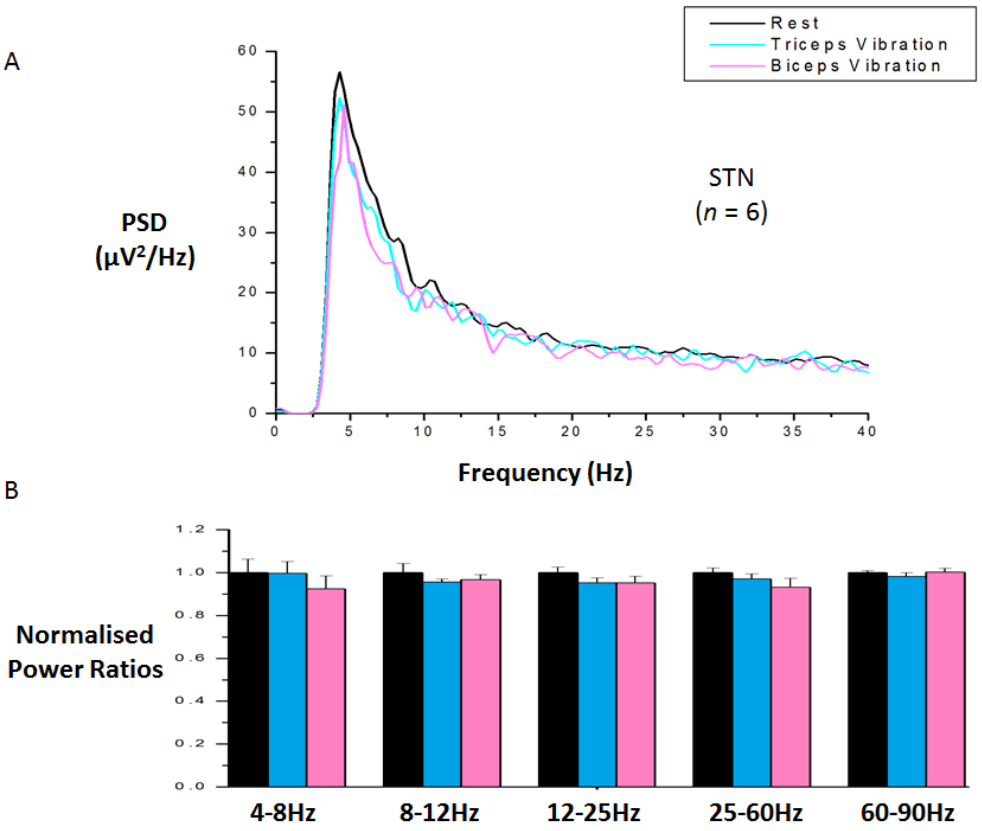

Figure 5.24 – *Graphs showing no significant changes in subthalamic nucleus (STN) neural activity during triceps vibration without contraction or during biceps vibration without contraction, compared to rest. (A) Mean power spectral density (PSD) for all six patients. (B) Normalised spectral changes (rest = 1.0) divided into frequency bands, showing no significant differences compared to rest. n = 6. Error bars represent standard error of the mean.*

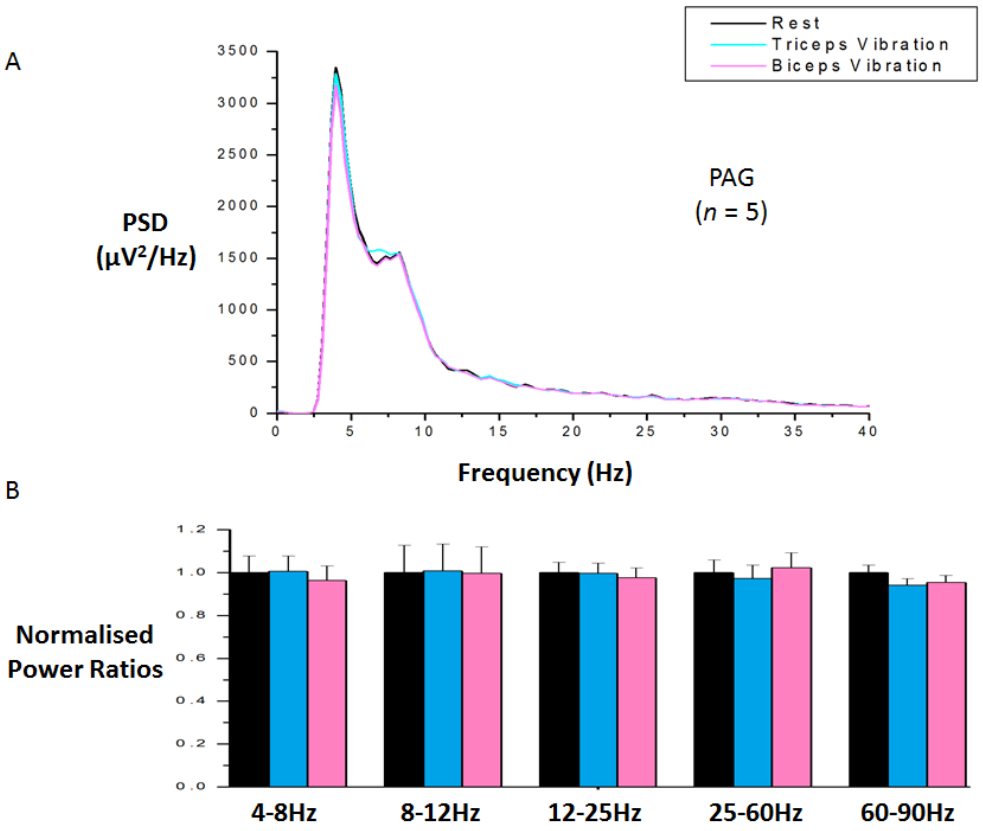

Figure 5.25 – *Graphs showing no significant changes in periaqueductal grey (PAG) neural activity during triceps vibration without contraction or during biceps vibration without contraction, compared to rest. (A) Mean power spectral density (PSD) for all five patients. (B) Normalised spectral changes (rest = 1.0) divided into frequency bands, showing no significant differences compared to rest. n = 5. Error bars represent standard error of the mean.*

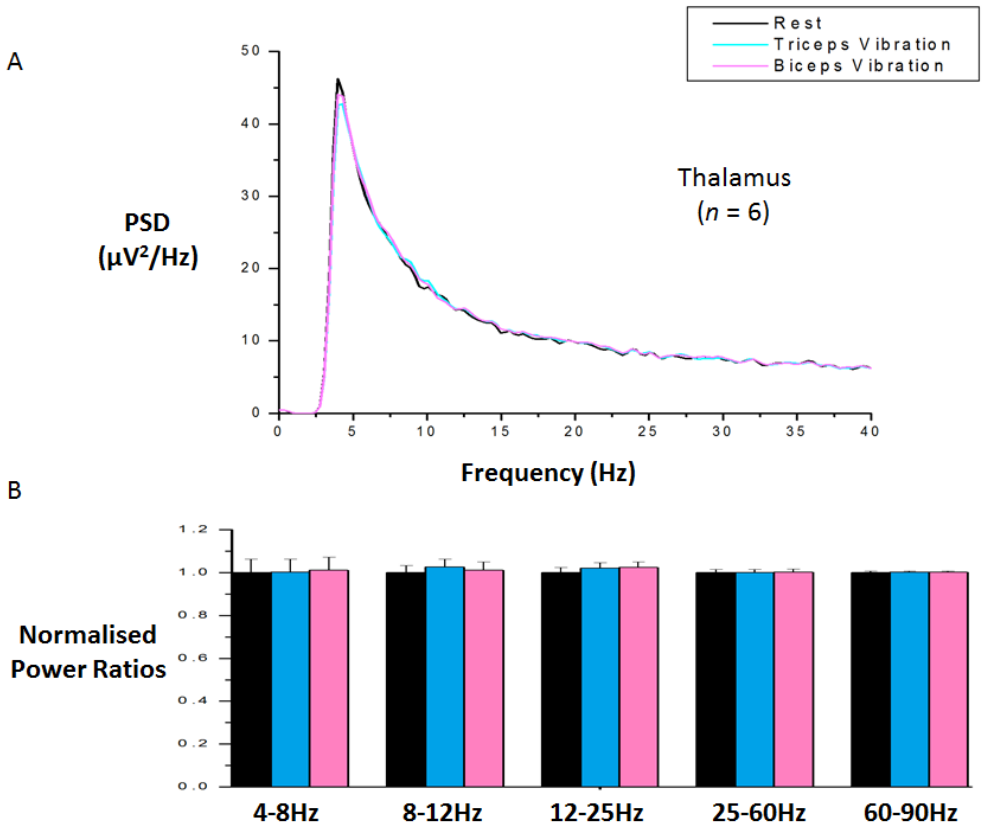

Figure 5.26 – *Graphs showing no significant changes in thalamic neural activity during triceps vibration without contraction or during biceps vibration without contraction, compared to rest. (A) Mean power spectral density (PSD) for all six patients. (B) Normalised spectral changes (rest = 1.0) divided into frequency bands, showing no significant differences compared to rest. n = 6. Error bars represent standard error of the mean.*

Discussion

Using the paradigm of Goodwin *et al* (1972), I have been able to demonstrate in humans that central command is associated with significantly decreased neural activity in the subthalamic nucleus (STN), which is consistent with the hypothesis that the STN is involved in the neurocircuitry controlling the cardiovascular responses to exercise. Furthermore, I have shown that neural activity in the STN is graded to the perception of the exercise task, i.e. the degree of central command. The other sites that were investigated (the periaqueductal grey [PAG] and the sensory thalamus) appear not to have as significant a role in the integration of central command during the light exercise that was undertaken, despite having been previously

identified as cardiovascularly active in both animals and humans (Thornton *et al*, 2002; Green *et al*, 2005; Green *et al*, 2007). Although there was increased neural activity in the PAG during exercise, the response was not graded to the degree of central command. Therefore, the response most likely represents the activation of the exercise pressor reflex (as discussed in Chapters 3 and 4). It is recognised that the sensation of the vibration itself does not correspond to a change in STN activity. Therefore, one can be confident that the decrease in STN activity seen during the exercise tasks is not due to the vibratory stimulus.

Role of the Subthalamic Nucleus in the Integration of Central Command

The findings in this chapter demonstrate a marked decrease in neural activity in the subthalamic nucleus (STN) during isometric biceps contractions, both with and without the vibration stimulus. For each patient, the tension achieved was always constant. Therefore, reflex responses from the exercising muscle would have remained the same, whereas responses dependent on central command would have varied. Essentially, on application of the vibrator to the biceps tendon during a biceps contraction, an element of reflex excitation is provided; subsequently, less central command is required to achieve a given tension – and subjects generally reported that they found it easier to hold the contraction even though there was no change in the force produced. Conversely, on application of the vibrator to the triceps tendon (i.e. the antagonist tendon) during a biceps contraction, an element of reflex inhibition is provided, due to the disynaptic inhibition of the active muscle motor neurons; accordingly, more central command is required to achieve a given tension – and subjects reported that they found it harder to hold the contraction even though, again, there was no change in the force produced.

Every subject experienced an increase in both blood pressure and heart rate during isometric effort. These increases were compared to those which occurred when the same force was held

by the same muscle for the same period of time, while the central command required to produce the tension was changed, via the vibration stimulus. These results show not only that both blood pressure and heart rate change with the level of central command (as demonstrated by Goodwin *et al*, 1972), but also that STN neural activity changes with the level of central command. When the degree of central command is high (i.e. triceps vibration during a biceps contraction), STN activity is decreased by a large amount, whereas when the degree of central command is low (i.e. biceps vibration during a biceps contraction), STN activity is decreased by a smaller amount.

The observation that STN activity decreased during the isometric contractions in the 4-8 Hz, 8-12 Hz and 12-25 Hz frequency bands is consistent with past experiments demonstrating suppression in STN activity following warning and 'go' cues (Williams *et al*, 2003; Kuhn *et al*, 2004; Green *et al*, 2007). This decrease in STN activity during contractions suggests that there is a release of the inhibitory drive on the cardiovascular nuclei which receive projections from the STN, as the changes are mirrored in terms of the subjects' cardiovascular parameters.

Interestingly, there was no increase in STN activity during isometric exercise in the 60-90 Hz band, as observed during the dynamic exercise tasks in Chapters 3 and 4 and during the cycle ergometry exercise task in the Green *et al* (2007) study. This is consistent with the theory that this increase in STN neural activity in the higher frequencies is associated with the movement itself i.e. the locomotor system, as opposed to the cardiovascular system (which appears to be associated with the lower frequency bands).

Classically, the STN has been thought of as playing a role in motor function (DeLong and Wichmann, 2007). However, it is also recognised to have a role in cardiovascular function, as there is evidence to suggest it is involved in the parallel activation of the cardiorespiratory and locomotor systems. Angyan and Angyan (1999b) used electrical stimulation of the STN in both freely moving and anaesthetised cats to elicit a significant increase in arterial blood pressure,

heart rate and respiratory rate. They showed that STN stimulation causes significant cardiorespiratory changes in anaesthetised cats, despite the absence of visible somatomotor activity, suggesting that the STN is directly involved in adjusting cardiorespiratory function, and that the cardiovascular responses to STN stimulation are not secondary to electrically elicited movement.

Not only is the STN itself implicated in the control of cardiovascular function, but the entire subthalamic area (including the subthalamic locomotor region of the hypothalamus) is also thought to be involved. Using electrical stimulation of the dorsal region of the STN in dogs, Smith *et al* (1960) were able to evoke cardiovascular responses of a similar magnitude to those elicited by volitional exercise. Eldridge *et al* (1981) electrically stimulated the subthalamic locomotor region in unanaesthetised decorticate cats and provided evidence to suggest that this area drives both cardiovascular and locomotor activity. In 1988, Spencer *et al* used glutamate in anaesthetised rats to show the involvement of the subthalamic region in modulating cardiovascular parameters. Both Van der Plas *et al* (1995) – using electrical stimulation of the same region in rats – and Iwamoto *et al* (1996) – using c-Fos expression in dynamically exercising rats – also demonstrated that this region is involved in the integration of the cardiovascular response to exercise.

There is a selection of experiments with human subjects in which high frequency stimulation of the STN evoked increases in arterial blood pressure, heart rate and facilitation of movement (Priori *et al*, 2001; Kaufmann *et al*, 2002; Thornton *et al*, 2002; Benedetti *et al*, 2004), although the underlying mechanisms of this pathway are poorly understood. STN stimulation is used to improve the motor symptoms in Parkinsonian patients (Limousin *et al*, 1998; Lopiano *et al*, 2001), which are thought to be related to an overactive STN. High frequency stimulation of the STN is thought to elicit a post-synaptic depolarisation block and activation of its afferent inhibitory fibres (Benazzouz and Hallett, 2000; Benedetti *et al*, 2004). This is consistent with

the results of this chapter, where decreased or 'inhibited' STN activity appears to be correlated with increased arterial blood pressure and heart rate.

A great deal of the research investigating the neurocircuitry involved in central command in humans comes from functional imaging studies. Positron emission tomography scanning has proved to be a useful tool in identifying increased regional cerebral blood flow within certain areas of the brain during activation of central command. Nowak *et al* (2005) demonstrated in paraplegic subjects that activation of the insular cortex is associated with both attempted exercise tasks and actual exercise tasks; the motor cortex and the sensory cortex were only shown to be active during actual exercise tasks, suggesting that the insular cortex could be involved in the activation of central command. Furthermore, it is believed that the insular cortex does not receive nerve afferents from working muscle, providing further indication that it is involved in central command. Williamson *et al* (1999) showed similar results regarding the insular cortex using single-photon-emission computed tomography scanning. In 2006, the same group implicated the cingulate cortex in the integration of central command (Williamson *et al*, 2006).

Limitations

There is much overlap between the limitations of this chapter and those of Chapters 3 and 4, with regards to directly translating the power spectral density (PSD) changes into changes in neural activity. To address this issue briefly, local field potentials are considered to be due to local synchronous neuronal population activity (Mitzdorf, 1985; Rasch *et al*, 2009). Therefore, increases in PSD are considered to be a reflection of increases in network synchrony or size (Logothetis *et al*, 2001; Katzner *et al*, 2009; Kelly *et al*, 2010).

It could be argued that the decrease in subthalamic nucleus (STN) neural activity observed was purely a coincidence and not linked to central command. However, this is very unlikely due to

the fact that the decrease in neural activity was graded to the degree of central command. It is also unlikely that the STN neural activity decrease was compensatory to central command, as there is so much evidence showing that direct stimulation of the nucleus evokes changes in cardiorespiratory parameters. Furthermore, during vibration of the triceps and biceps tendons without any contraction, there was no change in PSD, thus eliminating the possibility that STN activity is associated with the vibration stimulus itself. Hodgson and Matthews (1968) performed experiments on decerebrate cats which indicated that activation of the primary afferents of the triceps surae muscle spindles by vibration does not produce any cardiovascular responses. McCloskey and Mitchell (1972) also carried out experiments with decerebrate cats, using direct current anodal nerve block to block the large myelinated afferents (including muscle spindles and Golgi tendon organs) of the dorsal roots receiving projections from working muscle. They found that this had no effect on the cardiovascular responses which occurred during exercise.

The underlying pathology in the patient model is also a limitation, as it is known that the STN is affected in patients suffering from Parkinson's disease. This makes it difficult to translate the findings to healthy humans. Moreover, the nuclei available for investigation were limited, as only sites that provided therapeutic benefit to the subjects could be used to record from. Despite this, the nuclei examined have all been identified in animal models as being cardiovascularly active. Additionally, without histological data, the precise electrode locations of the electrodes within the nuclei could only be estimated, in spite of being carefully placed using stereotactic coordinates.

In terms of the experimental protocol itself, a number of possible limitations must be considered. First, when subjects held the biceps contraction while the antagonist triceps tendon was being vibrated, it might have been possible for the triceps muscle itself to have been contracting. It was ensured that this was not the case, by palpation of the triceps muscle,

and it was found that the reflex inhibition was not associated with any detectable contraction of the vibrated antagonist triceps muscle. This was expected, as the motor neurons of the triceps muscle were most likely being inhibited by both descending command and spinal reflexes from the contracting biceps muscle (Goodwin *et al*, 1972). Secondly, although subjects were specifically instructed to confine their efforts to the biceps muscle only during periods of isometric contraction, and to avoid changing their leverage by using shoulder, trunk or elbow movements, it was expected that there would still be some activity in the muscles fixating the shoulder joint. The activity of these other groups of muscles could have varied between different sections of the experiment. Nevertheless, Lind *et al* (1966) showed that the cardiovascular responses to isometric effort vary according to the percentage of the maximum capable contraction of the muscle group. If two muscle groups contract together, the response is determined by the muscle group achieving the larger proportion of its own maximum contraction. Therefore, changes in the activity of accessory muscles or other muscle groups in this study would only be expected to influence the cardiovascular responses if they were achieving over 50% of their maximum voluntary contraction, as this was the percentage that subjects were instructed to hold using their biceps muscles. However, it is highly unlikely that this would have gone unnoticed. Contraction by the vibrated antagonistic triceps muscle would have been a more obvious problem, as this would have resulted in the biceps muscle having to increase its own tension in order to externally register the required force. However, as discussed previously, the risk of this occurring was excluded by palpation of the muscle to ensure the absence of contraction.

As this experiment consisted of repeated comparisons between responses to the same muscular effort by the biceps, it is important to consider the potential influence of muscle fatigue. Fatigue could change the afferent neural activity responsible for the cardiovascular responses from the exercising muscle. Furthermore, it is possible that fatigued muscle requires a greater level of central command to hold a specific tension than it would under normal non-

fatigued conditions. These effects could have distorted the results of this study, where it is assumed that the reflex activity from the muscles is the same between contractions at a constant tension, and that the level of central command is only varied by the vibration stimulus. Therefore, the sequence of the different sections of the experiment was ordered to minimise any alterations to the recordings that might have arisen due to muscle fatigue. Contractions were only 50% of each subject's maximum voluntary contraction, and were spaced at least five minutes apart to allow good recovery. The reproducibility of the cardiovascular responses, particularly the arterial blood pressure response, to the normal isometric biceps contractions (without any vibration) was very good in all subjects. Experiments were conducted in sets of three contractions: the first was a normal biceps contraction, the second would involve vibration of either the biceps tendon or its antagonist tendon, and the third would be another normal biceps contraction. The set of contractions in which the central command would be increased during the vibration period, i.e. the set including the vibration of the triceps tendon, was always conducted before the set of contractions in which central command would be decreased during the vibration period, i.e. the set including the vibration of the biceps tendon. Therefore, the effects of fatigue were working against the way in which I interpreted the results, as central command was always greater in the first set of contractions. However, fatigue could only be greater in the second set.

The subjects were asked to comment on their experiences throughout the study. On application of vibration to the triceps muscle tendon (requiring an increase in central command), all subjects reported that it was more difficult to hold the required tension. On application of vibration to the tendon of the biceps muscle (so that less central command is required), most subjects reported that it was easier to hold the required tension. However, some subjects found the reflexly assisted biceps contraction more difficult than a normal

contraction. This could have been due to the increased concentration that was necessary to hold the required tension.

Conclusion

In conclusion, using direct neurophysiological recordings, this study provides evidence to suggest that the STN is a key component of the neurocircuitry responsible for integrating central command in humans, during light exercise involving a small muscle mass.

CHAPTER 6

Changes in Muscle Sympathetic Nerve Activity during Stimulation of Various Brain Nuclei in Humans

Introduction

The advent of microneurography has been an important development in terms of research into sympathetic nerve activity, both at rest and during exercise, and also in various disease states. In 1960, Hensel and Boman were the first to successfully record neural impulses from peripheral nerves in humans. They recorded single unit afferent discharges using glass microelectrodes from exposed peripheral nerves. The technique of microneurography in use today is much less invasive; a tungsten microelectrode is used to percutaneously penetrate into peripheral nerves in unanaesthetised humans. This method was first developed by Hagbarth and Vallbo in 1967.

Sympathetic nerve fibres characteristically exhibit spontaneous activity – this activity is usually synchronised amongst neighbouring nerve fibres. Therefore, sympathetic multi-unit nerve activity can be recorded as 'bursts' of neural impulses interspersed by periods of silence (Wallin and Charkoudian, 2007). The timing of the occurrence of these spontaneous bursts is different between multi-unit muscle sympathetic nerve activity (MSNA) and multi-unit skin sympathetic nerve activity (SSNA), allowing reliable differentiation between the two. MSNA is believed to be pulse synchronous (Delius *et al*, 1972), whereas SSNA occurrence is not thought to be related to the cardiac cycle.

In humans, resting MSNA is modulated by the arterial baroreflex. Delius *et al* (1972) showed that in the median or peroneal nerves of resting humans, series of pulse synchronous neural bursts appeared frequently when blood pressure was transiently decreased, whereas blood

pressure increases were associated with phases of neural silence. It has also been shown that changes in arterial baroreceptor firing can provoke reciprocal changes in the strength (or amplitude) of the neural burst impulses (Wallin *et al*, 1975; Wallin and Eckberg, 1982). Each sympathetic burst can be related to a particular cardiac cycle, as in each individual subject there is a constant baroreflex latency period (Delius *et al*, 1972). However, overall, some subjects have many sympathetic bursts, and others have few – these inter-individual differences in the occurrence of bursts are reproducible over significant lengths of time, suggesting that each subject has a constant level of MSNA individual to them (Sundlof and Wallin, 1977; Fagius and Wallin, 1993).

It was originally thought that, during systemic exercise, arterial blood pressure was maintained by the fact that the maximum level of cardiac output was closely linked to the amount by which the peripheral vasculature to skeletal muscle dilated. However, it has been shown that the capacity of peripheral blood flow can exceed the maximum cardiac output (Armstrong and Laughlin, 1984; Andersen and Saltin, 1985; Musch *et al*, 1987). Therefore, it is believed that a further controlling influence must be involved in the maintenance of arterial blood pressure, in order to ensure adequate perfusion of the various vascular beds. It is thought that this regulatory influence originates from the sympathetic nervous system (Khan and Sinoway, 2000).

Haemodynamic studies conducted in both animal and human models have led to the widely accepted belief that both static and dynamic exercise are associated with increases in heart rate, arterial blood pressure and sympathetic nerve activity (Lind *et al*, 1964; Delius *et al*, 1972; Mark *et al*, 1985; Victor *et al*, 1988; Savard *et al*, 1989; Sinoway *et al*, 1989; Leuenberger *et al*, 1993). The magnitude of the increase in sympathetic activity is thought to be dependent on the muscle mass being used (Mitchell *et al*, 1980; Seals, 1989), the intensity of the exercise task (Lind *et al*, 1964; Leuenberger *et al*, 1993), and the effects of fatigue (Saito *et al*, 1989;

Seals and Enoka, 1989). The precise mechanism of the increase in sympathetic nerve activity with exercise has not yet been firmly established. However, the arterial baroreflex, central command and the exercise pressor reflex have all been implicated (Rowell and O'Leary, 1990; Mitchell and Victor, 1996; Khan and Sinoway, 2000; Delp and O'Leary, 2004).

These three mechanisms have been discussed in detail in previous chapters. Briefly, central command refers to the cortically-initiated feed-forward regulatory response accompanying volitional exercise (Krogh and Lindhard, 1913; Goodwin *et al*, 1972), whereas the arterial baroreflex is a feedback reflex that makes regular autonomic neural adjustments so that resting arterial blood pressure operates around a set point. Originally, it was believed that the arterial baroreflex was 'switched off' at the onset of exercise, but a number of studies have demonstrated that during exercise, the arterial baroreflex is actually reset to a higher pressure (Potts *et al*, 1993; Collins *et al*, 2001). Therefore, as opposed to counteracting the increased sympathetic nerve activity during exercise, the arterial baroreflex is thought to play a role in the increase, by attempting to raise the arterial blood pressure to the higher baroreflex set point. The exercise pressor reflex is another feedback mechanism in which group III and IV nerve fibre afferents from skeletal muscle are activated by increased muscle tension and metabolites released during exercise, thereby providing additional influence on cardiovascular control (Alam and Smirk, 1937; McCloskey and Mitchell, 1972; Mark *et al*, 1985; Rotto and Kaufman, 1988).

The extent to which each of these mechanisms contributes to the regulation of sympathetic nerve outflow during exercise is uncertain. Microneurographic studies have shown that the relative contribution of each of these mechanisms can vary considerably according to the experimental model, the type of exercise being performed, the intensity of the exercise task and the specific outflow of sympathetic nerve activity being investigated (Mitchell and Victor, 1996; Delp and O'Leary, 2004).

For example, the metaboreflex portion of the exercise pressor reflex is not thought to be active during light dynamic exercise (as demonstrated in Chapters 3 and 4). This is similar to the findings of Mark *et al* (1985) who observed that only if the workload is sufficiently energetic and the exercise task is continued for a long enough length of time would the metabolic by-products of muscle contraction begin to accumulate, thereby activating the muscle metaboreflex. They recorded efferent sympathetic nerve activity in the leg during static arm exercise in humans and demonstrated that activation of the metaboreflex increased sympathetic nerve activity whereas activation of central command decreased sympathetic nerve activity. Saito *et al* (1986) showed in humans that the increase in sympathetic nerve activity recorded from the leg was related to the intensity of the static arm exercise being performed. The same group showed that the MSNA response to metaboreflex stimulation was activated by fatigue in the exercising muscles (Saito *et al*, 1989). In 1991**,** O'Leary *et al* used carotid occlusion in dogs to demonstrate that as the intensity of the exercise task increases, the arterial blood pressure response becomes increasingly dependent on vasoconstriction (and therefore increased sympathetic activity) within the working muscle.

The mechanoreflex portion of the exercise pressor reflex alone (Stebbins *et al*, 1988) is also believed to contribute to increased sympathetic outflow. Victor *et al* (1989b) used anaesthetised cats to show that stimulation of the group III mechanically sensitive muscle nerve fibres in the triceps surae muscles resulted in increased renal sympathetic nerve activity. McMahon and McWilliam (1992) used decerebrate cats to demonstrate that the mechanoreflex also modulates parasympathetic outflow to the heart (i.e. vagal withdrawal leading to increased heart rate) at the beginning of exercise.

It has been hypothesised by a number of research groups that central command responds to the metabolic needs of exercising skeletal muscle via the pattern of recruitment of motor units; as muscle fatigue arises, further motor units are recruited and sympathetic outflow is

thought to increase correspondingly (Krogh and Lindhard, 1913; Goodwin *et al*, 1972; Eldridge *et al*, 1985; Victor *et al*, 1989a; Khan and Sinoway, 2000). Victor *et al* (1989a) were able to demonstrate, using neuromuscular blockade in humans, that during static arm exercise, central command has a strong influence on parasympathetic outflow to the heart, but only a minor influence on sympathetic outflow to skeletal muscle in the leg. Six years later, the same group demonstrated that central command does have a significant influence on sympathetic nerve activity recorded from the leg during very intense intermittent static arm exercise (Victor *et al*, 1995). However, although central command does appear to make some contribution to sympathetic discharge in working muscle, particularly during high intensity exercise tasks (Victor *et al*, 1995), it seems that it plays a more significant role in sympathetic discharge in skin (Vissing *et al*, 1991; Victor *et al*, 1995; Silber *et al*, 2000).

Various methods have been trialled in an attempt to precisely quantify MSNA – the two major quantification methods involve burst 'incidence' and burst 'amplitude' (Sundlof and Wallin, 1978). Burst incidence describes the threshold of the neural activity; in simple terms, whether or not a sympathetic burst occurs. Burst amplitude describes the strength of the neural impulse. Furthermore, baroreflex sensitivity can be mapped by plotting the strength of the impulse against the diastolic pressure in its corresponding cardiac cycle (Sundlof and Wallin, 1978; Kienbaum *et al*, 2001).

Kienbaum *et al* (2001) conducted a study that provided evidence for differential baroreflex regulation of burst incidence and burst amplitude in muscle nerve afferents in humans. They recorded MSNA from the peroneal nerve in 60 healthy subjects, and observed that while the burst incidence in muscle sympathetic neurons was precisely linked to arterial blood pressure, burst amplitude had a poor relationship to arterial blood pressure. Furthermore, they found that the burst incidence was highly reproducible within individual subjects, whereas burst amplitude was not. They suggested that the modulation of the two factors of burst incidence

and burst amplitude occur at two different sites within the central nervous system – one to determine whether or not a burst occurs and the other to determine the strength of the discharge.

Prior to the Kienbaum study (Kienbaum *et al*, 2001), there had been other evidence to suggest differentiated control of burst incidence and burst amplitude. Hjemdahl *et al* (1989) demonstrated an increase in MSNA burst amplitude during mental stress in humans, but no change in burst incidence. Animal models have also been used to demonstrate the idea of two separate regulatory mechanisms – one group used an automated computer algorithm to show differentiated control of renal sympathetic activity in cats (Malpas and Ninomiya, 1992a; Malpas and Ninomiya, 1992b). DiBona *et al* (1997) showed that in both Wistar-Kyoto rats and spontaneously hypertensive rats, activation of the arterial baroreflex resulted in a decrease in renal sympathetic activity almost entirely by decreases in burst amplitude, but not burst incidence. DiBona and Jones (1998) demonstrated that heat stimulation applied to the tails of rats caused an increase in burst amplitude, whereas acute loading volume caused a decrease in burst amplitude; meanwhile, burst incidence remained unchanged in both scenarios. Sverrisdottir *et al* (2000) used a human disease model to demonstrate the differentiated control mechanisms of the two factors. They showed that in subjects suffering from congestive heart failure, there was an increase in both burst incidence and burst amplitude. However, in ageing healthy subjects, there was an increase in burst incidence but not in burst amplitude.

Studies performed by Mary and co-workers investigated the effects of ischaemic heart disease and myocardial infarction on MSNA burst incidence (Graham *et al*, 2002; Graham *et al*, 2004; Hogarth *et al*, 2006). They observed that patients suffering from stable coronary artery disease showed similar burst incidence to the healthy control group. However, following uncomplicated acute myocardial infarction, burst incidence was shown to be raised for up to

nine months compared to healthy controls and patients with stable coronary artery disease (Graham *et al*, 2002). Patients suffering from unstable angina also showed increased burst incidence compared to healthy controls, but they showed less of an increase than post-myocardial infarction patients (Graham *et al*, 2004). Patients suffering from hypertension prior to their myocardial infarction showed greater and more prolonged increases in burst incidence than patients who were normotensive prior to their myocardial infarction (Hogarth *et al*, 2006). The sympathetic hyperactivity demonstrated in these experiments was inversely correlated with left ventricular ejection fraction, but had no relationship to arterial blood pressure – this suggests that the mechanism of the increase in MSNA burst incidence could involve impairment of the reflexes from cardiac receptors.

The aim of this study was to investigate the changes in MSNA during direct electrical stimulation of various deep brain nuclei, in order to establish the central nervous system sites which are responsible for the modulation of burst incidence and burst amplitude. Structures which had previously been identified as cardiovascularly active in animals were stimulated whilst recording MSNA from the peroneal nerve. The recordings were used to test the hypothesis that stimulation of particular subcortical structures corresponds to increases in MSNA, either in terms of burst incidence or in terms of burst amplitude.

Methods

Twelve patients (8 male, 4 female), with a mean age of 51.8 years (range 33-67 years) were recruited for this study (Table 6.1). Four patients had electrodes implanted in the periaqueductal grey (PAG) for the treatment of chronic pain (mean age 47.8 years). Two more patients had electrodes implanted in the sensory thalamus, also for the treatment of chronic pain (mean age 53.5 years), either in the ventroposterolateral or ventroposteromedial nucleus for the treatment of limb pain or facial pain, respectively. Another four patients had

electrodes implanted in the subthalamic nucleus for the treatment of Parkinson's disease (mean age 58.5 years). One patient had an electrode in the internal globus pallidus for the treatment of generalised dystonia (age 45 years). Finally, one patient had an electrode in the anterior cingulate cortex for the treatment of chronic pain (age 45 years).

Table 6.1 *– Subject characteristics for muscle sympathetic nerve activity experiments. PAG, periaqueductal grey; STN, subthalamic nucleus; GPi, internal globus pallidus; ACC, anterior cingulate cortex.*

Patient	***Age (years)***	***Sex***	***Diagnosis***	***DBS Electrode Location***
1	60	M	Chronic pain following stroke	Dorsal PAG
2	58	M	Chronic right arm pain following brachial plexus injury	Dorsal PAG
3	33	M	Chronic left-sided neuropathic pain	Ventral PAG
4	40	F	Right-sided glossopharyngeal neuralgia	Ventral PAG
5	67	M	Chronic pain following stroke	Sensory Thalamus
6	40	F	Right-sided glossopharyngeal neuralgia	Sensory Thalamus
7	66	M	Parkinson's disease	STN
8	47	F	Parkinson's disease	STN
9	55	M	Parkinson's disease	STN
10	66	M	Parkinson's disease	STN
11	45	F	Generalised dystonia	GPi
12	45	M	Right-sided pain after complete C6 motor & sensory tetraplegia	ACC

Unlike those in Chapters 3, 4 and 5, these experiments did not have to be conducted within the first week following stage 1 of the deep brain stimulation surgical procedure, as the electrodes did not need to be externalised in order to turn the stimulation on and off within the targeted brain nuclei. Therefore, the patients had had their electrodes implanted for varying periods of time, ranging from less than one week to as long as three years. The protocol was as follows (Fig. 6.1): each patient was asked to lie down comfortably, with the knee from which muscle sympathetic nerve activity (MSNA) was being recorded slightly bent and elevated on a leg rest. The patients were asked before the experiment started whether their deep brain stimulation electrodes were switched on or off, and what settings (in terms of

amplitude, pulse width and frequency) they normally used for therapeutic benefit. Once a suitable recording site was identified within the peroneal nerve, cardiovascular parameters and MSNA were recorded for a period of five minutes, with the deep brain stimulation switched on to whatever settings the patients usually used. The stimulation was then turned off, and cardiovascular parameters and MSNA were recorded for another five minutes. The protocol was then repeated twice more, for a total of three sets of on/off recordings, in order to confirm the consistency of the response. If the response was consistent, the results were averaged together to give one set of results for each patient.

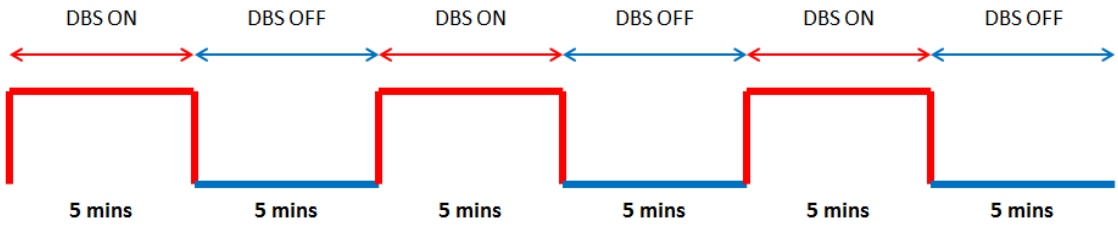

Figure 6.1 *– Protocol for muscle sympathetic nerve activity experiment. The raised lines indicate that the deep brain stimulation (DBS) is switched on.*

A different protocol was used for one of the PAG patients and one of the thalamus patients who had had their electrodes implanted less than a week before. Therefore, the best settings for their therapeutic benefit had not yet been decided upon. This allowed for some flexibility with the parameters that were tested and thus a graded protocol was followed (Figs. 6.2-6.3): cardiovascular parameters and MSNA were recorded for a period of five minutes, with the deep brain stimulation switched off. This was followed by five minutes of the stimulation switched on with an amplitude of 1V, then five minutes with an amplitude of 2V, etc. This continued up to 3V for the PAG electrode (Fig. 6.2), and up to 5V for the sensory thalamus electrode (Fig. 6.3). The experiments ended with a further five minutes of recordings with the stimulation switched off once more.

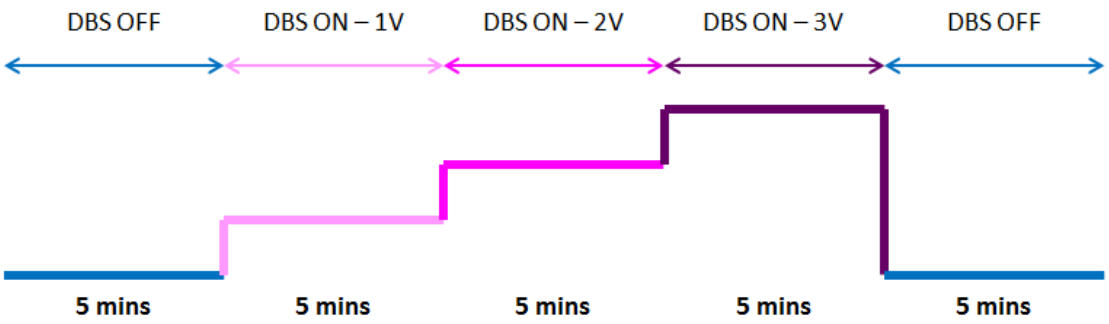

Figure 6.2 *– Graded protocol for muscle sympathetic nerve activity experiment in the periaqueductal grey patient with undetermined therapeutic parameters. The raised lines indicate the amplitude of the deep brain stimulation (DBS) when it is switched on.*

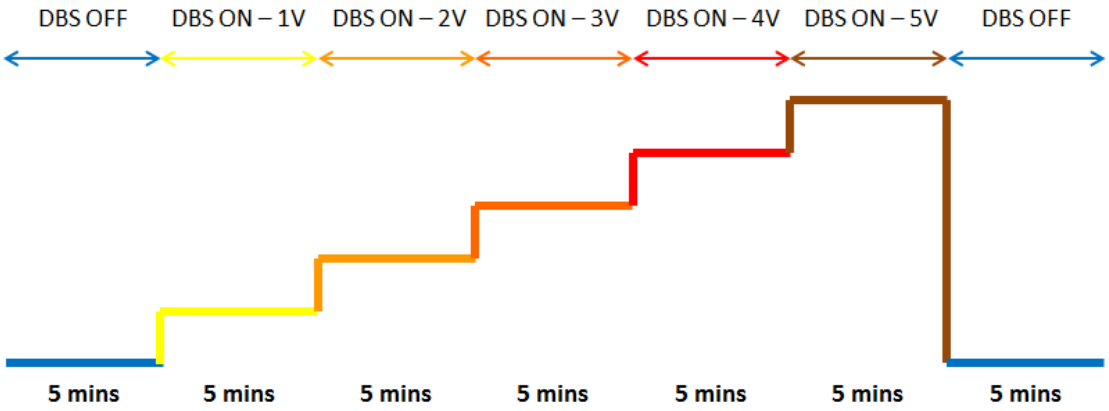

Figure 6.3 *– Graded protocol for muscle sympathetic nerve activity experiment in the sensory thalamus patient with undetermined therapeutic parameters. The raised lines indicate the amplitude of the deep brain stimulation (DBS) when it is switched on.*

Patients were asked to rate their levels of pain throughout the duration of the experiments using the Visual Analog Pain Severity Scale (VAPSS), in order to determine whether changes in MSNA could be due to the patient's pathology (for example, pain in PAG patients), as opposed to the neural responses to deep brain stimulation. Data segments in which the VAPSS score changed were excluded from analysis.

Results

As the results of this experiment were so variable, each patient is presented as a separate case study. I performed minute-by-minute analysis in each case, so that results could be compared and statistically analysed within each individual patient. Therefore, for patients performing the normal protocol, *n* = 15, as the stimulation was turned on for a total of 15 minutes and turned off for a total of 15 minutes. For the patients performing the graded protocol, *n* = 5, as each stimulation condition lasted 5 minutes. Fig. 6.4 shows the raw spectral data from one of the periaqueductal grey (PAG) patients, showing a five minute sample of the muscle sympathetic nerve activity recordings from each condition of the protocol.

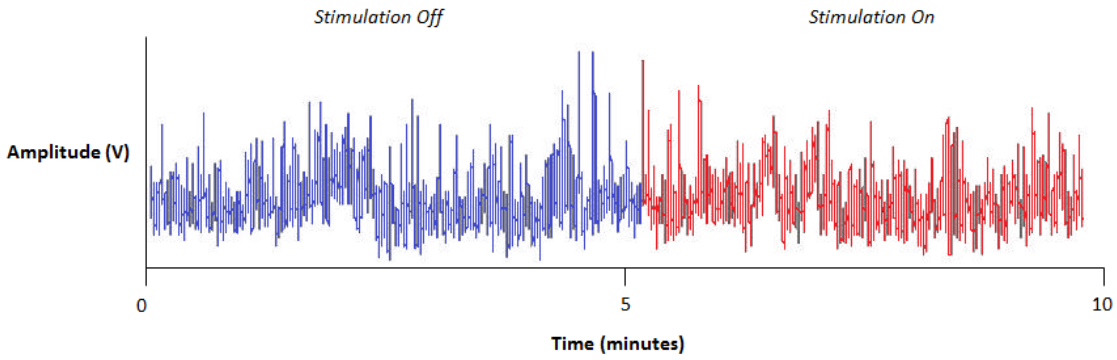

Figure 6.4 *– Raw data trace showing muscle sympathetic nerve activity recordings during each condition of the protocol from one of the periaqueductal grey patients.*

Periaqueductal Grey Stimulation

Case 1

In this patient, there was no significant change in mean arterial blood pressure (MABP) upon stimulation of the dorsal periaqueductal grey (PAG) (P = 0.361, *n* = 15) (Fig. 6.5A). Likewise, there were no significant changes in systolic blood pressure (SBP) or diastolic blood pressure (DBP) (P = 0.110 and P = 0.540, respectively; *n* = 15) (Figs. 6.5B-6.5C). However, there was a significant decrease in R-R interval of 0.035 ± 0.011 s when stimulation was turned on, equivalent to a 3.4% decrease (P = 0.003, *n* = 15) (Fig. 6.5D). The variability of these

cardiovascular parameters was also examined. It appears that stimulation of the dorsal PAG slightly decreased the variability of MABP, SBP and DBP, but increased the variability of R-R interval (Fig. 6.6). The relationship between the R-R interval and SBP can be used to determine cardiac baroreflex sensitivity; no significant change in cardiac baroreflex sensitivity could be detected upon stimulation of the dorsal PAG (P = 0.375, *n* = 15) (Fig. 6.7).

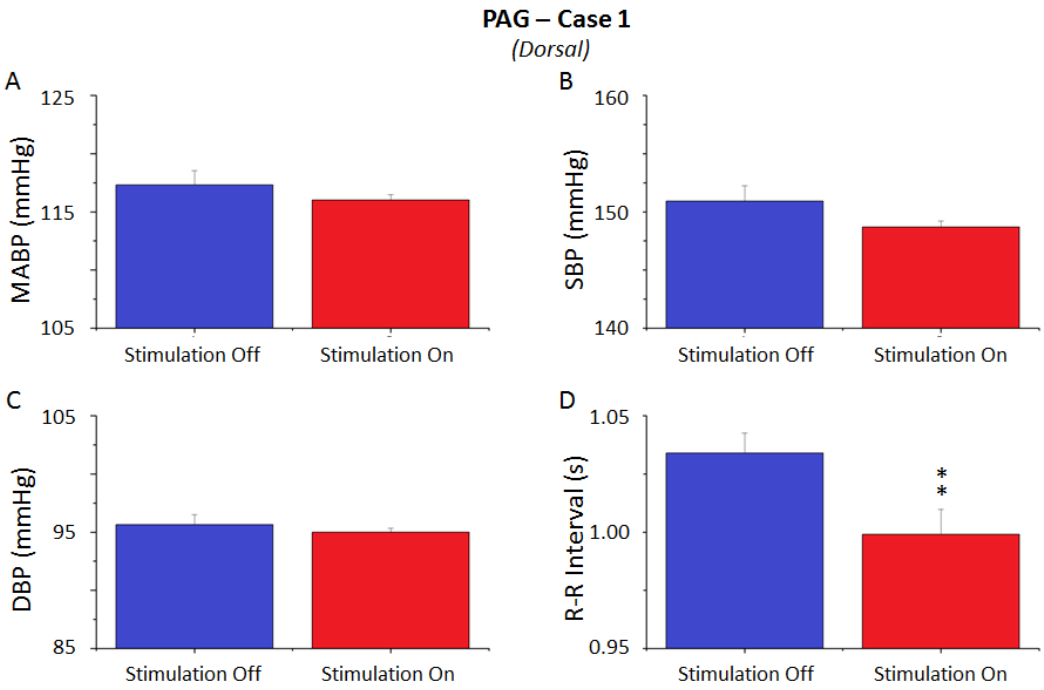

Figure 6.5 *– Graphs showing changes in cardiovascular parameters during stimulation of the dorsal periaqueductal grey (PAG) in the first PAG patient. There were no significant changes in (A) mean arterial blood pressure (MABP), (B) systolic blood pressure (SBP) or (C) diastolic blood pressure (DBP) during dorsal PAG stimulation. (D) There was a significant decrease in R-R interval (i.e. increase in heart rate) during dorsal PAG stimulation. n = 15, ** P < 0.01. Error bars represent standard error of the mean.*

Unfortunately, muscle sympathetic nerve activity could not be recorded from this patient as an appropriate recording site within the peroneal nerve could not be established.

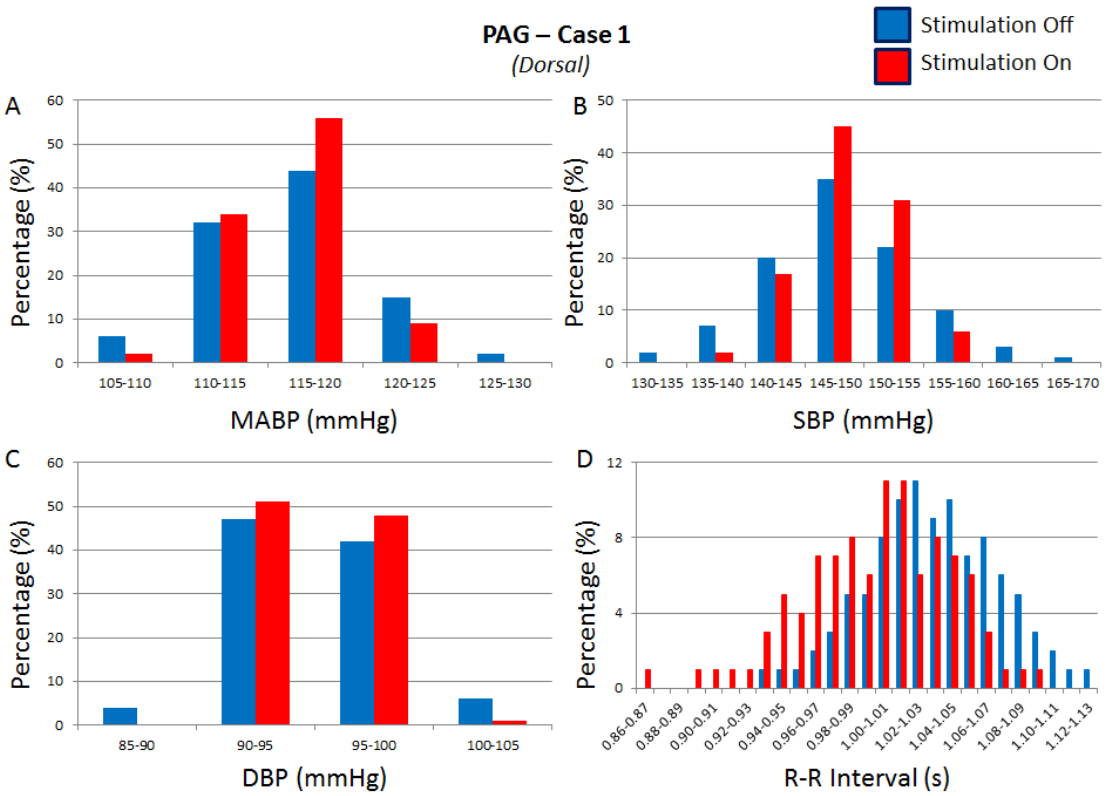

Figure 6.6 *– Graph showing the changes in variability of cardiovascular parameters during stimulation of the dorsal periaqueductal grey (PAG) in the first PAG patient. Stimulation appears to slightly decrease the variability of (A) mean arterial blood pressure (MABP), (B) systolic blood pressure (SBP) and (C) diastolic blood pressure (DBP). However, it appears to increase the variability of (D) the R-R interval.*

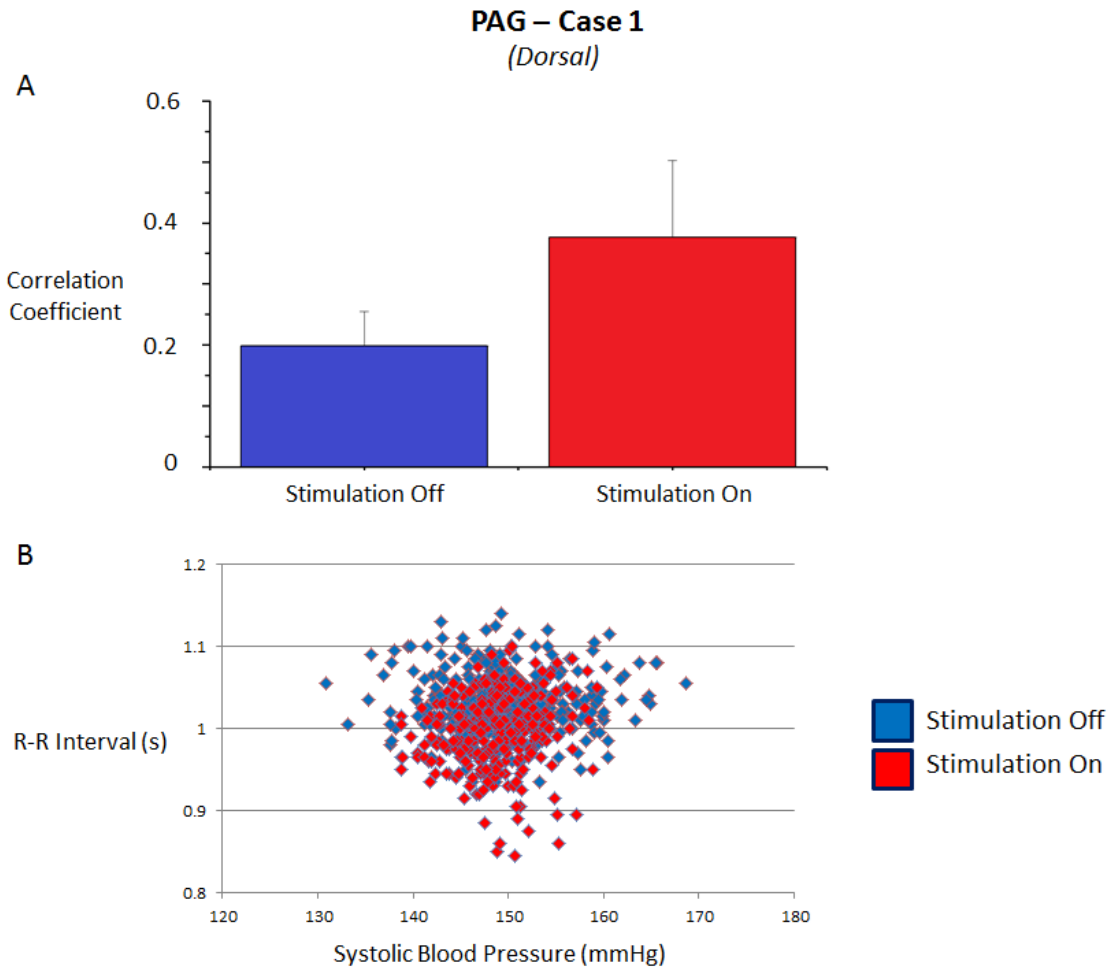

Figure 6.7 *– Graphs showing the changes in cardiac baroreflex sensitivity during stimulation of the dorsal periaqueductal grey (PAG) in the first PAG patient. (A) Graph showing no significant differences in the correlation between systolic blood pressure and R-R interval (indicative of cardiac baroreflex sensitivity) during dorsal PAG stimulation. (B) Scatter graph showing all the data points from the entire protocol. n = 15. Error bars represent standard error of the mean.*

Case 2

In the second dorsal periaqueductal grey (PAG) patient, there was no significant change in mean arterial blood pressure (MABP) upon stimulation (P = 0.088, *n* = 15) (Fig. 6.8A). Similarly, there were no significant changes in systolic blood pressure (SBP) or diastolic blood pressure (DBP) (P = 0.126 and P = 0.079, respectively; *n* = 15) (Figs 6.8B-6.8C). However, there was a significant decrease in R-R interval of 0.047 ± 0.019 s when stimulation was turned on, equivalent to a 5.7% decrease (P = 0.020, *n* = 15) (Fig. 6.8D), which is similar to *Case 1*. The

variability of these cardiovascular parameters was also examined. In this case, stimulation of the dorsal PAG appears to decrease the variability of MABP, SBP, DBP and R-R interval (Fig. 6.9). No significant change in cardiac baroreflex sensitivity could be detected upon dorsal PAG stimulation (P = 0.413, *n* = 15) (Fig. 6.10).

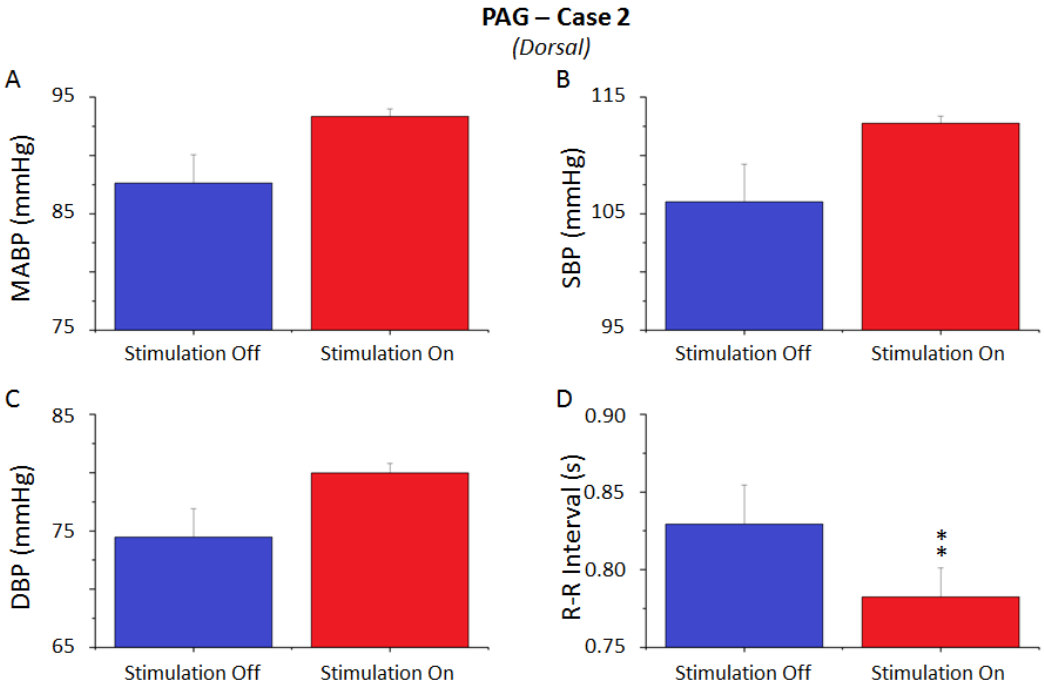

Figure 6.8 *– Graphs showing changes in cardiovascular parameters during stimulation of the dorsal periaqueductal grey (PAG) in the second PAG patient. There were no significant changes in (A) mean arterial blood pressure (MABP), (B) systolic blood pressure (SBP) or (C) diastolic blood pressure (DBP) during dorsal PAG stimulation. (D) There was a significant decrease in R-R interval (i.e. increase in heart rate) during dorsal PAG stimulation. n = 15, ** P < 0.01. Error bars represent standard error of the mean.*

In terms of muscle sympathetic nerve activity, burst incidence, burst amplitude, burst duration and burst latency were analysed. There was no significant difference in burst incidence upon stimulation of the dorsal PAG (P = 0.968, *n* = 15), nor in burst amplitude (P = 0.929, *n* = 15) or in burst duration (P = 0.434, *n* = 15) (Figs. 6.11A-6.11C). However, there was a significant difference in the latency period between each heart beat and its corresponding sympathetic burst – the burst latency decreased during dorsal PAG stimulation by 0.071 ± 0.083 s, an

equivalent of 5.5% (P = 0.048, *n* = 15) (Fig. 6.11D). The relationship between the burst amplitude and DBP can be used to determine vascular baroreflex sensitivity; no significant change in vascular baroreflex sensitivity could be detected upon stimulation of the dorsal PAG (P = 0.911, *n* = 15) (Fig. 6.12).

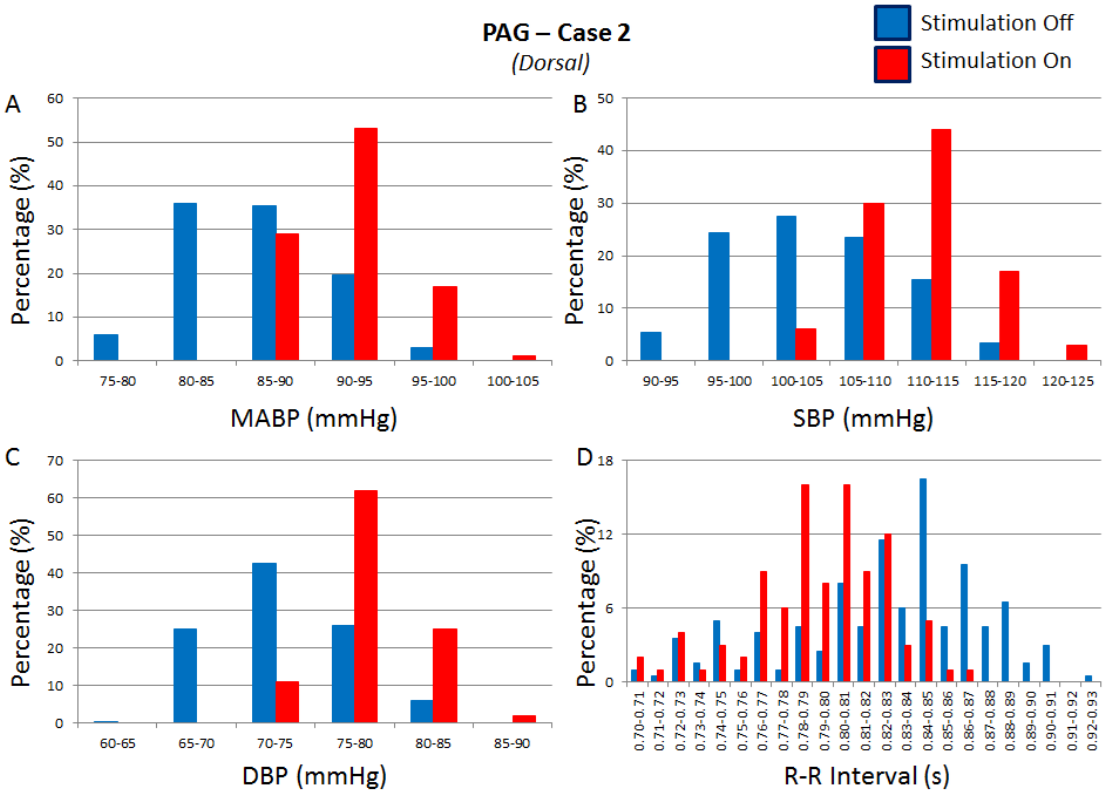

Figure 6.9 *– Graph showing the changes in variability of cardiovascular parameters during stimulation of the dorsal periaqueductal grey (PAG) in the second PAG patient. Stimulation appears to slightly decrease the variability of (A) mean arterial blood pressure (MABP), (B) systolic blood pressure (SBP), (C) diastolic blood pressure (DBP) and (D) the R-R interval.*

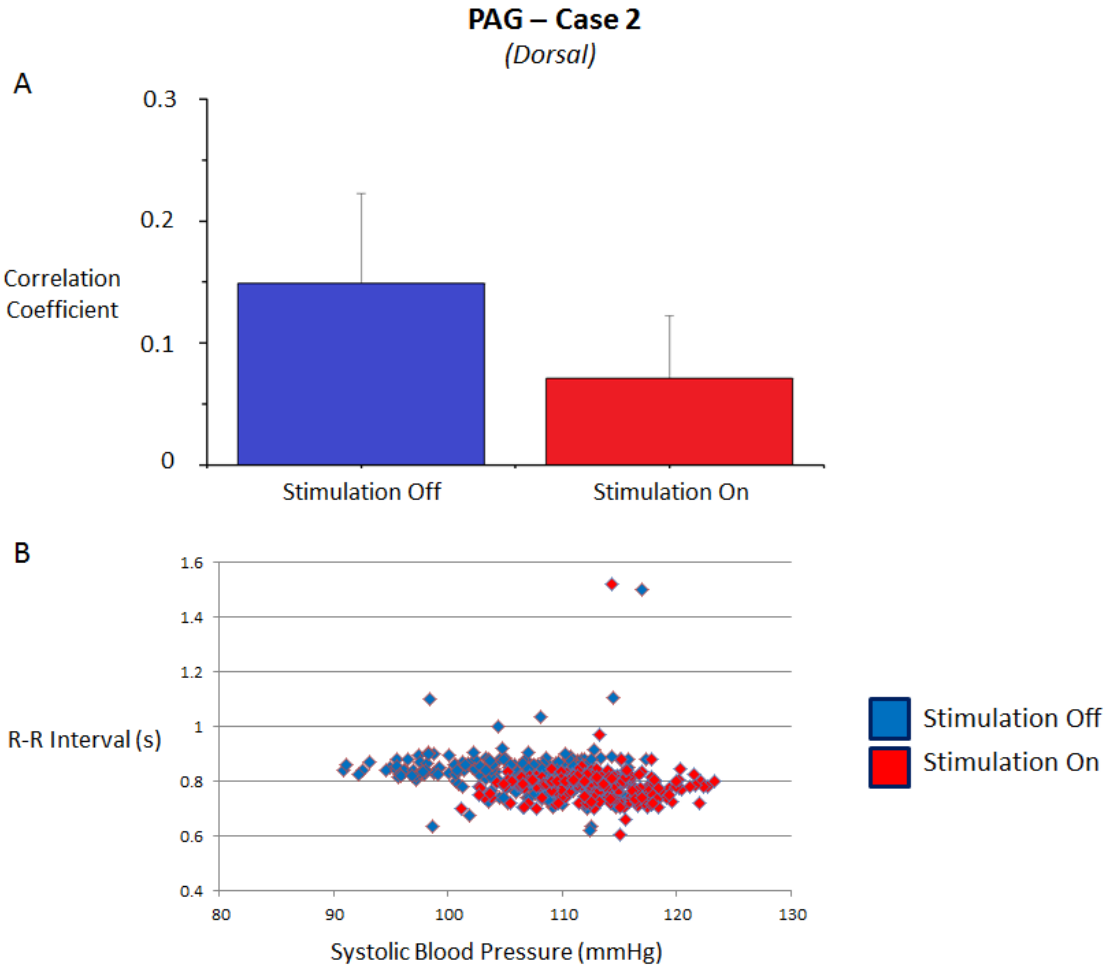

Figure 6.10 *– Graphs showing the changes in cardiac baroreflex sensitivity during stimulation of the dorsal periaqueductal grey (PAG) in the second PAG patient. (A) Graph showing no significant differences in the correlation between systolic blood pressure and R-R interval (indicative of cardiac baroreflex sensitivity) during dorsal PAG stimulation. (B) Scatter graph showing all the data points from the entire protocol. n =15. Error bars represent standard error of the mean.*

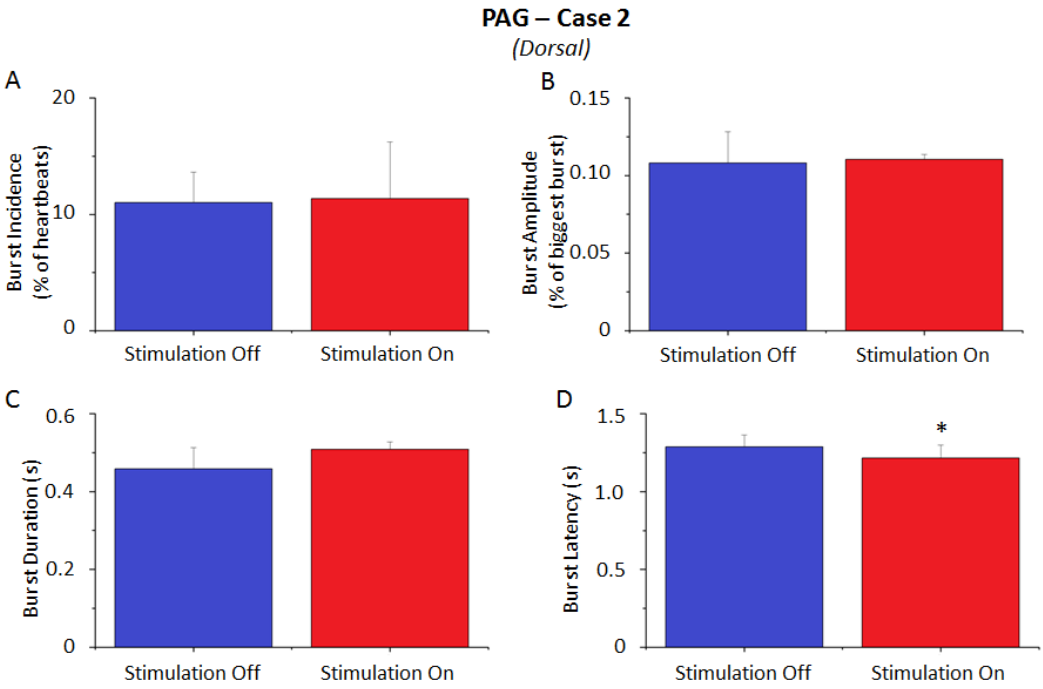

Figure 6.11 *– Graphs showing changes in muscle sympathetic nerve activity parameters during stimulation of the dorsal periaqueductal grey (PAG) in the second PAG patient. There were no significant changes in (A) burst incidence, (B) burst amplitude or (C) burst duration during dorsal PAG stimulation. (D) There was a significant decrease in burst latency during dorsal PAG stimulation. n = 15, * P < 0.05. Error bars represent standard error of the mean.*

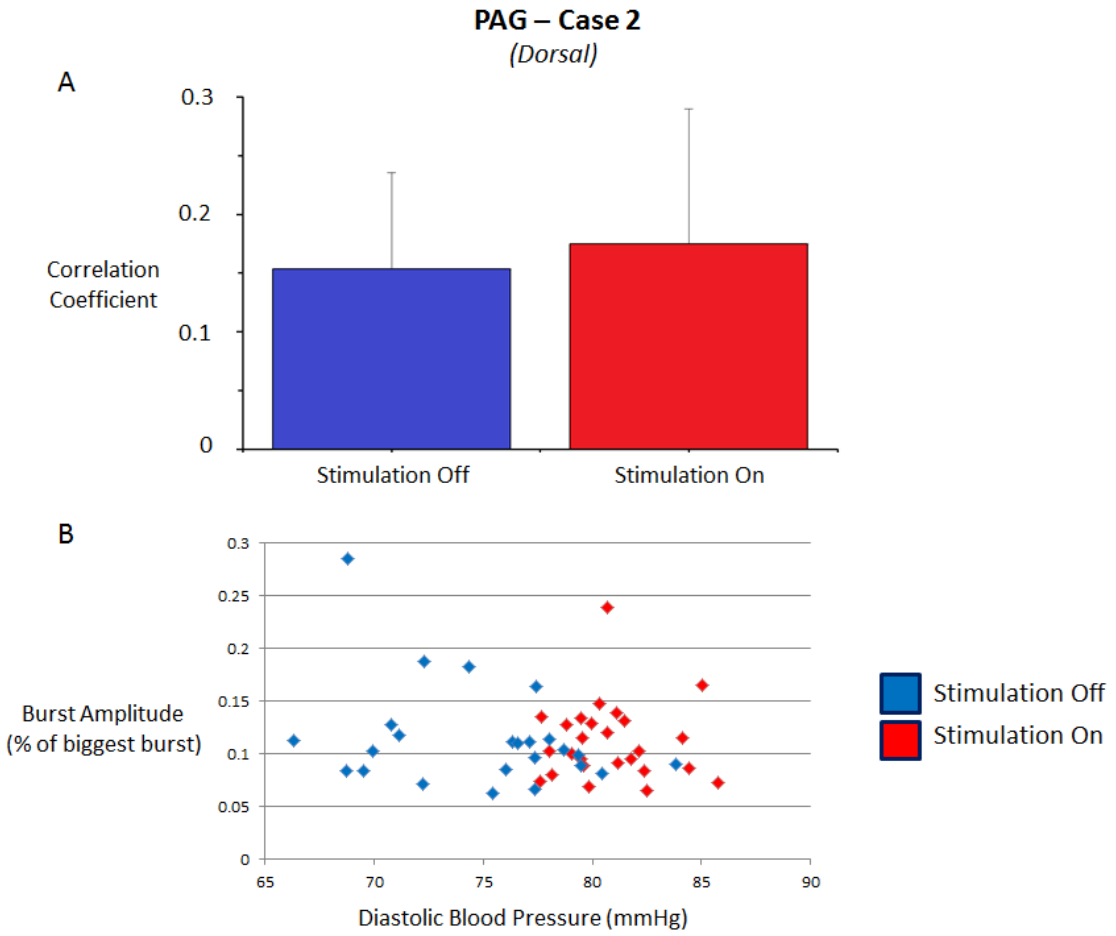

Figure 6.12 *– Graphs showing the changes in vascular baroreflex sensitivity during stimulation of the dorsal periaqueductal grey (PAG) in the second PAG patient. (A) Graph showing no significant differences in the correlation between diastolic blood pressure and burst amplitude (indicative of vascular baroreflex sensitivity) during dorsal PAG stimulation. (B) Scatter graph showing all the data points from the entire protocol. n = 15. Error bars represent standard error of the mean.*

Case 3

In the third periaqueductal grey (PAG) patient, the electrode was positioned in the ventral region. There was no significant change in mean arterial blood pressure (MABP) upon stimulation (P = 0.199, *n* = 15) (Fig. 6.13A). However, there was a significant decrease in systolic blood pressure (SBP) of 2.0 ± 0.5 mmHg during ventral PAG stimulation, equivalent to a decrease of 1.6% (P = 0.005, *n* = 15) (Fig. 6.13B). There was no significant change in diastolic blood pressure (DBP) during stimulation (P = 0.486, *n* = 15) (Fig. 6.13C), and no change in R-R

interval (P = 0.214, *n* = 15) (Fig. 6.13D). The variability of these cardiovascular parameters was also examined. In this case, stimulation of the ventral PAG appears to have little effect on the variability of MABP and the R-R interval, but slightly increases the variability of SBP and DBP (Fig. 6.14). No significant change in cardiac baroreflex sensitivity could be detected upon ventral PAG stimulation (P = 0.156, *n* = 15) (Fig. 6.15).

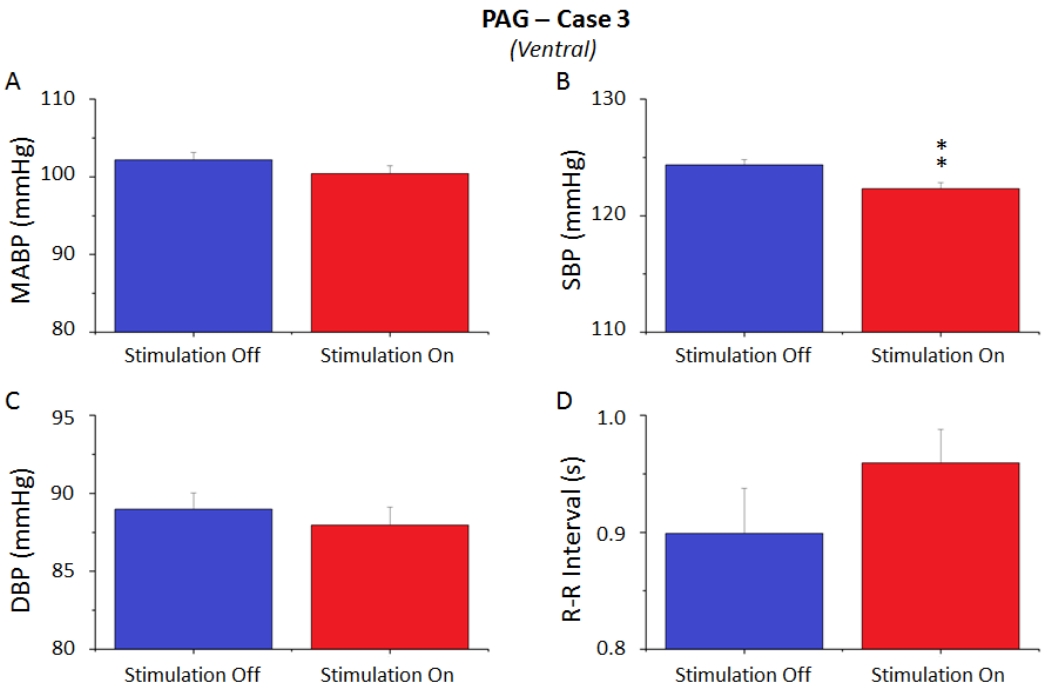

Figure 6.13 *– Graphs showing changes in cardiovascular parameters during stimulation of the ventral periaqueductal grey (PAG) in the third PAG patient. (A) There were no significant changes in mean arterial blood pressure (MABP) during ventral PAG stimulation. (B) There was a significant decrease in systolic blood pressure (SBP) during ventral PAG stimulation. There were no significant changes in (C) diastolic blood pressure (DBP) or (D) R-R interval during ventral PAG stimulation. n = 15, ** P < 0.01. Error bars represent standard error of the mean.*

Unfortunately, muscle sympathetic nerve activity could not be recorded from this patient as an appropriate recording site within the peroneal nerve could not be established.

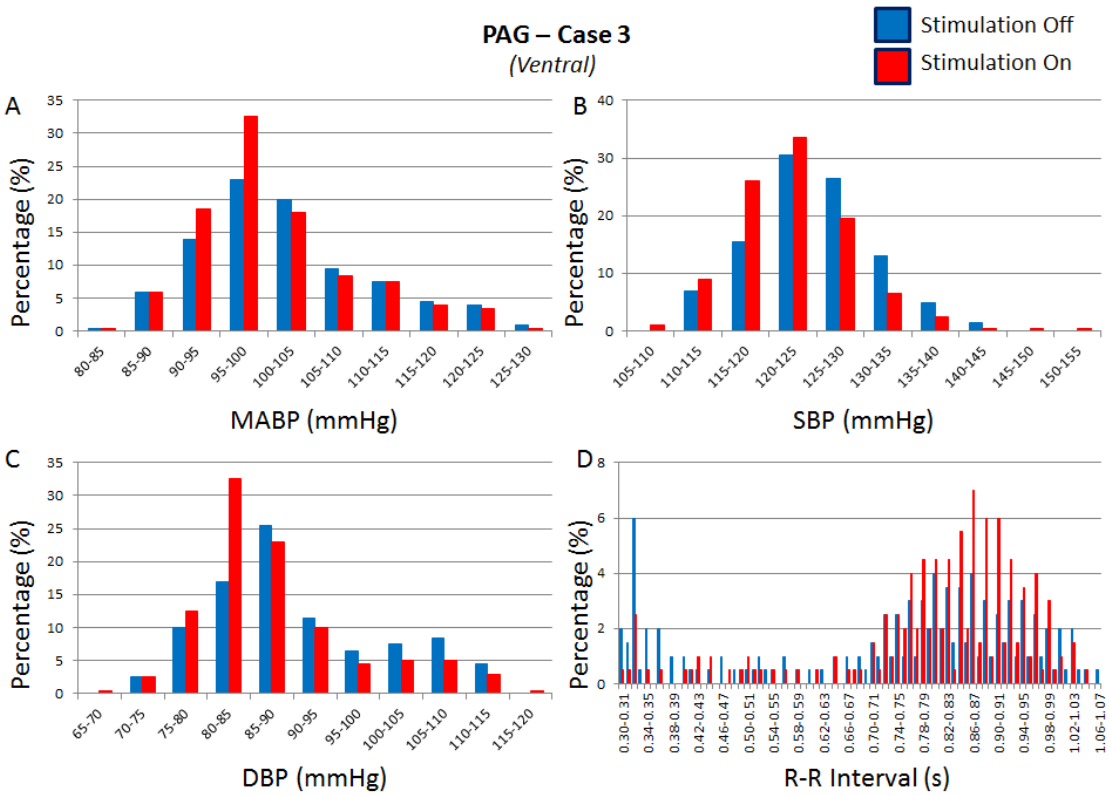

Figure 6.14 *– Graph showing the changes in variability of cardiovascular parameters during stimulation of the ventral periaqueductal grey (PAG) in the third PAG patient. (A) Stimulation appears to have little effect on mean arterial blood pressure (MABP). (B) Stimulation appears to slightly increase the variability of (B) systolic blood pressure (SBP) and (C) diastolic blood pressure (DBP). (D) Stimulation appears to have little effect on the R-R interval.*

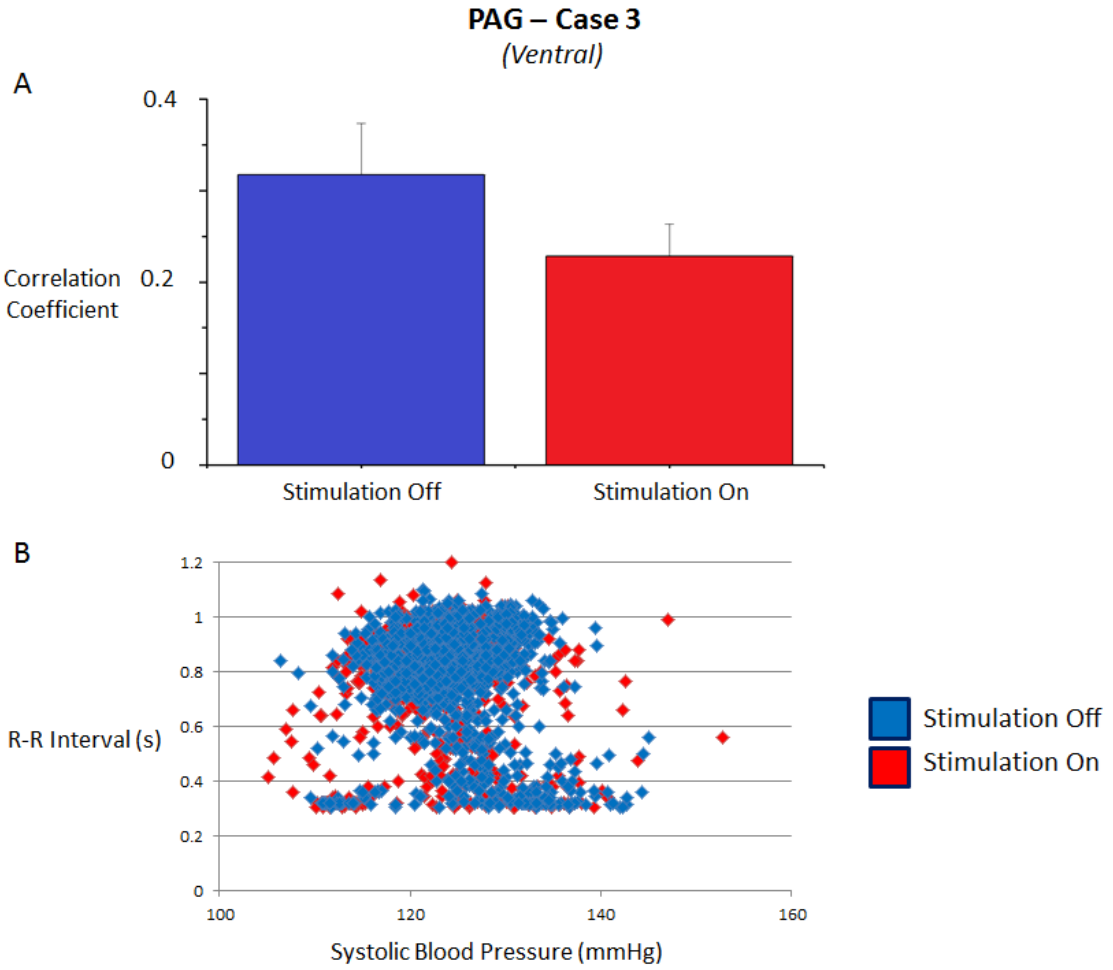

Figure 6.15 *– Graphs showing the changes in cardiac baroreflex sensitivity during stimulation of the ventral periaqueductal grey (PAG) in the third PAG patient. (A) Graph showing no significant differences in the correlation between systolic blood pressure and R-R interval (indicative of cardiac baroreflex sensitivity) during ventral PAG stimulation. (B) Scatter graph showing all the data points from the entire protocol. n = 5. Error bars represent standard error of the mean.*

Case 4

In this periaqueductal grey (PAG) case, the most therapeutically beneficial stimulation settings had not yet been established. Therefore, the patient underwent the graded protocol. The electrode was situated in the ventral area of the PAG. There was a significant decrease in mean arterial blood pressure (MABP) during 2 V ventral PAG stimulation of 5.0 ± 0.5 mmHg, equivalent to a decrease of 5.1%, compared to no stimulation (P = 0.002, *n* = 5) (Fig. 6.16A). However, there were no significant differences during 1 V stimulation (P = 0.730, *n* = 5) and 3

V stimulation (P = 0.661, *n* = 5). There were significant decreases in systolic blood pressure (SBP) during 2 V ventral PAG stimulation of 18.3 ± 2.0 mmHg (equivalent to a decrease of 12.7%) and during 3 V ventral PAG stimulation of 4.8 ± 1.5 mmHg (equivalent to a decrease of 3.3%) (P = 0.006 and P = 0.016, respectively; *n* = 5) (Fig. 6.16B). There were no significant differences during 1 V stimulation (P = 0.416, *n* = 5). There were no significant changes in diastolic blood pressure (DBP) throughout the protocol (Fig. 6.16C). In terms of the R-R interval, there was a significant decrease of 0.019 ± 0.007 s during 1 V ventral PAG stimulation compared to no stimulation, equivalent to a decrease of 2.6% (P = 0.016, *n* = 5) (Fig. 6.16D). There were no significant differences during 2 V stimulation (P = 0.863, *n* = 5) and 3 V stimulation (P = 0.052, *n* = 5).

The variability of these cardiovascular parameters was also examined. In this case, ventral PAG stimulation appears to increase the variability of MABP, SBP and the R-R interval (Figs. 6.17-6.18). DBP variability also appears to be increased by 1 V and 2 V stimulation, but not by 3 V stimulation (Fig. 6.18). There was also a significant increase in cardiac baroreflex sensitivity during 1 V ventral PAG stimulation – the correlation coefficient rose by 0.185 ± 0.051 (P = 0.007, *n* = 5). There was no significant change in cardiac baroreflex sensitivity during 2 V stimulation (P = 0.655, *n* = 5) and 3 V stimulation (P = 0.243, *n* = 5) (Fig. 6.19).

Unfortunately, muscle sympathetic nerve activity could not be recorded from this patient as an appropriate recording site could not be established due to the patient's phobia of needles.

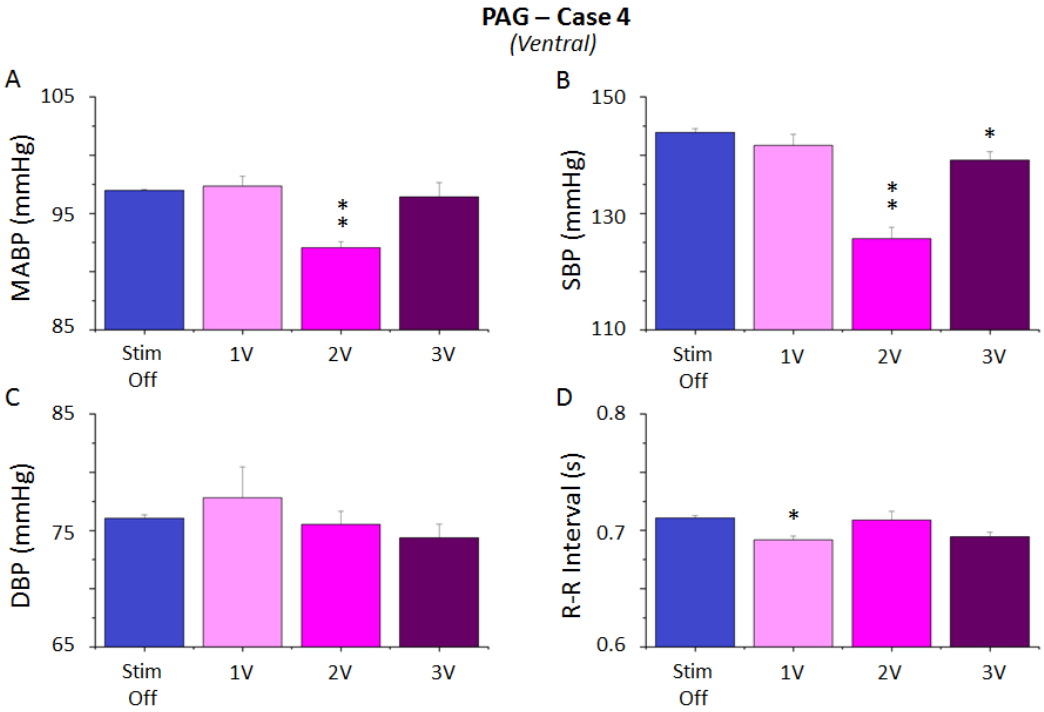

Figure 6.16 *– Graphs showing changes in cardiovascular parameters during stimulation of the ventral periaqueductal grey (PAG) in the fourth PAG patient, who followed the graded protocol. There was a significant decrease in (A) mean arterial blood pressure (MABP) during 2 V ventral PAG stimulation and in (B) systolic blood pressure (SBP) during 2 V ventral PAG stimulation and 3 V ventral PAG stimulation. (C) There were no significant changes in diastolic blood pressure (DBP) during stimulation of any amplitude. (D) There was a significant decrease in R-R interval during 1 V ventral PAG stimulation. n = 5, * P < 0.05, ** P < 0.01. Error bars represent standard error of the mean.*

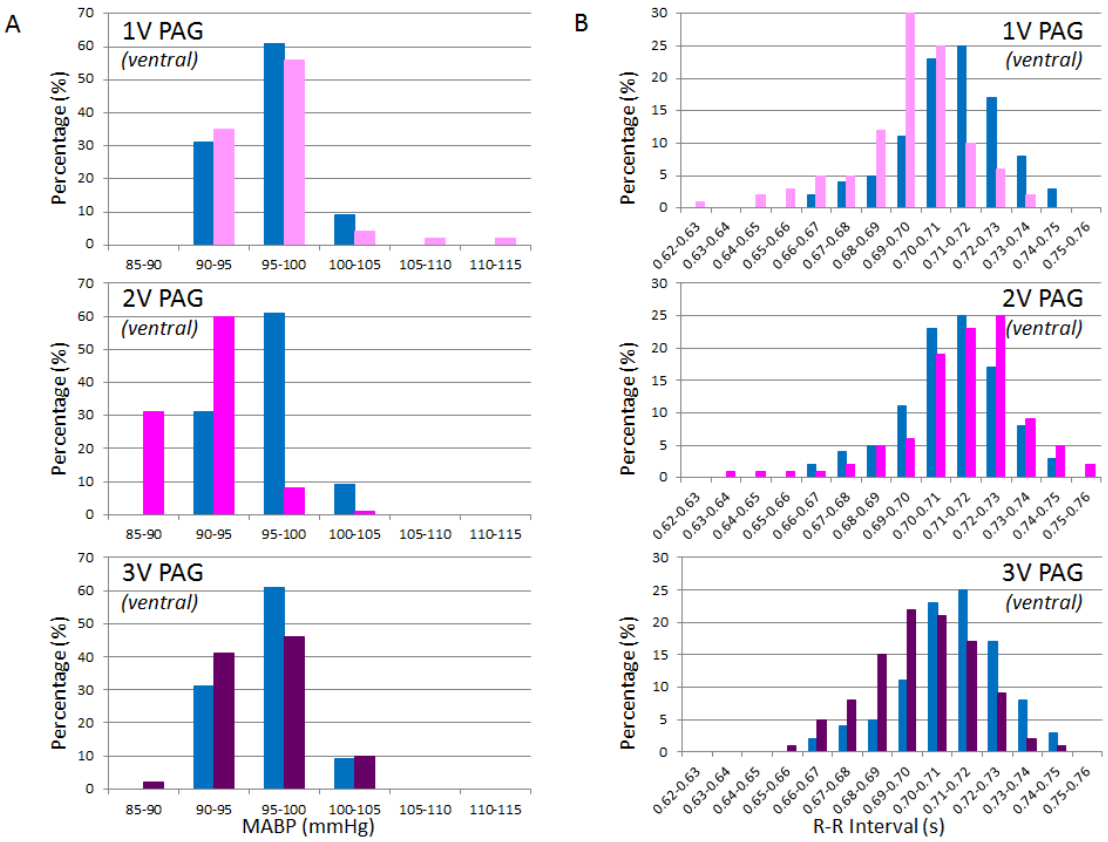

Figure 6.17 *– Graph showing the changes in variability of cardiovascular parameters during stimulation of the ventral periaqueductal grey (PAG) in the fourth PAG patient, who followed the graded protocol. Stimulation appears to increase the variability of (A) mean arterial blood pressure (MABP) and (B) the R-R interval.*

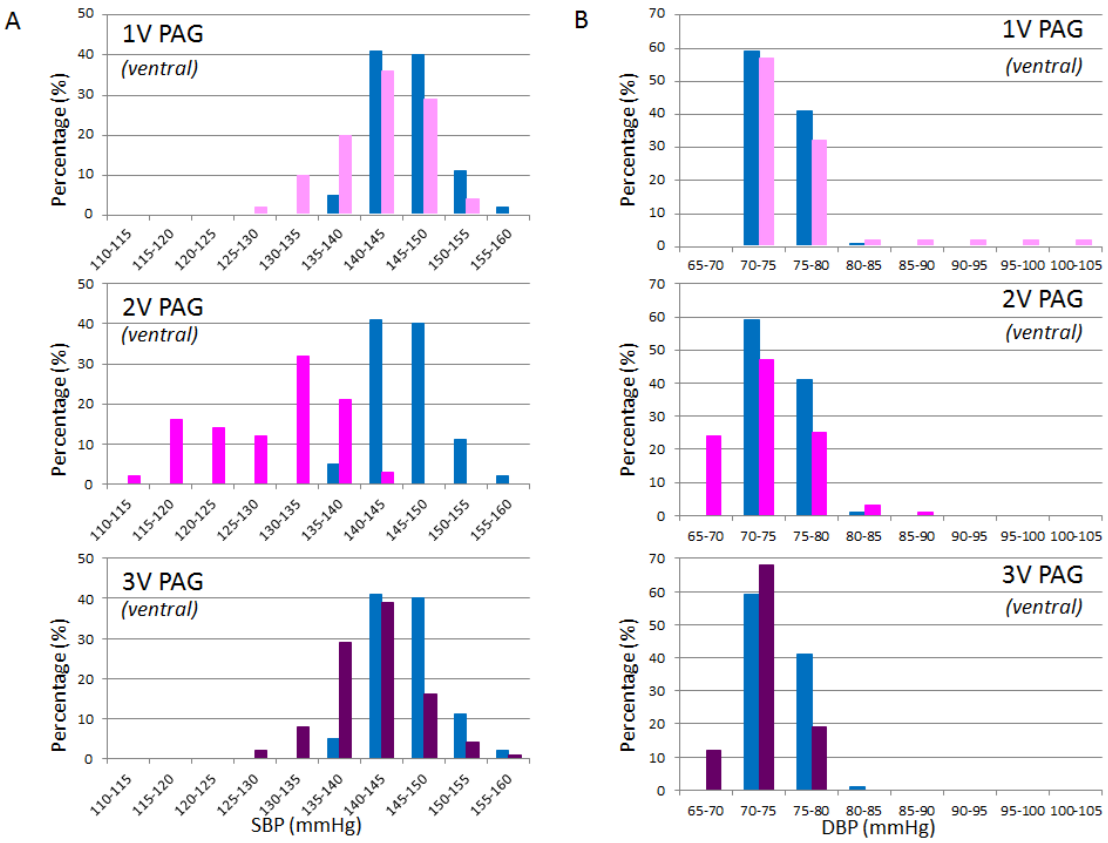

Figure 6.18 *– Graph showing the changes in variability of cardiovascular parameters during stimulation of the ventral periaqueductal grey (PAG) in the fourth PAG patient, who followed the graded protocol. Stimulation appears to increase the variability of (A) systolic blood pressure (SBP) during ventral PAG stimulation at any amplitude, and (B) diastolic blood pressure (DBP) during 1 V ventral PAG stimulation and 2 V ventral PAG stimulation.*

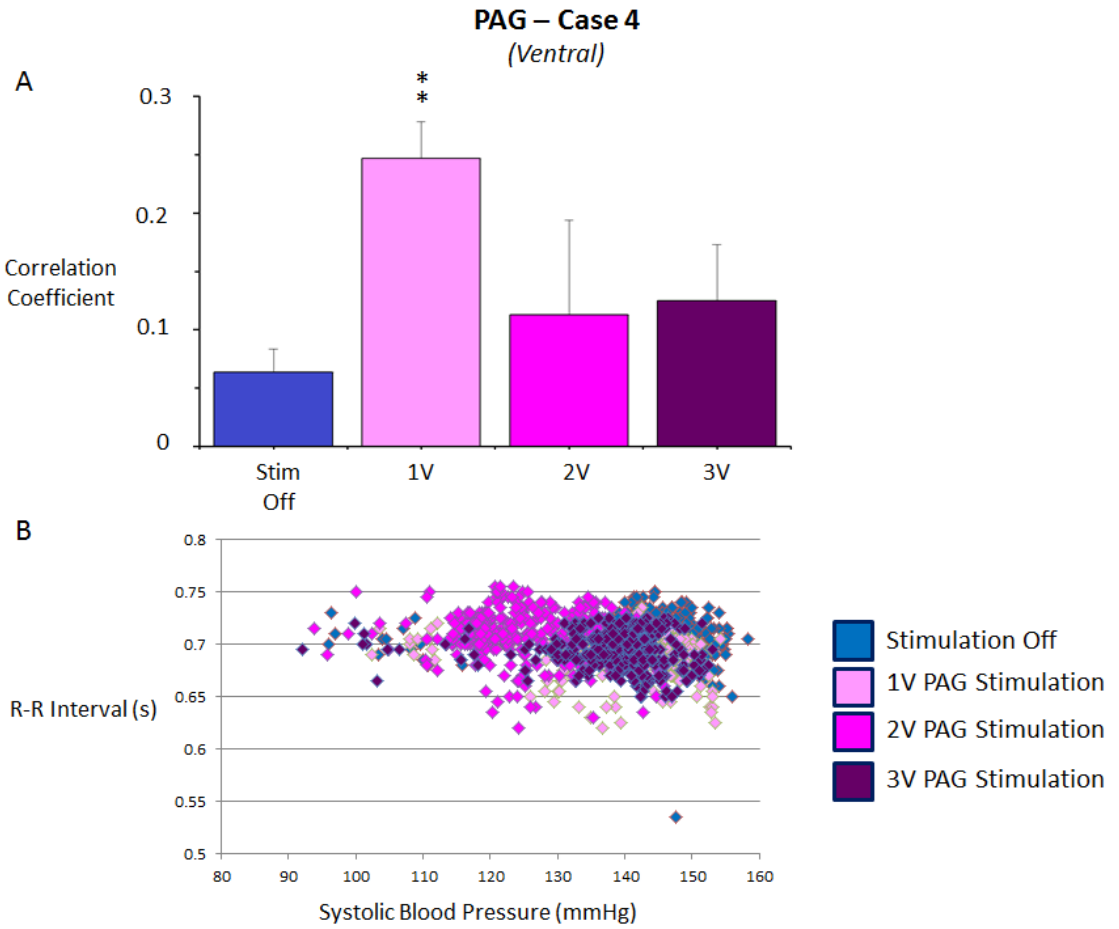

Figure 6.19 *– Graphs showing the changes in cardiac baroreflex sensitivity during stimulation of the ventral periaqueductal grey (PAG) in the fourth PAG patient, who followed the graded protocol. (A) Graph showing a significant increase in the correlation between systolic blood pressure and R-R interval (indicative of cardiac baroreflex sensitivity) during 1 V ventral PAG stimulation. (B) Scatter graph showing all the data points from the entire protocol. n = 5, ** P < 0.01. Error bars represent standard error of the mean.*

Subthalamic Nucleus Stimulation

Case 1

In the first subthalamic nucleus (STN) patient, mean arterial blood pressure (MABP) decreased significantly during stimulation by 19.5 ± 1.7 mmHg, which is equivalent to a decrease of 13.4% (P = 0.005, *n* = 15) (Fig. 6.20A). Likewise, systolic blood pressure (SBP) decreased significantly during stimulation by 27.1 ± 2.6 mmHg, which is equivalent to a decrease of 13.7% (P = 0.012, *n* = 15), and diastolic blood pressure (DBP) decreased significantly by 14.0 ±

1.5 mmHg, which is equivalent to a decrease of 12.1% (P = 0.006, *n* = 15) (Figs. 6.20B-6.20C). There was a significant increase in R-R interval during STN stimulation of 0.094 ± 0.024 s, which is equivalent to an increase of 13.5% (P = 0.004, *n* = 15) (Fig. 6.20D). The variability of these cardiovascular parameters was also examined. It appears that stimulation of the STN slightly increases the variability of MABP and DBP, but has little effect on SBP (Figs. 6.21A-6.21C). STN stimulation also significantly increases the variability of the R-R interval (Fig. 6.21D). No significant change in cardiac baroreflex sensitivity could be detected upon STN stimulation (P = 0.707, *n* = 15) (Fig. 6.22).

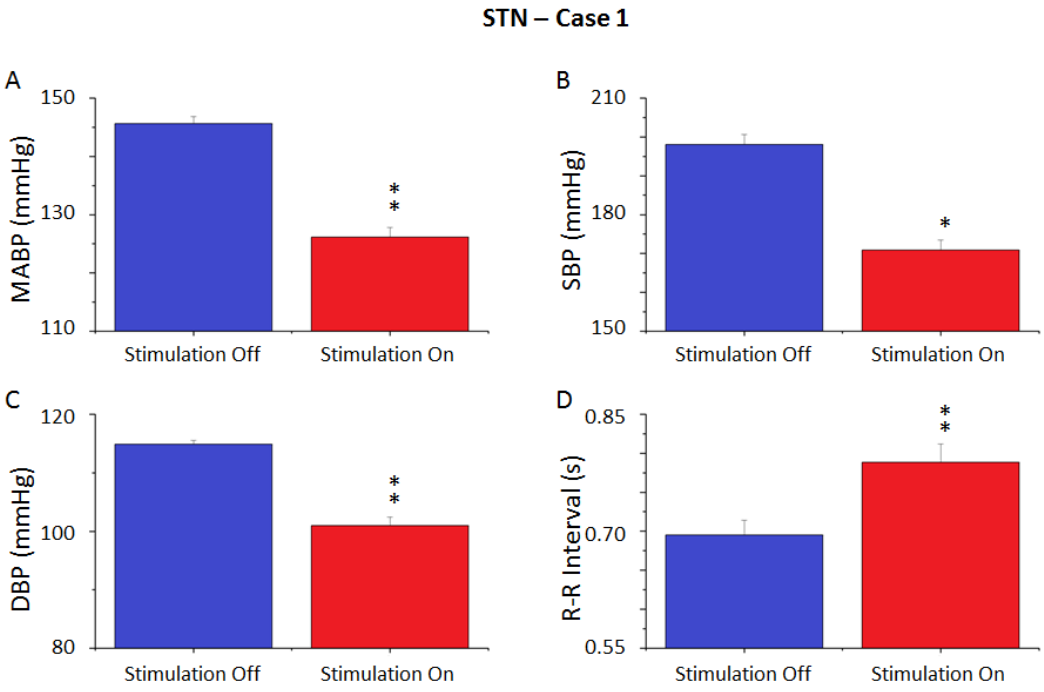

Figure 6.20 *– Graphs showing changes in cardiovascular parameters during stimulation of the subthalamic nucleus (STN) in the first STN patient. There was a significant decrease in (A) mean arterial blood pressure (MABP), (B) systolic blood pressure (SBP) and (C) diastolic blood pressure (DBP) during STN stimulation. (D) There was a significant increase in R-R interval (i.e. decrease in heart rate) during STN stimulation. n = 15, * P < 0.05, ** P < 0.01. Error bars represent standard error of the mean.*

In terms of muscle sympathetic nerve activity, there were no significant differences upon STN stimulation in burst incidence (P = 0.409, *n* = 15), burst amplitude (P = 0.067, *n* = 15), burst

duration (P = 0.259, *n* = 15) or burst latency (P = 0.106, *n* = 15) (Fig. 6.23). No significant change in vascular baroreflex sensitivity could be detected during stimulation of the STN (P = 0.290, *n* = 15) (Fig. 6.24).

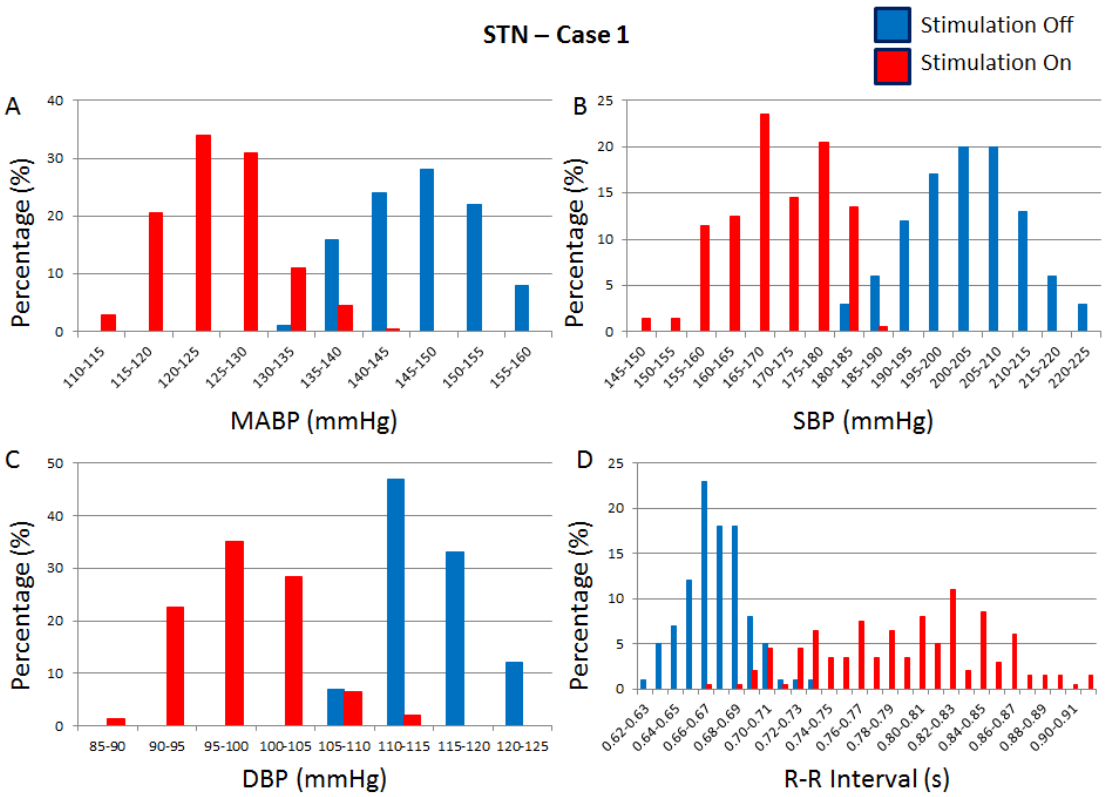

Figure 6.21 *– Graph showing the changes in variability of cardiovascular parameters during stimulation of the subthalamic nucleus (STN) in the first STN patient. (A) Stimulation appears to slightly increase the variability of mean arterial blood pressure (MABP). (B) Stimulation appears to have little effect on the variability of systolic blood pressure (SBP). Stimulation also appears to increase the variability of (C) diastolic blood pressure (DBP) and (D) the R-R interval.*

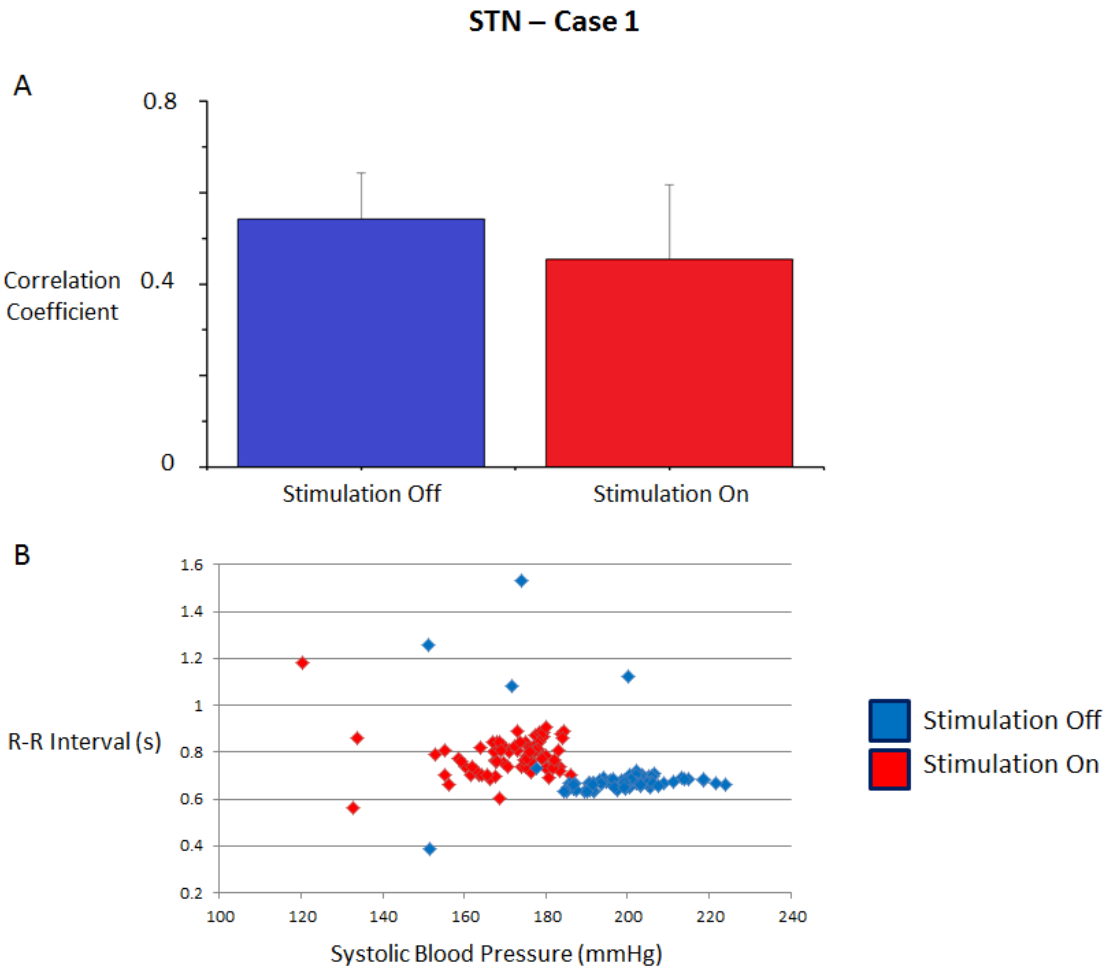

Figure 6.22 *– Graphs showing the changes in cardiac baroreflex sensitivity during stimulation of the subthalamic nucleus (STN) in the first STN patient. (A) Graph showing no significant differences in the correlation between systolic blood pressure and R-R interval (indicative of cardiac baroreflex sensitivity) during STN stimulation. (B) Scatter graph showing all the data points from the entire protocol. n = 15. Error bars represent standard error of the mean.*

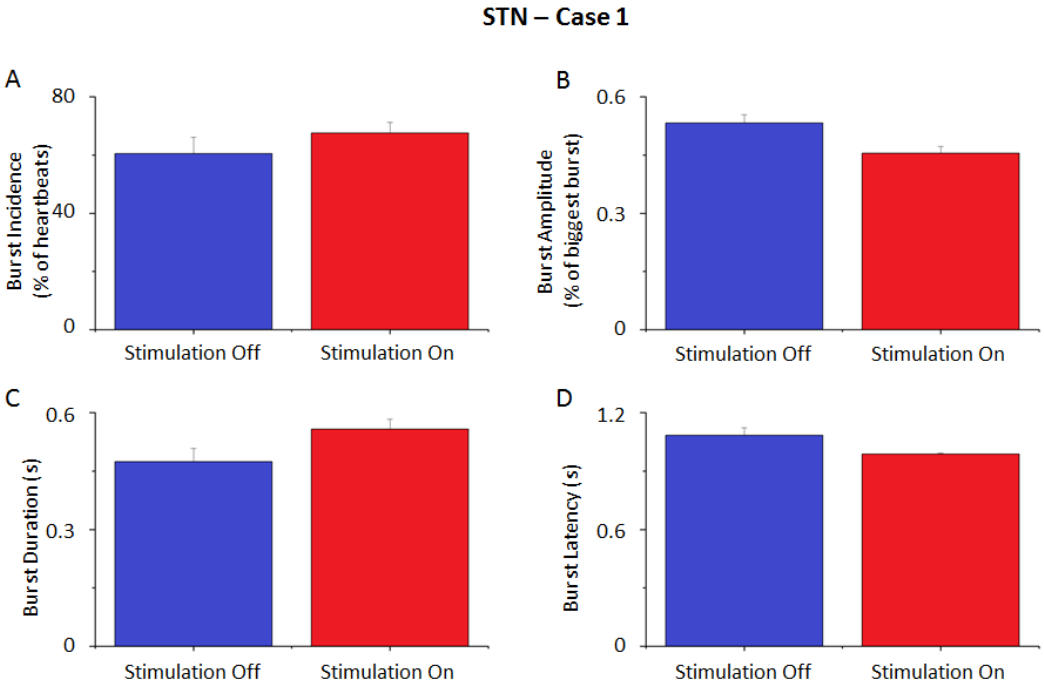

Figure 6.23 *– Graphs showing changes in muscle sympathetic nerve activity parameters during stimulation of the subthalamic nucleus (STN) in the first STN patient. There were no significant changes in (A) burst incidence, (B) burst amplitude, (C) burst duration or (D) burst latency during STN stimulation. n = 15. Error bars represent standard error of the mean.*

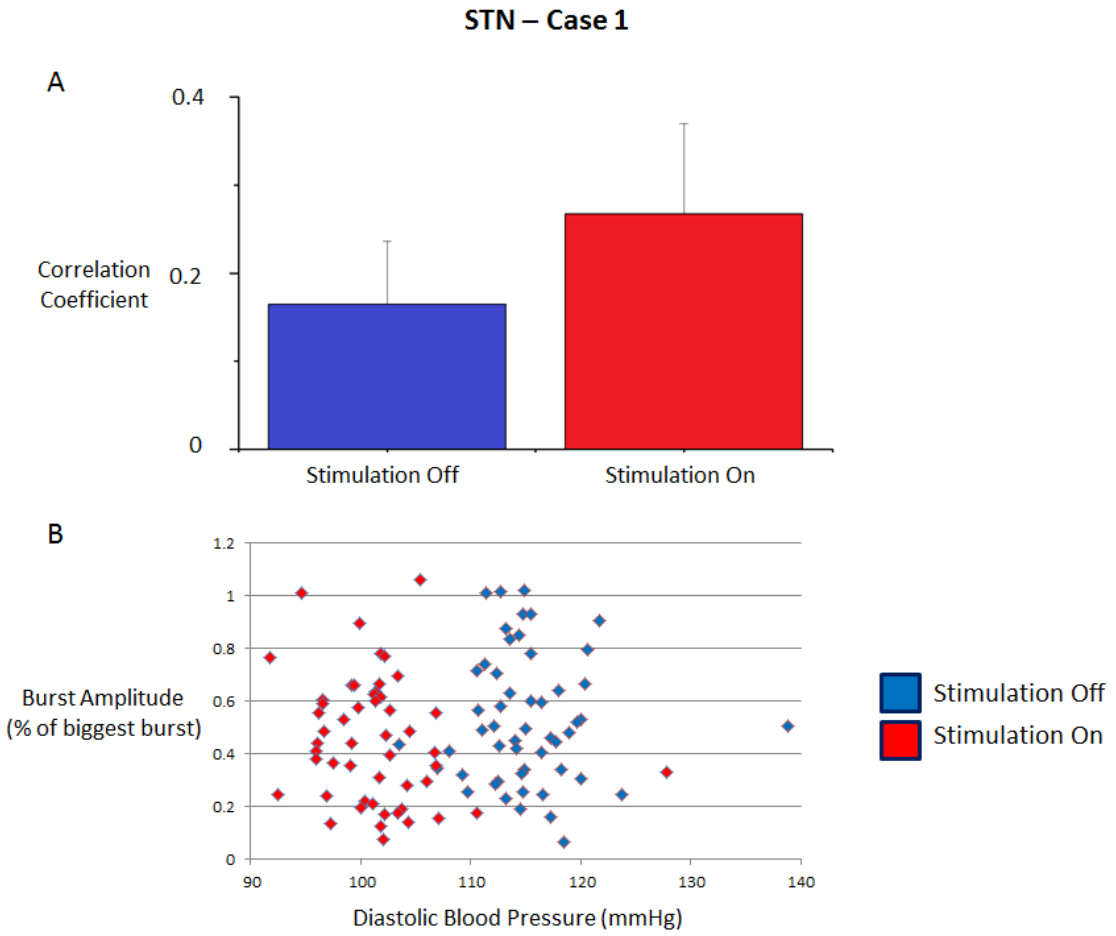

Figure 6.24 *– Graphs showing the changes in vascular baroreflex sensitivity during stimulation of the subthalamic nucleus (STN) in the first STN patient. (A) Graph showing no significant differences in the correlation between diastolic blood pressure and burst amplitude (indicative of vascular baroreflex sensitivity) during STN stimulation. (B) Scatter graph showing all the data points from the entire protocol. n = 15. Error bars represent standard error of the mean.*

Case 2

In the second subthalamic nucleus (STN) patient, there was no significant change in mean arterial blood pressure (MABP) during stimulation (P = 0.370, *n* = 15) (Fig. 6.25A). Similarly, systolic blood pressure (SBP) and diastolic blood pressure (DBP) also remained unchanged during STN stimulation (P = 0.115 and P = 0.504, respectively; *n* = 15) (Figs. 6.25B-6.25C). There was no significant change in R-R interval upon STN stimulation either (P = 0.748, *n* = 15) (Fig. 6.25D). The variability of these cardiovascular parameters was also examined. It appears that stimulation of the STN very slightly increases the variability of MABP, SBP, DBP and the R-R

interval (Fig. 6.26). No significant change in cardiac baroreflex sensitivity could be detected upon STN stimulation (P = 0.463, *n* = 15) (Fig. 6.27).

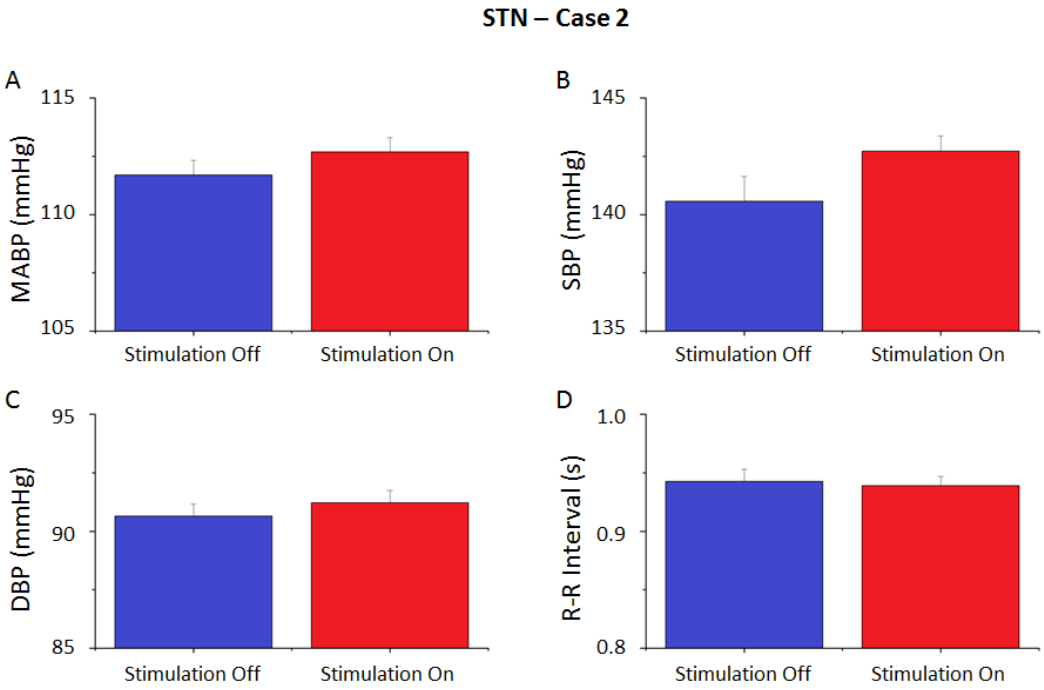

Figure 6.25 *– Graphs showing changes in cardiovascular parameters during stimulation of the subthalamic nucleus (STN) in the second STN patient. There were no significant changes in (A) mean arterial blood pressure (MABP), (B) systolic blood pressure (SBP), (C) diastolic blood pressure (DBP) or (D) R-R interval during STN stimulation. n = 15. Error bars represent standard error of the mean.*

In terms of muscle sympathetic nerve activity, there was a significant increase in burst incidence during STN stimulation – at rest, 62 ± 3% of heartbeats were associated with a sympathetic burst, whereas during stimulation, 74 ± 3% of heartbeats were associated with a burst (P = 0.002, *n* = 15) (Fig. 6.28A). There were no significant differences upon STN stimulation in burst amplitude (P = 0.224, *n* = 15), burst duration (P = 0.107, *n* = 15) or burst latency (P = 0.178, *n* = 15) (Figs. 6.28B-6.28D). No significant change in vascular baroreflex sensitivity could be detected during stimulation of the STN (P = 0.998, *n* = 15) (Fig. 6.29).

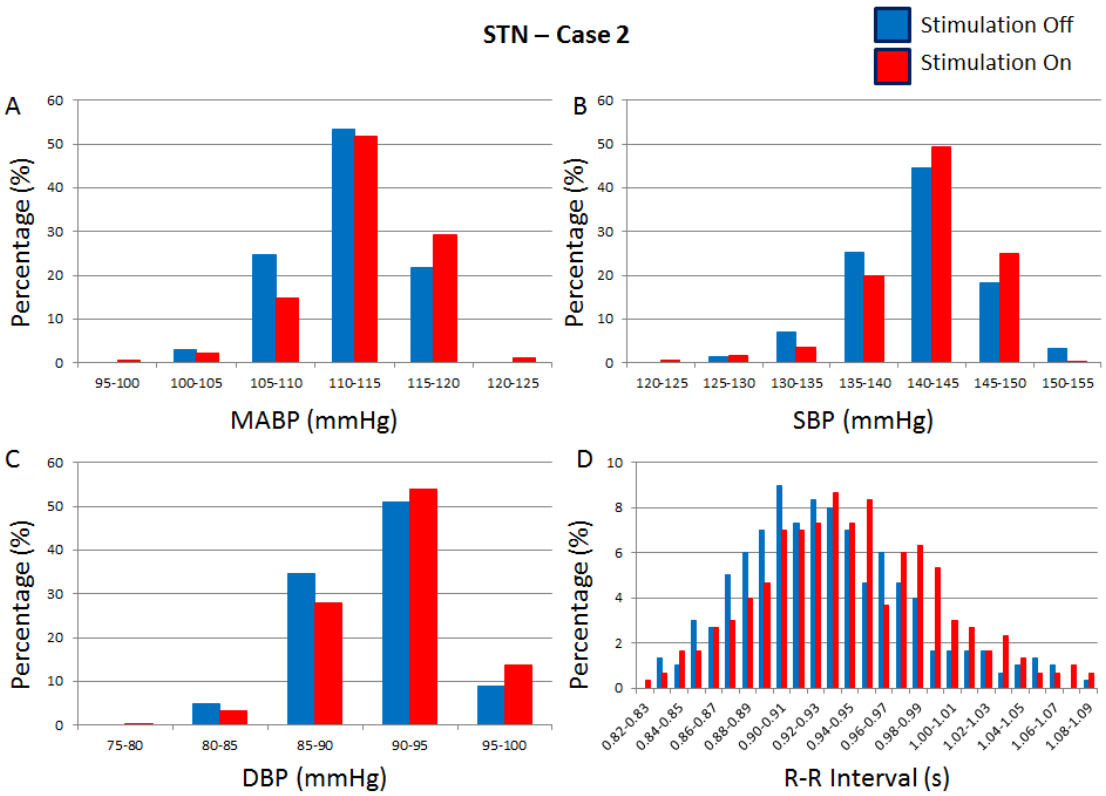

Figure 6.26 *– Graph showing the changes in variability of cardiovascular parameters during stimulation of the subthalamic nucleus (STN) in the second STN patient. Stimulation appears to very slightly increase the variability of (A) mean arterial blood pressure (MABP), (B) systolic blood pressure (SBP), (C) diastolic blood pressure (DBP) and (D) the R-R interval.*

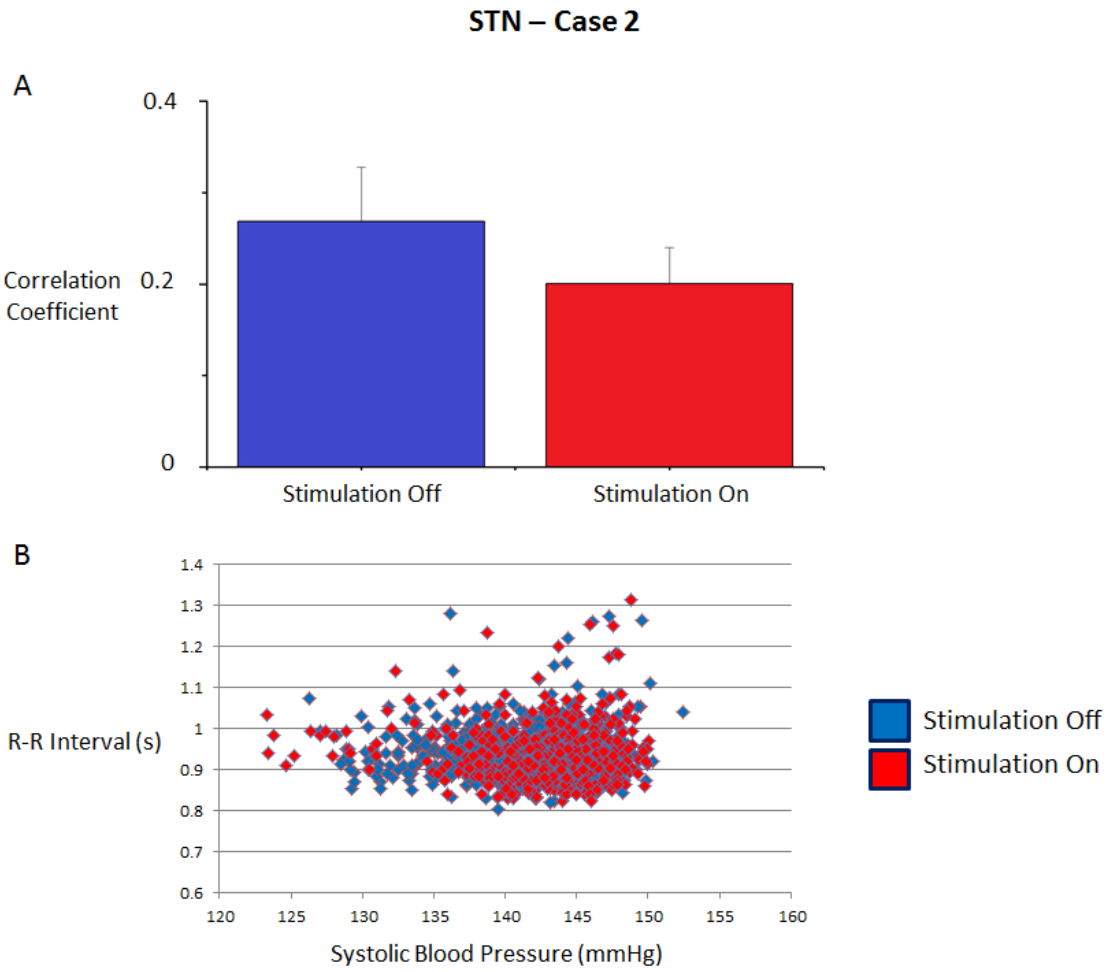

Figure 6.27 *– Graphs showing the changes in cardiac baroreflex sensitivity during stimulation of the subthalamic nucleus (STN) in the second STN patient. (A) Graph showing no significant differences in the correlation between systolic blood pressure and R-R interval (indicative of cardiac baroreflex sensitivity) during STN stimulation. (B) Scatter graph showing all the data points from the entire protocol. n = 15. Error bars represent standard error of the mean.*

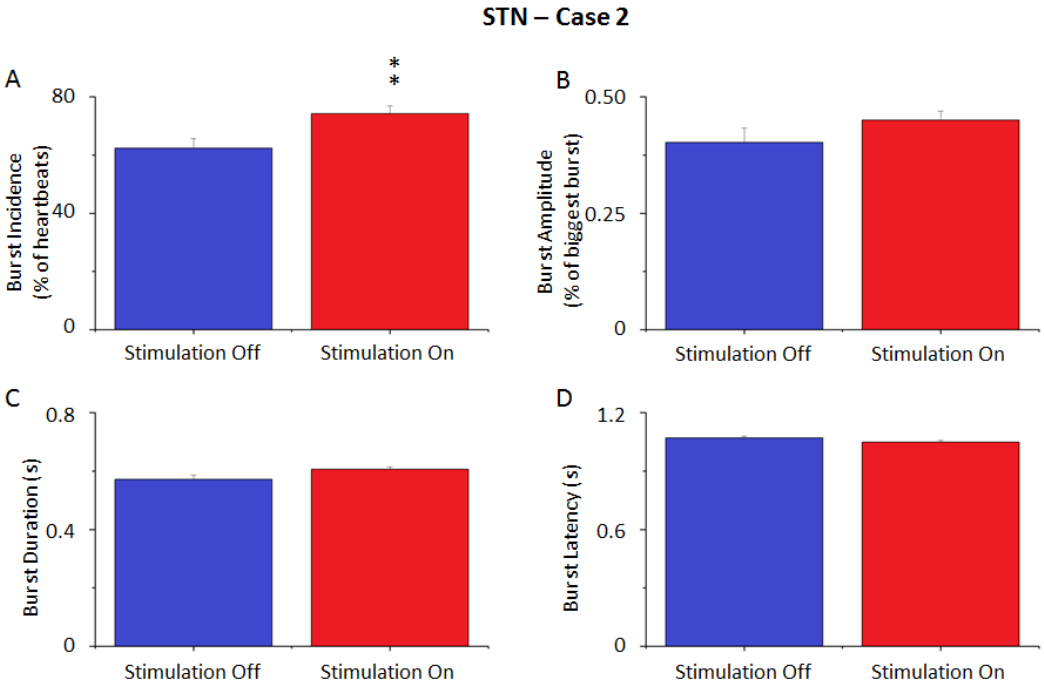

Figure 6.28 *– Graphs showing changes in muscle sympathetic nerve activity parameters during stimulation of the subthalamic nucleus (STN) in the second STN patient. (A) There was a significant increase in burst incidence during STN stimulation. There were no significant changes in (B) burst amplitude, (C) burst duration or (D) burst latency during STN stimulation. n = 15. Error bars represent standard error of the mean.*

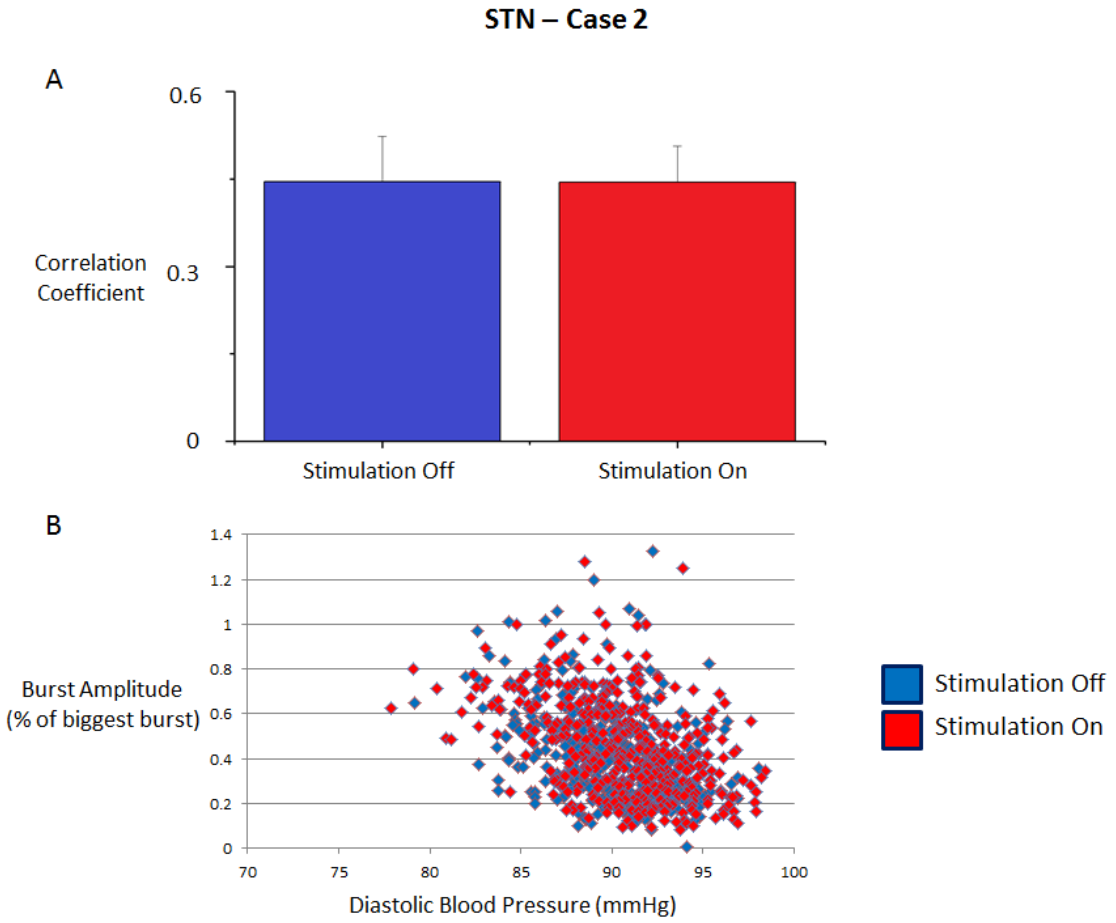

Figure 6.29 *– Graphs showing the changes in vascular baroreflex sensitivity during stimulation of the subthalamic nucleus (STN) in the second STN patient. (A) Graph showing no significant differences in the correlation between diastolic blood pressure and burst amplitude (indicative of vascular baroreflex sensitivity) during STN stimulation. (B) Scatter graph showing all the data points from the entire protocol. n = 15. Error bars represent standard error of the mean.*

Case 3

In the third subthalamic nucleus (STN) patient, there were no significant changes in mean arterial blood pressure (MABP) during stimulation (P = 0.122, *n* = 15) (Fig. 6.30A). Likewise, systolic blood pressure (SBP) and diastolic blood pressure (DBP) also remained unchanged during STN stimulation (P = 0.092 and P = 0.107, respectively; *n* = 15) (Figs. 6.30B-6.30C). There were no significant changes in R-R interval upon STN stimulation either (P = 0.834, *n* = 15) (Fig. 6.30D). The variability of these cardiovascular parameters was also examined. It appears that stimulation of the STN has little effect on MABP but slightly increases the variability of SBP,

DBP and the R-R interval (Fig. 6.31). There was also a significant decrease in cardiac baroreflex sensitivity during STN stimulation – the correlation coefficient dropped by 0.213 ± 0.052 (P = 0.014, *n* = 15) when the stimulation was switched on (Fig. 6.32).

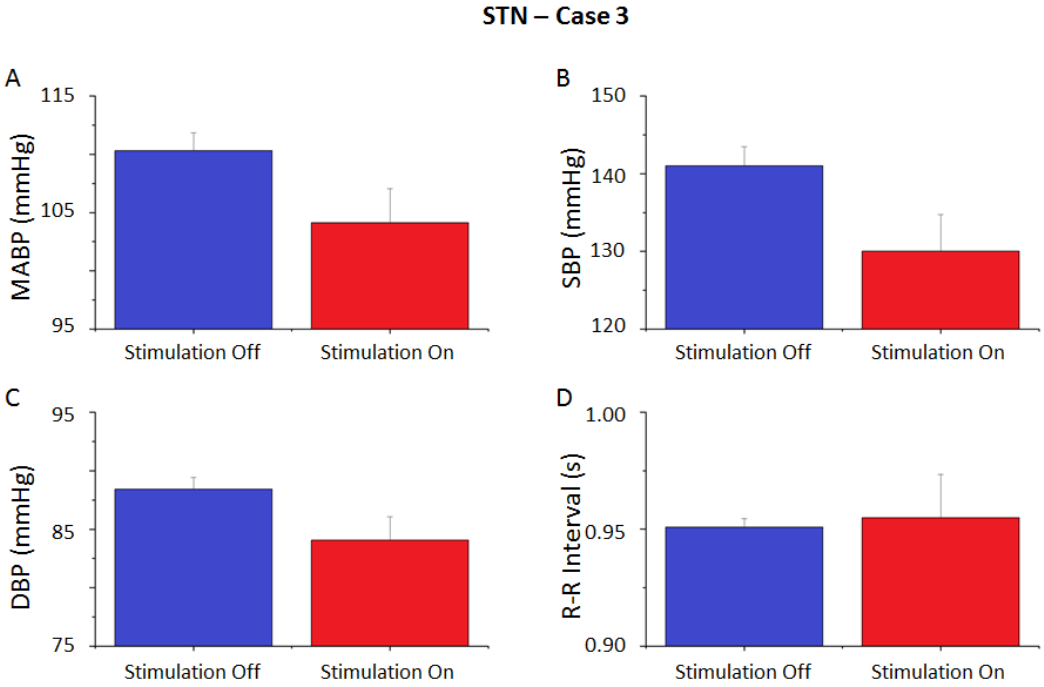

Figure 6.30 *– Graphs showing changes in cardiovascular parameters during stimulation of the subthalamic nucleus (STN) in the third STN patient. There were no significant changes in (A) mean arterial blood pressure (MABP), (B) systolic blood pressure (SBP), (C) diastolic blood pressure (DBP) or (D) R-R interval during STN stimulation. n = 15. Error bars represent standard error of the mean.*

In terms of muscle sympathetic nerve activity, there were no significant differences upon STN stimulation in burst incidence (P = 0.288, *n* = 15), burst amplitude (P = 0.311, *n* = 15), burst duration (P = 0.100, *n* = 15) or burst latency (P = 0.885, *n* = 15) (Fig. 6.33). No significant change in vascular baroreflex sensitivity could be detected during stimulation of the STN (P = 0.996, *n* = 15) (Fig. 6.34).

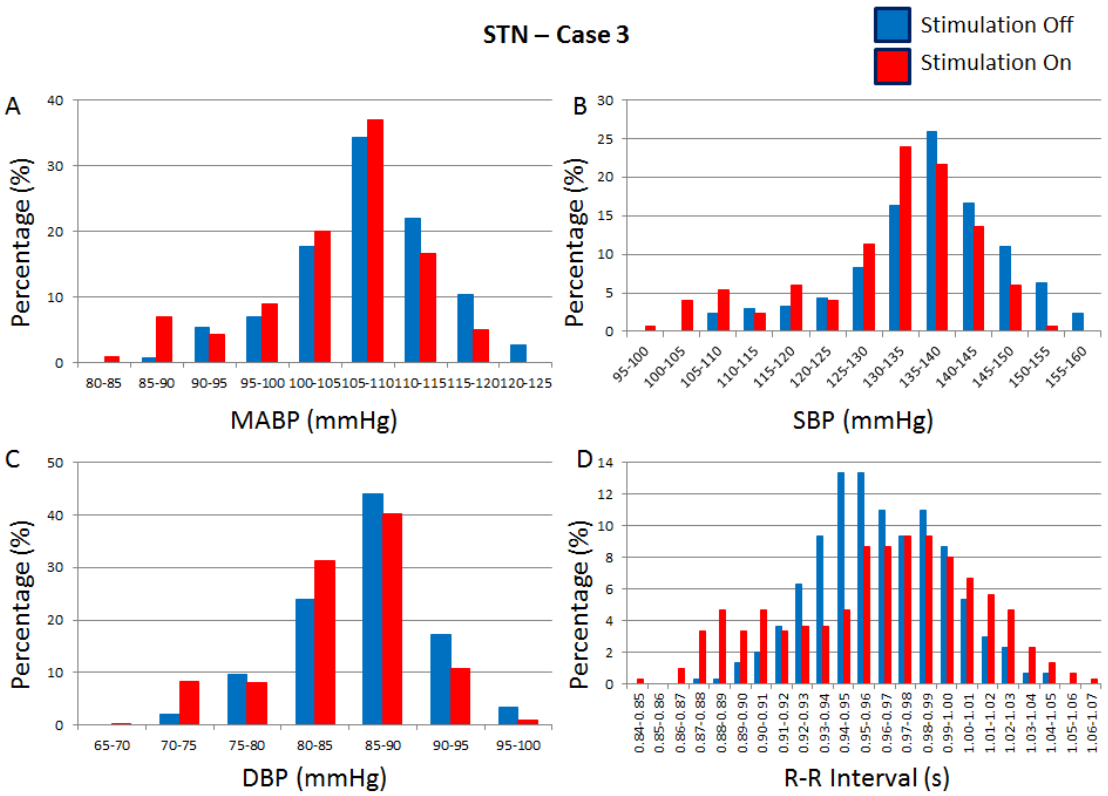

Figure 6.31 *– Graph showing the changes in variability of cardiovascular parameters during stimulation of the subthalamic nucleus (STN) in the third STN patient. (A) Stimulation appears to have little effect on the variability of mean arterial blood pressure (MABP). However, stimulation appears to increase the variability of (B) systolic blood pressure (SBP), (C) diastolic blood pressure (DBP) and (D) the R-R interval.*

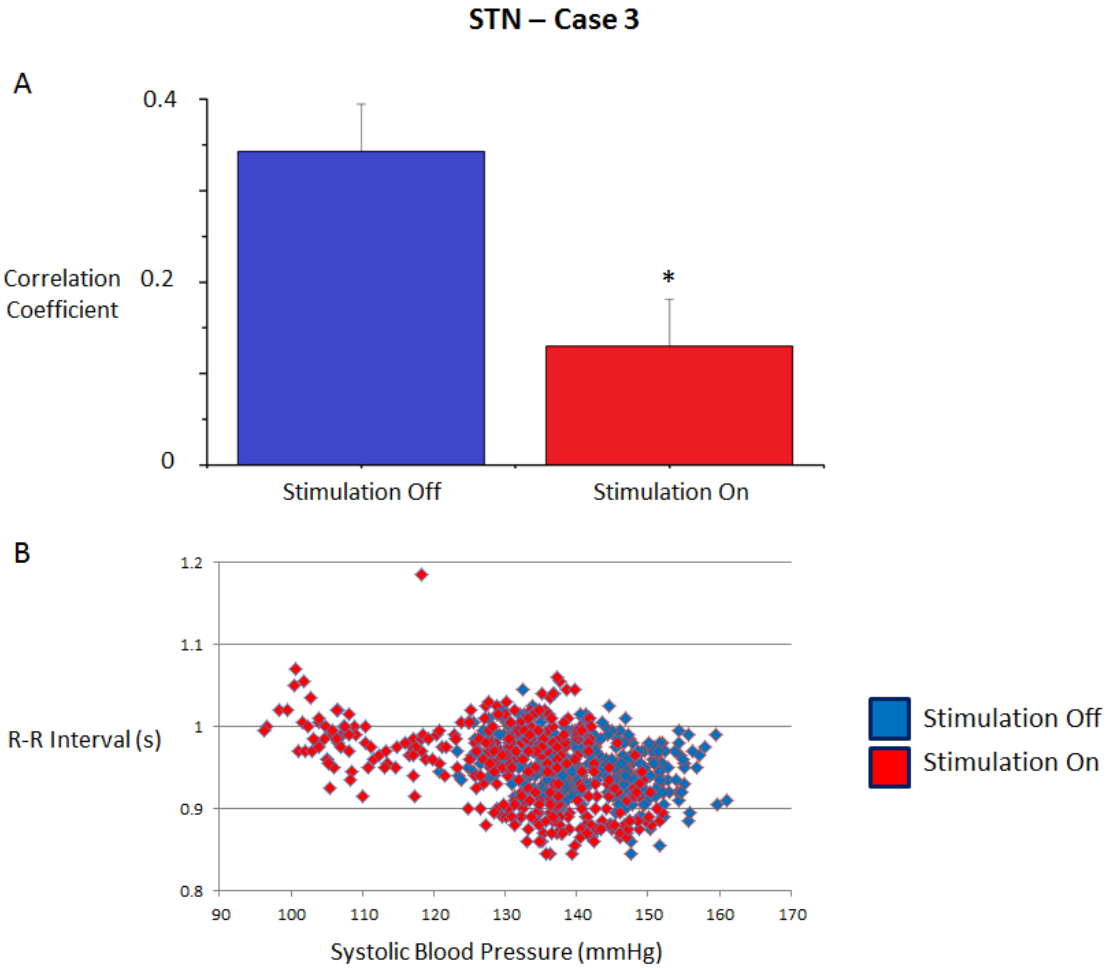

Figure 6.32 *– Graphs showing the changes in cardiac baroreflex sensitivity during stimulation of the subthalamic nucleus (STN) in the third STN patient. (A) Graph showing a significant decrease in the correlation between systolic blood pressure and R-R interval (indicative of cardiac baroreflex sensitivity) during STN stimulation. (B) Scatter graph showing all the data points from the entire protocol. n = 15, * P < 0.05. Error bars represent standard error of the mean.*

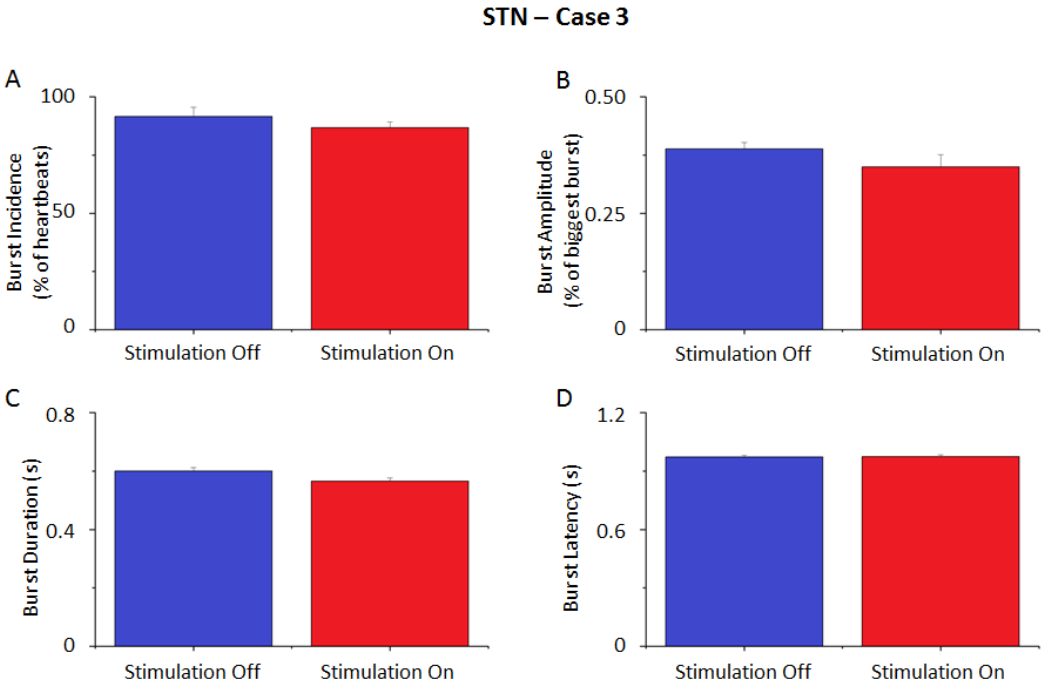

Figure 6.33 *– Graphs showing changes in muscle sympathetic nerve activity parameters during stimulation of the subthalamic nucleus (STN) in the third STN patient. There were no significant changes in (A) burst incidence, (B) burst amplitude, (C) burst duration or (D) burst latency during STN stimulation. n = 15. Error bars represent standard error of the mean.*

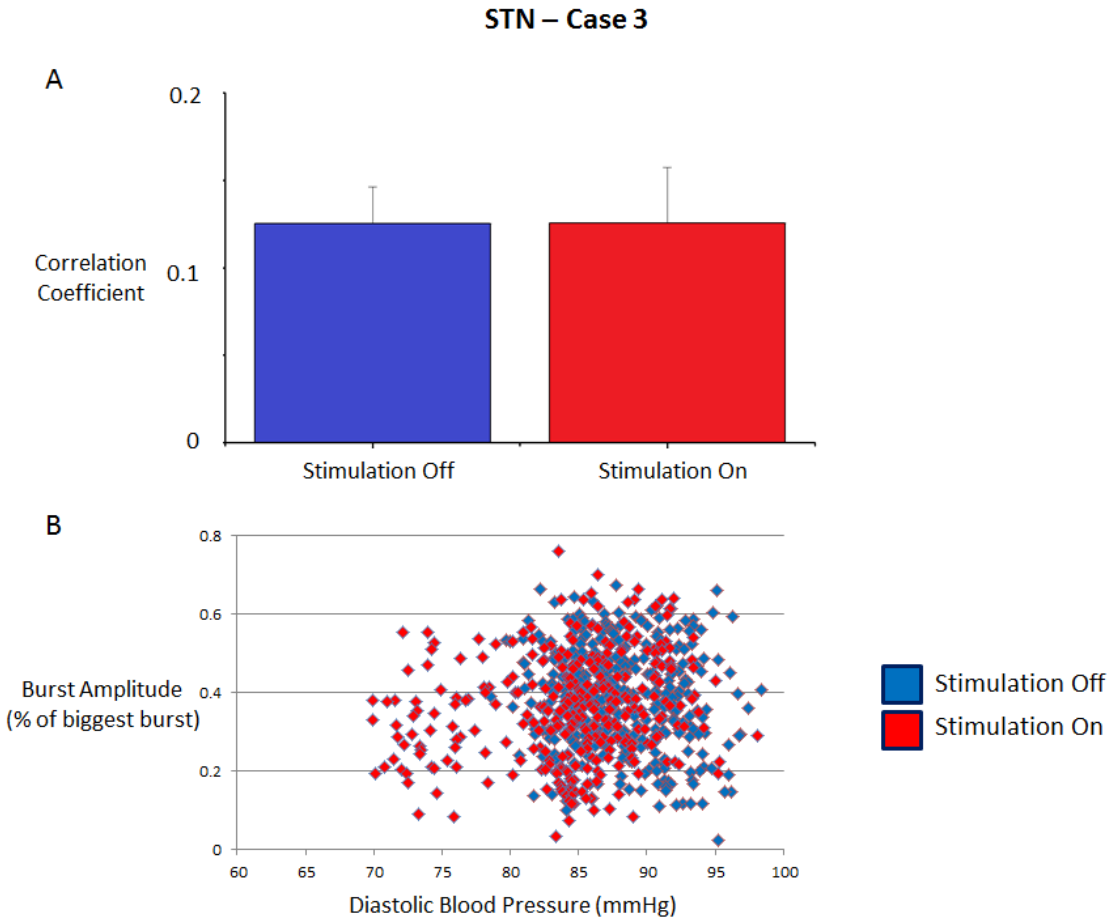

Figure 6.34 *– Graphs showing the changes in vascular baroreflex sensitivity during stimulation of the subthalamic nucleus (STN) in the third STN patient. (A) Graph showing no significant differences in the correlation between diastolic blood pressure and burst amplitude (indicative of vascular baroreflex sensitivity) during STN stimulation. (B) Scatter graph showing all the data points from the entire protocol. n = 15. Error bars represent standard error of the mean.*

Case 4

In the final subthalamic nucleus (STN) patient, there was a significant increase in mean arterial blood pressure (MABP) upon stimulation of 23.3 ± 0.8 mmHg, which is equivalent to an increase of 25.1% (P = 0.001, *n* = 15) (Fig. 6.35A). Similarly, systolic blood pressure (SBP) and diastolic blood pressure (DBP) also increased significantly during STN stimulation (Figs. 6.35B-6.35C). SBP increased by 29.1 ± 0.9 mmHg (equivalent to an increase of 23.6%) and DBP increased by 18.7 ± 1.3 mmHg (equivalent to an increase of 25.2%) (P <0.001 and P = 0.004, respectively; *n* = 15). The R-R interval did not change significantly during STN stimulation (P =

0.062, *n* = 15) (Fig. 6.35D). The variability of these cardiovascular parameters was also examined. It appears that stimulation of the STN increases the variability of MABP, SBP and DBP, but slightly decreases the variability of the R-R interval (Fig. 6.36). There was also a significant increase in cardiac baroreflex sensitivity during STN stimulation – the correlation coefficient rose by 0.180 ± 0.123 (P = 0.001, *n* = 15) when the stimulation was turned on (Fig. 6.37).

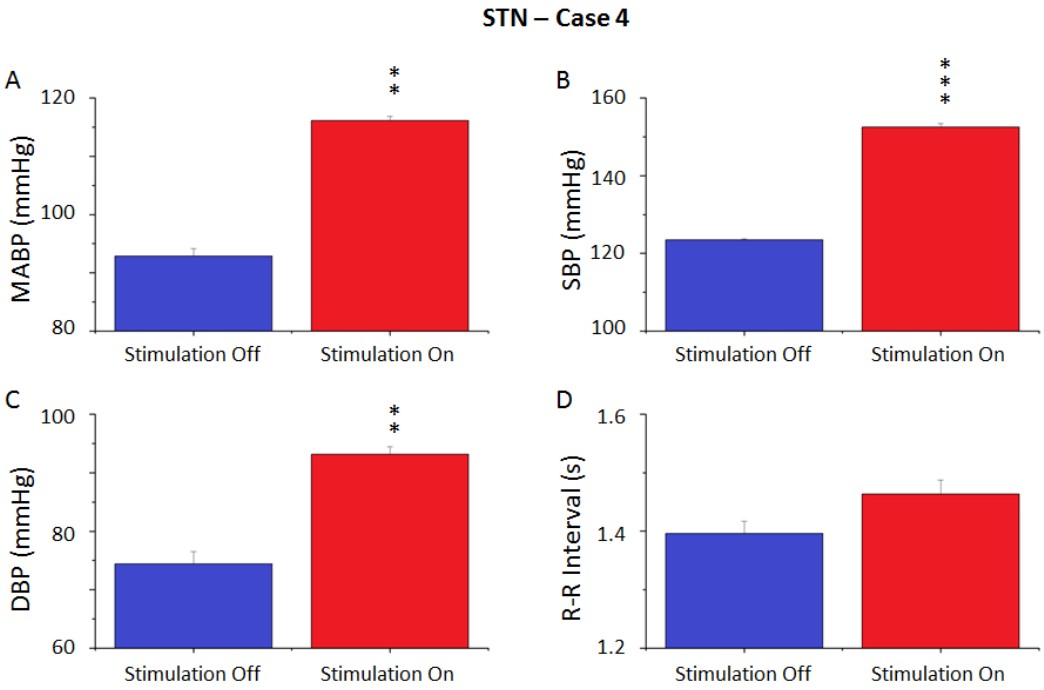

Figure 6.35 *– Graphs showing changes in cardiovascular parameters during stimulation of the subthalamic nucleus (STN) in the fourth STN patient. There was a significant increase in (A) mean arterial blood pressure (MABP), (B) systolic blood pressure (SBP) and (C) diastolic blood pressure (DBP) during STN stimulation. (D) There was no significant difference in R-R interval during STN stimulation. n = 15, ** P < 0.01, *** P < 0.001. Error bars represent standard error of the mean.*

In terms of muscle sympathetic nerve activity, there were no significant differences upon STN stimulation in burst incidence (P = 0.372, *n* = 15), burst amplitude (P = 0.462, *n* = 15), burst duration (P = 0.283, *n* = 15) or burst latency (P = 0.458, *n* = 15) (Fig. 6.38). No significant

change in vascular baroreflex sensitivity could be detected during stimulation of the STN (P = 0.782, *n* = 15) (Fig. 6.39).

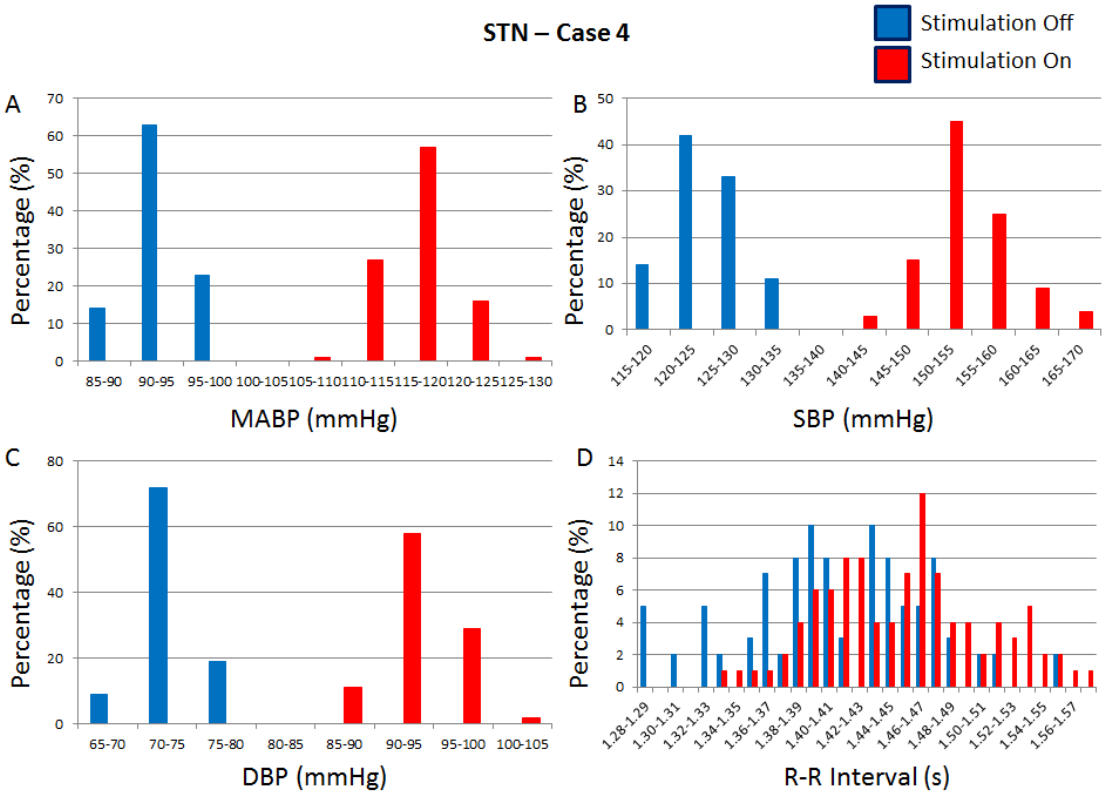

Figure 6.36 *– Graph showing the changes in variability of cardiovascular parameters during stimulation of the subthalamic nucleus (STN) in the fourth STN patient. Stimulation appears to increase the variability of (A) mean arterial blood pressure (MABP), (B) systolic blood pressure (SBP) and (C) diastolic blood pressure (DBP). (D) Stimulation appears to decrease the variability of the R-R interval.*

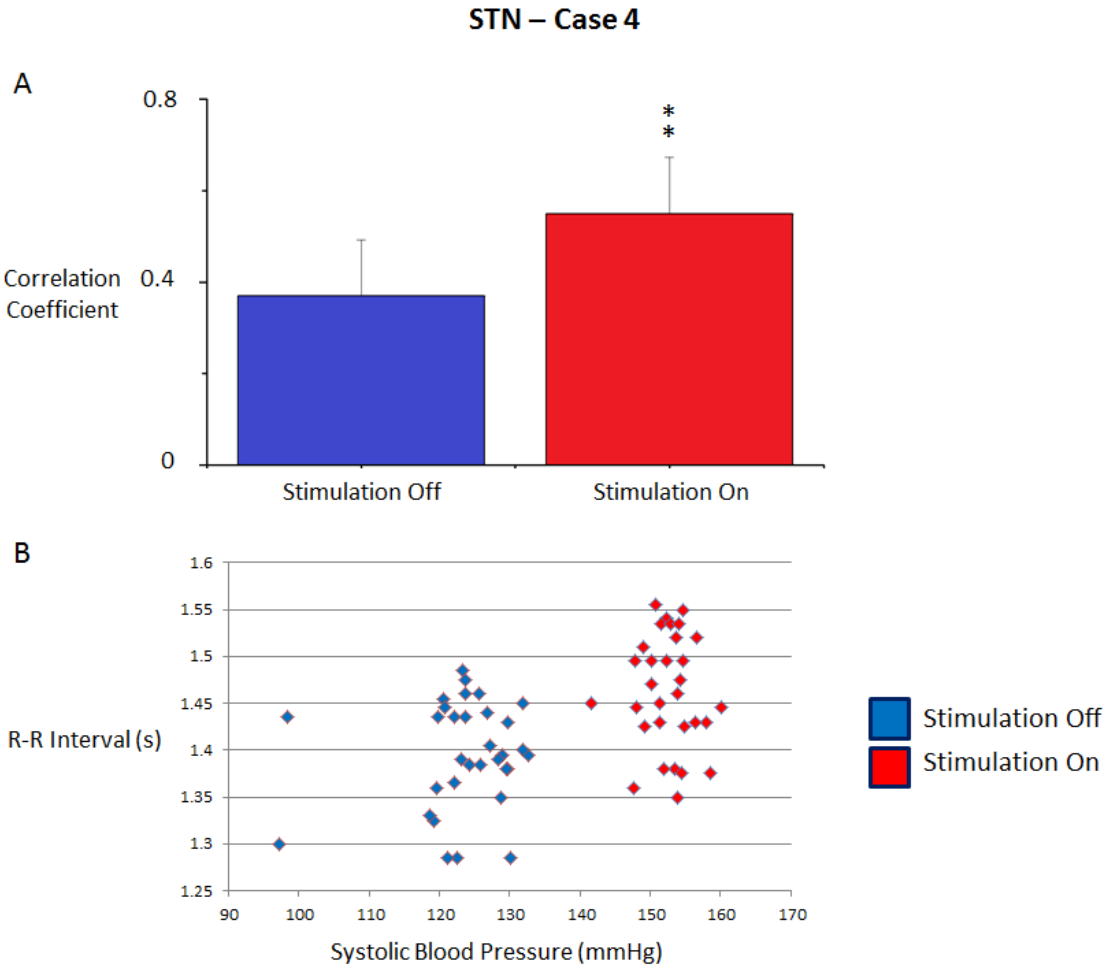

Figure 6.37 *– Graphs showing the changes in cardiac baroreflex sensitivity during stimulation of the subthalamic nucleus (STN) in the fourth STN patient. (A) Graph showing a significant increase in the correlation between systolic blood pressure and R-R interval (indicative of cardiac baroreflex sensitivity) during STN stimulation. (B) Scatter graph showing all the data points from the entire protocol. n = 15, ** P < 0.01. Error bars represent standard error of the mean.*

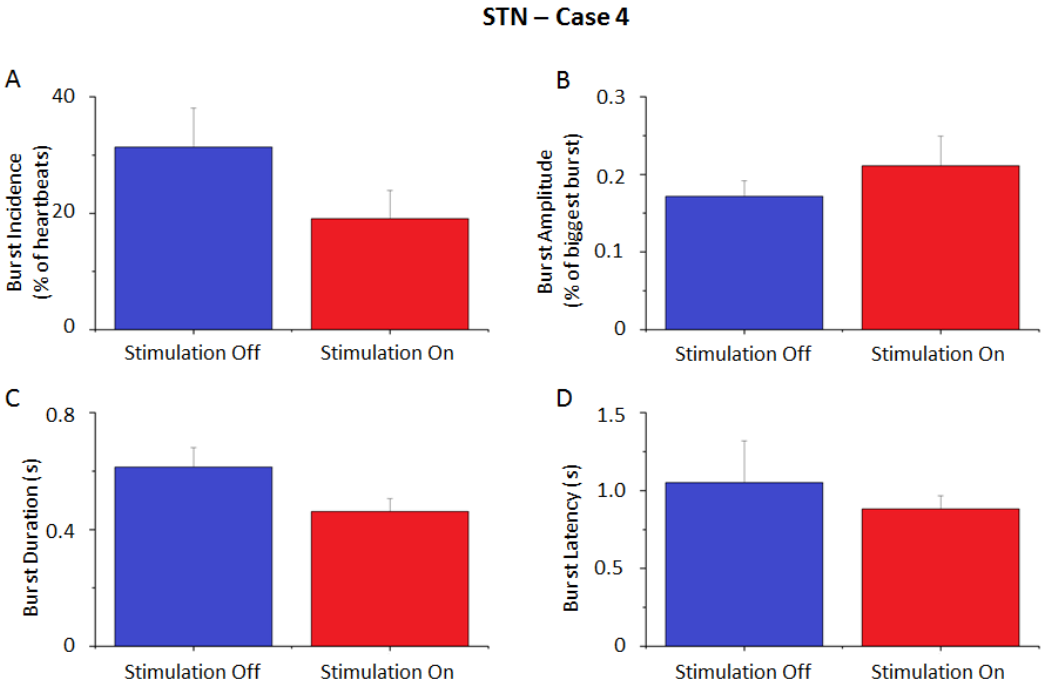

Figure 6.38 *– Graphs showing changes in muscle sympathetic nerve activity parameters during stimulation of the subthalamic nucleus (STN) in the fourth STN patient. There were no significant changes in (A) burst incidence, (B) burst amplitude, (C) burst duration or (D) burst latency during STN stimulation. n = 15. Error bars represent standard error of the mean.*

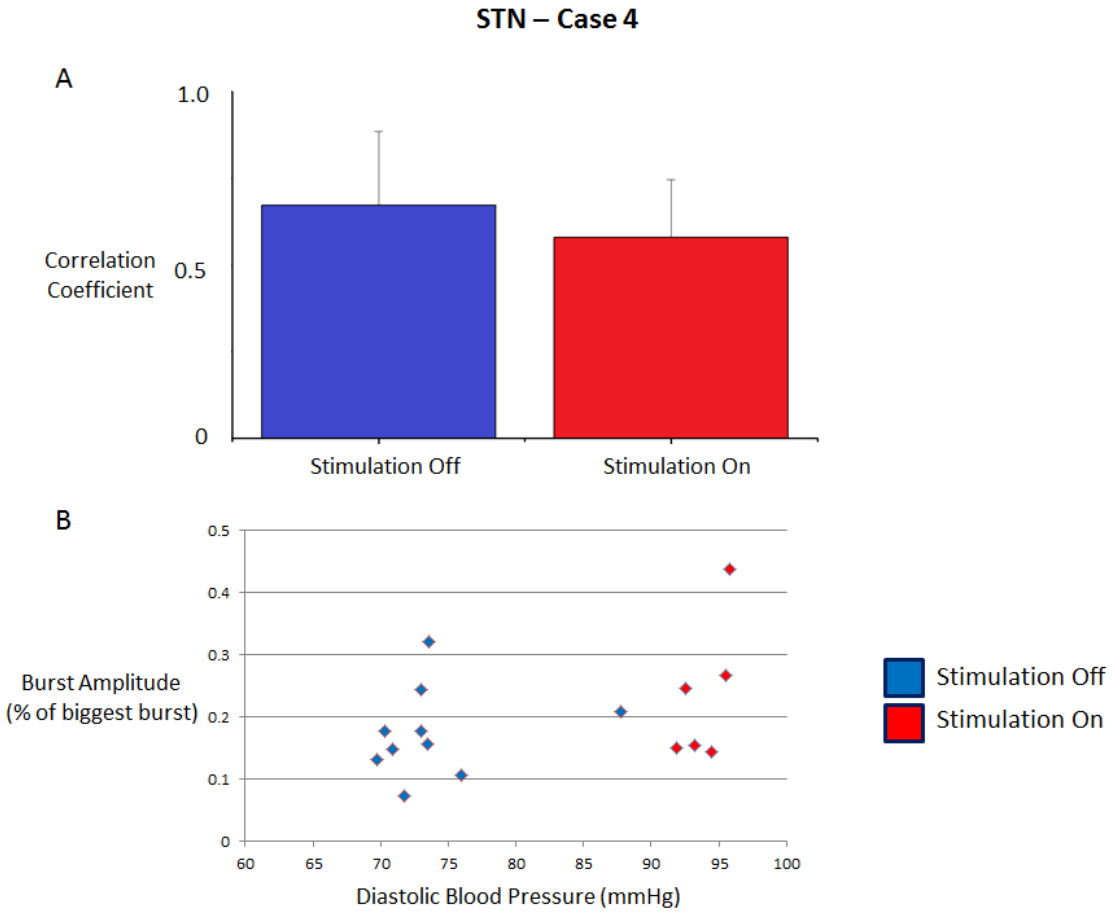

Figure 6.39 *– Graphs showing the changes in vascular baroreflex sensitivity during stimulation of the subthalamic nucleus (STN) in the fourth STN patient. (A) Graph showing no significant differences in the correlation between diastolic blood pressure and burst amplitude (indicative of vascular baroreflex sensitivity) during STN stimulation. (B) Scatter graph showing all the data points from the entire protocol. n = 15. Error bars represent standard error of the mean.*

Sensory Thalamus Stimulation

Case 1

In this patient, there were no significant changes in mean arterial blood pressure (MABP) during stimulation of the sensory thalamus (P = 0.249, *n* = 15) (Fig. 6.40A). Correspondingly, systolic blood pressure (SBP) and diastolic blood pressure (DBP) also remained unchanged during sensory thalamus stimulation (P = 0.895 and P = 0.136, respectively; *n* = 15) (Figs. 6.40B-6.40C). There were no significant changes in R-R interval upon sensory thalamus stimulation either (P = 0.148, *n* = 15) (Fig. 6.40D). The variability of these cardiovascular

parameters was also examined. It appears that stimulation of the sensory thalamus has little effect on the variability of MABP, SBP, DBP and the R-R interval (Fig. 6.41). No significant change in cardiac baroreflex sensitivity could be detected during stimulation of the sensory thalamus (P = 0.463, *n* = 15) (Fig. 6.42).

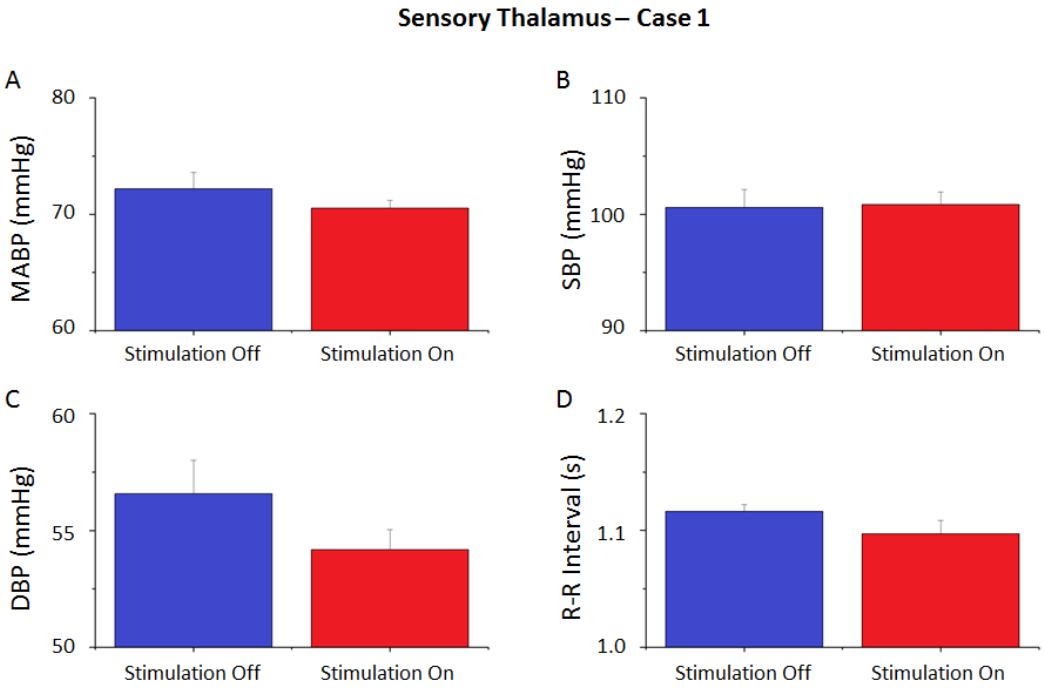

Figure 6.40 *– Graphs showing changes in cardiovascular parameters during stimulation of the sensory thalamus in the first patient. There were no significant changes in (A) mean arterial blood pressure (MABP), (B) systolic blood pressure (SBP), (C) diastolic blood pressure (DBP) and (D) R-R interval during stimulation of the sensory thalamus. n = 15. Error bars represent standard error of the mean.*

In terms of muscle sympathetic nerve activity, there were no significant differences upon sensory thalamus stimulation in burst incidence (P = 0.646, *n* = 15), burst amplitude (P = 0.057, *n* = 15), burst duration (P = 0.062, *n* = 15) or burst latency (P = 0.447, *n* = 15) (Fig. 6.43). No significant change in vascular baroreflex sensitivity could be detected during stimulation of the sensory thalamus (P = 0.949, *n* = 15) (Fig. 6.44).

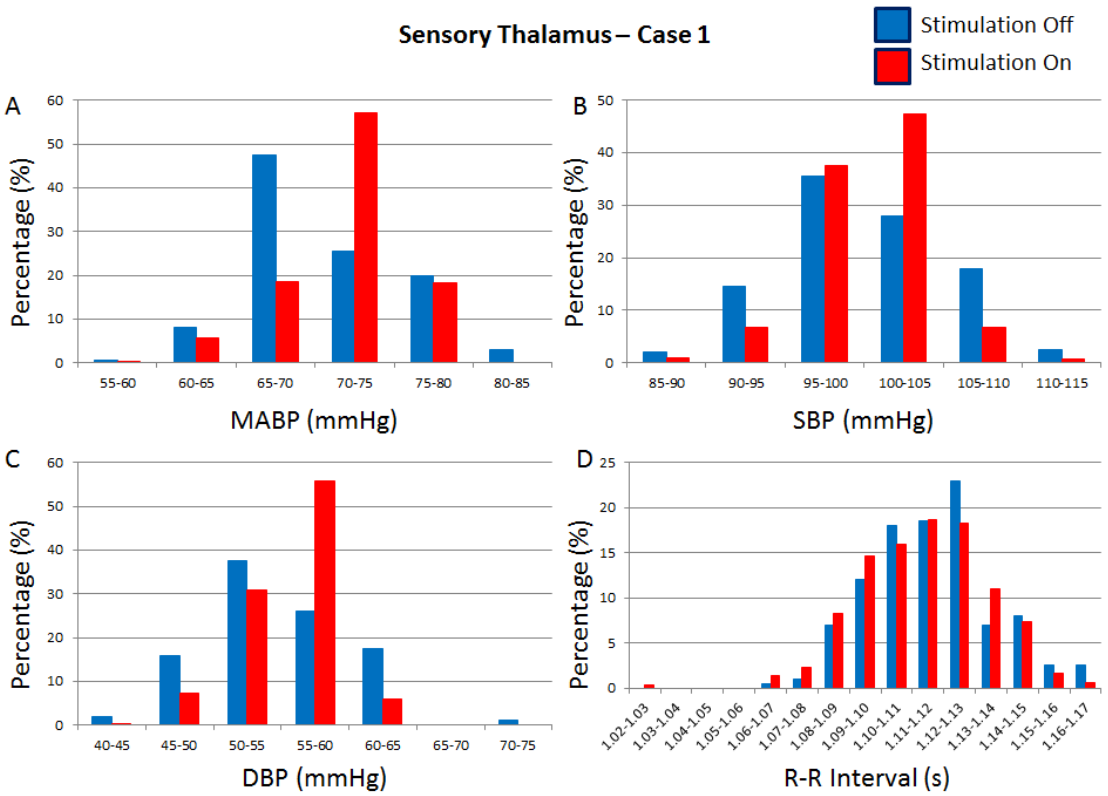

Figure 6.41 *– Graph showing the changes in variability of cardiovascular parameters during stimulation of the sensory thalamus in the first patient. Stimulation appears to have little effect on the variability of (A) mean arterial blood pressure (MABP), (B) systolic blood pressure (SBP), (C) diastolic blood pressure (DBP) and (D) the R-R interval.*

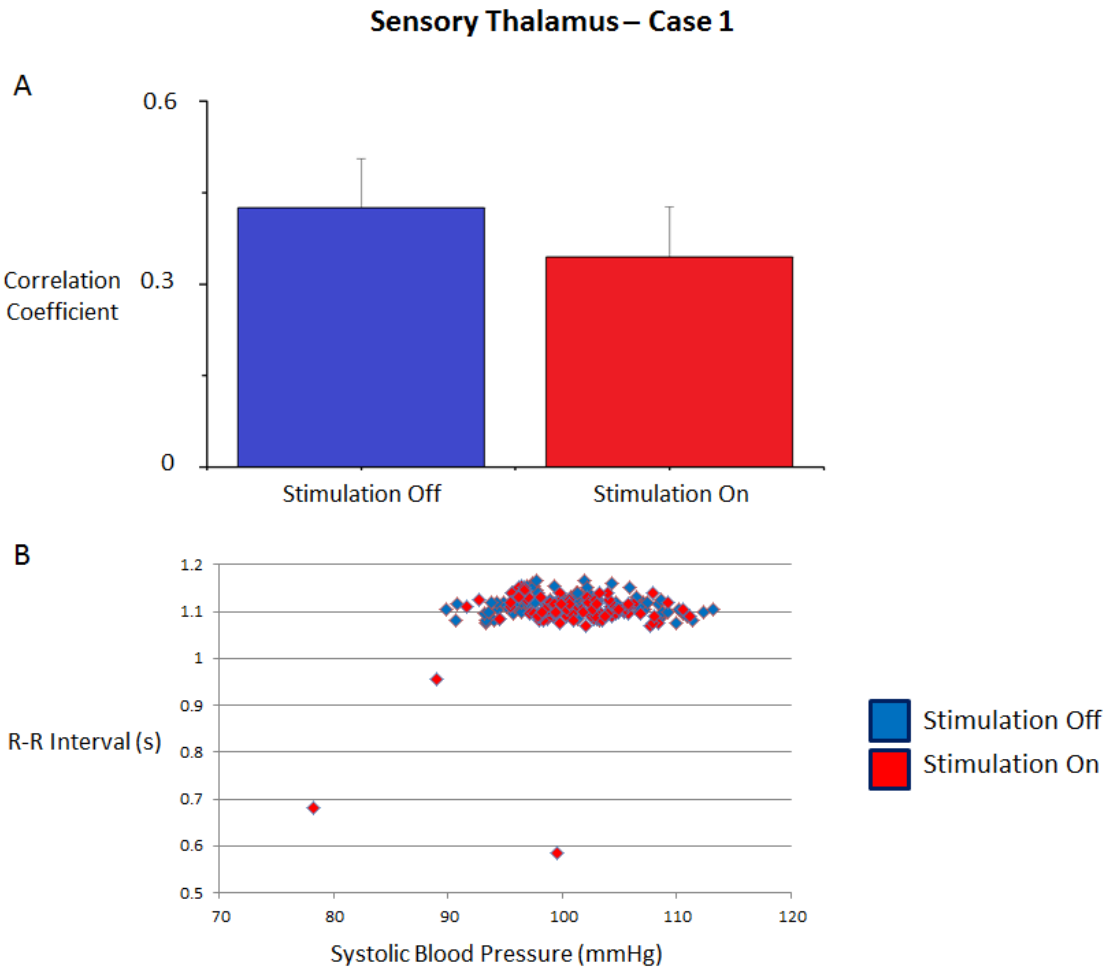

Figure 6.42 *– Graphs showing the changes in cardiac baroreflex sensitivity during stimulation of the sensory thalamus in the first patient. (A) Graph showing no significant differences in the correlation between systolic blood pressure and R-R interval (indicative of cardiac baroreflex sensitivity) during stimulation of the sensory thalamus. (B) Scatter graph showing all the data points from the entire protocol. n = 15. Error bars represent standard error of the mean.*

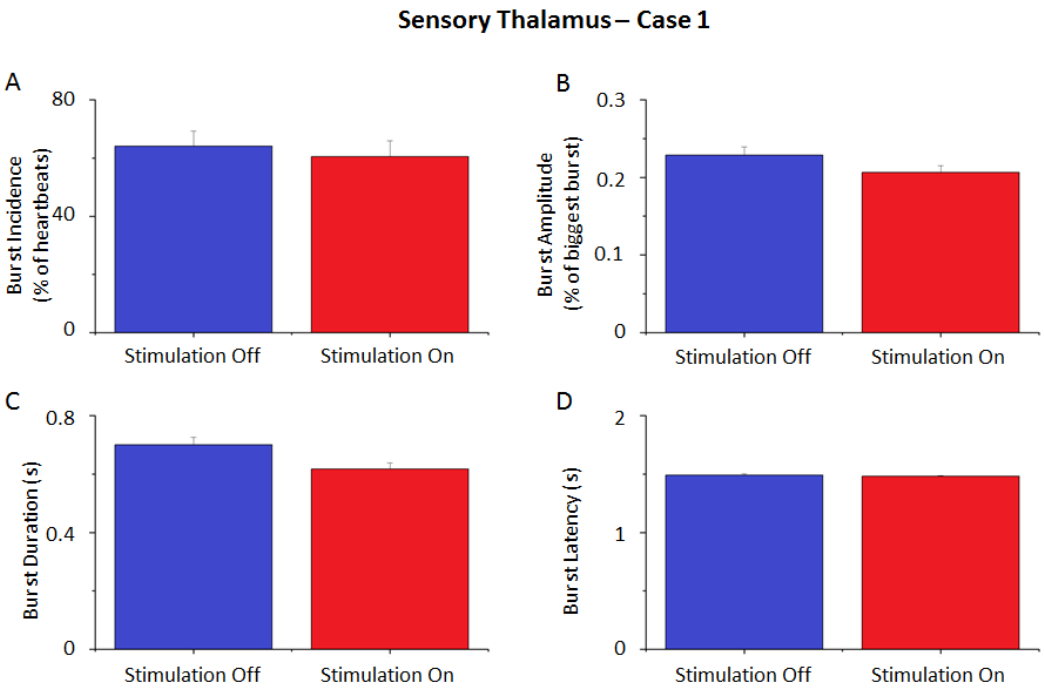

Figure 6.43 *– Graphs showing changes in muscle sympathetic nerve activity parameters during stimulation of the sensory thalamus in the first patient. There were no significant changes in (A) burst incidence, (B) burst amplitude, (C) burst duration or (D) burst latency during STN stimulation. n = 15. Error bars represent standard error of the mean.*

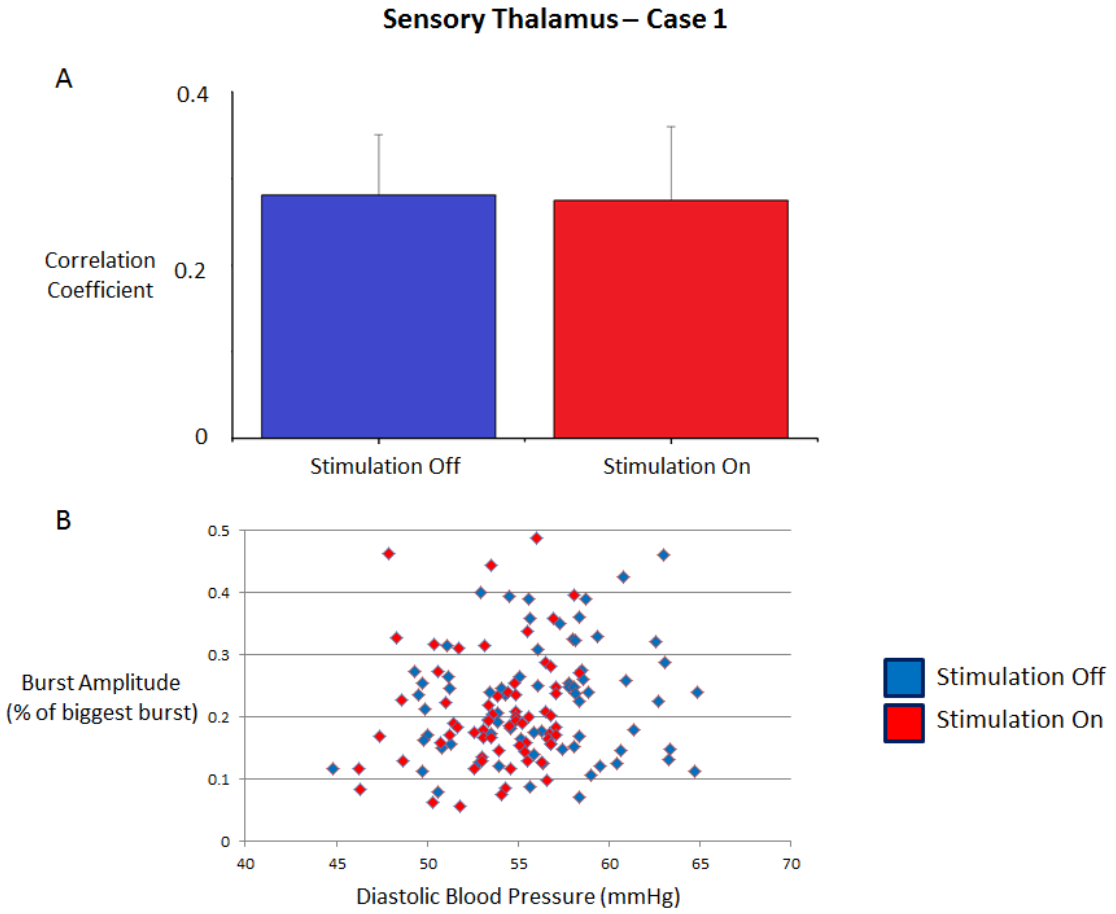

Figure 6.44 *– Graphs showing the changes in vascular baroreflex sensitivity during stimulation of the sensory thalamus in the first patient. (A) Graph showing no significant differences in the correlation between diastolic blood pressure and burst amplitude (indicative of vascular baroreflex sensitivity) during stimulation of the sensory thalamus. (B) Scatter graph showing all the data points from the entire protocol. n = 15. Error bars represent standard error of the mean.*

Case 2

In this sensory thalamus case, the most therapeutically beneficial stimulation settings had not yet been established. Therefore, the patient underwent the graded protocol. There were no significant differences, compared to no stimulation, during 1 V stimulation (P = 0.064, *n* = 5), 2 V stimulation (P = 0.763, *n* = 5), 3 V stimulation (P = 0.121, *n* = 5), 4 V stimulation (P = 0.102, *n* = 5), and 5 V stimulation (P = 0.319, *n* = 5) (Fig. 6.45A). Systolic blood pressure (SBP) decreased significantly by 8.9 ± 2.4 mmHg, which is equivalent to a decrease of 7.6%, during 3 V stimulation (P = 0.002, *n* = 5). However, SBP remained unchanged during 1 V stimulation (P =

0.537, *n* = 5), 2 V stimulation (P = 0.064, *n* = 5), 4 V stimulation (P = 0.450, *n* = 5), and 5 V stimulation (P = 0.732, *n* = 5) (Fig. 6.45B). Diastolic blood pressure (DBP) increased significantly by 7.2 ± 1.4 mmHg (equivalent to an increase of 10.4%) during 1 V stimulation and by 3.3 ± 0.5 mmHg (equivalent to an increase of 4.7%) during 2 V stimulation (P = 0.005 and P = 0.024, respectively; *n* = 5); DBP decreased significantly by 3.0 ± 0.9 mmHg (equivalent to a decrease of 4.3%) during 4 V stimulation (P = 0.011, *n* = 5) (Fig. 6.45C). However, there were no significant changes in DBP during 3 V stimulation (P = 0.485, *n* = 5) and during 5 V stimulation (P = 0.105, *n* = 5). In terms of the R-R interval, there was a significant decrease in R-R interval of 0.012 ± 0.004 s, which is equivalent to a decrease of 1.7%, during 4 V stimulation (P = 0.019, *n* = 5). However, there were no significant changes during 1 V stimulation (P = 0.391, *n* = 5), during 2 V stimulation (P = 0.106, *n* = 5), during 3 V stimulation (P = 0.316, *n* = 5), and during 5 V stimulation (P = 0.099, *n* = 5) (Fig. 6.45D).

The variability of these cardiovascular parameters was also examined (Figs. 6.46-6.47). In this case, sensory thalamus stimulation appeared to have little effect on MABP variability. SBP variability was increased by 1 V stimulation, slightly decreased by 2-4 V stimulation, and considerably decreased by 5 V stimulation. DBP variability was increased by 1 V and 2 V stimulation, remained unchanged by 3 V stimulation, and was decreased by 4 V and 5 V stimulation. The R-R interval variability did not appear to be affected by sensory thalamus stimulation. No significant change in cardiac baroreflex sensitivity could be detected during stimulation of the sensory thalamus throughout the protocol (Fig. 6.48).

Unfortunately, muscle sympathetic nerve activity could not be recorded from this patient as an appropriate recording site within the peroneal nerve could not be established.

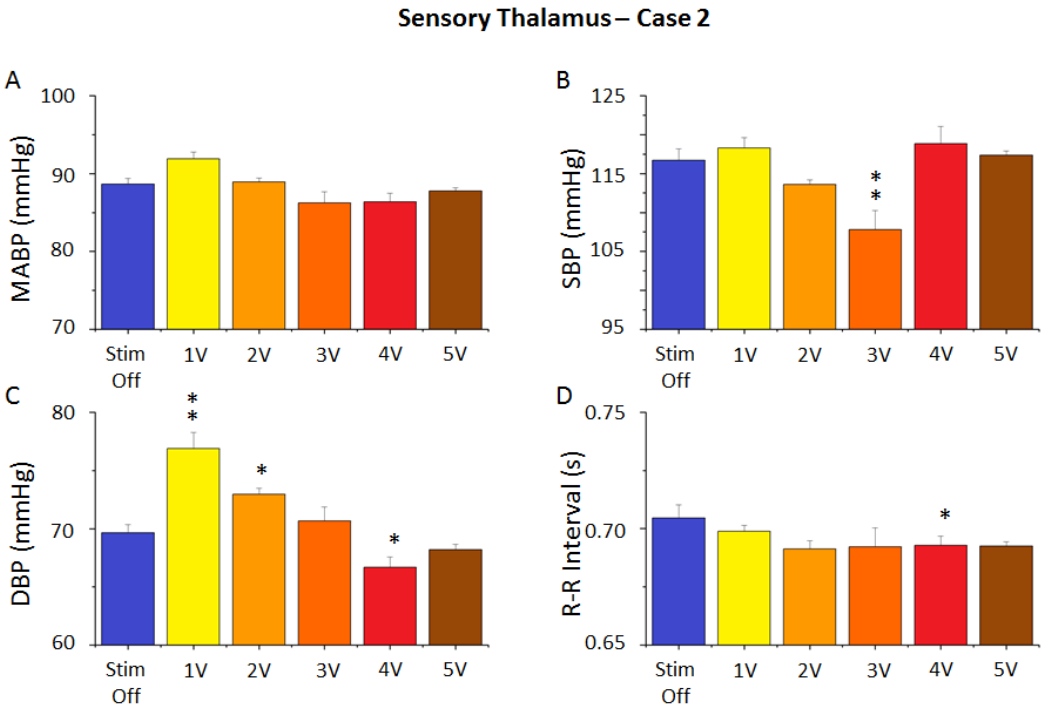

Figure 6.45 *– Graphs showing changes in cardiovascular parameters during stimulation of the sensory thalamus in the second patient, who followed the graded protocol. (A) There were no significant changes in mean arterial blood pressure (MABP) during stimulation of any amplitude. (B) There was a significant decrease in systolic blood pressure (SBP) during 3 V stimulation. (C) There was a significant increase in diastolic blood pressure (DBP) during 1 V stimulation and 2 V stimulation, and a significant decrease in DBP during 4 V stimulation. (D) There was a significant decrease in R-R interval during 4 V stimulation. n = 5, * P < 0.05, ** P < 0.01. Error bars represent standard error of the mean.*

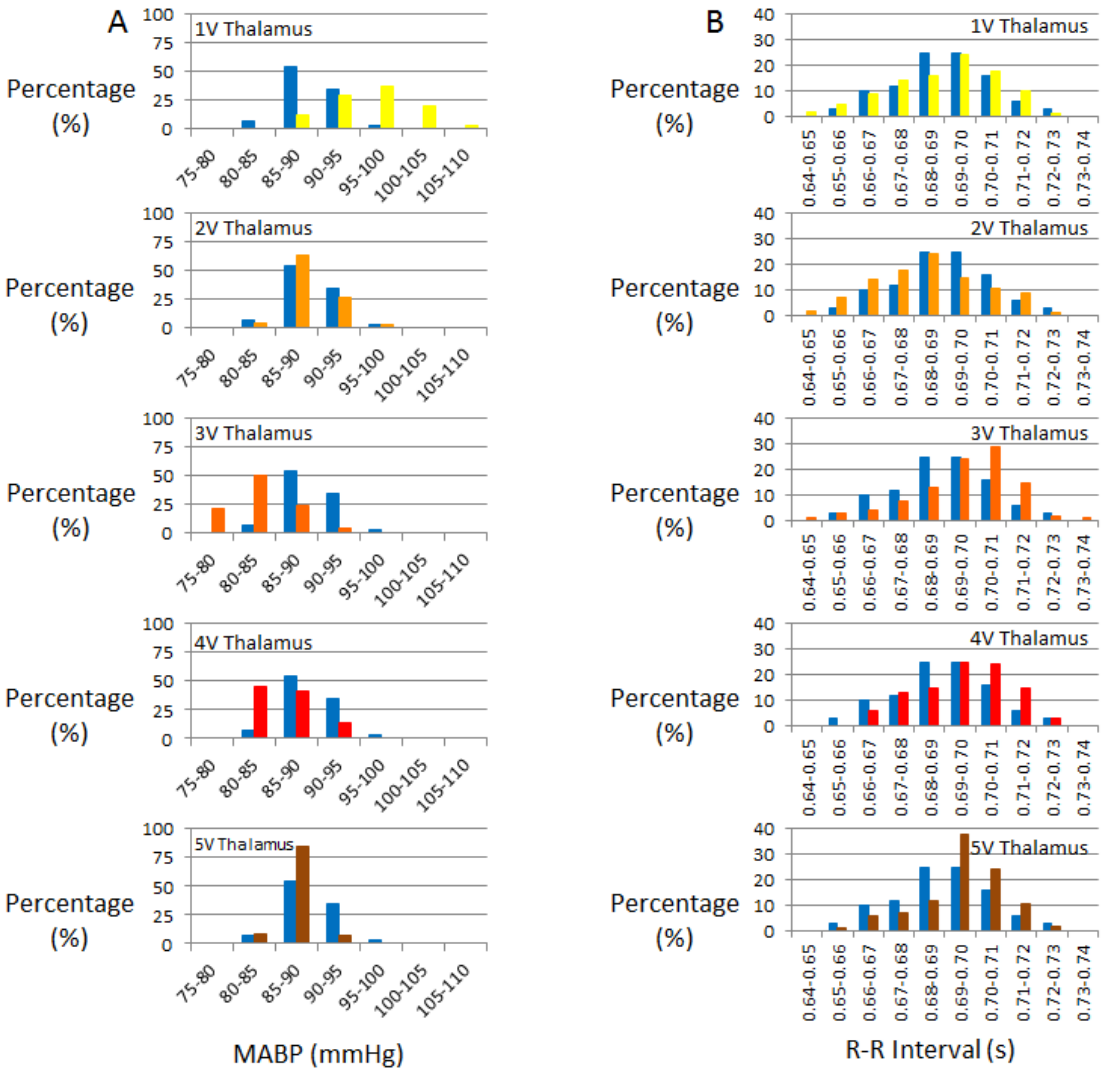

Figure 6.46 *– Graph showing the changes in variability of cardiovascular parameters during stimulation of the sensory thalamus in the second patient, who followed the graded protocol. Stimulation appears to have little effect on the variability of (A) mean arterial blood pressure (MABP) and (B) the R-R interval.*

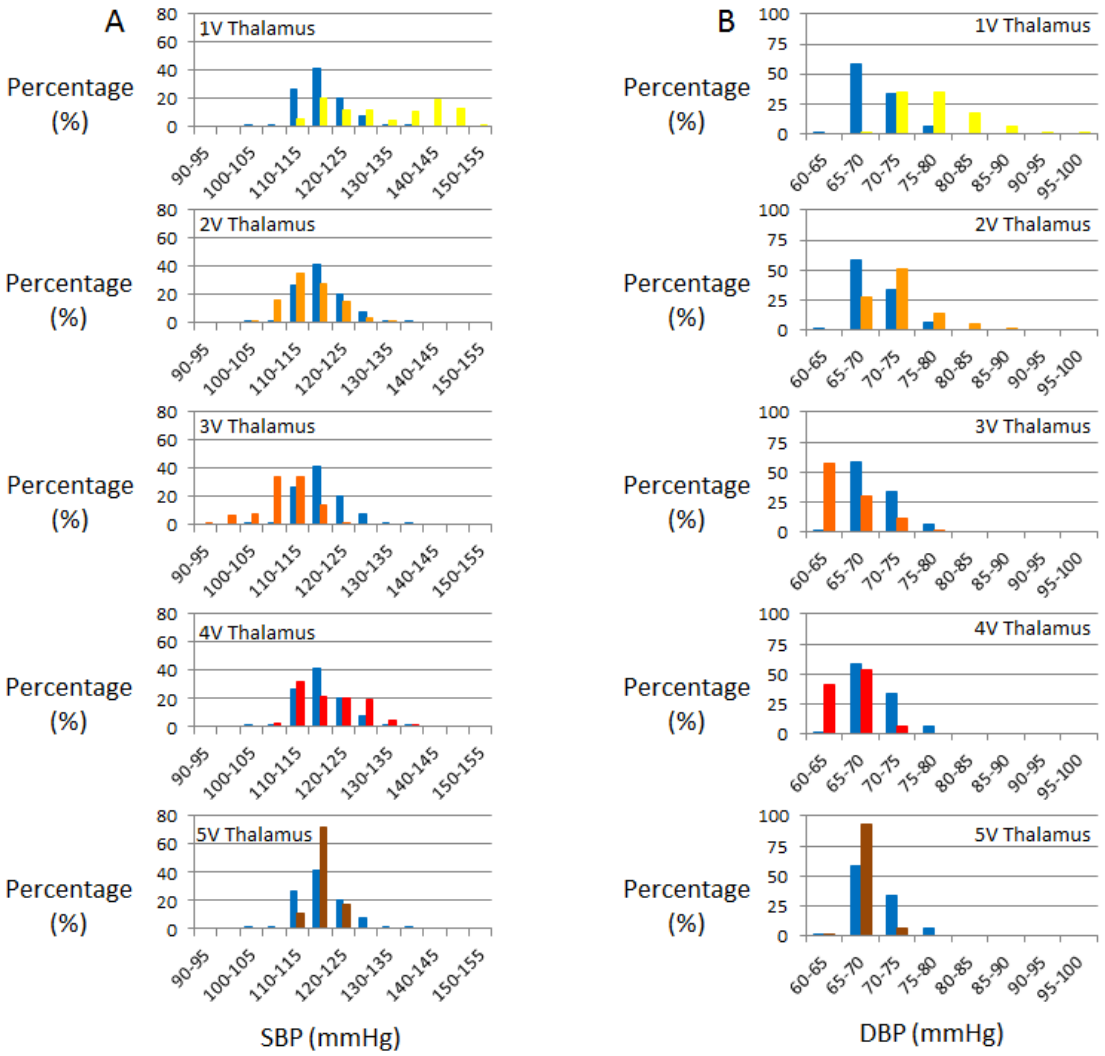

Figure 6.47 *– Graph showing the changes in variability of cardiovascular parameters during stimulation of the sensory thalamus in the second patient, who followed the graded protocol. (A) Stimulation at 1 V appears to increase the variability of systolic blood pressure (SBP), whereas stimulation at 2-5 V appears to decrease the variability of SBP. (B) Stimulation at 1 V and 2 V appears to increase the variability of diastolic blood pressure (DBP), stimulation at 3 V appears to have little effect on the variability of DBP, and stimulation at 4 V and 5 V appears to decrease the variability of DBP.*

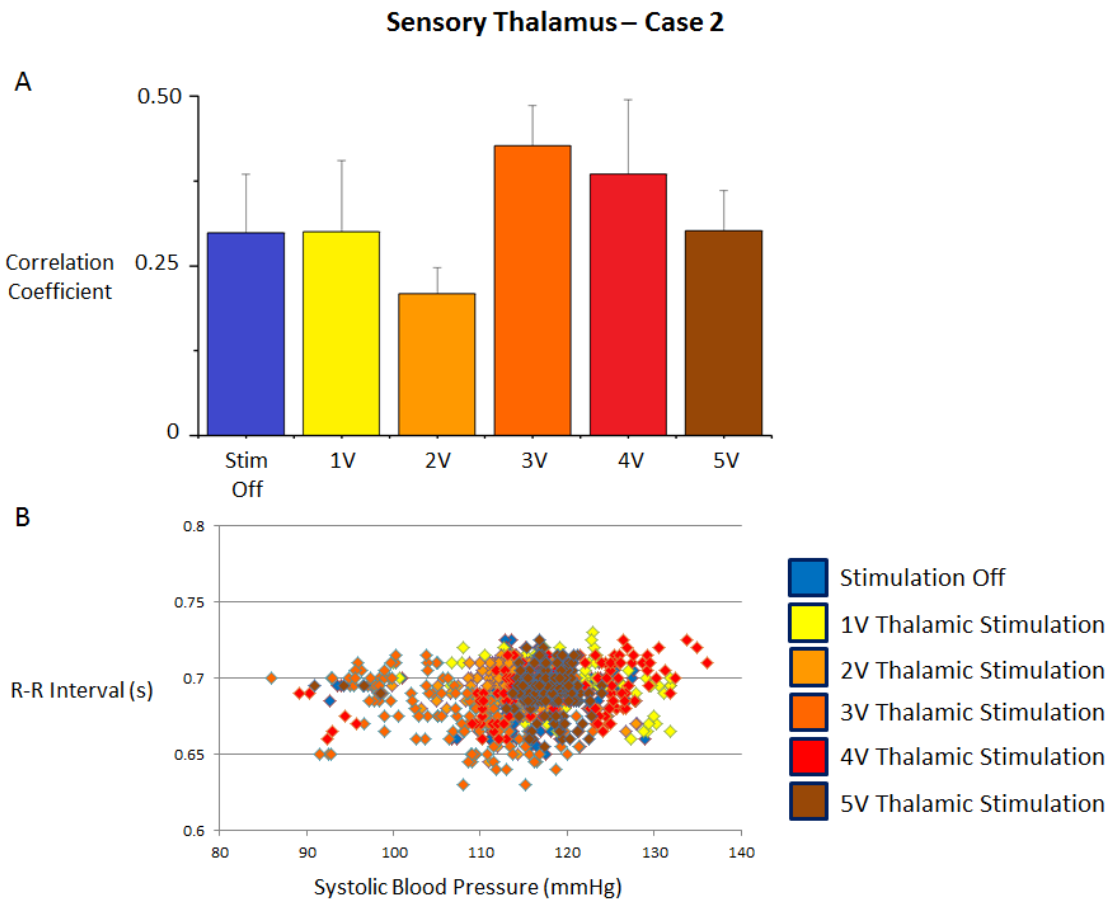

Figure 6.48 *– Graphs showing the changes in cardiac baroreflex sensitivity during stimulation of the sensory thalamus in the second patient, who followed the graded protocol. (A) Graph showing no significant differences in the correlation between systolic blood pressure and R-R interval (indicative of cardiac baroreflex sensitivity) during stimulation of the sensory thalamus at any amplitude. (B) Scatter graph showing all the data points from the entire protocol. n = 5. Error bars represent standard error of the mean.*

Internal Globus Pallidus Stimulation

Case 1

In this patient, there were no significant changes in mean arterial blood pressure (MABP) during stimulation of the internal globus pallidus (GPi) (P = 0.258, *n* = 15) (Fig. 6.49A). Likewise, systolic blood pressure (SBP) and diastolic blood pressure (DBP) also remained unchanged during GPi stimulation (P = 0.223 and P = 0.291, respectively; *n* = 15) (Figs. 6.49B-6.49C). There were no significant changes in R-R interval upon GPi stimulation either (P = 0.255, *n* = 15) (Fig. 6.49D). The variability of these cardiovascular parameters was also examined. It appears that

stimulation of the GPi increased the variability of SBP, had little effect on the variability of MABP and DBP, and decreased the variability of the R-R interval (Fig. 6.50). No significant change in cardiac baroreflex sensitivity could be detected during stimulation of the GPi (P = 0.866, *n* = 15) (Fig. 6.51).

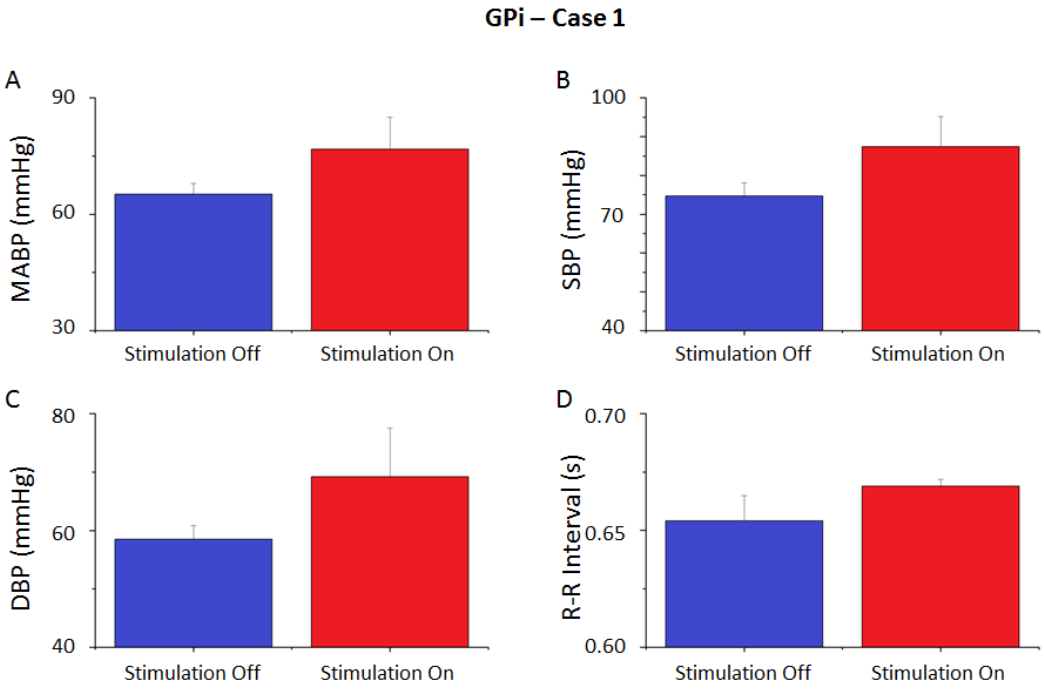

Figure 6.49 *– Graphs showing changes in cardiovascular parameters during stimulation of the internal globus pallidus (GPi). There were no significant changes in (A) mean arterial blood pressure (MABP), (B) systolic blood pressure (SBP), (C) diastolic blood pressure (DBP) and (D) R-R interval during stimulation of the sensory thalamus. n = 15. Error bars represent standard error of the mean.*

In terms of muscle sympathetic nerve activity, there were no significant differences upon GPi stimulation in burst incidence (P = 0.964, *n* = 15), burst amplitude (P = 0.639, *n* = 15), burst duration (P = 0.092, *n* = 15) or burst latency (P = 0.300, *n* = 15) (Fig. 6.52). No significant change in vascular baroreflex sensitivity could be detected during stimulation of the GPi (P = 0.695, *n* = 15) (Fig. 6.53).

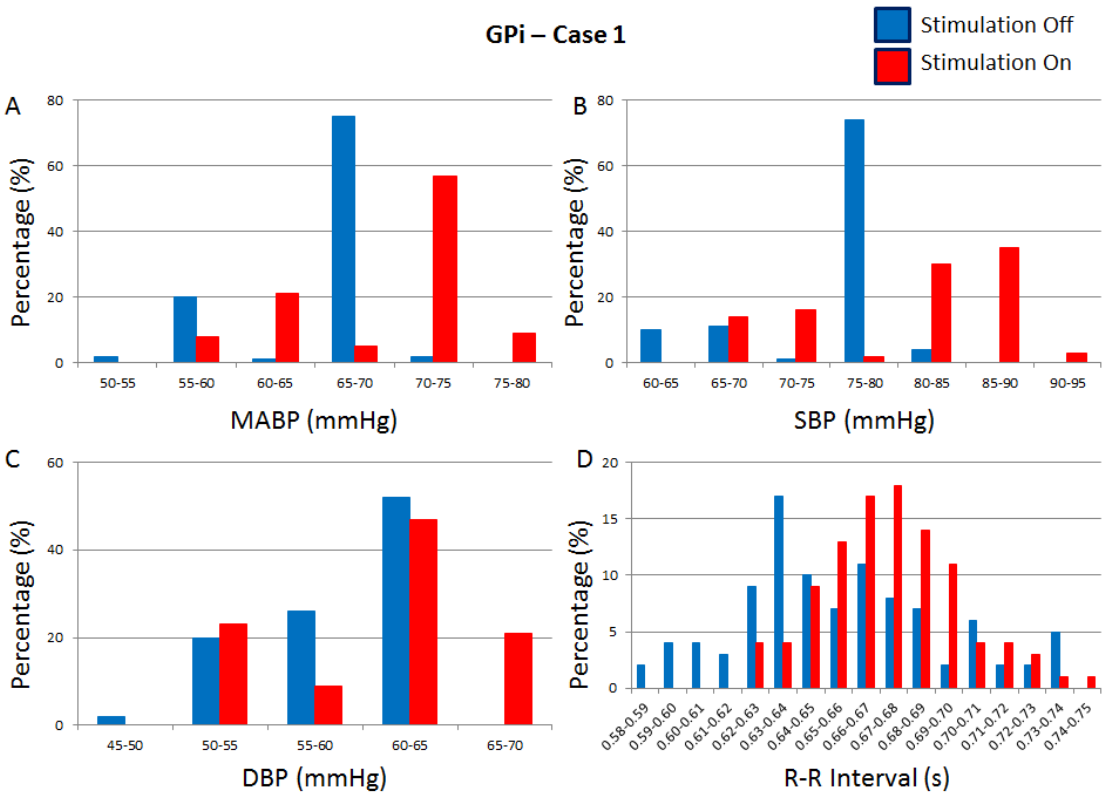

Figure 6.50 *– Graph showing the changes in variability of cardiovascular parameters during stimulation of the internal globus pallidus (GPi). (A) Stimulation appears to have little effect on the variability of mean arterial blood pressure (MABP). (B) Stimulation appears to increase the variability of systolic blood pressure (SBP). (C) Stimulation appears to have little effect on diastolic blood pressure (DBP). (D) Stimulation appears to decrease the variability of the R-R interval.*

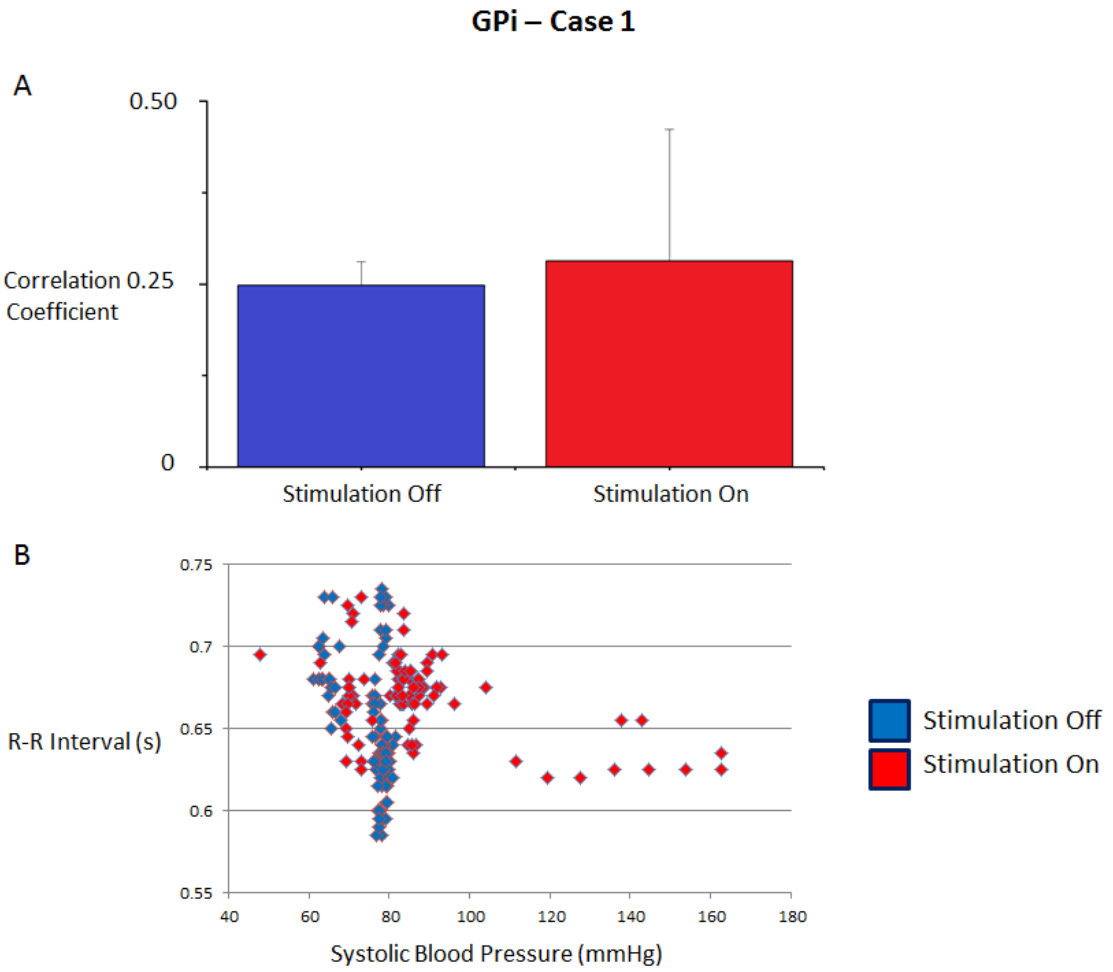

Figure 6.51 *– Graphs showing the changes in cardiac baroreflex sensitivity during stimulation of the internal globus pallidus (GPi). (A) Graph showing no significant differences in the correlation between systolic blood pressure and R-R interval (indicative of cardiac baroreflex sensitivity) during stimulation of the GPi. (B) Scatter graph showing all the data points from the entire protocol. n = 15. Error bars represent standard error of the mean.*

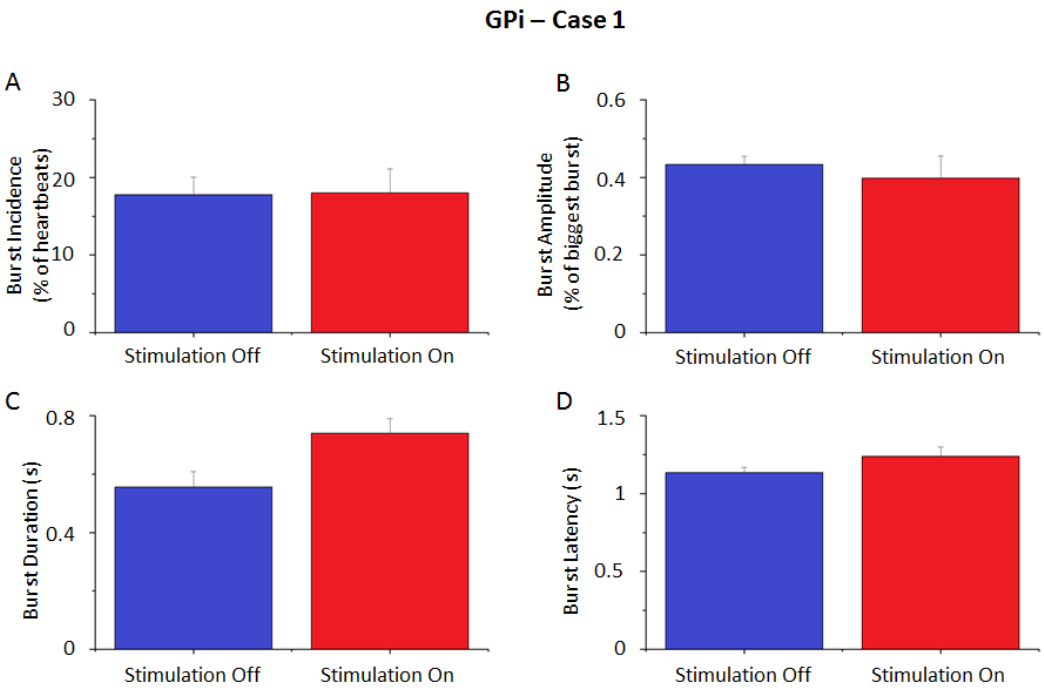

Figure 6.52 *– Graphs showing changes in muscle sympathetic nerve activity parameters during stimulation of the internal globus pallidus (GPi). There were no significant changes in (A) burst incidence, (B) burst amplitude, (C) burst duration or (D) burst latency during STN stimulation. n = 15. Error bars represent standard error of the mean.*

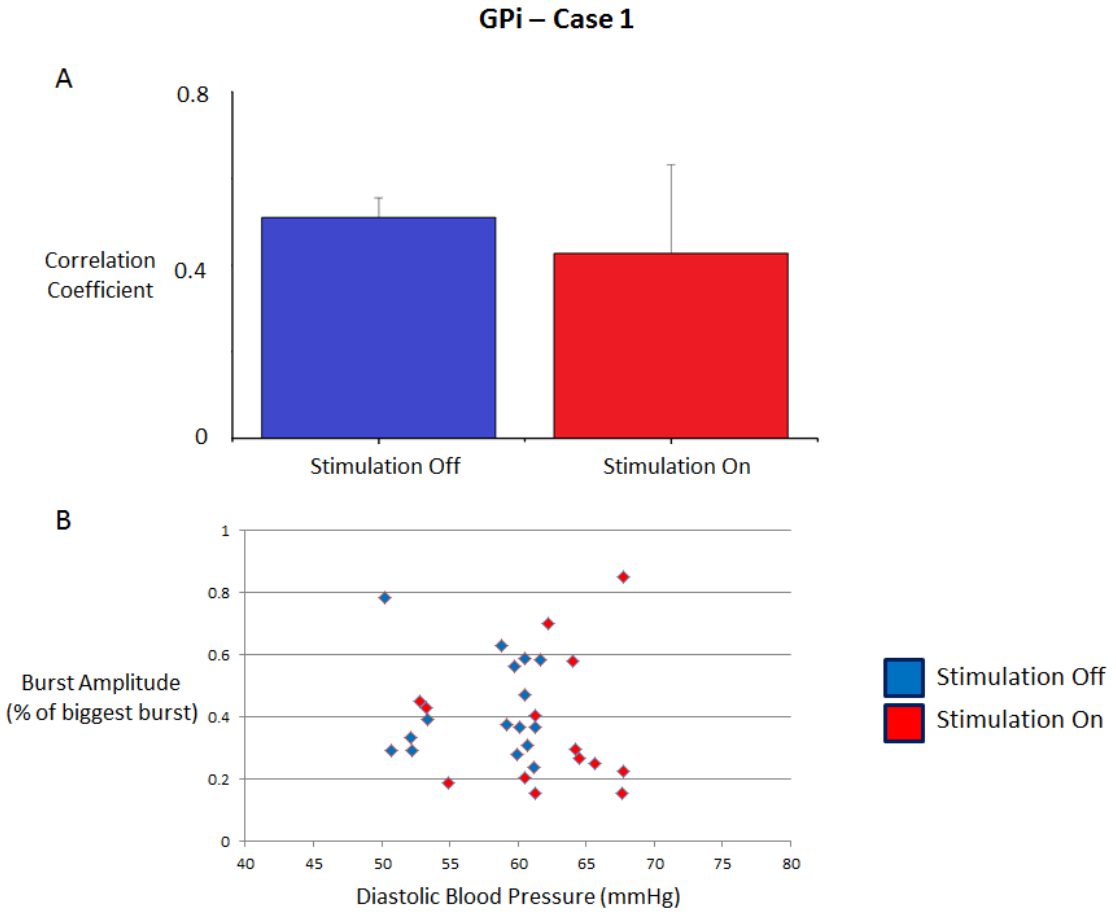

Figure 6.53 *– Graphs showing the changes in vascular baroreflex sensitivity during stimulation of the internal globus pallidus (GPi). (A) Graph showing no significant differences in the correlation between diastolic blood pressure and burst amplitude (indicative of vascular baroreflex sensitivity) during stimulation of the GPi. (B) Scatter graph showing all the data points from the entire protocol. n = 15. Error bars represent standard error of the mean.*

Anterior Cingulate Cortex Stimulation

Case 1

In this anterior cingulate cortex (ACC) patient, there was a significant decrease in mean arterial blood pressure (MABP) during stimulation compared to no stimulation of 12.2 ± 2.4 mmHg, which is equivalent to a decrease of 14.7% ($P < 0.001$, $n = 15$) (Fig. 6.54A). Similarly, during ACC stimulation, systolic blood pressure (SBP) decreased by 18.7 ± 3.1 mmHg (equivalent to a decrease of 18.2%) and diastolic blood pressure (DBP) decreased by 9.8 ± 2.0 mmHg (equivalent to a decrease of 13.9%) ($P < 0.001$ and $P < 0.001$, respectively; $n = 15$) (Figs. 6.54B-

6.54C). However, there were no significant changes in R-R interval upon ACC stimulation (P = 0.115, *n* = 15) (Fig. 6.54D). The variability of these cardiovascular parameters was also examined. It appears that stimulation of the ACC increased the variability of MABP, SBP, DBP and the R-R interval (Fig. 6.55). No significant change in cardiac baroreflex sensitivity could be detected during stimulation of the ACC (P = 0.274, *n* = 15) (Fig. 6.56).

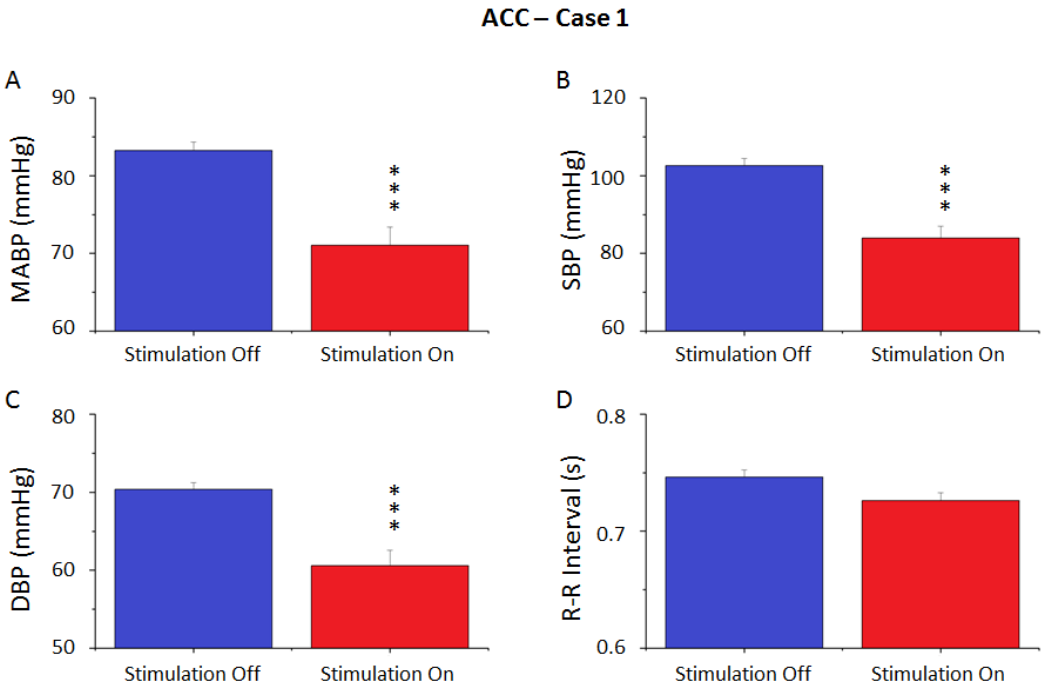

Figure 6.54 *– Graphs showing changes in cardiovascular parameters during stimulation of the anterior cingulate cortex (ACC). There was a significant decrease in (A) mean arterial blood pressure (MABP), (B) systolic blood pressure (SBP) and (C) diastolic blood pressure (DBP) during ACC stimulation. (D) There was no significant difference in R-R interval during ACC stimulation. n = 15, *** P < 0.001. Error bars represent standard error of the mean.*

Unfortunately, muscle sympathetic nerve activity could not be recorded from this patient as an appropriate recording site within the peroneal nerve could not be established.

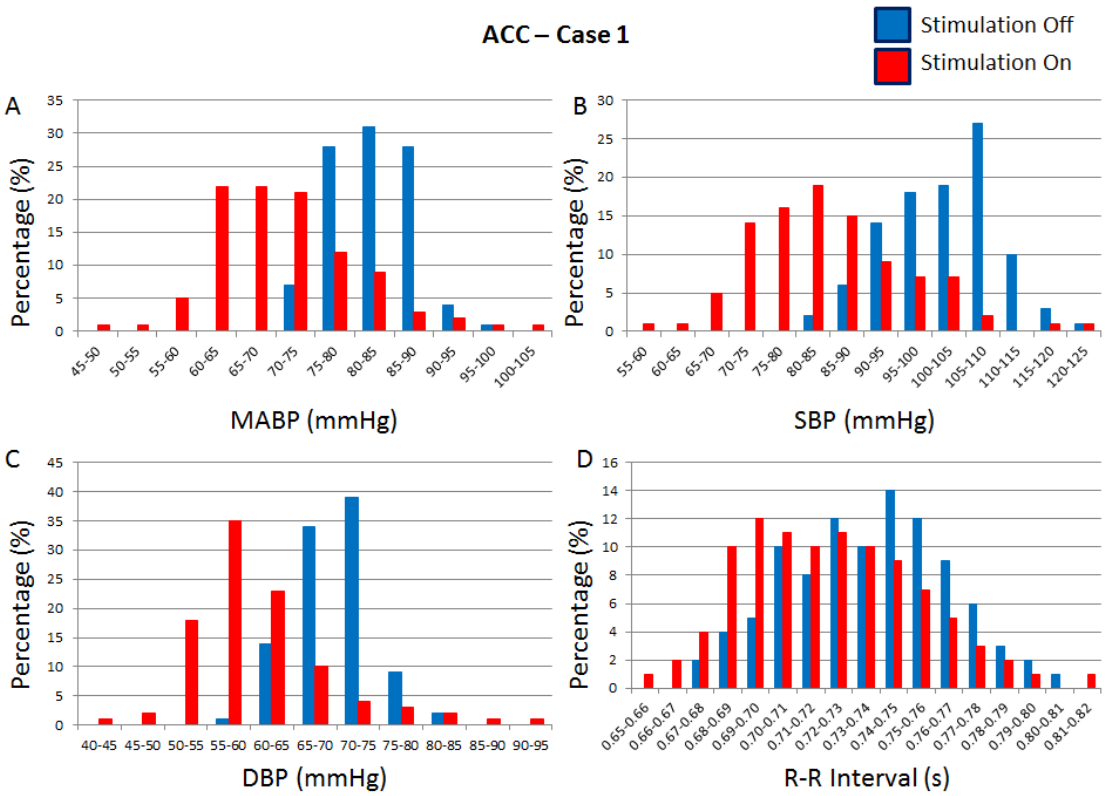

Figure 6.55 *– Graph showing the changes in variability of cardiovascular parameters during stimulation of the anterior cingulate cortex (ACC). Stimulation appears to increase the variability of (A) mean arterial blood pressure (MABP), (B) systolic blood pressure (SBP), (C) diastolic blood pressure (DBP) and (D) the R-R interval.*

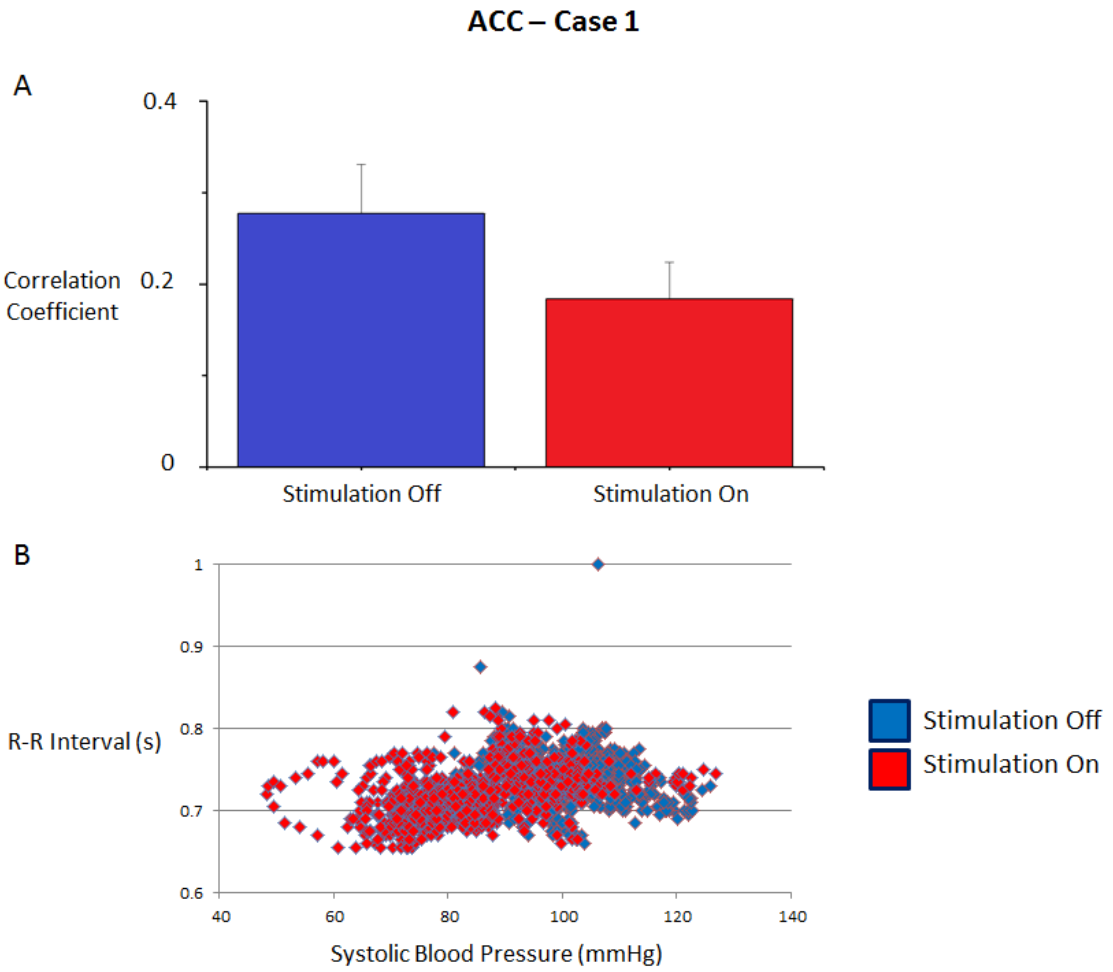

Figure 6.56 *– Graphs showing the changes in cardiac baroreflex sensitivity during stimulation of the anterior cingulate cortex (ACC). (A) Graph showing no significant differences in the correlation between systolic blood pressure and R-R interval (indicative of cardiac baroreflex sensitivity) during stimulation of the ACC. (B) Scatter graph showing all the data points from the entire protocol. n = 15. Error bars represent standard error of the mean.*

Discussion

This is the first ever study in awake humans to examine changes in muscle sympathetic nerve activity (MSNA) in response to deep brain stimulation, albeit on a case-by-case analysis. Unfortunately, the results presented in this chapter are not convincing enough to support the hypothesis that stimulation of particular subcortical structures corresponds to increases in MSNA, either in terms of burst incidence or in terms of burst amplitude. However, the cardiovascular changes that were recorded during stimulation of the different subcortical

structures are congruous with previous studies in both animal models and in humans. The experiments conducted in this chapter had several limitations, which need to be highlighted. Furthermore, although it is not possible to discuss the specific roles in the modulation of MSNA of any of the neural structures examined, I can reflect upon the rationale for hypothesising that some of these structures could be involved.

Limitations

The most obvious limitation in this study was the difficulty in finding an appropriate recording site for monitoring muscle sympathetic nerve activity (MSNA) within the peroneal nerve. Many of the patients in whom recording sites could not be established were intolerant to the insertion of the recording electrode. Therefore, in most cases if the recording site could not be established on the first attempt, the patients were reluctant to allow a second or third attempt. This study clearly needs to be expanded and performed with more patients.

It could also be argued that one cannot be certain of the positional accuracy when establishing a recording site within the peroneal nerve. The quality of the MSNA recording is based on the proximity of the tip of the electrode to the sympathetic nerve bundle (Lambert *et al*, 2008). Therefore, considerable time was spent making minute adjustments in the positioning of the electrode to ensure the best possible recording site, before the start of the experimental protocol. Moreover, one cannot be certain whether the recordings were from afferent or efferent nerves, nor whether they were muscle sympathetic nerves or skin sympathetic nerves. This was assessed by passively contracting the foot and listening for an afferent signal, and by lightly stroking the skin of the foot and ensuring the absence of an afferent signal. MSNA is also known to display strict cardiac rhythmicity (Lambert *et al*, 2008). Furthermore, MSNA is known to increase during breath-holding and manoeuvres designed to increase intra-thoracic pressure, such as Valsalva's manoeuvre (Mano *et al*, 2006), both of which were

performed by the patients in order to confirm the correctness of the recording site. On the other hand, skin sympathetic nerve activity can be elicited by mental stress or by sensory stimuli, such as sound (Mano *et al*, 2006). Therefore, a loud and unexpected noise was made to startle the patients, in order to confirm that the recordings were not from skin sympathetic nerves.

A possible limitation is the underlying pathology within the patient model. There is no evidence that the periaqueductal grey (PAG) is dysfunctional in the patients suffering from chronic pain, although it is understood that the subthalamic nucleus (STN) is affected in the patients suffering from Parkinson's disease (DeLong and Wichmann, 2007; Benarroch, 2008). This makes it challenging to translate the findings to healthy humans. Furthermore, the specific nuclei investigated in this experiment were limited, as only sites that provided therapeutic benefit to the patients could be stimulated. Nevertheless, the nuclei that were stimulated have all been identified as being cardiovascularly active. Additionally, without histological data, the precise location of the electrodes within the various nuclei can only be estimated, despite their careful placement using stereotactic coordinates.

Muscle Sympathetic Nerve Activity Is Modulated By Two Different Neural Sites

Kienbaum *et al* (2001) postulated that, in humans, two separate sites within the central nervous system were responsible for the control of muscle sympathetic nerve activity (MSNA) – one site responsible for the regulation of sympathetic burst incidence, i.e. whether or not a burst occurs, and another responsible for the regulation of sympathetic burst amplitude, i.e. the strength of the discharge. They observed that while the burst incidence in muscle sympathetic neurons was precisely linked to arterial blood pressure, burst amplitude had a poor relationship to arterial blood pressure. This implies that blood pressure changes at rest are compensated for, in terms of sympathetic activity, mostly by changes in burst incidence. It

also indicates that the baroreflex mechanisms responsible for the control of burst incidence and burst strength are differentiated.

Additionally, there have been other studies which have suggested differentiated regulation of burst incidence and burst amplitude. Hjemdahl *et al* (1989) observed increased burst amplitude in humans undergoing mental stress, but no variations in burst incidence. Malpas and Ninomiya (1992a; 1992b) demonstrated differentiated control of renal sympathetic activity in cats. DiBona *et al* (1997) showed that arterial baroreflex activation results in decreased renal sympathetic activity mostly by decreased burst amplitude, but not burst incidence, in both Wistar-Kyoto rats and spontaneously hypertensive rats. DiBona and Jones (1998) observed that heat stimulation in rats causes increased burst amplitude, whereas acute loading volume causes decreased burst amplitude. However, burst incidence remains unchanged in both cases. Sverrisdottir *et al* (2000) showed that in humans suffering from congestive heart failure, there was increased burst incidence and increased burst amplitude. However, in age-matched healthy subjects, there was increased burst incidence but no variation in burst amplitude.

The precise mechanisms of this differentiated control of burst incidence and burst amplitude have not yet been established (McAllen and Malpas, 1997). Kienbaum *et al* (2001) proposed a model in which afferent baroreceptor activity is thought to influence two separate central nervous system sites. They proposed that at one site the arterial baroreceptor afferent input might act together with other afferent inputs in order to cause a graded MSNA effect, which would be dependent on the strength of the respective input. At a separate site, the baroreceptor afferent input might act as a 'gate control', only allowing the descending sympathetic impulse to transmit across the synapse depending on its strength and character.

The experiments in this chapter were conducted in the hope of identifying these two hypothetical control sites. It was anticipated that, in particular, the periaqueductal grey and/or

the subthalamic nucleus could be involved in the modulation of MSNA, given their key roles in the cardiovascular responses to exercise, i.e. in the integration of the exercise pressor reflex and central command.

Role of the Periaqueductal Grey in the Modulation of Muscle Sympathetic Nerve Activity

The findings presented with regards to the changes in muscle sympathetic nerve activity (MSNA) during periaqueductal grey (PAG) stimulation are inconclusive. Unfortunately, MSNA could only be recorded from one of the four PAG patients, due to the difficulty of obtaining appropriate recordings sites within the peroneal nerve. In the patient from whom MSNA was recorded (Case 2), PAG stimulation was associated with a slight decrease in burst latency; there was no difference in burst incidence or in burst amplitude. Additionally, there was no change in baroreflex sensitivity during stimulation.

In terms of the changes in cardiovascular parameters during PAG stimulation, the data were, once again, inconclusive. In Case 1 and Case 2, there were no significant changes in arterial blood pressure, but in both cases R-R interval decreased, i.e. the heart rate increased, during stimulation. This is partially consistent with the work of Green *et al* (2005), who demonstrated that in some subjects PVG (periventricular grey)/PAG stimulation caused no significant changes in arterial blood pressure. However, they found that R-R interval always remained unchanged during stimulation regardless of the effects on arterial blood pressure. In Case 3 and Case 4, arterial blood pressure decreased during PAG stimulation, which is also consistent with what Green *et al* (2005) demonstrated, in that stimulation of the ventral PVG/PAG can result in decreased arterial blood pressure. In Case 4, in which the graded protocol was followed, a significant decrease was only observed at 2 V stimulation, and not at 1 V or 3 V.

The PAG was a strong candidate for playing a role in modulation of MSNA due to the vital role it plays in the integration of the exercise pressor reflex. Alam and Smirk (1937) suggested that the chemical by-products of muscle contraction caused a pressor response to exercise. It is well established that when this metaboreflex component of the exercise pressor reflex is activated, sympathetic tone is dramatically increased and is directed to skeletal muscle vasculature (Mark *et al*, 1985; Mitchell and Victor, 1996; Boushel, 2010).

Mark *et al* (1985) were the first researchers to study MSNA in humans during static exercise tasks. They recorded MSNA from the peroneal nerve at rest and during static handgrip contraction at 30% of the subject's maximum voluntary contraction. They observed a delay of almost one minute in the onset of increased MSNA, which was maintained until the exercise task ended, at which point MSNA returned to resting values. They also noted that if blood flow was occluded at the end of the exercise task, the MSNA remained elevated even though exercise had stopped, suggesting that the metaboreflex component of the exercise pressor reflex, and not the mechanoreflex or central command, was predominantly responsible for maintaining the increase in MSNA during static exercise.

Further experiments have been conducted since this pioneering study showing similar results, both in static exercise and in dynamic exercise (Victor *et al*, 1987; Sinoway *et al*, 1988; Victor and Seals, 1989; Wallin *et al*, 1989; Saito *et al*, 1993b; Hansen *et al*, 1994). However, some studies have shown a decrease in MSNA during dynamic exercise (Ray *et al*, 1993; Ray *et al*, 1994); this was perhaps due to the low intensity level of the dynamic exercise tasks, as metaboreflex-mediated MSNA has been shown to be dependent on exercise intensity (Seals *et al*, 1988; Ray and Mark, 1993; Saito *et al*, 1993a). More specifically, it appears that increases in MSNA are only observed during moderate to severe dynamic exercise, and not during mild dynamic exercise.

The close relationship between MSNA and the metaboreflex has been further evidenced by studies which demonstrate the latent onset of increased MSNA coinciding with increased metabolic products of exercise within the muscle, measured with ^{31}P magnetic resonance spectroscopy (Victor *et al*, 1988; Sinoway *et al*, 1989; Sinoway *et al*, 1994).

Role of the Subthalamic Nucleus in the Modulation of Muscle Sympathetic Nerve Activity

The findings presented with regards to the changes in muscle sympathetic nerve activity (MSNA) during subthalamic nucleus (STN) stimulation are also inconclusive. Although MSNA was recorded from all four of the STN patients, only one patient showed any significant changes in MSNA during stimulation. In this patient (Case 2), STN stimulation was associated with an increase in burst incidence; there was no change in burst amplitude. There was also no change in baroreflex sensitivity during stimulation in this patient.

In terms of changes in cardiovascular parameters during STN stimulation, the results were inconsistent. In Case 2 and Case 3, there were no significant changes in arterial blood pressure or in R-R interval during stimulation. Thornton *et al* (2002) noted that during low frequency stimulation of the STN (i.e. 14 ± 9 Hz), there was no effect on mean arterial blood pressure or heart rate, and that during high frequency stimulation of the STN (i.e. 100 ± 3 Hz), both the mean arterial blood pressure and the heart rate increased significantly. However, in Case 2 stimulation was at 150 Hz and in Case 3 stimulation was at 130 Hz, both which can be classified as 'high frequency stimulation'. In Case 1, there was a significant decrease in arterial blood pressure and a significant increase in R-R interval (i.e. a decrease in heart rate) during STN stimulation. In Case 4, there was a significant increase in arterial blood pressure during STN stimulation, which is consistent with what Thornton *et al* (2002) observed. This inconsistency in cardiovascular responses to stimulation of the STN has been previously

documented in both animal models (Spencer *et al*, 1988; Angyan and Angyan, 1999b) and in human subjects (Kaufmann *et al*, 2002; Benedetti *et al*, 2004).

The STN was a strong candidate for playing a role in modulation of MSNA due to the vital role it appears to play in the integration of central command. Experiments using neuromuscular blockade have shown that central command can increase MSNA, even when uncoupled from the effects of the exercise pressor reflex. Victor *et al* (1989a) was one of the first groups to conduct such an experiment. Subjects were asked to perform static handgrip exercise at 15% of their maximum voluntary contraction (MVC), which had no effect on MSNA. Subjects were then asked to perform static handgrip exercise at 30% MVC, which resulted in the typical slow progressive rise in MSNA. During attempted static handgrip exercise following partial neuromuscular blockade with curare, MSNA increased modestly as the patient fatigued, even when the generated force had fallen to zero.

The same group (Victor *et al*, 1995) also investigated the effects of central command on MSNA during intermittent episodes of static exercise. Subjects were asked to contract their forearm muscles for three seconds and then release for nine seconds, repeatedly. Contractions were performed at 25%, 50% and 75% MVC. They showed that during 75% intermittent static handgrip, each contraction was accompanied by bursts of MSNA; in other words, the neural activity appeared to be synchronised with the muscle contraction. This synchronisation was not present at 25% or 50% intermittent static handgrip. The synchronisation at 75% MVC was unlikely to be a result of the muscle metaboreflex, as the onset of this reflex has a latency of almost a minute (Victor *et al*, 1995; Mitchell and Victor, 1996). Following partial neuromuscular blockade with curare, synchronisation between neural activity and attempted contraction was observed, even when the force actually generated was less than 25% MVC. This indicates a key role for central command in the modulation of MSNA.

Roles of Other Nuclei in the Modulation of Muscle Sympathetic Nerve Activity

With regards to the rest of the patients who were studied (two sensory thalamus patients, one internal globus pallidus patient [GPi] and one anterior cingulate cortex [ACC] patient), there was no effect on MSNA during stimulation in those patients in whom a suitable recording site could be established. Similarly, there were no changes in baroreflex sensitivity during stimulation.

In one of the sensory thalamus patients (Case 1), there were no changes in cardiovascular parameters during thalamic stimulation. However, in the other patient (Case 2), a graded protocol was followed, and although there were no significant changes in mean arterial blood pressure at any of the amplitudes of stimulation, there were significant variations in systolic and diastolic blood pressure. There was also a small decrease in R-R interval (i.e. increase in heart rate) at 4 V stimulation. Thornton *et al* (2002) demonstrated increased mean arterial blood pressure and increased heart rate during high frequency stimulation of the sensory thalamus in humans. In the GPi patient, there were no changes in cardiovascular parameters during stimulation. In the ACC patient, there was a significant decrease in arterial blood pressure during stimulation, but no change in R-R interval. This depressor response to ACC stimulation has been shown in both anaesthetised and non-anaesthetised rats (Burns and Wyss, 1985).

Conclusion

In conclusion, using direct electrical stimulation, this study provides preliminary evidence that could suggest a role for the STN in the modulation of MSNA in humans, particularly in terms of burst incidence. However, it is essential that further experiments are conducted in order to verify (1) the involvement of the STN and (2) the involvement of the other nuclei, stimulation of which, in this instance, had no effect on MSNA.

CHAPTER 7

Conclusion

The concept of a link between the central and peripheral nervous systems during exercise has been supported by almost a centuries worth of experiments, since the classical studies of Krogh and Lindhard (1913), Alam and Smirk (1937), Coote *et al* (1971), McCloskey and Mitchell (1972), and Goodwin *et al* (1972). Furthermore, there is a wealth of data from both animal and human models attempting to identify the specific neural circuitry involved in cardiovascular control during exercise. The studies included in this thesis have used the technique of deep brain stimulation to provide evidence to suggest that both the periaqueductal grey (PAG) and the subthalamic nucleus (STN) are major sites of integration of the cardiovascular responses during exercise in humans (Fig. 7.1).

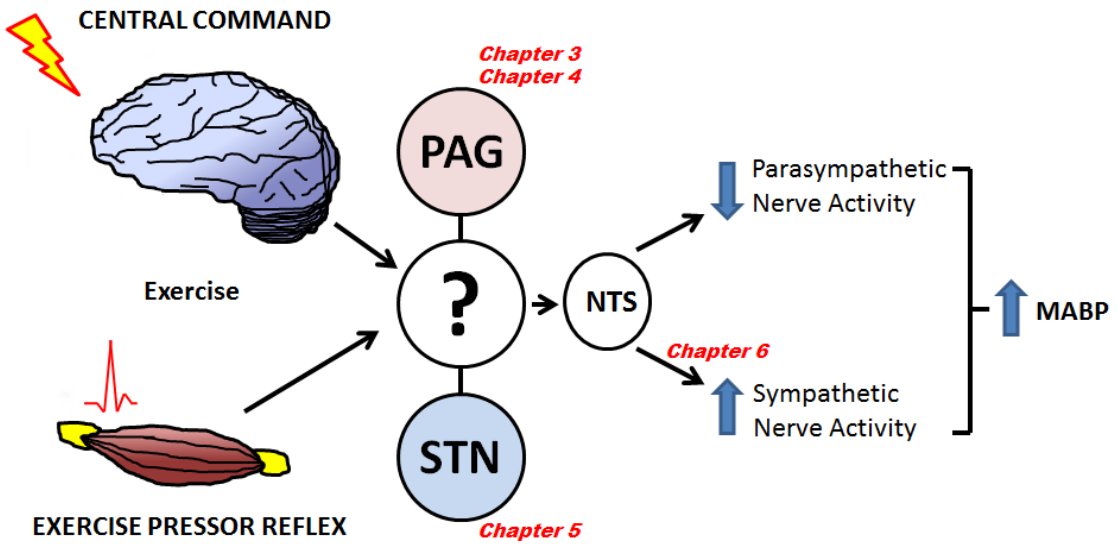

Figure 7.1 – *Hypothesised neurocircuitry for the neural control of the cardiovascular system during exercise, with reference to the studies carried out as part of this thesis.*

Considering existing data identifying detailed neurocircuitry in small animal models and the measurements of neuropeptides from these circuits during simulated exercise, together with

Chapters 3 and 4 of this thesis, the PAG appears to be a key site of integration of the exercise pressor reflex; in particular the dorsolateral PAG in animals (Lovick, 1985; Bandler and Carrive, 1988; Horiuchi *et al*, 2009) and the dorsal PVG (periventricular grey)/PAG in humans (Green *et al*, 2007). I have demonstrated that the exercise pressor reflex is associated with significant increases in dorsal PAG activity, and that this response is graded to exercise intensity and is greater during ischaemic exercise.

With regards to the STN, previous studies taken together with Chapter 5 of this thesis provide evidence to suggest that it is involved in the parallel activation of the cardiovascular and the locomotor systems (Smith *et al*, 1960; Eldridge *et al*, 1981; Thornton *et al*, 2002; Angyan and Angyan, 2003). I have shown that the STN is not only involved in the control of movement, but is also an important aspect of the circuitry underpinning the cardiovascular responses to exercise. It appears to be a key component of the neurocircuitry responsible for integrating central command. I have also provided evidence to suggest that the STN is involved in the neurogenic pathway of the remote ischaemic preconditioning stimulus. Furthermore, I have been able to suggest a role for the STN in the modulation of muscle sympathetic nerve activity burst incidence.

Although the PAG and STN may not be the “command” sites controlling the exercise pressor reflex and central command responses, these nuclei have all the properties of being key integrating sites or relay stations within the neural pathways controlling the cardiovascular responses to exercise.

CHAPTER 8

References

Abols IA & Basbaum AI (1981). Afferent connections of the rostral medulla of the cat: a neural substrate for midbrain-medullary interactions in the modulation of pain. *J Comp Neurol* **201**, 285-297.

Abrahams VC, Hilton SM & Zbrozyna A (1960). Active muscle vasodilatation produced by stimulation of the brain stem: it significance in the defence reaction. *J Physiol* **154**, 491-513.

Adreani CM, Hill JM & Kaufman MP (1997). Responses of group III and IV muscle afferents to dynamic exercise. *J Appl Physiol* **82**, 1811-1817.

Alam M & Smirk FH (1937). Observations in man upon a blood pressure raising reflex arising from the voluntary muscles. *J Physiol* **89**, 372-383.

Ally A (1998). Ventrolateral medullary control of cardiovascular activity during muscle contraction. *Neurosci Biobehav Rev* **23**, 65-86.

Andersen P & Saltin B (1985). Maximal perfusion of skeletal muscle in man. *J Physiol* **366**, 233-249.

Angyan L & Angyan Z (1999a). Characterization of cardiorespiratory responses to electrical stimulation of the globus pallidus in cat. *Physiol Behav* **66**, 53-58.

Angyan L & Angyan Z (1999b). Subthalamic influences on the cardiorespiratory functions in the cat. *Brain Res* **847**, 130-133.

Angyan Z & Angyan L (2003). Differential blood pressure and heart rate responses to supramedullary brain stimulation in cats. *Acta Physiol Hung* **90**, 9-16.

Armstrong RB, Delp MD, Goljan EF & Laughlin MH (1987). Distribution of blood flow in muscles of miniature swine during exercise. *J Appl Physiol* **62**, 1285-1298.

Armstrong RB & Laughlin MH (1984). Exercise blood flow patterns within and among rat muscles after training. *Am J Physiol* **246**, H59-H68.

Asmussen E, Johansen SH, Jorgensen M & Nielsen M (1965). On the nervous factors controlling respiration and circulation during exercise. Experiments with curarization. *Acta Physiol Scand* **63**, 343-350.

Awan NR, Lozano A & Hamani C (2009). Deep brain stimulation: current and future perspectives. *Neurosurg Focus* **27**, E2.

Aziz TZ, Peggs D, Sambrook MA & Crossman AR (1991). Lesion of the subthalamic nucleus for the alleviation of 1-methyl-4-phenyl-1,2,3,6-tetrahydropyridine (MPTP)-induced parkinsonism in the primate. *Mov Disord* **6**, 288-292.

Bailey SP, Hall EE, Folger SE & Miller PC (2008). Changes in EEG during graded exercise on a recumbent cycle ergometer. *Journal of Sports Science and Medicine* **7**, 505-511.

Bandler R & Carrive P (1988). Integrated defence reaction elicited by excitatory amino acid microinjection in the midbrain periaqueductal grey region of the unrestrained cat. *Brain Res* **439**, 95-106.

Bandler R, Carrive P & Depaulis A (1991). Emerging principles of organization in the midbrain periaqueductal gray matter. In *The Midbrain periaqueductal gray matter: functional, anatomical, and neurochemical organization / edited by A Depaulis & R Bandler. New York; London: Plenum*, pp. 1-8.

Bandler R, Keay KA, Floyd N & Price J (2000). Central circuits mediating patterned autonomic activity during active vs. passive emotional coping. *Brain Res Bull* **53**, 95-104.

Bauer RM, Iwamoto GA & Waldrop TG (1989). Ventrolateral medullary neurons modulate pressor reflex to muscular contraction. *Am J Physiol Regul Integr Comp Physiol* **257**, R1154-R1161.

Behbehani MM (1995). Functional characteristics of the midbrain periaqueductal gray. *Prog Neurobiol* **46**, 575-605.

Beitz AJ (1985). The midbrain periaqueductal gray in the rat. I. Nuclear volume, cell number, density, orientation, and regional subdivisions. *J Comp Neurol* **237**, 445-459.

Beitz AJ, Mullett MA & Weiner LL (1983). The periaqueductal gray projections to the rat spinal trigeminal, raphe magnus, gigantocellular pars alpha and paragigantocellular nuclei arise from separate neurons. *Brain Res* **288**, 307-314.

Benabid AL, Pollak P, Gervason C, Hoffmann D, Gao DM, Hommel M, Perret JE & de Rougemont J (1991). Long-term suppression of tremor by chronic stimulation of the ventral intermediate thalamic nucleus. *Lancet* **337**, 403-406.

Benarroch EE (2008). Subthalamic nucleus and its connections: anatomic substrate for the network effects of deep brain stimulation. *Neurology* **70**, 1991-1995.

Benazzouz A, Gross C, Feger J, Boraud T & Bioulac B (1993). Reversal of rigidity and improvement in motor performance by subthalamic high-frequency stimulation in MPTP-treated monkeys. *Eur J Neurosci* **5**, 382-389.

Benazzouz A & Hallett M (2000). Mechanism of action of deep brain stimulation. *Neurology* **55**, S13-S16.

Benedetti F, Colloca L, Lanotte M, Bergamasco B, Torre E & Lopiano L (2004). Autonomic and emotional responses to open and hidden stimulations of the human subthalamic region. *Brain Res Bull* **63**, 203-211.

Bergman H, Wichmann T & DeLong MR (1990). Reversal of experimental parkinsonism by lesions of the subthalamic nucleus. *Science* **249**, 1436-1438.

Birnbaum Y, Hale SL & Kloner RA (1997). Ischemic preconditioning at a distance: reduction of myocardial infarct size by partial reduction of blood supply combined with rapid stimulation of the gastrocnemius muscle in the rabbit. *Circulation* **96**, 1641-1666.

Bittar RG, Kar-Purkayastha I, Owen SL, Bear RE, Green A, Wang S & Aziz TZ (2005). Deep brain stimulation for pain relief: a meta-analysis. *J Clin Neurosci* **12**, 515-519.

Boushel R (2010). Muscle metaboreflex control of the circulation during exercise. *Acta Physiol (Oxf)* **199**, 367-383.

Brazier MA, Cobb WA, Fischgold H, Gastaut H, Gloor P, Hess R, Jasper H, Loeb C, Magnus O, Pampiglione G, Remond A, Storm van Leeuwen W & Grey Walter W (1961). Preliminary proposal for an EEG terminology by the Terminology Committee of the International Federation for Electroencephalography and Clinical Neurophysiology. *Electroencephalogr Clin Neurophysiol* **13**, 646-650.

Brown MC, Engberg I & Matthews PB (1967). The relative sensitivity to vibration of muscle receptors of the cat. *J Physiol* **192**, 773-800.

Burns SM & Wyss JM (1985). The involvement of the anterior cingulate cortex in blood pressure control. *Brain Res* **340**, 71-77.

Calaresu FR, Faiers AA & Mogenson GJ (1975). Central neural regulation of heart and blood vessels in mammals. *Prog Neurobiol* **5**, 1-35.

Calaresu FR & Yardley CP (1988). Medullary basal sympathetic tone. *Annu Rev Physiol* **50**, 511-524.

Cameron AA, Khan IA, Westlund KN, Cliffer KD & Willis WD (1995). The efferent projections of the periaqueductal gray in the rat: a Phaseolus vulgaris-leucoagglutinin study. I. Ascending projections. *J Comp Neurol* **351**, 568-584.

Carrive P (1993). The periaqueductal gray and defensive behaviour: functional representation and neuronal organization. *Behav Brain Res* **58**, 27-47.

Carrive P & Bandler R (1991a). Control of extracranial and hindlimb blood flow by the midbrain periaqueductal grey of the cat. *Exp Brain Res* **84**, 599-606.

Carrive P & Bandler R (1991b). Viscerotopic organization of neurons subserving hypotensive reactions within the midbrain periaqueductal grey: a correlative functional and anatomical study. *Brain Res* **541**, 206-215.

Carrive P, Bandler R & Dampney RAL (1988). Anatomical evidence that hypertension associated with the defence reaction in the cat is mediated by a direct projection from a restricted portion of the midbrain periaqueductal grey to the subretrofacial nucleus of the medulla. *Brain Res* **460**, 339-345.

Carrive P, Bandler R & Dampney RAL (1989). Viscerotopic control of regional vascular beds by discrete groups of neurons within the midbrain periaqueductal grey. *Brain Res* **493**, 385-390.

Carrive P, Dampney RA & Bandler R (1987). Excitation of neurones in a restricted portion of the midbrain periaqueductal grey elicits both behavioural and cardiovascular components of the defence reaction in the unanaesthetised decerebrate cat. *Neurosci Lett* **81**, 273-278.

Castiglioni P, Parati G, Omboni S, Mancia G, Imholz BP, Wesseling KH & Di Rienzo M (1999). Broad-band spectral analysis of 24 h continuous finger blood pressure: comparison with intra-arterial recordings. *Clin Sci* **97**, 129-139.

Chang JY, Shi LH, Luo F & Woodward DJ (2006). Neural responses in multiple basal ganglia regions following unilateral dopamine depletion in behaving rats performing a treadmill locomotion task. *Exp Brain Res* **172**, 193-207.

Cheung MM, Kharbanda RK, Konstantinov IE, Shimizu M, Frndova H, Li J, Holtby HM, Cox PN, Smallhorn JF, Van Arsdell GS & Redington AN (2006). Randomized controlled trial of the effects of remote ischemic preconditioning on children undergoing cardiac surgery: first clinical application in humans. *J Am Coll Cardiol* **47**, 2277-2282.

Ciriello J & Calaresu FR (1981). Projections from buffer nerves to the nucleus of the solitary tract: an anatomical and electrophysiological study in the cat. *J Auton Nerv Syst* **3**, 299-310.

Ciriello J, Caverson MM & Polosa C (1986). Function of the ventrolateral medulla in the control of the circulation. *Brain Res* **11**, 359-391.

Cohen MV, Liu GS & Downey JM (1991). Preconditioning causes improved wall motion as well as smaller infarcts after transient coronary occlusion in rabbits. *Circulation* **84**, 341-349.

Collins HL, Augustyniak RA, Ansorge EJ & O'Leary DS (2001). Carotid baroreflex pressor responses at rest and during exercise: cardiac output vs. regional vasoconstriction. *Am J Physiol Heart Circ Physiol* **280**, H642-H648.

Coote JH (1995). Cardiovascular function of the paraventricular nucleus of the hypothalamus. *Biol Signals* **4**, 142-149.

Coote JH, Hilton SM & Perez-Gonzalez JF (1971). The reflex nature of the pressor response to muscular exercise. *J Physiol* **215**, 789-804.

Coote JH, Hilton SM & Zbrozyna AW (1973). The ponto-medullary area integrating the defence reaction in the cat and its influence on muscle blood flow. *J Physiol* **229**, 257-274.

Craig AD & Mense S (1983). The distribution of afferent fibers from the gastrocnemius-soleus muscle in the dorsal horn of the cat, as revealed by the transport of horseradish peroxidase. *Neurosci Lett* **41**, 233-238.

Crayton SC, Mitchell JH & Payne FC III (1981). Reflex cardiovascular response during injection of capsaicin into skeletal muscle. *Am J Physiol* **240**, H315-H319.

Critchley HD, Melmed RN, Featherstone E, Mathias CJ & Dolan RJ (2001). Brain activity during biofeedback relaxation: a functional neuroimaging investigation. *Brain* **124**, 1003-1012.

Dampney RA (1994). Functional organization of central pathways regulating the cardiovascular system. *Physiol Rev* **74**, 323-364.

Dampney RA, Coleman MJ, Fontes MA, Hirooka Y, Horiuchi J, Li YW, Polson JW, Potts PD & Tagawa T (2002). Central mechanisms underlying short- and long-term regulation of the cardiovascular system. *Clin Exp Pharmacol Physiol* **29**, 261-268.

Dampney RA, Czachurski J, Dembowsky K, Goodchild AK & Seller H (1987). Afferent connections and spinal projections of the pressor region in the rostral ventrolateral medulla of the cat. *J Auton Nerv Syst* **20**, 73-86.

Dampney RA, Goodchild AK & Tan E (1985). Vasopressor neurons in the rostral ventrolateral medulla of the rabbit. *J Auton Nerv Syst* **14**, 239-254.

Dampney RA, Horiuchi J & McDowall LM (2008). Hypothalamic mechanisms coordinating cardiorespiratory function during exercise and defensive behaviour. *Auton Neurosci* **142**, 3-10.

De Castro F (2009). The discovery of sensory nature of the carotid bodies—invited article. *Adv Exp Med Biol* **648**, 1-18.

De Gail P, Lance JW & Neilson PD (1966). Differential effects on tonic and phasic reflex mechanisms produced by vibration of muscles in man. *J Neurol Neurosurg Psychiatry* **29**, 1-11.

Delius W, Hagbarth KE, Hongell A & Wallin BG (1972). Manoeuvres affecting sympathetic outflow in human muscle nerves. *Acta Physiol Scand* **84**, 82-94.

DeLong MR & Wichmann T (2007). Circuits and circuit disorders of the basal ganglia. *Arch Neurol* **64**, 20-24.

Delp MD & Laughlin MH (1998). Regulation of skeletal muscle perfusion during exercise. *Acta Physiol Scand* **162**, 411-419.

Delp MD & O'Leary DS (2004). Integrative control of the skeletal muscle microcirculation in the maintenance of arterial pressure during exercise. *J Appl Physiol* **97**, 1112-1118.

Dennis SG, Choiniere M & Melzack R (1980). Stimulation-produced analgesia in rats: assessment by two pain tests and correlation with self-stimulation. *Exp Neurol* **68**, 295-309.

DiBona GF & Jones SY (1998). Reflex effects on components of synchronized renal sympathetic nerve activity. *Am J Physiol Renal Physiol* **275**, F441-F446.

DiBona GF, Jones SY & Sawin LL (1997). Reflex effects on renal nerve activity characteristics in spontaneously hypertensive rats. *Hypertension* **30**, 1089-1096.

Dickson EW, Lorbar M, Porcaro WA, Fenton RA, Reinhardt CP, Gysembergh A & Przyklenk K (1999). Rabbit heart can be "preconditioned" via transfer of coronary effluent. *Am J Physiol* **277**, H2451-2457.

Duggan AW & Morton CR (1983). Periaqueductal grey stimulation: an association between selective inhibition of dorsal horn neurones and changes in peripheral circulation. *Pain* **15**, 237-248.

Eckert S & Horstkotte D (2002). Comparison of Portapres non-invasive blood pressure measurement in the finger with intra-aortic pressure measurement during incremental bicycle exercise. *Blood Press Monit* **7**, 179-183.

Eldridge FL, Millhorn DE, Kiley JP & Waldrop TG (1985). Stimulation by central command of locomotion, respiration and circulation during exercise. *Respir Physiol* **59**, 313-337.

Eldridge FL, Millhorn DE & Waldrop TG (1981). Exercise hyperpnea and locomotion: parallel activation from the hypothalamus. *Science* **211**, 844-846.

Fadel PJ (2008). Arterial baroreflex control of the peripheral vasculature in humans: rest and exercise. *Med Sci Sports Exerc* **40**, 2055-2062.

Fagius J & Wallin BG (1993). Long-term variability and reproducibility of resting human muscle nerve sympathetic activity at rest, as reassessed after a decade. *Clin Auton Res* **3**, 201-205.

Farkas E, Jansen AS & Loewy AD (1997). Periaqueductal gray matter projection to vagal preganglionic neurons and the nucleus tractus solitarius. *Brain Res* **764**, 257-261.

Farkas E, Jansen AS & Loewy AD (1998). Periaqueductal gray matter input to cardiac-related sympathetic premotor neurons. *Brain Res* **792**, 179-192.

Fernandes A, Galbo H, Kjaer M, Mitchell JH, Secher NH & Thomas SN (1990). Cardiovascular and ventilatory responses to dynamic exercise during epidural anaesthesia in man. *J Physiol* **420**, 281-293.

Fink GR, Adams L, Watson JD, Innes JA, Wuyam B, Kobayashi I, Corfield DR, Murphy K, Jones T, Frackowiak RS & Guz A (1995). Hyperpnoea during and immediately after exercise in man: evidence of motor cortical involvement. *J Physiol* **489**, 663-675.

Finnegan TF, Chen SR & Pan HL (2005). Effect of the μ opioid on excitatory and inhibitory synaptic inputs to periaqueductal gray-projecting neurons in the amygdale. *J Pharmacol Exp Ther* **312**, 441-448.

Francois C, Savy C, Jan C, Tande D, Hirsch EC & Yelnik J (2000). Dopaminergic innervations of the subthalamic nucleus in the normal state, in MPTP-treated monkeys, and in Parkinson's disease patients. *J Comp Neurol* **425**, 121-129.

Franzini A, Ferroli P, Leone M & Broggi G (2003). Stimulation of the posterior hypothalamus for treatment of chronic intractable cluster headaches: first reported series. *Neurosurgery* **52**, 1095-1099.

Freund PR, Rowell LB, Murphy TM, Hobbs SF & Butler SH (1979). Blockade of the pressor response to muscle ischemia by sensory nerve block in man. *Am J Physiol* **237**, H433-H439.

Fye WB (2000). Profiles in cardiology. Ernst, Wilhelm, and Eduard Weber. *Clin Cardiol* **23**, 709-710.

Gandevia SC, Killian K, McKenzie DK, Crawford M, Allen GM, Gorman RB & Hales JP (1993). Respiratory sensations, cardiovascular control, kinaesthesia and transcranial stimulation during paralysis in humans. *J Physiol* **470**, 85-107.

Gho BC, Schoemaker RG, van den Doel MA, Duncker DJ & Verdouw PD (1996). Myocardial protection by brief ischemia in noncardiac tissue. *Circulation* **94**, 2193-2200.

Gioia M, Tredici G & Bianchi R (1985). A Golgi study of the periaqueductal gray matter in the cat. Neuronal types and their distribution. *Exp Brain Res* **58**, 318-332.

Gonzalez-Hernandez T, Conde-Sendin M & Meyer G (1992). Laminar distribution and morphology of NADPH-diaphorase containing neurons in the superior colliculus and underlying periaqueductal gray of the rat. *Anat Embryol* **186**, 245-250.

Goodchild AK, Dampney RA & Bandler R (1982). A method for evoking physiological responses by stimulation of cell bodies, but not axons of passage, within localized regions of the central nervous system. *J Neurosci Methods* **6**, 351-363.

Goodwin GM, McCloskey DI & Mitchell JH (1972). Cardiovascular and respiratory responses to changes in central command during isometric exercise at constant muscle tension. *J Physiol* **226**, 173-190.

Grace AA, Floresco SB, Goto Y & Lodge DJ (2007). Regulation of firing of dopaminergic neurons and control of goal-directed behaviors. *Trends Neurosci* **30**, 220-227.

Grace PA (1994). Ischaemia-reperfusion injury. *Br J Surg* **81**, 637-647.

Graham LN, Smith PA, Stoker JB, Mackintosh AF & Mary DA (2002). Time course of sympathetic neural hyperactivity after uncomplicated acute myocardial infarction. *Circulation* **106**, 793-797.

Graham LN, Smith PA, Stoker JB, Mackintosh AF & Mary DA (2004). Sympathetic neural hyperactivity and its normalization following unstable angina and acute myocardial infarction. *Clin Sci (Lond)* **106**, 605-611.

Granata AR, Ruggiero DA, Park DH, Joh TH & Reis DJ (1985). Brain stem area with C1 epinephrine neurons mediates baroreflex vasodepressor responses. *Am J Physiol* **248**, H547-567.

Green AL & Paterson DJ (2008). Identification of neurocircuitry controlling cardiovascular function in humans using functional neurosurgery: implications for exercise control. *Exp Physiol* **93**, 1022-1028.

Green AL, Wang S, Owen SL, Xie K, Liu X, Paterson DJ, Stein JF, Bain PG & Aziz TZ (2005). Deep brain stimulation can regulate arterial blood pressure in awake humans. *Neuroreport* **16**, 1741-1745.

Green AL, Wang S, Purvis S, Owen SL, Bain PG, Stein JF, Guz A, Aziz TZ & Paterson DJ (2007). Identifying cardiorespiratory neurocircuitry involved in central command during exercise in humans. *J Physiol* **578**, 605-612.

Gross C, Rougier A, Guehl D, Boraud T, Julien J & Bioulac B (1997). High-frequency stimulation of the globus pallidus internalis in Parkinson's disease: a study of seven cases. *J Neurosurg* **87**, 491-498.

Gubellini P, Salin P, Kerkerian-Le Goff L & Baunez C (2009). Deep brain stimulation in neurological diseases and experimental models: from molecule to complex behavior. *Prog Neurobiol* **89**, 79-123.

Guertzenstein PG & Silver A (1974). Fall in blood pressure produced from discrete regions of the ventral surface of the medulla by glycine and lesions. *J Physiol* **242**, 489-503.

Guyenet PG (2006). The sympathetic control of blood pressure. *Nat Rev Neurosci* **7**, 335-346.

Hagbarth KE & Vallbo AB (1967). Mechanoreceptor activity recorded percutaneously with semi-microelectrodes in human peripheral nerves. *Acta Physiol Scand* **69**, 121-122.

Hansen J, Thomas GD, Jacobsen TN & Victor RG (1994). Muscle metaboreflex triggers parallel sympathetic activation in exercising and resting human skeletal muscle. *Am J Physiol Heart Circ Physiol* **266**, H2508-H2514.

Hariz MI, Blomstedt P & Zrinzo L (2010). Deep brain stimulation between 1947 and 1987: the untold story. *Neurosurg Focus* **29**, E1.

Haselton JR, Winters RW, Liskowsky DR, Haselton CL, McCabe PM & Schneiderman N (1988a). Anatomical and functional connections of neurons of the rostral medullary raphe of the rabbit. *Brain Res* **453**, 176-182.

Haselton JR, Winters RW, Liskowsky DR, Haselton CL, McCabe PM & Schneiderman N (1988b). Cardiovascular responses elicited by electrical and chemical stimulation of the rostral medullary raphe of the rabbit. *Brain Res* **453**, 167-175.

Hausenloy DJ, Mwamure PK, Venugopal V, Harris J, Barnard M, Grundy E, Ashley E, Vichare S, Di Salvo C, Kolvekar S, Hayward M, Keogh B, MacAllister RJ & Yellon DM (2007). Effect of remote ischaemic preconditioning on myocardial injury in patients undergoing coronary artery bypass graft surgery: a randomised controlled trial. *Lancet* **370**, 575-579.

Hensel H & Boman KK (1960). Afferent impulses in cutaneous sensory nerves in human subjects. *J Neurophysiol* **23**, 564-578.

Herbert H & Saper CB (1992). Organization of medullary adrenergic and noradrenergic projections to the periaqueductal gray matter in the rat. *J Comp Neurol* **315**, 34-52.

Heymans C & Neil E (1958). *Reflexogenic Areas of the Cardiovascular System*, pp. 1-271. Boston (MA): Little, Brown and Company.

Hilton SM (1966). Hypothalamic regulation of the cardiovascular system. *Br Med Bull* **22**, 243-248.

Hilton SM (1975). Ways of viewing the central nervous control of the circulation—old and new. *Brain Res* **87**, 213-219.

Hilton SM (1982). The defence-arousal system and its relevance for circulatory and respiratory control. *J Exp Biol* **100**, 159-174.

Hilton SM & Redfern WS (1986). A search for brain stem cell groups integrating the defence reaction in the rat. *J Physiol* **378**, 213-228.

Hilton SM & Spyer KM (1980). Central nervous regulation of vascular resistance. *Annu Rev Physiol* **42**, 399-441.

Hjemdahl P, Fagius J, Freyschuss U, Wallin BG, Daleskog M, Bohlin G & Perski A (1989). Muscle sympathetic activity and norepinephrine release during mental challenge in humans. *Am J Physiol Endocrin Metab* **257**, E654-E664.

Hobbs SF & Gandevia SC (1985). Cardiovascular responses and the sense of effort during attempts to contract paralysed muscles: role of the spinal cord. *Neurosci Lett* **57**, 85-90.

Hodgson HJ & Matthews PB (1968). The ineffectiveness of excitation of the primary endings of the muscle spindle by vibration as a respiratory stimulant in the decerebrate cat. *J Physiol* **194**, 555-563.

Hogarth AJ, Mackintosh AF & Mary DA (2006). The sympathetic drive after acute myocardial infarction in hypertensive patients. *Am J Hypertens* **19**, 1070-1076.

Horiuchi J, McDowall LM & Dampney RA (2009). Vasomotor and respiratory responses evoked from the dorsolateral periaqueductal grey are mediated by the dorsomedial hypothalamus. *J Physiol* **587**, 5149-5162.

Hosobuchi Y, Adams JE & Rutkin B (1973). Chronic thalamic stimulation for the control of facial anesthesia dolorosa. *Arch Neurol* **29**, 158-161.

Ichiyama RM, Gilbert AB, Waldrop TG & Iwamoto GA (2002). Changes in the exercise activation of diencephalic and brainstem cardiorespiratory areas after training. *Brain Res* **947**, 225-233.

Iellamo F, Pizzinelli P, Massaro M, Raimondi G, Peruzzi G & Legramante JM (1999). Muscle metaboreflex contribution to sinus node regulation during static exercise: insights from spectral analysis of heart rate variability. *Circulation* **100**, 27-32.

Iwamoto GA, Wappel SM, Fox GM, Buetow KA & Waldrop TG (1996). Identification of diencephalic and brainstem cardiorespiratory areas activated during exercise. *Brain Res* **726**, 109-122.

Jansen AS, Farkas E, Mac Sams J & Loewy AD (1998). Local connections between the columns of the periaqueductal gray matter: a case for intrinsic neuromodulation. *Brain Res* **784**, 329-336.

Johannson JE (1893). Uber die einwirkung der muskelthatigkeit auf die athmung und die herzthatigkeit. *Skand Arch Physiol* **5**, 20-66.

Johnson PL, Lightman SL & Lowry CA (2004). A functional subset of serotonergic neurons in the rat ventrolateral periaqueductal gray implicated in the inhibition of sympathoexcitation and panic. *Ann N Y Acad Sci* **1018**, 58-64.

Jordan D & Spyer KM (1977). Studies on the termination of sinus nerve afferents. *Pflugers Arch* **369**, 65-73.

Jurgens U & Pratt R (1979). Role of the periaqueductal grey in vocal expression of emotion. *Brain Res* **167**, 367-378.

Kakizaki T (1988). Effects of bicycle exercise on occipital EEG amplitude in male students. *Ind Health* **26**, 191-195.

Katzner S, Nauhaus I, Benucci A, Bonin V, Ringach DL & Carandini M (2009). Local origin of field potentials in visual cortex. *Neuron* **61**, 35-41.

Kaufman MP, Iwamoto GA, Longhurst JC & Mitchell JH (1982). Effects of capsaicin and bradykinin on afferent fibers with ending in skeletal muscle. *Circ Res* **50**, 133-139.

Kaufman MP, Longhurst JC, Rybicki KJ, Wallach JH & Mitchell JH (1983). Effects of static muscular contraction on impulse activity of groups III and IV afferents in cats. *J Appl Physiol* **55**, 105-112.

Kaufman MP, Rybicki KJ, Waldrop TG & Ordway GA (1984). Effect of ischemia on responses of group III and IV afferents to contraction. *J Appl Physiol* **57**, 644-650.

Kaufmann H, Bhattacharya KF, Voustianiouk A & Gracies JM (2002). Stimulation of the subthalamic nucleus increases heart rate in patients with Parkinson disease. *Neurology* **59**, 1657-1658.

Kelly RC, Smith MA, Kass RE & Lee TS (2010). Local field potentials indicate network state and account for neuronal response variability. *J Comput Neurosci* **29**, 567-579.

Khan MH & Sinoway LI (2000). Muscle reflex control of sympathetic nerve activity in heart failure: the role of exercise conditioning. *Heart Fail Rev* **5**, 87-100.

Kharbanda RK, Mortensen UM, White PA, Kristiansen SB, Schmidt MR, Hoschtitzky JA, Vogel M, Sorensen K, Redington AN & MacAllister R (2002). Transient limb ischemia induces remote ischemic preconditioning in vivo. *Circulation* **106**, 2881-2883.

Kharbanda RK, Nielsen TT & Redington AN (2009). Translation of remote ischaemic preconditioning into clinical practice. *Lancet* **374**, 1557-1565.

Kienbaum P, Karlssonn T, Sverrisdottir YB, Elam M & Wallin BG (2001). Two sites for modulation of human sympathetic activity by arterial baroreceptors? *J Physiol* **531**, 861-869.

Kirchheim HR (1976). Systemic arterial baroreceptor reflexes. *Physiol Rev* **56**, 100-177.

Kita H & Kitai ST (1987). Efferent projections of the subthalamic nucleus in the rat: light and electron microscopic analysis with the PHA-L method. *J Comp Neurol* **260**, 435-452.

Kopell BH & Greenberg BD (2008). Anatomy and physiology of the basal ganglia: implications for DBS in psychiatry. *Neurosci Biobehav Rev* **32**, 408-422.

Kramer JM, Jarboe MO & Waldrop TG (1996). Periaqueductal gray neuronal responses to hindlimb muscle contraction in the cat. *Soc Neurosci Abstr* **22**, 89.

Kringelbach ML, Green AL, Owen SL, Schweder PM & Aziz TZ (2010). Sing the mind electric – principles of deep brain stimulation. *Eur J Neurosurg* **32**, 1070-1079.

Krogh A & Lindhard J (1913). The regulation of respiration and circulation during the initial stages of muscular work. *J Physiol* **47**, 112-136.

Krout KE & Loewy AD (2000). Periaqueductal gray matter projections to midline and intralaminar thalamic nuclei of the rat. *J Comp Neurol* **424**, 111-141.

Kuhn AA, Williams D, Kupsch A, Limousin P, Hariz M, Schneider GH, Yarrow K & Brown P (2004). Event-related beta desynchronization in human subthalamic nucleus correlates with motor performance. *Brain* **127**, 735-746.

Kuncel AM & Grill WM (2004). Selection of stimulus parameters for deep brain stimulation. *Clin Neurophysiol* **115**, 2431-2441.

Lambert E, Dawood T, Schlaich M, Straznicky N, Esler M & Lambert G (2008). Single-unit sympathetic discharge pattern in pathological conditions associated with elevated cardiovascular risk. *Clin Exp Pharmacol Physiol* **35**, 503-507.

Larson CR & Kistler MK (1986). The relationship of periaqueductal gray neurons to vocalization and laryngeal EMG in the behaving monkey. *Exp Brain Res* **63**, 596-606.

Lenz FA, Gracely RH, Hope EJ, Baker FH, Rowland LH, Dougherty PM & Richardson RT (1994). The sensation of angina can be evoked by stimulation of the human thalamus. *Pain* **59**, 119-125.

Leuenberger U, Sinoway L, Gubin S, Gaul L, Davis D & Zelis R (1993). Effects of exercise intensity and duration on norepinephrine spillover and clearance in humans. *J Appl Physiol* **75**, 668-674.

Levy R, Ashby P, Hutchison WD, Lang AE, Lozano AM & Dostrovsky JO (2002). Dependence of subthalamic nucleus oscillations on movement and dopamine in Parkinson's disease. *Brain* **125**, 1196-1209.

Levy RM, Lamb S & Adams JE (1987). Treatment of chronic pain by deep brain stimulation: long term follow-up and review of the literature. *Neurosurgery* **21**, 885-893.

Li P & Lovick TA (1985). Excitatory projections from hypothalamic and midbrain defence regions to nucleus paragigantocellularis lateralis in the rat. *Exp Neurol* **89**, 543-553.

Li J & Mitchell JH (2000). c-Fos expression in the midbrain periaqueductal gray during static muscle contraction. *Am J Physiol Heart Circ Physiol* **279**, H2986-H2993.

Liebeskind JC, Guilbaud G, Besson JM & Oliveras JL (1973). Analgesia from electrical stimulation of the periaqueductal gray matter in the cat: behavioral observations and inhibitory effects on spinal cord interneurons. *Brain Res* **50**, 441-446.

Liebman JM, Mayer DJ & Liebeskind JC (1973). Self-stimulation loci in the midbrain central gray matter of the rat. *Behav Biol* **9**, 299-306.

Liem DA, Verdouw PD, Ploeg H, Kazim S & Duncker DJ (2002). Sites of action of adenosine in interorgan preconditioning of the heart. *Am J Physiol Heart Circ Physiol* **283**, H29-H37.

Light AR & Perl ER (1979). Reexamination of the dorsal root projection to the spinal dorsal horn including observations on the differential termination of coarse and fine fibers. *J Comp Neurol* **186**, 117-131.

Lim SY, Yellon DM & Hausenloy DJ (2010). The neural and humoral pathways in remote limb ischemic preconditioning. *Basic Res Cardiol* **105**, 651-655.

Limousin P, Krack P, Pollak P, Benazzouz A, Ardouin C, Hoffmann D & Benabid AL (1998). Electrical stimulation of the subthalamic nucleus in advanced Parkinson's disease. *N Engl J Med* **339**, 1105-1111.

Limousin P, Pollak P, Benazzouz A, Hoffmann D, Le Bas JF, Broussolle E, Perret JE & Benabid AL (1995). Effect of parkinsonian signs and symptoms of bilateral subthalamic nucleus stimulation. *Lancet* **345**, 91-95.

Lind AR, McNicol GW & Donald KW (1966). Circulatory adjustments to sustained (static) muscular activity. In *Physical activity in health and disease: Proceedings of the Beitostolen Symposium 1966 / Edited by Evang K & Andersen KL*, pp. 36-63. Oslo: Universitesforlaget.

Lind AR, Taylor SH, Humphreys PW, Kennelly BM & Donald KW (1964). The circulatory effects of sustained voluntary muscle contraction. *Clin Sci* **27**, 229-244.

Logothetis NK, Pauls J, Augath M, Trinath T & Oeltermann A (2001). Neurophysiological investigation of the basis of the fMRI signal. *Nature* **412**, 150-157.

Lopiano L, Rizzone M, Bergamasco B, Tavella A, Torre E, Perozzo P, Valentini MC & Lanotte M (2001). Deep brain stimulation of the subthalamic nucleus: clinical effectiveness and safety. *Neurology* **56**, 552-554.

Loukogeorgakis SP, Panagiotidou AT, Broadhead MW, Donald A, Deanfield JE & MacAllister RJ (2005). Remote ischemic preconditioning provides early and late protection against endothelial ischemia-reperfusion injury in humans: role of the autonomic nervous system. *J Am Coll Cardiol* **46**, 450-456.

Lovick TA (1985). Ventrolateral medullary lesions block the antinociceptive and cardiovascular responses elicited by stimulating the dorsal periaqueductal grey matter in rats. *Pain* **21**, 241-252.

Lovick TA (1986). Projections from brainstem nuclei to the nucleus paragigantocellularis lateralis in the cat. *J Auton Nerv Syst* **16**, 1-11.

Lovick TA (1987). Differential control of cardiac and vasomotor activity by neurones in nucleus paragigantocellularis lateralis in the cat. *J Physiol* **389**, 23-35.

Lovick TA (1992a). Inhibitory modulation of the cardiovascular defence response by the ventrolateral periaqueductal grey matter in rats. *Exp Brain Res* **89**, 133-139.

Lovick TA (1992b). Midbrain influences on ventrolateral medullo-spinal neurones in the rat. *Exp Brain Res* **90**, 147-152.

Lovick TA & Hilton SM (1985). Vasodilator and vasoconstrictor neurones of the ventrolateral medulla in the cat. *Brain Res* **331**, 353-357.

Luiten PG, ter Horst GJ & Steffens AB (1987). The hypothalamus, intrinsic connections and outflow pathways to the endocrine system in relation to the control of feeding and metabolism. *Prog Neurobiol* **28**, 1-54.

Mai JK, Assheuer JK & Paxinos G (1997). *Atlas of the Human Brain. San Diego; London: Academic.*

Mallet L, Schupbach M, N'Diaye K, Remy P, Bardinet E, Czernecki V, Welter ML, Pelissolo A, Ruberg M, Agid Y & Yelnik J (2007). Stimulation of subterritories of the subthalamic nucleus reveals its role in the integration of the emotional and motor aspects of behavior. *Proc Natl Acad Sci USA* **104**, 10661-10666.

Malpas SC & Ninomiya I (1992a). A new approach to analysis of synchronized sympathetic nerve activity. *Am J Physiol* **263**, H1311-H1317.

Malpas SC & Ninomiya I (1992b). Effect of chemoreceptor stimulation on the periodicity of renal sympathetic nerve activity in anesthetized cats. *J Auton Nerv Syst* **37**, 19-28.

Mano T, Iwase S & Toma S (2006). Microneurography as a tool in clinical neurophysiology to investigate peripheral neural traffic in humans. *Clin Neurophysiol* **117**, 2357-2384.

Marcinkiewicz M, Morcos R & Chretien M (1989). CNS connections with the median raphe nucleus: retrograde tracing with WGA-apoHRP-Gold complex in the rat.

Mark AL, Victor RG, Nerhed C & Wallin BG (1985). Microneurographic studies of the mechanisms of sympathetic nerve responses to static exercise in humans. *Circ Res* **57**, 461-469.

Martin DS, Egland MC, Barnes LU & Vogel EM (2006). Adrenergic nerves mediate the venoconstrictor response to PVN stimulation. *Brain Res* **1076**, 93-100.

Mazzone P, Lozano A, Stanzione P, Galati S, Scarnati E, Peppe A & Stefani A (2005). Implantation of human pedunculopontine nucleus: a safe and clinically relevant target in Parkinson's disease. *Neuroreport* **16**, 1877-1881.

McAllen RM & Dampney RA (1990). Vasomotor neurons in the rostral ventrolateral medulla are organized topographically with respect to type of vascular bed but not body region. *Neurosci Lett* **110**, 91-96.

McAllen RM & Malpas SC (1997). Sympathetic burst activity: characteristics and significance. *Clin Exp Pharmacol Physiol* **24**, 791-799.

McCall RB (1984). Evidence for a serotonergically mediated sympathoexcitatory response to stimulation of medullary raphe nuclei. *Brain Res* **311**, 131-139.

McCloskey DI & Mitchell JH (1972). Reflex cardiovascular and respiratory responses originating in exercising muscle. *J Physiol* **224**, 173-186.

McIntyre CC & Hahn PJ (2010). Network perspectives on the mechanisms of deep brain stimulation. *Neurobiol Dis* **38**, 329-337.

McIntyre CC, Savasta M, Kerkerian-Le Goff L & Vitek JL (2004). Uncovering the mechanism(s) of action of deep brain stimulation: activation, inhibition, or both. *Clin Neurophysiol* **115**, 1239-1248.

McMahon SE & McWilliam PN (1992). Changes in R-R interval at the start of muscle contraction in the decerebrate cat. *J Physiol* **447**, 549-562.

Mena-Segovia J, Bolam JP & Magill PJ (2004). Pedunculopontine nucleus and basal ganglia: distant relatives or part of the same family? *Trends Neurosci* **27**, 585-588.

Mense S & Craig AD Jr (1988). Spinal and supraspinal terminations of primary afferent fibers from the gastrocnemius-soleus muscle in the cat. *Neuroscience* **26**, 1023-1035.

Mense S & Stahnke M (1983). Responses in muscle afferent fibres of slow conduction velocity to contractions and ischaemia in the cat. *J Physiol* **342**, 383-397.

Mitchell JH (1985). Cardiovascular control during exercise: central and reflex neural mechanisms. *Am J Cardiol* **55**, 34D-41D.

Mitchell JH, Payne FC, Saltin B & Schibye B (1980). The role of muscle mass in the cardiovascular response to static contractions. *J Physiol* **309**, 45-54.

Mitchell JH, Reeves DR Jr, Rogers HB & Secher NH (1989). Epidural anaesthesia and cardiovascular responses to static exercise in man. *J Physiol* **417**, 13-24.

Mitchell JH & Victor RG (1996). Neural control of the cardiovascular system: insights from muscle sympathetic nerve recordings in humans. *Med Sci Sports Exerc* **28**, S60-S69.

Mitzdorf U (1985). Current source-density method and application in cat cerebral cortex: investigation of evoked potentials and EEG phenomena. *Physiol Rev* **65**, 37-100.

Montastruc JL, Rascol O & Senard JM (1996). The discovery of vasomotor nerves. *Clin Auton Res* **6**, 183-187.

Murphy AZ, Ennis M, Rizvi TA, Behbehani MM & Shipley MT (1995). Fos expression induced by changes in arterial pressure is localized in distinct, longitudinally organized columns of neurons in the rat midbrain periaqueductal gray. *J Comp Neurol* **360**, 286-300.

Murry CE, Jennings RB & Reimer KA (1986). Preconditioning with ischemia: a delay of lethal cell injury in ischemic myocardium. *Circulation* **74**, 1124-1136.

Musch TI, Haidet GC, Ordway GA, Longhurst JC & Mitchell JH (1987). Training effects on regional blood flow response to maximal exercise in foxhounds. *J Appl Physiol* **62**, 1724-1732.

Muthusamy KA, Aravamuthan BR, Kringelbach ML, Jenkinson N, Voets NL, Johansen-Berg H, Stein JF & Aziz TZ (2007). Connectivity of the human pedunculopontine nucleus region and diffusion tensor imaging in surgical targeting. *J Neurosurg* **107**, 814-820.

Nagai M, Hoshide S & Kario K (2010). The insular cortex and cardiovascular system: a new insight into the brain-heart axis. *J Am Soc Hypertens* **4**, 174-182.

Nashold BS Jr, Wilson WP & Slaughter DG (1969). Sensations evoked by stimulation in the midbrain of man. *J Neurosurg* **30**, 14-24.

Ni HF, Zhang JX & Harper RM (1990). Respiratory-related discharge of periaqueductal gray neurons during sleep-waking states. *Brain Res* **511**, 319-325.

Nowak M, Holm S, Biering-Sorensen F, Secher NH & Friberg L (2005). “Central command” and insular activation during attempted foot lifting in paraplegic humans. *Hum Brain Mapp* **25**, 259-265.

O’Leary DS, Rowell LB & Scher AM (1991). Baroreflex-induced vasoconstriction in active skeletal muscle of conscious dogs. *Am J Physiol Heart Circ Physiol* **260**, H37-H41.

Oppenheimer SM, Gelb A, Girvin JP & Hachinski VC (1992). Cardiovascular effects of human insular cortex stimulation. *Neurology* **42**, 1727-1732.

Oppenheimer SM, Kulshreshtha N, Lenz FA, Zhang Z, Rowland LH & Dougherty PM (1998). Distribution of cardiovascular related cells within the human thalamus. *Clin Auton Res* **8**, 173-179.

Ott I (1891). Vaso-tonic centres in the thalami. *J Nerv Ment Dis* **17**, 483-488.

Pahapill PA & Lozano AM (2000). The pedunculopontine nucleus and Parkinson’s disease. *Brain* **123**, 1767-1783.

Pahwa R, Wilkinson S, Smith D, Lyons K, Miyawaki E & Koller WC (1997). High-frequency stimulation of the globus pallidus for the treatment of Parkinson’s disease. *Neurology* **49**, 249-253.

Pajolla GP, Tavares RF, Pelosi GG & Correa FM (2005). Involvement of the periaqueductal gray in the hypotensive response evoked by L-glutamate microinjection in the lateral hypothalamus of unanesthetized rats. *Auton Neurosci* **122**, 84-93.

Panneton WM, Gan Q & Juric R (2005). The central termination of sensory fibers from nerves to the gastrocnemius muscle of the rat. *Neuroscience* **134**, 175-187.

Papanastassiou V, Rowe J, Scott R, Silburn P, Davies L & Aziz T (1998). Use of the Radionics Image Fusion™ and Stereoplan™ programs for target localization in functional neurosurgery. *J Clin Neurosci* **5**, 28-32.

Parent A & Hazrati LN (1995). Functional anatomy of the basal ganglia. II. The place of subthalamic nucleus and external pallidum in basal ganglia circuitry. *Brain Res Brain Res Rev* **20**, 128-154.

Pfurtscheller G & Lopes da Silva FH (1999). Event-related EEG/MEG synchronization and desynchronization: basic principles. *Clin Neurophysiol* **110**, 1842-1857.

Plaha P & Gill SS (2005). Bilateral deep brain stimulation of the pedunculopontine nucleus for Parkinson's disease. *Neuroreport* **16**, 1883-1887.

Potts JT, Shi XR & Raven PB (1993). Carotid baroreflex responsiveness during dynamic exercise in humans. *Am J Physiol Heart Circ Physiol* **265**, H1928-H1938.

Priori A, Cinnante C, Genitrini S, Pesenti A, Tortora G, Bencini C, Barelli MV, Buonamici V, Carella F, Girotti F, Soliveri P, Magrini F, Morganti A, Albanese A, Broggi S, Scarlato G & Barbieri S (2001). Non-motor effects of deep brain stimulation of the subthalamic nucleus in Parkinson's disease: preliminary physiological results. *Neurol Sci* **22**, 85-86.

Przyklenk K, Bauer B, Ovize M, Kloner RA & Whittaker P (1993). Regional ischemic 'preconditioning' protects remote virgin myocardium from subsequent sustained coronary occlusion. *Circulation* **87**, 893-899.

Rasch M, Logothetis NK & Kreiman G (2009). From neurons to circuits: linear estimation of local field potentials. *J Neurosci* **29**, 13785-13796.

Ray CA & Mark AL (1993). Augmentation of muscle sympathetic nerve activity during fatiguing isometric leg exercise. *J Appl Physiol* **75**, 228-232.

Ray CA, Rea RF, Clary MP & Mark AL (1993). Muscle sympathetic nerve responses to dynamic one-legged exercise: effect of body posture. *Am J Physiol* **264**, H1-H7.

Ray CA, Secher NH & Mark AL (1994). Modulation of sympathetic nerve activity during posthandgrip muscle ischemia in humans. *Am J Physiol Heart Circ Physiol* **266**, H79-H83.

Richardson DE & Akil H (1977a). Pain reduction by electrical brain stimulation in man. Part 1: Acute administration in periaqueductal and periventricular sites. *J Neurosurg* **47**, 178-183.

Richardson DE & Akil H (1977b). Pain reduction by electrical brain stimulation in man. Part 2: Chronic self-administration in the periventricular gray matter. *J Neurosurg* **47**, 184-194.

Risold PY, Thompson RH & Swanson LW (1997). The structural organization of connections between hypothalamus and cerebral cortex. *Brain Res Brain Res Rev* **24**, 197-254.

Rizvi TA, Ennis M, Behbehani MM & Shipley MT (1991). Connections between the central nucleus of the amygdala and the midbrain periaqueductal gray: topography and reciprocity. *J Comp Neurol* **303**, 121-131.

Rosen SD, Paulesu E, Nihoyannopoulos P, Tousoulis D, Frackowiak RS, Frith CD, Jones T & Camici PG (1996). Silent ischemia as a central problem: regional brain activation compared in silent and painful myocardial ischemia. *Ann Intern Med* **124**, 939-949.

Rotto DM & Kaufman MP (1988). Effect of metabolic products of muscular contraction on discharge of group III and IV afferents. *J Appl Physiol* **64**, 2306-2313.

Rowell LB & O'Leary DS (1990). Reflex control of the circulation during exercise: chemoreflexes and mechanoreflexes. *J Appl Physiol* **69**, 407-418.

Sagawa K (1983). Baroreflex control of systemic arterial pressure and vascular bed. In *Handbook of Physiology. The Cardiovascular System*, pp. 453-496. Bethesda (MD): Am. Physiol. Soc.

Saito M, Mano T, Abe H & Iwase S (1986). Responses in muscle sympathetic nerve activity to sustained hand-grips of different tensions in humans. *Eur J Appl Physiol Occup Physiol* **55**, 493-498.

Saito M, Mano T & Iwase S (1989). Sympathetic nerve activity related to local fatigue sensation during static contraction. *J Appl Physiol* **67**, 980-984.

Saito M, Tsukanaka A, Yanagihara D & Mano T (1993a). Muscle sympathetic nerve responses to graded leg cycling. *J Appl Physiol* **75**, 663-667.

Saito M, Watanabe H & Mano T (1993b). Comparison of muscle sympathetic nerve activity during exercise in dominant and nondominant forearm. *Eur J Appl Physiol Occup Physiol* **66**, 108-115.

Savard GK, Richter EA, Strange S, Kiens B, Christensen NJ & Saltin B (1989). Norepinephrine spillover from skeletal muscle during exercise in humans: role of muscle mass. *Am J Physiol* **257**, H1812-H1818.

Schenberg LC, Povoa RM, Costa AL, Caldellas AV, Tufik S & Bittencourt AS (2005). Functional specializations within the tectum defence systems of the rat. *Neurosci Biobehav Rev* **29**, 1279-1298.

Schoemaker RG & van Heijningen CL (2000). Bradykinin mediates cardiac preconditioning at a distance. *Am J Physiol Heart Circ Physiol* **278**, H1571-H1576.

Schott RJ, Rohmann S, Braun ER & Schaper W (1990). Ischemic preconditioning reduces infarct size in swine myocardium. *Circ Res* **66**, 1133-1142.

Schwalb JM & Hamani C (2008). The history and future of deep brain stimulation. *Neurotherapeutics* **5**, 3-13.

Seals DR (1989). Influence of muscle mass on sympathetic neural activation during isometric exercise. *J Appl Physiol* **67**, 1801-1806.

Seals DR, Chase PB & Taylor JA (1988). Autonomic mediation of the pressor responses to isometric exercise in humans. *J Appl Physiol* **64**, 2190-2196.

Seals DR & Enoka RM (1989). Sympathetic activation is associated with increases in EMG during fatiguing exercise. *J Appl Physiol* **66**, 88-95.

Shackman AJ, McMenamin BW, Maxwell JS, Greischar LL & Davidson RJ (2010). Identifying robust and sensitive frequency bands for interrogating neural oscillations. *Neuroimage* **51**, 1319-1333.

Sheehan D, Mullholland JH & Safiroff B (1941). Surgical anatomy of the carotid sinus nerve. *Anat Rec* **80**, 431-442.

Shimizu M, Tropak M, Diaz RJ, Suto F, Surendra H, Kuzmin E, Li J, Gross G, Wilson GJ, Callahan J & Redington AN (2009). Transient limb ischaemia remotely preconditions through a humoral mechanism acting directly on the myocardium: evidence suggesting cross-species protection. *Clin Sci (Lond)* **117**, 191-200.

Silber DH, Sinoway LI, Leuenberger UA & Amassian VE (2000). Magnetic stimulation of the human motor cortex evokes skin sympathetic nerve activity. *J Appl Physiol* **88**, 126-134.

Sinoway LI, Hill JM, Pickar JG & Kaufman MP (1993). Effects of contraction and lactic acid on the discharge of group III muscle afferents in cats. *J Neurophysiol* **69**, 1053-1059.

Sinoway L, Prophet S, Gorman I, Mosher T, Shenberger J, Dolecki M, Briggs R & Zelis R (1989). Muscle acidosis during static exercise is associated with calf vasoconstriction. *J Appl Physiol* **66**, 429-436.

Sinoway LI, Smith MB, Enders B, Leuenberger U, Dzwonczyk T, Gray K, Whisler S & Moore RL (1994). Role of diprotonated phosphate in evoking muscle reflex responses in cats and humans. *Am J Physiol* **267**, H770-H778.

Sinoway LI, Wilson JS, Zelis R, Schenberger J, McLaughlin DP, Morris DL & Day FP (1988). Sympathetic tone affects human limb vascular resistance during a maximal metabolic stimulus. *Am J Physiol* **255**, H937-H946.

Skultety FM (1962). Circus movements in cats following midbrain stimulation through chronically implanted electrodes. *J Neurophysiol* **25**, 152-164.

Skultety FM (1965). Mutism in cats with rostral midbrain lesions. 1. *Arch Neurol* **12**, 211-225.

Smith OA Jr, Rushmer RF & Lasher EP (1960). Similarity of cardiovascular responses to exercise and to diencephalic stimulation. *Am J Physiol* **198**, 1139-1142.

Smith SM, Jenkinson M, Woolrich MW, Beckmann CF, Behrens TE, Johansen-Berg H, Bannister PR, De Luca M, Drobnjak I, Flitney DE, Niazy RK, Saunders J, Vickers J, Zhang Y, De Stefano N, Brady JM & Matthews PM (2004). Advances in functional and structural MR image analysis and implementation as FSL. *Neuroimage* **23**, S208-S219.

Soya H, Mukai A, Deocaris CC, Ohiwa N, Chang H, Nishijima T, Fujikawa T, Togashi K & Saito T (2007). Threshold-like pattern of neuronal activation in the hypothalamus during treadmill running: establishment of a minimum running stress (MRS) rat model. *Neurosci Res* **58**, 341-348.

Spencer SE, Sawyer WB & Loewy AD (1988). L-glutamate stimulation of the zona incerta in the rat decreases heart rate and blood pressure. *Brain Res* **458**, 72-81.

Spiegel EA, Wycis HT, Marks M & Lee AJ (1947). Stereotaxic apparatus for operations on the human brain. *Science* **106**, 349-350.

Stebbins CL, Brown B, Levin D & Longhurst JC (1988). Reflex effect of skeletal muscle mechanoreceptor stimulation on the cardiovascular system. *J Appl Physiol* **65**, 1539-1547.

Strange S, Secher NH, Pawelczyk JA, Karpakka J, Christensen NJ, Mitchell JH & Saltin B (1993). Neural control of cardiovascular responses and of ventilation during dynamic exercise in man. *J Physiol* **470**, 693-704.

Sun MK, Hackett JT & Guyenet PG (1988). Sympathoexcitatory neurons of rostral ventrolateral medulla exhibit pacemaker properties in the presence of a glutamate-receptor antagonist. *Brain Res* **438**, 23-40.

Sundlof G & Wallin BG (1977). The variability of muscle nerve sympathetic activity in resting recumbent man. *J Physiol* **272**, 383-397.

Sundlof G & Wallin BG (1978). Human muscle nerve sympathetic activity at rest. Relationship to blood pressure and age. *J Physiol* **274**, 621-637.

Sverrisdottir YB, Rundgvist B, Johannsson G & Elam M (2000). Sympathetic neural burst amplitude distribution: A more specific indicator of sympathoexcitation in human heart failure. *Circulation* **102**, 2076-2081.

Tan E & Dampney RA (1983). Cardiovascular effects of stimulation of neurones within the 'defence area' of the hypothalamus and midbrain of the rabbit. *Clin Exp Pharmacol Physiol* **10**, 299-303.

Tasker RR (2004). One man's recollection of 50 years of functional and stereotactic neurosurgery. *Neurosurgery* **55**, 968-976.

Thornton JM, Aziz T, Schlugman D & Paterson DJ (2002). Electrical stimulation of the midbrain increased heart rate and arterial blood pressure in awake humans. *J Physiol* **539**, 615-621.

Thornton JM, Guz A, Murphy K, Griffith AR, Pedersen DL, Kardos A, Leff A, Adams L, Casadei B & Paterson DJ (2001). Identification of higher brain centres that may encode the cardiorespiratory response to exercise in humans. *J Physiol* **533**, 823-836.

Tibes U (1977). Reflex inputs to the cardiovascular and respiratory centers from dynamically working canine muscles. Some evidence for involvement of group III and IV nerve fibers. *Circ Res* **41**, 332-341.

Turnbull IM, Shulman R & Woodhurst WB (1980). Thalamic stimulation for neuropathic pain. *J Neurosurg* **52**, 486-493.

Vallbo AB, Hagbarth KE, Torebjork HE & Wallin BG (1979). Somatosensory, proprioceptive, and sympathetic activity in human peripheral nerves. *Physiol Rev* **59**, 919-957.

Van Bockstaele EJ, Pieribone VA & Aston-Jones G (1989). Diverse afferents converge on the nucleus paragigantocellularis in the rat ventrolateral medulla: retrograde and anterograde tracing studies. *J Comp Neurol* **290**, 561-584.

Van der Plas J, Wiersinga-Post JE, Maes FW & Bohus B (1995). Cardiovascular effects and changes in midbrain periaqueductal grey neuronal activity induced by electrical stimulation of the hypothalamus in the rat. *Brain Res Bull* **37**, 645-656.

Verberne AJ & Struyker Boudier HA (1991). Midbrain central grey: regional haemodynamic control and excitatory amino acidergic mechanisms. *Brain Res* **550**, 86-94.

Victor RG, Bertocci LA, Pryor SL & Nunnally RL (1988). Sympathetic nerve discharge is coupled to muscle cell pH during exercise in humans. *J Clin Invest* **82**, 1301-1305.

Victor RG, Pryor SL, Secher NH & Mitchell JH (1989a). Effects of partial neuromuscular blockade on sympathetic nerve responses to static exercise in humans. *Circ Res* **65**, 468-476.

Victor RG, Rotto DM, Pryor SL & Kaufman MP (1989b). Stimulation of renal sympathetic activity by static contraction: evidence for mechanoreceptor-induced reflexes from skeletal muscle. *Circ Res* **64**, 592-599.

Victor RG & Seals DR (1989). Reflex stimulation of sympathetic outflow during rhythmic exercise in humans. *Am J Physiol* **257**, H2017-H2024.

Victor RG, Seals DR & Mark AL (1987). Differential control of heart rate and sympathetic nerve activity during dynamic exercise. Insight from intraneural recordings in humans. *J Clin Invest* **79**, 508-516.

Victor RG, Secher NH, Lyson T & Mitchell JH (1995). Central command increases muscle sympathetic nerve activity during intense intermittent isometric exercise in humans. *Circ Res* **76**, 127-131.

Vissing SF, Scherrer U & Victor RG (1991). Stimulation of skin sympathetic nerve discharge by central command. Differential control of sympathetic outflow to skin and skeletal muscle during static exercise. *Circ Res* **69**, 228-238.

Vitek JL, Bakay RA, Hashimoto T, Kaneoke Y, Mewes K, Zhang JY, Rye D, Starr P, Baron M, Turner R & DeLong MR (1998). Microelectrode-guided pallidotomy: technical approach and its application in medically intractable Parkinson's disease. *J Neurosurg* **88**, 1027-1043.

Volkmann J, Herzog J, Kopper F & Deuschl G (2002). Introduction to the programming of deep brain stimulators. *17*, S181-S187.

Waldrop TG, Rybicki KJ & Kaufman MP (1984). Chemical activation of group I and II muscle afferents has no cardiorespiratory effects. *J Appl Physiol* **56**, 1223-1228.

Wallin BG & Charkoudian N (2007). Sympathetic neural control of integrated cardiovascular function: insights from measurement of human sympathetic nerve activity. *Muscle Nerve* **36**, 595-614.

Wallin BG & Eckberg DL (1982). Sympathetic transients caused by abrupt alterations of carotid baroreceptor activity in humans. *Am J Physiol Heart Circ Physiol* **242**, H185-H190.

Wallin BG, Sundlof G & Delius W (1975). The effect of carotid sinus nerve stimulation on muscle and skin nerve sympathetic activity in man. *Pflugers Arch* **358**, 101-110.

Wallin BG, Victor RG & Mark AL (1989). Sympathetic outflow to resting muscles during static handgrip and postcontraction muscle ischemia. *Am J Physiol* **256**, H105-H110.

Ward DG & Darlington DN (1987a). Lesions of the caudal periaqueductal gray prevent compensation of arterial pressure during hemorrhage. *Brain Res* **407**, 369-375.

Ward DG & Darlington DN (1987b). A blood pressure lowering effect of lesions of the caudal periaqueductal gray: relationship to basal pressure. *Brain Res* **423**, 373-377.

Wiles JD, Allum SR, Coleman DA & Swaine IL (2008). The relationships between exercise intensity, heart rate, and blood pressure during an incremental isometric exercise test. *J Sports Sci* **26**, 155-162.

Williams CA (1985). Effect of clonidine and naloxone on the pressor response during contraction of cat hind-limb muscles. *Cardiovasc Res* **19**, 474-482.

Williams CA (1996). Neuropeptide Y-like substances are released from the rostral brainstem of cats during the muscle pressor response. *J Physiol* **495**, 267-277.

Williams CA, Blevins LS & Paul DJ (1987). Possible catecholaminergic-opiodergic control of blood pressure during muscular contraction. *Cardiovasc Res* **21**, 471-480.

Williams CA, Holtsclaw LI & Chiverton JA (1992). Release of immunoreactive enkephalinergic substances in the periaqueductal grey of the cat during fatiguing isometric contractions. *Neurosci Lett* **139**, 19-23.

Williams CA, Loyd SD, Hampton TA & Hoover DB (2000). Expression of c-fos-like immunoreactivity in the feline brainstem in response to isometric muscle contraction and baroreceptor reflex changes in arterial pressure. *Brain Res* **852**, 424-435.

Williams CA, Roberts JR & Freels DB (1990). Changes in blood pressure during isometric contractions to fatigue in the cat after brain stem lesions: effects of clonidine. *Cardiovasc Res* **24**, 821-833.

Williams D, Kuhn A, Kupsch A, Tijssen M, van Bruggen G, Speelman H, Hotton G, Yarrow K & Brown P (2003). Behavioural cues are associated with modulations of synchronous oscillations in the human subthalamic nucleus. *Brain* **126**, 1975-1985.

Williamson JW, Fadel PJ & Mitchell JH (2006). New insights into central cardiovascular control during exercise in humans: a central command update. *Exp Physiol* **91**, 51-58.

Williamson JW, McColl R, Mathews D, Ginsburg M & Mitchell JH (1999). Activation of the insular cortex is affected by the intensity of exercise. *J Appl Physiol* **87**, 1213-1219.

Williamson JW, McColl R, Matthews D, Mitchell JH, Raven PB & Morgan WP (2001). Hypnotic manipulation of effort sense during dynamic exercise: cardiovascular responses and brain activation. *J Appl Physiol* **90**, 1392-1399.

Wolfrum S, Schneider K, Heidbreder M, Nienstedt J, Dominiak P & Dendorfer A (2002). Remote preconditioning protects the heart by activating myocardial PKCepsilon-isoform. *Cardiovasc Res* **55**, 583-589.

Woolrich MW, Jbabdi S, Patenaude B, Chappell M, Makni S, Behrens T, Beckmann C, Jenkinson M & Smith SM (2009). Bayesian analysis of neuroimaging data in FSL. *Neuroimage* **45**, S173-S186.

Yaksh TL, Yeung JC & Rudy TA (1976). Systematic examination in the rat of brain sites sensitive to the direct application of morphine: observation of differential effects within the periaqueductal gray. *Brain Res* **114**, 83-103.

Yardley CP & Hilton SM (1986). The hypothalamic and brainstem areas from which the cardiovascular and behavioural components of the defence reaction are elicited in the rat. *J Auton Nerv Syst* **15**, 227-244.

Yellon DM, Alkhulaifi AM, Browne EE & Pugsley WB (1992). Ischaemic preconditioning limits infarct size in the rat heart. *Cardiovasc Res* **26**, 983-987.

Yezierski RP (1988). Spinomesencephalic tract: projections from the lumbosacral spinal cord of the rat, cat, and monkey. *J Comp Neurol* **267**, 131-146.

Zhang SP, Bandler R & Carrive P (1990). Flight and immobility evoked by excitatory amino acid microinjection within distinct parts of the subtentorial midbrain periaqueductal gray of the cat. *Brain Res* **520**, 73-82.

Zuntz N & Geppert J (1886). Uber die natur der normalen atemreize und den ort ihrer wirkung. *Arch General Physiol* **38**, 337-338.